Thorium based Nuclear Materials

SOCIETY FOR MATERIALS CHEMISTRY

Society for Materials Chemistry

Society for Materials Chemistry was mooted in 2007 with following aims and objectives:

(a) to help the advancement, dissemination and application of the knowledge in the field of materials chemistry,

(b) to promote active interaction among all material scientists, bodies, institutions and industries interested in achieving the advancement, dissemination and application of the knowledge of materials chemistry,

(c) to disseminate information in the field of materials chemistry by publication of bulletins, reports, newsletters, journals.

(d) to provide a common platform to young researchers and active scientists by arranging seminars, lectures, workshops, conferences on current research topics in the area of materials chemistry,

(e) to provide financial and other assistance to needy deserving researchers for participation to present their work in symposia, conference, etc.

(f) to provide an incentive by way of cash awards to researchers for best thesis, best paper published in journal/national/international conferences for the advancement of materials chemistry,

(g) to undertake and execute all other acts as mentioned in the constitution of SMC.

Executive Committee

President
Dr. T. Mukherjee
Bhabha Atomic Research Centre
Trombay, Mumbai, 400 085
mukherji@barc.gov.in

Vice-Presidents
Dr. D. Das
Bhabha Atomic Research Centre
Trombay, Mumbai, 400 085
dasd@barc.gov.in

Dr. K. Nagarajan
Indira Gandhi Centre for Atomic Research
Kalpakkam, 603102 (TN)
knag@igcar.gov.in

Secretary
Dr. A.K. Tyagi
Bhabha Atomic Research Centre
Trombay, Mumbai, 400 085
aktyagi@barc.gov.in

Treasurer
Dr. R.K. Vatsa
Bhabha Atomic Research Centre
Trombay, Mumbai, 400 085
rkvatsa@barc.gov.in

Members
Dr. P.R. Vasudeva Rao
Indira Gandhi Centre for Atomic Research
Kalpakkam, 603102 (TN)
vasu@igcar.gov.in

Dr. S.K. Kulshrestha
Atomic Energy Education Society
Western Sector, AEES-6
Anushaktinagar, Mumbai, 400 094
kulshres@gmail.com

Dr. V.K. Jain
Bhabha Atomic Research Centre
Trombay, Mumbai, 400 085
jainvk@barc.gov.in

Dr. C.G.S. Pillai
Bhabha Atomic Research Centre
Trombay, Mumbai, 400 085
cgspil@barc.gov.in

Dr. S.R. Bharadwaj
Bhabha Atomic Research Centre
Trombay, Mumbai, 400 085
shyamala@barc.gov.in

Dr. Manidipa Basu
Bhabha Atomic Research Centre
Trombay, Mumbai, 400 085
deepa@barc.gov.in

Dr. Sandeep Nigam
Bhabha Atomic Research Centre
Trombay, Mumbai, 400 085
snigam@barc.gov.in

Co-opted Members
Dr. Aparna Banerjee
Bhabha Atomic Research Centre
Trombay, Mumbai, 400 085
aparnab@barc.gov.in

Dr. A.K. Tripathi
Bhabha Atomic Research Centre
Trombay, Mumbai, 400 085
catal@barc.gov.in

Prof. S.D. Samant
Institute of Chemical Technology
Matunga, Mumbai-400 019
samantsd@udct.org

Prof. G.P. Das
Indian Association for the
Cultivation of Science (IACS)
Jadavpur, Kolkata-700 032,
msgpd@iacs.res.in

Prof. Ashok K. Ganguli
Indian Institute of Technology
Hauz Khas, New Delhi 110 016
ashok@chemistry.iitd.ernet.in

Contact address
Society for Materials Chemistry
C/o Chemistry Division
Bhabha Atomic Research Centre, Trombay, Mumbai, 400 085, India
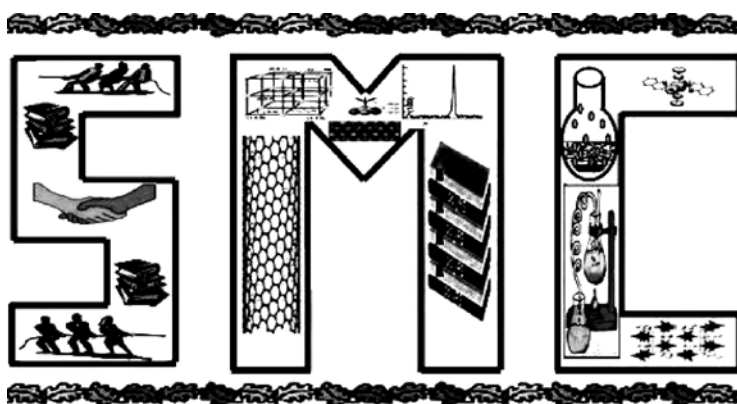Tel: +91-22-25592001, E-mail: socmatchem@gmail.com

SMC Bulletin

A Publication of the Society for Materials Chemistry

Volume 4   **No. 1**   **April 2013**

SMC Bulletin

Please note that the authors of the paper are alone responsible for the technical contents of papers and references cited therein.
Front cover shows a photograph of washed & vacuum dried as-prepared thorium metal powders

Guest Editorial

Siddhartha Kolay

Manidipa Basu

It is imperative that India should launch thorium (Th) cycle at the earliest for its energy security and sustainability because thorium based fuels have several advantages. Thorium has higher natural abundance (nearly thrice) than uranium and wide distribution in easily extractable forms. It has superior structural, physical, chemical, thermal and thermophysical properties as compared to those of uranium and/or plutonium. In addition, it is bestowed with attractive fertile characteristics (nuclear properties). Thorium based fuels are inherently safe and non-proliferative in nature, irrespective of their chemical states. In view of these, thorium is a potential fuel for nuclear reactors. However, the major disadvantage with thorium is that it is not fissile and has to be converted to U-233 for using it as a sustainable source of energy. In fact, separating ^{233}U from irradiated thorium and fabricating newer fuel with the bred ^{233}U are technologically challenging tasks that have been undertaken by scientists and engineers working in the field of nuclear technology. Continuous research efforts are being put into all aspects of the thorium fuel cycle. Currently, research is going on towards design and development of Advanced Heavy Water Reactor (AHWR), Compact High Temperature Reactor (CHTR) and Innovative High Temperature Reactor (IHTR) all of which would be using thorium based fuels.

In this perspective the chosen theme 'Thorium based Nuclear Materials' for this issue is highly relevant for our theme-based issues of SMC bulletin. This issue includes articles which cover almost all the important aspects of thorium-based fuel technology. One of the articles covers the physics aspects like neutronic characteristics and performance potential of thorium. The same article also gives an overview of thorium utilization in our country. Several articles deal with key issues like extractive metallurgy or production of thorium metal and some others deal with important issues like thoria dissolution at both ends of the thorium based fuel cycle and separation of essential radionuclides in the context of recycling and reprocessing of spent fuel. This issue also contains overview on thorium based metallic alloy fuels and on thermo-chemical investigations of Th-based oxide fuels. There is also an article dealing with issues of immobilization of waste from thorium based oxide fuels.

We take this opportunity to thank all the contributors who have spared some of their valuable time to provide such informative articles for the benefit of all our readers. We also thank the editorial committee of SMC bulletin for inviting us to be guest editors for this issue. We hope the readers would find this issue interesting and useful.

(S. Kolay and M. Basu)

Editorial Note

We are happy to bring forth the first issue of volume four (April 2013) of SMC bulletin on the theme of **"Thorium based Nuclear Materials'** which contains articles covering almost all the essential aspects of thorium fuel technology. We thank the guest editors, Manidipa Basu and Siddhartha Kolay, whose well coordinated efforts helped in timely release of this bulletin.

We hope that our readers would appreciate the articles presented therein and would send us their feedback which would enable us in improving the quality of this bulletin in future.

The next issue of the bulletin will be on the theme of Computational Materials Chemistry. We request all our members to come forward and contribute their theme-based articles to this forthcoming issue.

Editors

From the President's Desk

Dear Fellow Members,

The 4th biennial symposium, "Interdisciplinary Symposium on Materials Chemistry (ISMC-2012)" which was hosted in BARC, Mumbai, in December, 2012, has brought an overwhelming response from the young scientists that shows their eagerness to participate actively in all events of this society, thus increasing their scientific awareness and getting scientifically enriched. We look forward to active participation from all our members in the forthcoming National Workshop on Materials Chemistry, (NWMC-2013) to be held this year. It is also very satisfying to note the enthusiasm which is being shown by young researchers and academicians in contributing articles for the theme-based issues of the SMC bulletin.

The theme of this issue of SMC bulletin, 'Thorium based Nuclear Materials' is highly relevant to the research carried out by scientists of the DAE family. However, I feel that the information contained in the articles presented therein will also be of great value to all other materials scientists. I hope that the bulletin, in form of these theme-based issues will continue to serve as a medium for highlighting the advances made in the field of materials chemistry and the members will keep enriching it with quality articles.

T. Mukherjee

CONTENTS

x

Extractive metallurgy of thorium

A. Awasthi

Materials Processing Division
Bhabha Atomic Research Centre, Mumbai – 400085
*E-mail: aawasthi@barc.gov.in*

1. Introduction

The utilization of thorium in nuclear power reactors has been envisaged in the form of oxides to begin with. However, as the use of thorium in elemental form would result in a shorter doubling time, the time may not be very far when the large quantities of thorium would be required at a reasonable cost. Thorium is a metal and its isolation in elemental form in large quantities requires sound understanding of metallurgical thermochemistry principles besides those of metallurgical engineering.

Thorium occurs in nature mainly in beach sand deposits as monazite mineral, which is a phosphate of rare earths and thorium, $(RE,Th)PO_4$, and contains 8-10% thorium oxide (ThO_2). The percentage of monazite in beach sands happens to be around 1%. It is separated from the other constituents of the beach sand by making use of the fact that it is electrically non-conducting and feebly magnetic in comparison to other co-occurring minerals. Thorium oxide is recovered from monazite by selective chemical removal of rare earth compounds. Thorium oxide, also known as thoria, is the starting material for production of thorium metal.

## 2. Reduction of Thorium Oxide and Ellingham Diagram

The reduction of thorium oxide could be represented by the following reaction:

$$x\,ThO_2 + 2\,R = x\,Th + 2\,RO_x \tag{1}$$
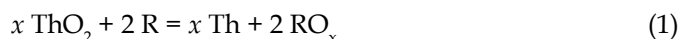
where $2x$ is the valency of the reductant R. Assessment whether R would be able to reduce thoria could be made by finding out the Gibbs free energy change of the reaction (1). When the products and the reactants are in standard state (i.e., in pure form at one atmospheric pressure in the most stable state), a convenient way of assessing the Gibbs free energy change at a given temperature is to use Ellingham diagram, which is a graphical representation of the variation in standard Gibbs free energies of formation of various oxides per mole of oxygen with temperature. For example, for elements M and N, the standard Gibbs free energies of the following reactions (2-3) would be plotted respectively:

$$(2/y)\,M + O_2 = (2/y)\,MO_y \tag{2}$$

$$(2/z)\,N + O_2 = (2/z)\,NO_z \tag{3}$$

where $2y$ and $2z$ are the valencies of M and N respectively. For assessing whether MO_y could be reduced by N, one would normally calculate whether the standard Gibbs free energy change for reaction (4) is negative:

$$MO_y + (y/z)\,N = M + (y/z)\,NO_z \tag{4}$$
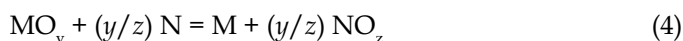
However, according to Hess's law, standard Gibbs free energies, $\Delta G^o_{reaction}$, of various reactions are related as follows:

$$\Delta G^o_{[4]} = (y/2)\left(\Delta G^o_{[3]} - \Delta G^o_{[2]}\right)$$

As standard Gibbs free energy of formation of a compound (thus $\Delta G^o_{[2]}$ and $\Delta G^o_{[3]}$, both) is negative, this expression would be negative if $\Delta G^o_{[3]}$ is more negative than $\Delta G^o_{[2]}$. In other words, N should be below M in Ellingham diagram for reaction (4) to be feasible (or for N to be able to reduce MO).

Figure 1 shows the Ellingham diagram of oxides calculated using the data compiled by Kubaschewski and Alcock [1]. Thorium occurs quite at the bottom of this diagram indicating that its oxide is amongst the most stable oxides.

2.1 Carbon as reductant for thoria

The most common reductant used in metallurgical industries is carbon (in the form of coal). Carbon has a special feature amongst the reductants that the stability of its oxide, CO, increases with temperature. However, as seen from Figure 1, the line of CO does not cut the line of ThO_2 upto 2000 K; in fact the two lines would cut each other around 2800 K. This is too high a temperature to be achieved in a controlled way and would lead to container problems.

Ellingham diagrams are normally plotted for the reactions occurring in standard states. However, the Gibbs free energy change for CO has also been plotted in Figure 1 when its equilibrium partial pressure, p_{CO}, is 1×10^{-5} atm:

As p_{CO} is less than one, the value of the logarithmic term in this equation is negative, which makes ΔG_{CO}

more negative than ΔG_{CO}. The line of CO with reduced equilibrium partial pressure cuts the thorium line around 1850 K. Therefore, with continuous removal of CO at pressures lower than 1×10^{-5} atm it should prima facie be possible to reduce thoria with carbon at this temperature.

However, this analysis does not consider the formation of thorium carbide, ThC. The following reaction (5)

$$ThO_2 + 3\,C = ThC + 2\,CO \tag{5}$$

can be considered as the sum of the two reactions (6) and (7):

$$ThO_2 + 2\,C = Th + 2\,CO \tag{6}$$

$$Th + C = ThC \tag{7}$$

Thorium carbide is known to exist and hence the $\Delta G^o_{[7]}$ would be negative. Therefore, according to Hess's law, $\Delta G^o_{[5]}$ would be more negative than $\Delta G^o_{[6]}$. In other words, ThC will first form until entire carbon present in the reactants gets consumed. ThO_2 and ThC will finally react to form Th and the overall reaction sequence could be written as

$$2\,(ThO_2 + 3\,C) + ThO_2 = 2\,(ThC + 2\,CO\,) + ThO_2$$
$$(2 \times 5 + ThO_2)$$

$$ThO_2 + 2ThC = 3\,Th + 2\,CO \tag{8}$$
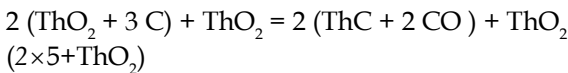
The equilibrium partial pressure of CO for reaction (8) could be given as

$$p_{CO} = \exp\left[-\left(2\Delta G^o_{CO} - \Delta G^o_{ThO_2} - 2\,DG^o_{ThC}\right)/(2RT)\right]$$

Since ΔG^o_{Thc} is highly negative as thorium is a strong carbide former, the introduction of this term in would result in further substantial decrease in p_{CO} values as compared to the case when the existence of ThC was not considered. In other words, for reduction of ThO_2 by carbon at around 1850 K, CO will have to be continuously removed at pressures many orders lower than 1×10^{-5} atm. Evaporation of thorium as ThO vapour also becomes appreciable under such conditions.

Therefore, the reduction of thoria by carbon is not practical even with the application of vacuum.

2.2 Hydrogen as reductant for thoria

Hydrogen in Ellingham diagram occurs quite at top (Figure 1) and the stability of its oxide, H_2O, decreases with temperature. Therefore, an increase in temperature would tend to decompose H_2O instead of favouring the reduction of ThO_2. However, H_2O is a vapour at temperatures important for reduction of oxides and it would not be

reasonable to assume its equilibrium partial pressure as 1 atm, particularly when the reduction is attempted in flowing hydrogen. The Gibbs free energy change when the equilibrium partial pressure of H_2O (or equilibrium H_2O/H_2 mole ratio) is 1×10^{-8} atm is plotted in Figure 1. This line cuts the thorium line around 1950 K. This is still a high temperature for industrial handling of an explosive gas like hydrogen. Besides, the reduction reaction would stop when the H_2O content of the gas increases above 1×10^{-8}, which indicates that the reaction would be very slow despite requiring high flow rate of hydrogen. Hydrogen is therefore not considered for reduction of ThO_2 to thorium metal.

2.3 Metals as the reductant for thoria

Aluminium is the most common metal used for the reduction of oxides in metallurgical industries.

However, it is reasonably above thorium in Ellingham diagram (Figure 1). Decreasing the activity of the product alumina by fluxing it with other oxides to form aluminates does not help much in making the Gibbs free energy of the reduction reaction negative, as the activity coefficients of Al_2O_3 in aluminates are not so less. Therefore, the reduction of thoria by aluminium is not possible practically.

Magnesium is another metal commonly used for the reduction of oxides. However, as seen from Figure 1, magnesium is also above thorium in Ellingham diagram and cannot be therefore used for the reduction of thoria.

This limits the choice of the reductant to calcium, which is the only element occurring partially below thorium in Ellingham diagram (Figure 1). However, the calcium line
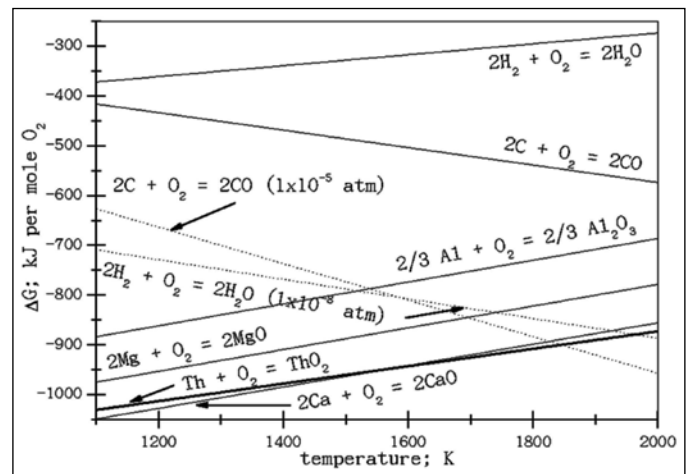
Fig 1: Free energy change for given reactions as a function of temperature (Ellingham diagram for oxides). Al, Mg and Ca are in liquid state. Rest of the reactants and the products are in standard state wherever not stated.

Table 1 Melting and boiling points of thorium and possible reductants and of their chlorides and fluorides [2]

Element	Melting Point (°C)	Boiling Point (°C)	Chloride	Melting Point (°C)	Boiling Point (°C)	Fluoride	Melting Point (°C)	Boiling Point (°C)
Mg	649	1107	$MgCl_2$	718	1415	MgF_2	1263	2227
Na	98	883	NaCl	800	1445	NaF	997	1704
Ca	839	1484	$CaCl_2$	772	1900	CaF_2	1418	2500
Th	1755	4787	$ThCl_4$	770	857	ThF_4	1050	1700

crosses the line of thorium in Ellingham diagram around 1575 K, which indicates that the reduction of thorium has to be carried out below this temperature. If the reduction was carried out at a lower temperature and the products, Th and CaO, were not separated, then on crossing this temperature, the products would revert to ThO_2 and calcium.

Calcium is taken as granules and is usually taken in hyperstoichiometric amount to compensate for its loss in oxidation. It is mixed with thoria powder, filled in a retort of Inconel and heated to 900-1000 °C in inert atmosphere. The product is leached in dilute acid below room temperature. CaO and excess calcium get dissolved and thorium powder remains.

As the difference between the stabilities of calcium oxide and thoria is not much (Figure 1), substantial oxygen (upto about 1 wt%) remains in the thorium powder thus obtained. However, this powder is ductile enough for compaction and conversion to sheets and other shapes. Further

Fig 2: Ellingham diagram of chlorides [2]

Fig 3: Ellingham diagram of fluorides [2]

purification occurs if the powder is vacuum-melted. The dissolved oxygen gets removed as ThO vapour, which becomes stable at high temperatures under vacuum. However, this does result in substantial loss of thorium metal as well. As the atomic weight of thorium is about fifteen times that of oxygen, the removal of oxygen as ThO results in the simultaneous loss of fifteen times thorium.

3. Reduction of thorium chloride
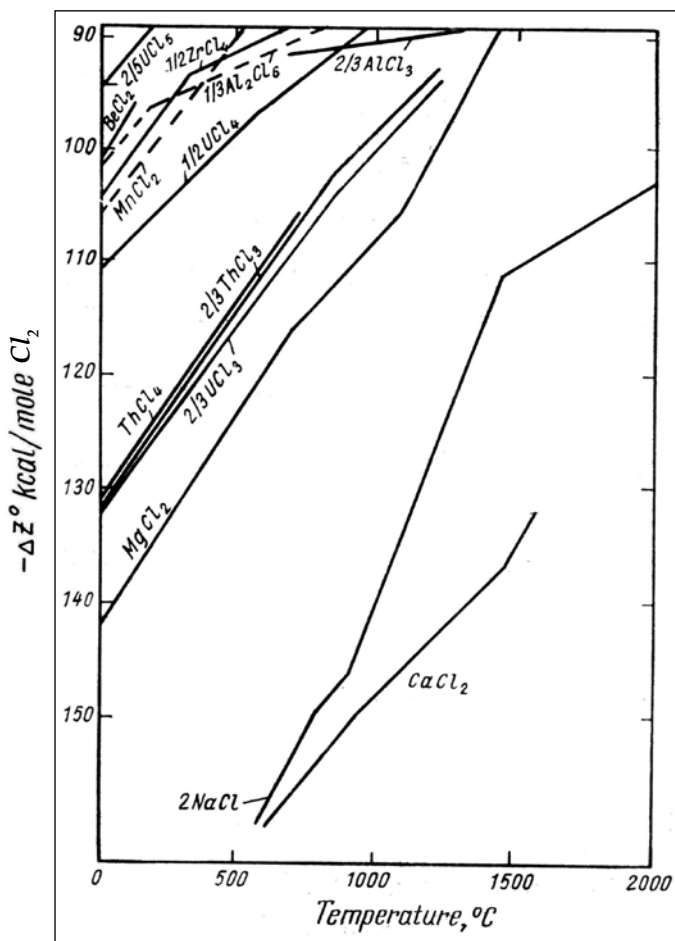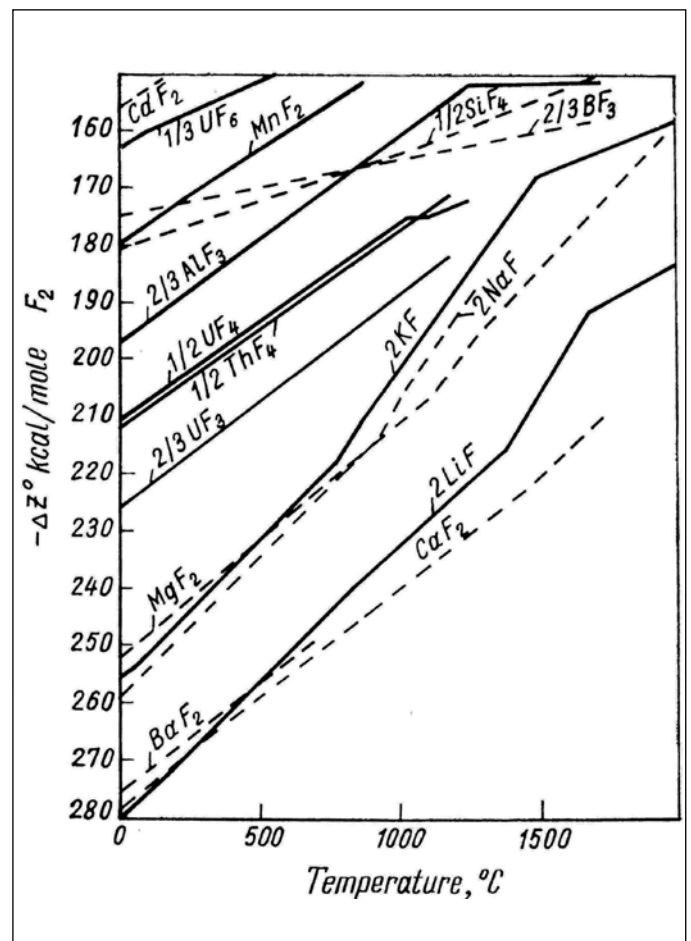
If pure thorium chloride could be used as the starting material, which is reduced further to thorium under inert atmosphere, then this thorium should have acceptable amount of oxygen impurity. Ellingham diagram of chlorides [2] is shown in Figure 2. The choice of reductants is wider for thorium chloride as compared to that for thorium oxide. Chlorides of magnesium, sodium, calcium and many rare earth elements occur below thorium chloride in Ellingham diagram. Reduction of thorium chloride has been demonstrated using cheaper magnesium and sodium, eliminating the need to use expensive calcium. The reduction is carried out at a temperature, when both $ThCl_4$ and the reductant are liquid. The product slags are also liquid at these temperatures, whereas thorium forms in solid form due to its much higher melting point (Table 1). Thorium being much heavier as compared to slag, its particles settle down in the molten slag. As the temperature is high enough, these particles sinter and thorium is obtained as sponge on cooling. Excess reductant and entrapped chlorides in this case are removed by distilling them off.

However, the chlorides are hygroscopic and corrosive, and therefore are not easy to handle. Besides, the conversion of ThO_2 to $ThCl_4$ requires good control on moisture and atmosphere as otherwise $ThOCl_2$ remains in the product chloride as contaminant defeating the purpose of going for the chloride process.

4. Reduction of thorium fluoride

Fluorides are less volatile as compared to chlorides besides being non-hygroscopic; however, they are expensive. Like the chloride reduction, the fluoride processes also result in low-oxygen thorium metal. It is much easier to avoid the formation of oxyfluorides as compared to that of oxychlorides. Thorium fluoride, ThF_4, is obtained from thoria by interacting it with HF, F_2, NH_4HF_2 or NH_4F.

Ellingham diagram for fluorides [2] is shown in Figure 3, according to which the choice of magnesium,

sodium, calcium etc is thermodynamically available as reductants. However, calcium is preferred as its vapour pressure is lower and manageable at reaction temperatures (Table 1).

In the process normally employed for the preparation of thorium metal from its fluoride, sufficient amount of $ZnCl_2$ is also added. The reaction of $ZnCl_2$ with calcium is highly exothermic. The product zinc, alloys with thorium, to result in a eutectic composition thereby lowering the melting temperature of the product. The overall heat of reaction is sufficient to melt all the products. As the densities of the two liquids are substantially different, good slag-metal separation is achieved. The reaction is carried out in a closed reactor made from steel suitably lined with refractory material. After cooling to room temperature, the slag phase and the metal phase are separated. The thorium-zinc alloy thus-obtained as the metal phase is purified by distilling-off zinc in vacuum to obtain pure thorium sponge. This process is therefore a two-step process. Besides, as this highly exothermic process is carried out in a closed reactor, it is potentially dangerous.

With high temperature furnaces being easily available now, a modified-fluoride process was proposed by Dr N. Krishnamurthy, BARC. As the reduction of ThF_4 by calcium is mildly exothermic, the heat of the reaction is not sufficient for raising the temperature to that above the melting point of thorium, which is 1755 °C. In the modified fluoride process, ThF_4 powder is mixed with excess amount of calcium granules and this charge is heated in a furnace to carry out the reduction reaction. The products, Th and CaF_2 both, are solid at the reaction temperature. The temperature of the furnace is then raised to above 1800 °C. Before the melting of thorium, the excess calcium evaporates and the slag CaF_2 melts. Sufficient time is allowed for the slag and the metal to separate in liquid state due to the difference in their densities. The metal and the slag are mechanically separated on cooling. A few trial runs of the modified-fluoride process have been performed and solutions are being looked into to sort out the container problems encountered.

5. Conclusions

Although calciothermic reduction of thorium oxide is the simplest process for the extraction of thorium, the yield and the purity of the product remain an issue. Alternate processes that solve these issues are still at development stage.

Acknowledgement

References:

1. O. Kubaschewski and C.B. Alcock, Metallurgical Thermochemistry, Pergamon Press, (1989), 5th edition.

2. A. Volsky and E. Sergievskaya, Theory of Metallurgical Processes: Pyrometallurgical Processes, Mir Publishers, (1978), 2nd edition.

Dr. A. Awasthi *is a Scientific Officer in Materials Processing Division of Bhabha Atomic research Centre (BARC), Mumbai. After completion of B.E.(Met.) from University of Roorkee (now IIT Roorkee), he joined BARC through the 33rd batch of Training School. He has a doctoral degree from Kyoto University and his research interests are vacuum metallurgy, extractive metallurgy of refractory and reactive metals, molten salt electrolysis, thermal analysis and experimental metallurgical thermodynamics.*

Production of Thorium Metal Foil

M. T. Saify#, S. K. Jha and K. K. Abdulla

Atomic Fuels Division
Bhabha Atomic Research Centre, Mumbai - 400 085
#Email: msaify@barc.gov.in

1. Introduction

Thorium metal has a high melting point and is reactive in nature, especially at elevated temperatures. The oxide being very stable, thorium metal gets oxidized on contact with air. Processes for production of high purity thorium metal foil therefore have been developed at Atomic Fuels Division, Bhabha Atomic Research Centre (AFD, BARC) so as to overcome these challenges.

There are several methods for production of thorium metal. Calcio-thermic reduction of thorium oxide and fused salt electrolysis of thorium compounds such as ThF_4, $ThCl_4$ and $KThF_5$ leads to the production of thorium metal in powder form. However, magnesium reduction of thorium chloride and calcium reduction of thorium fluoride yields thorium in sponge form. Among these methods, calcium reduction of thorium oxide has been adapted at AFD, BARC.

2. Calcio-thermic reduction of Thorium Oxide

Calcium is thermodynamically the most favorable reducing agent for thoria. This method of producing thorium metal was one of the first to be developed for producing thorium in the form of powder on kilogram scale. This method was adopted at AFD, BARC on the basis of following advantages:

i. The process is simple and economic

ii. Thorium oxide is stable, non-hygroscopic and non-corrosive posing no handling problems

iii. Equipment for preparing the reactants, performing the reaction and post reduction treatment of metal are simple

iv. High purity metal powder is produced

The calcio-thermic reduction of thoria is based on the reaction:

$$ThO_2 + 2Ca \rightleftharpoons Th + 2CaO \quad \Delta F^o_{298K} = -8.88 \text{ Kcal/mole of } ThO_2$$

$$\Delta H^o_{298K} = -10.00 \text{ Kcal/mole of } ThO_2$$
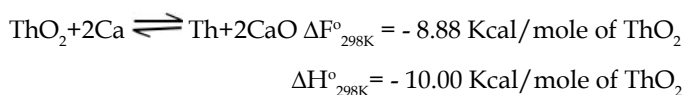
3. Fabrication of Thorium Metal Foil

Flow-sheet for the production of thorium metal foil is depicted in Fig. 1. The steps involved can be broadly classified into two main categories. First is the production of thorium metal powder by calico-thermic reduction of thorium oxide and secondly, fabrication of foil by consolidation of powder and cold rolling.

3.1 Production of thorium metal powder

Thorium oxide powder is first calcined at 900°C in calcination furnace (Fig. 2) to remove absorbed moisture and other volatile impurities. Thereafter it is handled in an inert atmosphere to prevent moisture pickup. Calcined thoria is then mixed with double distilled (99.9% purity) calcium granules (Fig. 3) in excess of
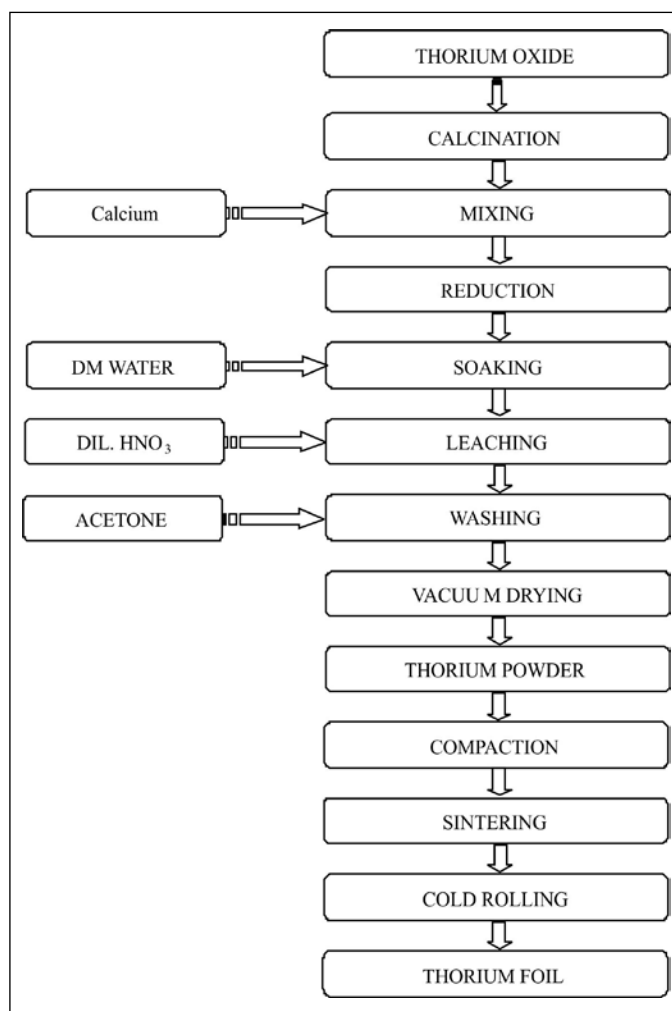
Fig 1: Flow-sheet for the production of thorium metal foil

Fig 2: Calcination of thorium oxide powder

Fig 4: Loading of reactants into reduction retort

Fig 3: Mixing of thorium oxide powder and calcium

about 20% over the stoichiometric requirement to ensure complete reduction. The weighing, mixing and charging into reaction containers are carried out under inert atmosphere.

Mixed reactants are then charged into heat resistant steel (310 grade) containers. The containers are lined from inside with molybdenum in order to prevent the eutectic reaction between thorium and iron. These containers are further loaded in a heat resistant steel (310 grade) retort for reduction (Fig. 4). The reduction is carried out in the temperature range of 950 - 1000°C for 2 hrs. in a protective atmosphere of flowing argon. Reacted mass comprises of thorium metal powder particles embedded in calcium oxide slag and excess calcium.

The reduced mass is taken out of reduction furnace and soaked in cold demineralised water and allowed to

disintegrate statically. After soaking for sufficient time for complete disintegration, supernatant liquor containing the fines, which are of lower purity, is decanted and the fines are recovered separately. The powder is subsequently leached with dilute nitric (Fig. 5).
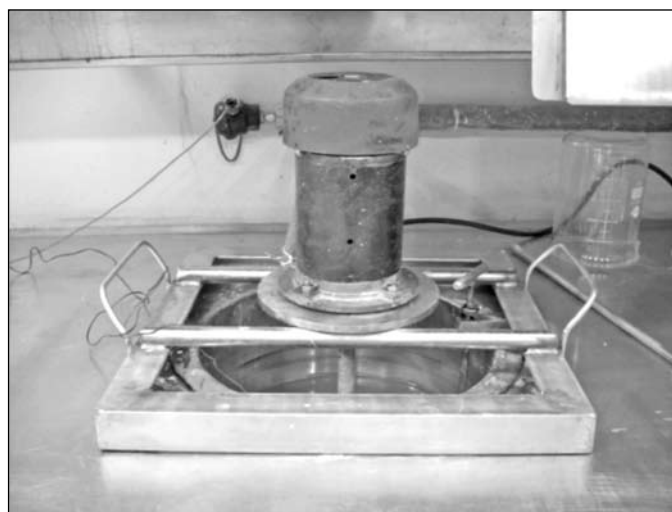
Fig 5: Leaching operation in SS tank

The leaching is continued until the supernatant liquor is neutral. During leaching, temperature is maintained at ~10°C to prevent oxidation of thorium powder. The metal powder is then washed with cold demineralised water several times followed with acetone washing and subsequently the powder is vacuum dried (Fig. 6). Resulting thorium powder is highly pyrophoric on account of finer particle size; hence requires handling in an inert atmosphere.

Fig 6: (a) Wet thorium powder and (b) Thorium powder after vacuum drying

Fig 7: Hydraulically operated compaction press

3.2 Consolidation and fabrication for the production of foil

Consolidation of thorium by conventional methods of melting and casting is difficult because of its high melting point (1755°C) and its high reactivity in molten condition with almost all the crucible materials. Hence, powder metallurgy techniques have been adopted for fabrication of thorium shapes. Thorium metal powder produced by calico-thermic reduction of oxide is compacted in hydraulically operated compaction press at 5 t/cm² pressure to obtain green compact (Fig. 7).

The green compact is then sintered at 1350°C under vacuum of 1×10^{-5} Torr for 2 hrs. in sintering furnace (Fig. 8). Sintered thorium metal (Fig. 9) has sufficient ductility to be cold rolled to produce sheets and foils on account of face centered cubic crystal structure. Hence the sintered thorium metal was cold rolled in a 2-high rolling mill (Fig. 9) to produce foils having thickness in the range of 0.4 to
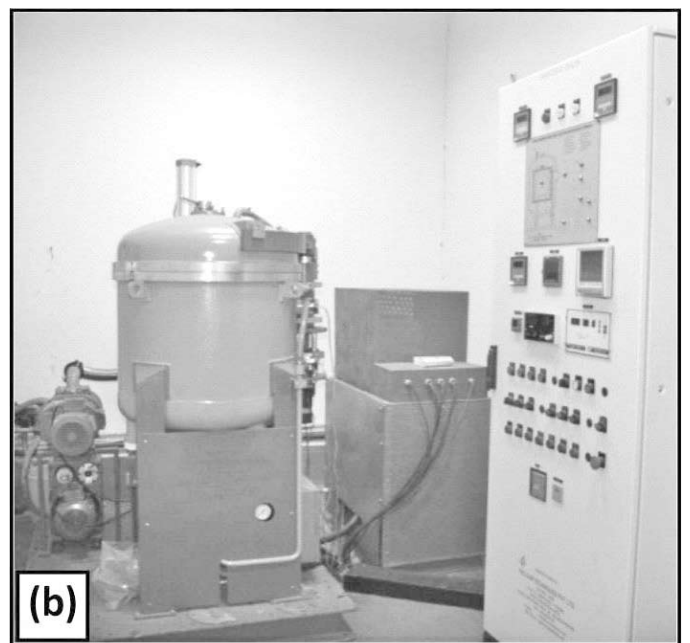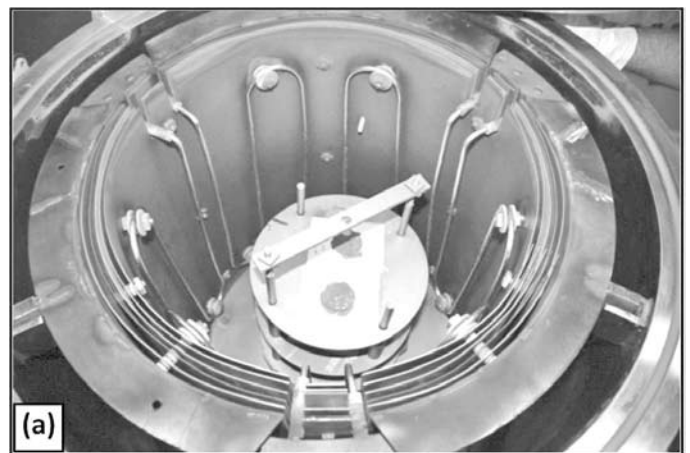
Fig 8: High temperature high vacuum sintering furnace (a) Inside view and (b) Outside view

Fig 9: Sintered metal for rolling in 2-high rolling mill
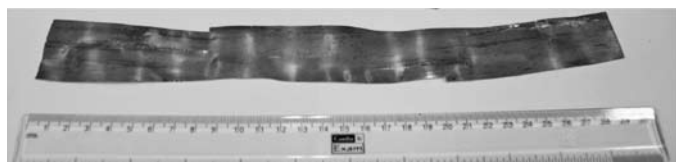
Fig 10: Thorium metal foil

0.8 mm (Fig. 10). The foils thus produced were supplied to various divisions within BARC for further studies.

5. Conclusion

Thorium metal foil of thickness varying from 0.4 mm to 0.8 mm of acceptable quality was produced by calico-thermic reduction of the oxide, compaction sintering and cold rolling.

Acknowledgements

References

1. B. Prakash, S. K. Kantan, and N. K. Rao, Metallurgy of Thorium Production, *IAEA,* (1962)*Vienna.*

2. N. Furhman, R. B. Holden, and C. I. Whitman, *J. Electrochem. Soc.,*, 107(1960)127.

3. K. R. Gurumurthy, S. V. Paibhale, S. P. Singh, and R. V. Raghavan, Fabrication of Thorium Shapes by Powder Metallurgy Techniques, *Transactions of the PMAI*, 3, (1976).

Mr M.T. Saify is B.E. (Metallurgy & Materials Science). After joining Bhabha Atomic Research Centre in the year 2002, he has been working in the field of development and fabrication of metallic fuels for nuclear research reactors and fast breeder reactors.

Mr S.K. Jha is B. Tech. (Metallurgy Engg.). After joining Bhabha Atomic Research Centre in the year 1986, he has been working in the field of development and fabrication of fuels for compact light water reactor and metallic fuels for nuclear research and fast breeder reactors. Presently Mr Jha is Head, Special Fuel Development Section, AFD, BARC.

Mr K.K. Abdulla is BSc Engg. (Mechanical Engg.). After joining Bhabha Atomic Research Centre in the year 1978, he has been working in the field of quality assurance for fabrication of components and equipments. Currently, he is associated with development and fabrication of fuels for compact light water reactor, metallic fuels for nuclear research and fast breeder reactors and fabrication of CICC superconductors. Presently Mr Abdulla is Head, Atomic Fuels Division, BARC.

Fabrication of Thoria Based Fuels – An Overview

N. Kumar, R. V. Pai and S. K. Mukerjee

Fuel Chemistry Division
Bhabha Atomic Research Centre, Mumbai - 400 085
E-mail: smukerji@barc.gov.in

Presently, India occupies an important place among the Asian nations in the indigenous design, development, construction, and operation of nuclear power reactors. Nuclear power generation in India is based on a three-stage plan to eventually make use of the abundant national resources of thorium. To achieve this long-range goal, India started with the setting up of heavy water moderated, natural uranium-fueled Pressurised Heavy Water Reactors (PHWR) in the first phase to produce plutonium, required for the subsequent stages, from fertile ^{238}U. The second stage of the power program commenced with the setting up of Fast Breeder Test Reactor (FBTR) at Indira Gandhi Centre for Atomic Research (IGCAR), Kalpakkam, which uses plutonium-uranium carbide as fuel. In the fast breeder reactor thorium is used as a blanket, which yields another fissile material ^{233}U. In the third stage, the ^{233}U thus produced, would be used along with fertile ^{232}Th as fuel in Thermal/fast Breeder Reactor. India is already in the process of developing the technology to utilise its abundant resources of thorium along with the ^{233}U produced, as a nuclear fuel, in order to sustain the Indian Nuclear power program for many centuries[1].

The development of a successful nuclear fuel is one of the important requirements for any nuclear power program. Nuclear fuel could be broadly classified as metallic fuel and ceramic fuel. Ceramic fuel can be an oxide, carbide or nitride. The most commercially used power reactor fuel is oxide fuel. India, has mastered the technology of fabricating ceramic oxide fuels for all its power reactors.

1. Fuels for Nuclear Reactor

The preparation of oxide fuel involves the conversion of metal nitrate solutions to its oxide. The oxide powder thus formed is converted to oxide pellets of desired dimension and density by powder metallurgical routes. In India, this route is used both for fabrication of natural and low-enriched uranium oxide fuels [2]. However, with the increasing demand of electricity at an affordable cost and depleting resources of uranium, introduction of thorium in the fuel cycle has been essential. The large scale utilization of thorium requires adoption of closed fuel cycle scheme. Although, many of the fuel cycle technologies developed for uranium can be readily adopted for thorium, the man-rem problem associated with these fuels is a major concern.

Therefore, fuel fabricators in recent past have initiated new R&D programmes to solve this problem either through elimination of powder handling or making the unit operations of the production process amenable to remote handling and automation. During the last 4 decades, several countries have manufactured thorium based oxide fuels. The following techniques have been developed so far for manufacturing thorium based fuels:

1. **Powder-pellet route:** Preparation of high density fuel pellets using ThO_2, UO_2, and PuO_2 powders as starting materials; the fuel pellet stacks are encapsulated in cladding tubes.

2. **Sphere-pac route:** Preparation of fuel microspheres using nitrate solutions of uranium, plutonium and thorium or their mixtures as starting materials and adapting ammonia external gelation or ammonia internal gelation process for obtaining hydrated gel microspheres. The microspheres are sintered and vibro packed in cladding tubes followed by encapsulation.

3. **Coated particles fuel for HTGR**: Sol-gel derived, high density, fuel microspheres are subjected to multi layer coating of pyrolytic carbon and silicon carbide, popularly known as TRISO and BISO particles, which are embedded in graphite matrix.

4. **Sol-gel microsphere pelletisation (SGMP):** Soft sol-gel derived fuel microspheres which are free flowing are used for direct pelletisation and sintering.

5. **Coated Agglomerate Pelletisation(CAP):** ThO_2 powder is converted to free flowing agglomerate by extrusion spherodisation which are then coated with uranium oxide powder, calcined, pellatised and sintered to obtain dense $(Th,U)O_2$ pellets, which are encapsulated in a cladding tube.

6. **Impregnation technique**: where (a) partially sintered ThO_2 pellets of relatively low density (≤75% theoretical density) or (b) porous ThO_2 microspheres are vacuum impregnated in uranyl nitrate (U as ^{233}U) or Pu–nitrate solution followed by calcinations, pelletisation and sintering to form high density ThO_2 based mixed oxide fuel pellets, which are encapsulated in cladding tubes.

7. **Molten salt fuel**: The fuel material is in the form of the fluoride salt AcF_4 (actinide fluoride) dissolved in a

molten salt carrier whose composition is a mixture of ^{7}LiF and ^{9}BeF$_2$. The molten salt flows over the outside of a close-packed set of high-purity graphite blocks serving both as fuel and heat transfer material.

1.1 Powder-pellet route

The ceramic nuclear fuels such as ThO$_2$, UO$_2$ and PuO$_2$ are generally fabricated as cylindrical pellets by powder metallurgy technique, and sintered in reducing atmosphere at around 1700°C. Thoria powder derived from the oxalate process has been used in major ThO$_2$-based fuel production campaigns. The oxalate derived ThO$_2$ powder has a flat, square platelet morphology, which requires pre-milling for making it sinter active. The flow sheet for the preparation mixed uranium thorium oxide by powder pellet route is given in Fig. 1. Since ThO$_2$ has a very high melting point (~3350°C), the sintering has to be carried out at temperatures higher than 1800°C to obtain high-density pellets. However, with small addition of sintering aids like Nb$_2$O$_5$, high-density ThO$_2$ pellets could be obtained by sintering in air at temperature as low as 1150°C [3]. Small addition of divalent metal oxide, like CaO and MgO, also enhances the diffusion of Th^{+4} by creating anion vacancies [4]. Studies showed that addition of around 2% U$_3$O$_8$ enhances the densification of ThO$_2$ and results into high density pellets (96% T.D.) by sintering in air even at 1100°C [5]. This has paved the way for manufacturing high density (Th,U)O$_2$ pellets without the addition of dopants like CaO, MgO or Nb$_2$O$_5$. The key step in the production of the above mixed oxide fuels, is the preparation of homogeneous oxide mixtures. However, a special feature of ^{232}Th–^{233}U fuel cycle is the high gamma dose associated the daughter products of ^{232}U, which is always associated with ^{233}U and the high specific radioactivity of ^{233}U. Hence, handling of ^{233}U bearing materials require remote and automated operation in hot cells or shielded glove boxes. The process flowsheets for fabrication of ^{233}U or Pu bearing fuels should preferably be dust-free and amenable to remotisation and automation. The powder pellet route is suitable for fabrication of high-density fuel pellets but has the disadvantage of radiotoxic dust hazard as it involves handling of fine fuel particles. Further, fine powders have poor flowability, which makes automation and remote fabrication difficult. Therefore, alternate fabrication routes that are more amenable to remote controlled operations and automation procedures are being considered for the fabrication of fuels containing highly radioactive materials, like ^{233}U.

1.2 Sphere-pac route

Sol-gel derived ThO$_2$ and (Th,U)O$_2$ microspheres have been prepared in the past [6] for manufacturing fuel
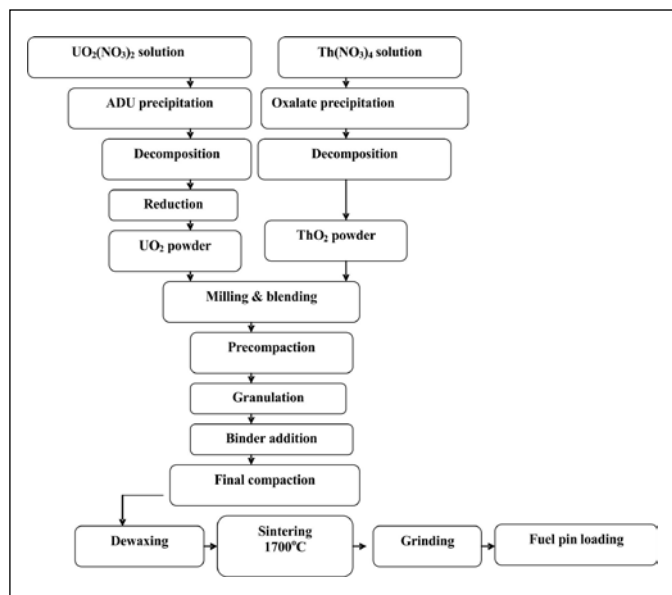
Fig. 1 Process flow-sheet for the fabrication of (Th,U)O$_2$ Pellets by powder pellet route

microspheres of controlled density for Sphere-pac fuel pins, where usually high density fuel microspheres of two or three size fractions (typically 1000 μm, 100 μm and 10 μm) are vibro compacted in fuel cladding tube to obtain fuel pins of controlled smear density. This route is highly suitable for remotisation and automation but has the limitation of maximum achievable smeared density of only 90%T.D., which makes it less attractive for use as water cooled reactor fuel. For the preparation of carbide and nitride fuel microspheres, the sol-gel process is modified for obtaining microspheres containing an intimate mixture of oxide/mixed oxide and carbon. These microspheres are subjected to carbothermic synthesis in vacuum or high purity flowing argon/nitrogen atmosphere to obtain high density carbide or nitride microspheres.The sol dehydration process was developed at ORNL, USA. Apart from (U,Pu)O$_2$ production, the process was also demonstrated for the production of ThO$_2$, UO$_2$, and (U,Th)O$_2$ microspheres. The sol-gel microspheres of the mixed oxide were prepared from mixed thorium nitrate and uranium nitrate solution by steam pyrolysis in a batch de-nitrator. The ORNL sol-gel process based on dehydration reaction was replaced by the more efficient 'ammonia gelation' processes, developed in Europe in the 1970s, which cause rapid gelation of droplets of sols or solutions of the nitrates of U, Th or Pu either externally by ammonia gas and ammonium hydroxide or internally by an added ammonia generator such as hexamethylenetetraamine (HMTA). Table-1 summarizes the popular sol-gel routes utilized for preparation of ThO$_2$ and ThO$_2$-based mixed oxide microspheres [7].

Table-1. Principal sol gel routes for the preparation of hydrated gel microspheres of oxides of U, Th and Pu

Process	Materials prepared	Laboratory/country
External gelation	ThO_2, UO_2 and $(Th,U)O_2$	NUKEM, FRG
External gelation of thorium (EGT)	ThO_2 and $(Th,U)O_2$	KFA, FRG
Internal gelation	ThO_2 and $(Th,U)O_2$	KFA, FRG
Internal gelation	ThO_2 and $(Th,U)O_2$	BARC, India

1.2.1 Ammonia external gelation process

At KFA, Germany, a solution-based process called external gelation (KFA) process was developed for ThO_2 and UO_2 microspheres. The external gelation of thorium (EGT) [8] has several advantages over the other sol-gel processes. The EGT process utilizes simple and reliable equipment and a few chemicals like ammonia and ammonium hydroxide, which are not flammable and have high radiolytical stability. The EGT process takes full advantage of the gelation features and sol-gel chemistry of $Th(OH)_4$, unlike other gelation processes, which use gel-supporting polymers or apply the buoyant force of an organic environment. The gel particles thus produced can be washed within a short time using small quantities of water that can be dried in minutes in a simple continuous manner. Fig. 2 shows the major steps of EGT process developed in Germany. First, the sol is prepared by controlled addition of gaseous ammonia through a hollow, rotating disperser shaft immersed in a jacketed and water heated glass vessel containing the nitrate solutions of thorium and uranium or plutonium. The solution is constantly monitored for pH and viscosity during the pre-neutralization step for preparing the ideal hydro-sol. An optimum sol has pH in the range of 3.25 to 3.50 and viscosity 3×10^{-2} Pa.s. Droplets of the sol are introduced through an electromechanical vibrator with a horizontal jetting nozzle inside a containment box that houses 2 horizontal ammonia gas pipes and the gelation bath. Thus, the droplets pass through a curtain of NH_3 gas and quickly coat themselves with a gel-skin before falling into the NH_4OH gelation bath. The gel microspheres containing NH_4NO_3 are washed with 1% NH_3 for removing ammonium nitrate. The washed microspheres are dried in humid air on a continuous belt drier at 200°C to obtain gel microspheres of excellent sphericity. The EGT process could be tailored to obtain oxide or mixed oxide microspheres of high density suitable for vibratory compaction in fuel cladding tubes. The only
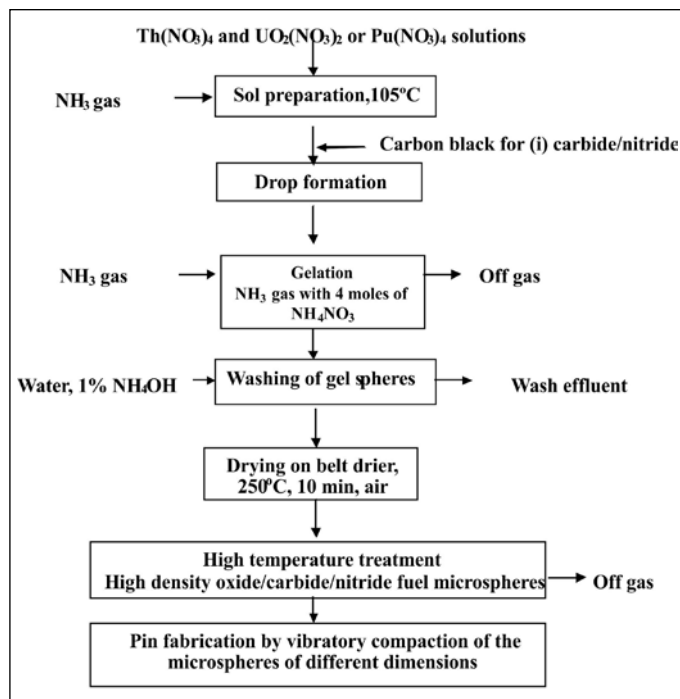
Fig. 2 Flowsheet based on KFA-EGT process of Germany for preparation of Th based oxide & non-oxide fuel microspheres for fabrication of pellet-pin, vipac pin

waste of the process is the wash water containing NH_4NO_3, which could either be completely decomposed into the gases NO_x, N_2O, N_2 and H_2O or reconverted to ammonia and nitric acid, which can be recycled. The EGT process was extensively utilized in Germany for manufacturing high density ThO_2 and $(Th, U)O_2$ microspheres in the diameter range of 400-500 micron for manufacturing coated fuel particles for the HTGRs in Germany, namely AVR and THTR. However, without changes of process and equipment, microspheres in the diameter range of 100-800 micron could be easily produced.

1.2.2 Ammonia internal gelation process

The ammonia internal gelation process was first reported by KEMA Laboratories, Netherlands for preparation of UO_2 microspheres. The KEMA internal gelation process [9] was modified in India for preparation of ThO_2 and $(Th,U)O_2$ microspheres. The internal gelation process is based on the hydrolysis of hexa methylenetetraamine [HMTA: $(CH_2)_6N_4$], which releases ammonia rapidly at temperature above 90°C. The nitrate solutions of thorium and uranium or plutonium are mixed with HMTA at around 0°C and urea to form the feed solution. Droplets of the feed solution are gelled into spherical particles by contacting them with hot silicon oil above 90°C, which is an inert and immiscible medium. The ammonia released from HMTA cause the precipitation of

the metal ion into a hydrated oxide gel. The properties of the gel depend on the composition of the feed solution, the temperature of the gelation medium and the contact time of the droplet with gelation medium. Extensive work has been carried out in BARC [10] to study the gelation behaviour of partially denitrated thorium nitrate solution with HMTA and urea on the basis of which a gelation field diagram has been developed, which outlines regions of opaque gel formation that yield good quality ThO_2 and $(Th,U)O_2$ microspheres containing up to 10 mole% uranium. Unlike that of UO_2, good quality ThO_2 and ThO_2-based microspheres can be obtained in very narrow region with precise control of the composition of feed solution. The stream of the feed solution was forced through a stainless steel capillary at a constant flow rate and broken into droplets of uniform size with the use of electromagnetic vibrator. The droplets gelled in a few seconds and were collected at the belt separator. The gelled product was first washed several times with carbon tetrachloride to remove silicone oil and then with 2-3 M NH_4OH solution to remove any unreacted HMTA and urea as well as ammonium nitrate formed during gelation. The washed gel particles were dried in air oven and heated to 1250–1650°C to form spherical microspheres in the diameter range of 100-400 micron. However, the major disadvantages of the process are: (i) the narrow range of stable feed solution composition that would yield good quality microspheres, (ii) the use of more number of chemicals and inflammable organic materials and (iii) excessive washing cycles and waste generation. Lab scale studies have indicated the possibility of recovery and recycle [11].

1.2.3 Vibratory compaction

Sphere-pac fuel pins of Zircaloy clad $(Th,^{233}U)O_2$, containing 3% $^{233}UO_2$, have first been successfully manufactured on a pilot plant scale in USA, in the 1960s, in the unshielded glove-box facility of Babcock and Wilcox (B&W) Company, and the shielded Kilorod set-up of Oak Ridge National Laboratory (ORNL) [12, 13]. In the B&W facility, the fuel is deactivated by removing the first daughter product of ^{232}U i.e., ^{228}Th and is then re-fabricated rapidly before the increase in the ^{232}U daughters and the associated gamma activity. The maximum ^{232}U content in the unshielded facility of B&W was 42 ppm. A total of 192 fuel rods of 10 feet length were vibratory compacted in the glove box line. The Kilorod facility has been designed for semi remote operations with the capability of handling of ^{233}U containing up to 200 ppm ^{232}U and with frequent decontamination up to 600 ppm ^{232}U. In all, some 980 kg of $(Th,^{233}U)O_2$ microspheres have been vibratory compacted into 1100 clad fuel pins in the smear density of 88–91%T.D. Based on the successful experience of the Kilorod facility,

two remote fabrication facilities for handling highly radioactive ^{233}U–bearing material, namely Thorium Uranium Recycle Facility (TURF) at ORNL and Programma Ciclo Uranio Torio (PCUT) at CNEN, Italy were set-up but not utilized because of the change in programme [14]. In FRG, as part of the heavy water moderated thorium breeder reactor programme, a few 'vi-pac' $(Th, U)O_2$ fuel containing HEU with 93% ^{235}U were fabricated in the 1960s for irradiation-testing experiments [15].

1.3 Coated fuel particles for HTGR

The higher melting point of thorium oxide and di-carbide as compared to their uranium counterparts, make thorium-based ceramic coated fuel particles in graphite matrix, an ideal choice of fuel for HTGRs, where the objective is to have a high coolant outlet temperature (750–900°C) and more particularly high fuel surface temperature (900–1100°C) and a compact core. R&D and manufacturing of coated fuel particles for HTGRs are underway for more than three decades in several countries. The core of an HTGR essentially consist of tiny, multilayer coated fuel particles, popularly known as TRISO, of ThO_2, $(Th,U)O_2$, ThC_2 or $(Th,U)C_2$ dispersed in graphite matrix and shaped in different forms depending on the design. Two major directions for the fuel element designs have emerged, namely the German spherical fuel element design pursued in Germany, Russia and China and the block type US design that have been utilized in USA and Japan. In the German design, kernels of ~500 µm of 'fissile' and 'fertile' materials, surrounded by layers of carbon buffer (~95 µm), inner pyrocarbon (40 µm), silicon carbide (35 µm) and finally outer pyrocarbon (~40 µm) as shown in Fig. 3(a), are homogeneously distributed in graphite matrix and shaped in the form of fuel element balls of diameter 60 mm with a 5 mm fuel free zone in the outer shell [16]. In HTGRs, the coated layers confine fission products released from the 'fissile' or 'fertile' kernels. The pyrolytic carbon (PyC) layers essentially retain Kr and Xe, whereas the silicon carbide layer is effective in retaining solid fission products. The disadvantage of high brittleness of SiC is overcome by embedding in dense PyC coatings, for which these particles are called TRISO. Earlier, the 'fissile' and 'fertile' kernels were coated with only PyC and were known as BISO particles. The reference fuel sphere contains approximately 11000 TRISO coated 'fissile' particles. The active core of the German THTR reactor consists of 360000 such spherical fuel elements. The modular HTGR of Russian Federation and China are also Pebble-Bed type reactors containing spherical fuel elements like the German HTGR. The US fuel element [Fig. 3(b)] is a hexagonal graphite block, 793 mm in length and 360 mm width across the flat surface contain some 102 coolant channels of diameter 15.9 mm and 210 fuel holes, which are filled with TRISO fuel compacts

of diameter 12 mm and sealed. The Japanese design [Fig. 3(c)] consists of block-type fuel, similar to the 'pin-inblock' design of the Dragon HTGR fuel of UK. Manufacturing of HTGR fuel element is carried out in 3 steps, namely preparation of 'fertile' (ThO$_2$ or ThC$_2$) and 'fissile' [(Th,U)O$_2$ or (Th, U)C$_2$] containing LEU or ^{233}U] kernels, multilayer coating to form TRISO particles and fabrication of fuel elements in the form of spherical balls or prismatic blocks. The spherical fuel kernels are prepared by 'ammonia external or internal gelation' process starting with nitrate solution of thorium and uranium followed by reduction at 900°C and sintering at 1500°C to form high density fuel microspheres. For preparation of the carbide fuel particles, carbon-black is added to the sol prior to gelation and the hydrated sol containing a homogenous mixture of oxide and carbon particles are subjected to reaction sintering at ~1400–1500°C. The coating is carried out in fluidized bed reactor using different hydrocarbon gas and methyl trichlorosilane (MTS: CH$_3$SiCl$_3$). The buffer layer is coated in the temperature range 1100–1400°C using a mixture of argon and acetylene (C$_2$H$_2$ + Ar). The inner pyrolytic

carbon layer is coated at 1370-1470°C using a mixture of Ar + C$_3$H$_6$. The SiC layer is coated at 1500–1570°C using methyl trichlorosilane (MTS: CH$_3$SiCl$_3$), a source for Si and C. Argon and hydrogen are used as the carrier gas along with MTS for the SiC coating. In recent years, ZrC coating is preferred for higher burnup in place of SiC. The process parameter for the outer pyrolytic carbon (PyC) layer is the same as that of inner PyC layer.

The coated fuel particles are embedded in carbon matrix and graphite shim. The carbon matrix consisting of 47% petroleum pitch, 38% filler, 10% octadecanol and 5% polystyrene is injected into a mould at 160°C. On cooling, the compact solidifies after which it is carbonized at 900°C to decompose organic compounds and to obtain a solid carbon contact. Thereafter, the compacts are heated at 1650°C for stabilization. The spherical fuel element is formed in a rubber mould, under quasi-isostatic pressing condition with pre-pressing pressure of 30 MPa and final forming pressure of 300 MPa. The spherical fuel elements thus formed is first carbonized at ~800°C and later heat treated at 1950°C.
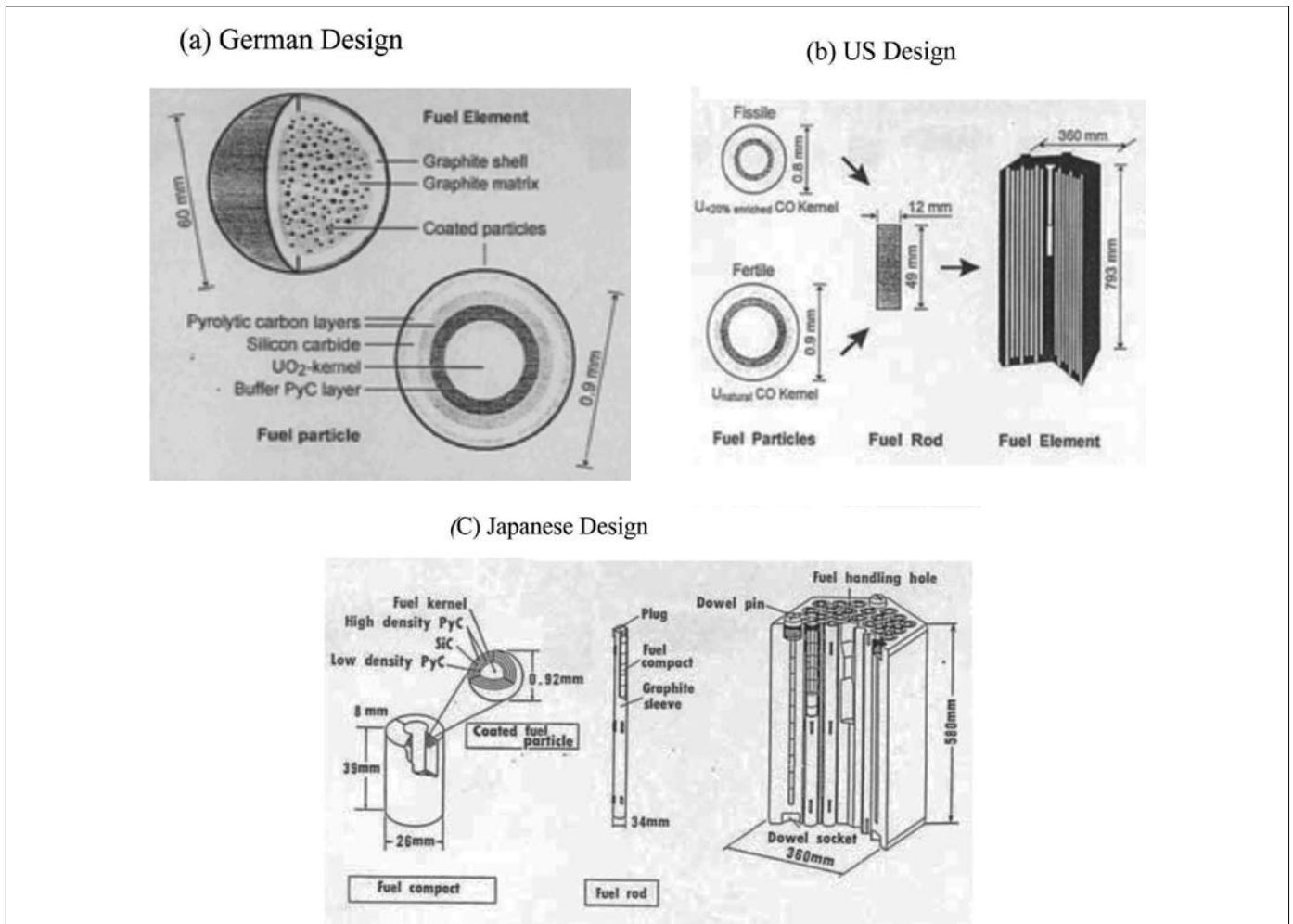
Fig. 3(a-c) Reference design of coated fuel particles and fuel elements for high temperature gas cooled reactors

1.4 Sol-Gel Microsphere Pelletisation technique

Sol-gel microsphere pelletisation (SGMP) is a novel concept for fabrication of oxide and non oxide ceramic nuclear fuel pellets of controlled density and microstructure by using sol-gel derived dust-free and free flowing fuel microspheres, rather than fine powder derived granules, for compaction of fuel pellets and sintering. The advantages of SGMP process are as follows:

(i) Radiotoxic dusts and aerosols are not produced and process losses are minimized;

(ii) Dust free and free flowing nature of microspheres facilitate remote and automated fuel fabrication inside shielded glove boxes or hot cells;

(iii) High microhomogeneity in case of mixed oxide, carbide and nitride fuels since nitrate solutions of Th, U and Pu are mixed and used as starting materials;

(iv) Possibility of controlled density and tailored microstructure of fuel pellets; and

(v) The process is ideal for manufacturing highly radiotoxic thorium-based and [233]U and Pu bearing fuel pellets for nuclear power reactors.

The SGMP process has been successfully developed initially in Germany and later in India (Fig. 4) for manufacturing high density ThO_2, $(Th,U)O_2$ and $(Th,Ce)O_2$ (Ce for simulating Pu) pellets containing uniform distribution of closed spherical pores in the ideal diameter range of 2–5 micron. The EGT process of Germany was modified for obtaining dust free and free flowing 'porous' ThO_2–based oxide and mixed oxide microspheres, which could be easily pelletised by cold compaction and sintered to high density pellets. For this, the following three major modifications have been made [17]:

(i) Preparation of mixed thorium uranium nitrate or mixed thorium plutonium nitrate solutions of relatively low molarity (1-1.2 M).
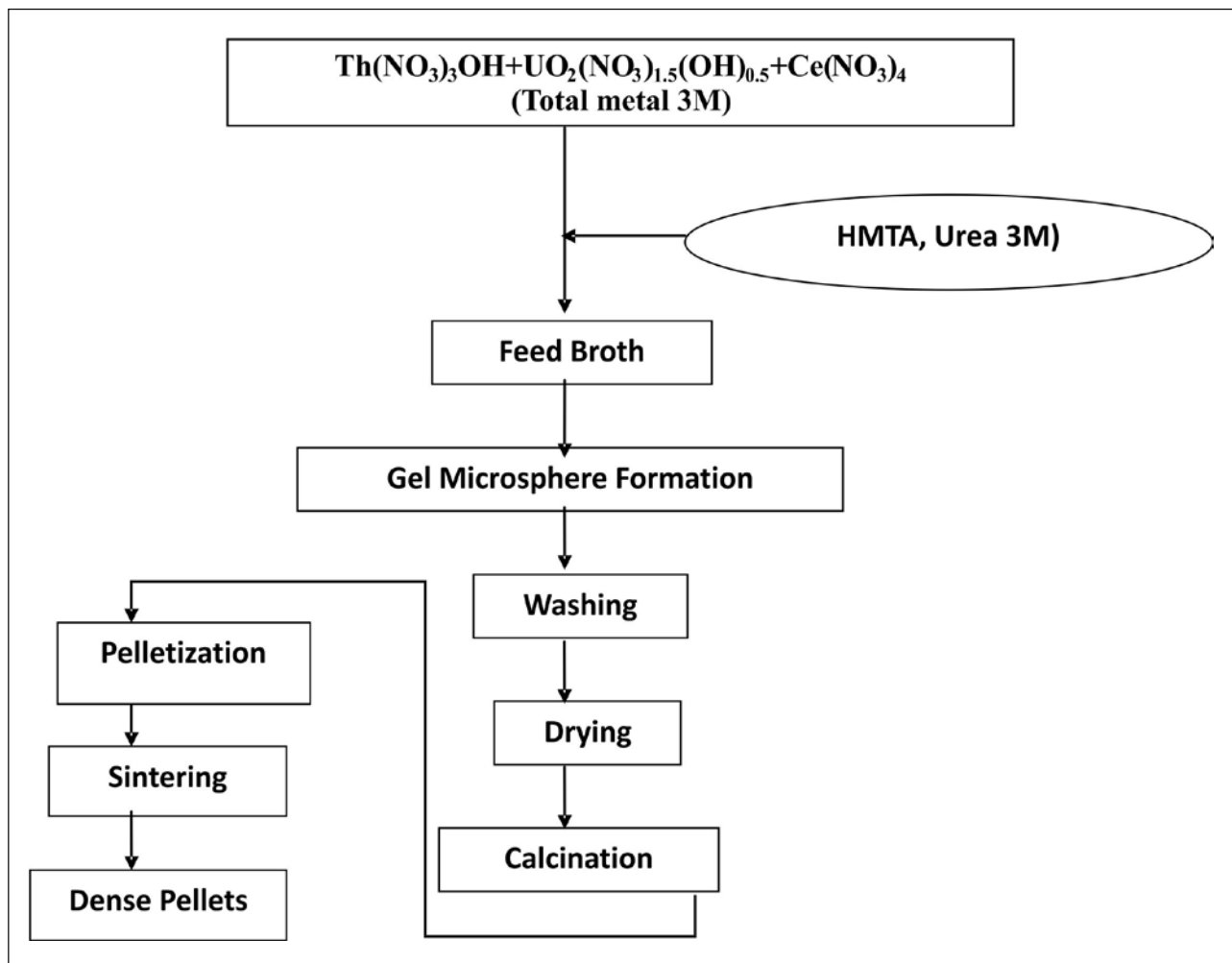
Fig. 4 Flow-sheet for the fabrication of ThO_2, $(Th,U)O_2$ and $(Th,Ce)O_2$ pellets by SGMP route

(ii) Addition of 'carbon black' pore former to the 'sol' prior to gelation and later removing carbon by controlled air calcinations at 700°C to obtain 'porous microspheres' The porous microspheres have very low crushing strength and lose their individual identity during pelletisation and also facilitate uniform pore size, shape and distribution in sintered pellets.

(iii) Addition of around 1wt% $Ca(NO_3)_2.6H_2O$ to the heavy nitrate feed solution to obtain 0.4% CaO.

In BARC, an internal gelation process has been developed for obtaining soft $(Th,U)O_2$ microspheres without any addition of carbon as pore formers which can be readily pelletised and sintered in to high density pellets [18].

1.5 Coated Particle Agglomerate Pelletisation

The coated agglomerate pelletization (CAP) process was developed by Bhabha Atomic Research Centre (BARC) to replace the conventional powder metallurgy process that consists of direct blending of $^{233}UO_2$ and ThO_2 powders [19, 20]. The radiation exposure problems can be minimized by quick processing of ^{233}U into finished fuel, as the first decay of ^{232}U has a comparatively longer half-life compared to the remaining daughter products. This technique is being developed to fabricate the fuel for the forthcoming Indian Advanced Heavy Water Reactor (AHWR). In this process, a wide option is possible for the ThO_2 starting material.

ThO_2 should be in the form of free flowing agglomerate which can be obtained either by pre-compaction and granulation technique or by extrusion of powders. The ThO_2 microspheres obtained by sol–gel technique can also be used in the CAP process. To make free flowing agglomerates in the extrusion route, the ThO_2 powder is mixed with an organic binder and extruded through perforated rollers. The CAP process is schematically shown in Fig. 5. The extruded ThO_2 paste is converted to agglomerates in a spherodiser. The agglomerates are sieved and subsequently dried to remove the organic binder. As only ThO_2 is handled up to this stage, all these operations are carried out in a normal alpha tight glove-box facility. The operations carried out under shielding are (a) coating of ThO_2 agglomerates with desired amount of ^{233}U oxide, (b) compaction in a multi-station rotary press into green pellets, (c) sintering in air and (d) pellet loading and encapsulation into fuel rods.

Despite these advantages, the CAP route has certain disadvantages such as sticking of U_3O_8 powder during coating to processing equipments and glove boxes, non-uniform microstructure and inhomogeneous uranium concentration in thoria matrix [21].

1.6 Impregnation technique

The impregnation technique is an attractive alternative for manufacturing highly radiotoxic ^{233}U or Pu –bearing
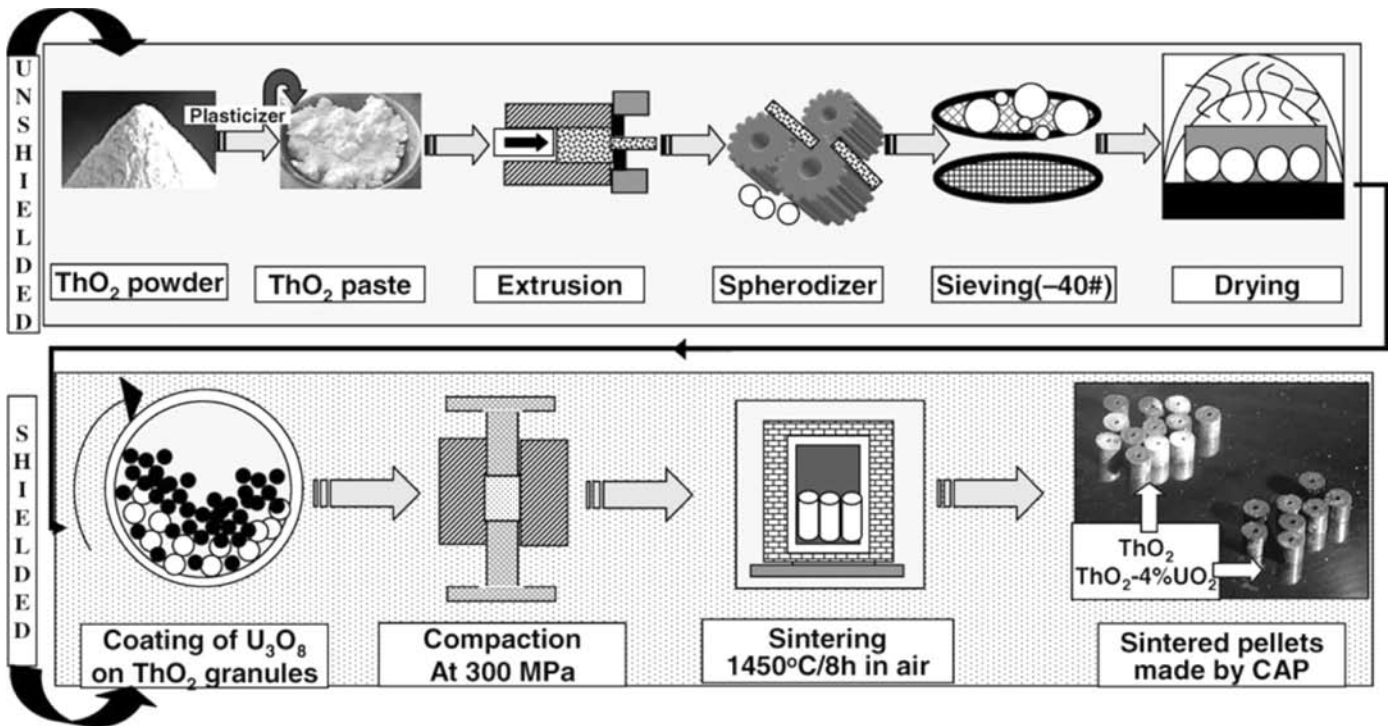
Fig. 5 Schematic diagram of the CAP process for the fabrication of (Th,^{233}U)O$_2$ pellets.

thoria based mixed oxide fuel pellets, remotely in a hot cell or shielded glove-box facility, taking advantage of the chemical inertness of ThO_2. In this process, the relatively less radioactive natural ThO_2 is first prepared in an unshielded area in the form of 'low density pellets' (≤80%T.D.) with 'open porosity' or sol-gel derived 'porous microspheres'. The ThO_2 pellets or microspheres thus prepared are impregnated in uranyl nitrate ([233]U) or plutonium nitrate solution of molarity in the range of 1 to 3, in a shielded facility, followed by sintering in case of the pellets or cold pelletisation followed by sintering in case of the microspheres to obtain ThO_2–based mixed oxide pellets of high density and excellent microhomogeneity, particularly when the impregnation was carried out in nitrate solutions of low molarity (0.5 to 1.0). The solid solution between ThO_2 and UO_2 or PuO_2 is formed during the sintering step. Thus, fine [233]U or Pu bearing powders are avoided and handling of these materials is restricted only in certain parts of the fuel fabrication plants. Process steps like precipitation of ammonium di uranate or plutonium oxalate, calcination, mixing, grinding, granulation, etc., which are associated with 'radiotoxic dust hazard', are eliminated. Use of microwave during impregnation for local heating of the partially sintered low density ThO_2 pellets or 'porous microspheres' facilitates expulsion of entrapped gas and impregnation operation. Annular ThO_2 pellets are suitable for enhancing the impregnation operation, leading to uniform distribution of [233]U of Pu in sintered pellets. With 'pellet impregnation' technique, it was possible to prepare high density (Th, U)O_2 pellets containing up to 2.5% U and with microsphere impregnation, it was possible to produce (Th,U)O_2 containing up to 20% U.

1.6.1 Pellet impregnation

The impregnation technique developed at Bhabha Atomic Research Centre (BARC) relies on the action of capillary forces to draw the solution into the pores of the host material. The amount of the second material introduced into the pellet can be controlled by adjusting the concentration of the infiltrant solution. It is important that many of the porosities are interconnected and distributed uniformly across the pellet otherwise the impregnation will not be effective. Use of microwave during impregnation for local heating of the partially sintered low density pellets has been tested for expulsion of entrapped gas to accelerate impregnation. For uniform distribution of actinide in the sintered pellets, annular pellets are more suitable than the conventional ones. The concentration of the added material can be increased by multiple impregnation or by the use of the solution containing higher concentration of the material. The flow-sheet of fabrication of ThO_2–4% UO_2 pellets by impregnation process is given in Fig. 6. The

U loading in ThO_2 pellet can be varied by controlling the following parameters:

(a) Density of the pre-sintered ThO_2 pellets.

(b) Concentration of uranyl nitrate solution.

(c) Duration of impregnation.

The density of the host pellets (ThO_2) is optimized by choosing the proper pre-sintering temperature. For attaining up to higher (4% U) loading with 1.5 M uranyl nitrate solution, multiple impregnation is necessary. Final sintered density of these pellets was in the range of 93-96%T.D.

1.6.2 Microsphere Impregnation

In a variation of pellet impregnation process, the ThO_2 gel microspheres/ agglomerates can also be used for impregnation instead of low-density pellets. It is seen that gel/agglomerate impregnation permits more uniform and higher concentration of U loading resulting in more homogeneous ThO_2-UO_2 pellets. The microsphere impregnation technique has been developed in FCD, BARC, based on sol-gel microsphere pelletisation technique, in which the (Th,U)O_2 microspheres containing 3-4 mole% of natural U were prepared by microsphere impregnation technique which uses porous thoria microspheres prepared by internal gelation process for impregnation of uranium [22]. This process requires minimum manual handling and radiation shielding especially if fresh thorium is used. The principal steps involved for the preparation of high density pellets are:

Preparation of porous ThO_2 microspheres:

– Conversion of feed droplets into solid gel spheres (gelation).

– Washing of gel spheres, heat treatment of the gel spheres to obtain calcined ThO_2 microspheres.

Impregnation of Uranyl nitrate solution:

– Impregnation of uranyl nitrate solution into calcined ThO_2 microspheres under vacuum.

– Heat treatment of uranium impregnated ThO_2 microspheres for decomposition of uranyl nitrate to uranium oxide.

– Pelletization and sintering to obtain high density (Th,U)O_2 pellets.

(i) The loading of uranium in the ThO_2 microspheres depends on the morphology of the microspheres, i.e., pore size, shape, volume and their inter connectivity

(ii) Extent of evacuation and degassing achieved before impregnation.

(iii) Time of impregnation.

(iv) Concentration of uranyl nitrate solution used.

The preparation of natural ThO_2 microspheres and its characterization which is the major step could be carried out outside shielding facility and vacuum impregnation of uranyl nitrate solution into these microspheres, pelletisation and sintering in air atmosphere would be carried out in a shielding facility. The green pellets prepared from these microspheres could be sintered in air up to ~96% of T.D by heating at 1350^oC for duration of 4h.

1.6.3 Impregnated Agglomerate Pelletisation (IAP)

Impregnated Agglomerate Pelletization (IAP) technique was developed at Advanced Fuel Fabrication Facility (AFFF), Bhabha Atomic Research Centre (BARC), which uses uranyl nitrate solution for coating instead of UO_2 powder used in CAP route [23]. In the IAP route, spheroids obtained through extrusion route were spray coated with uranyl nitrate solution instead of dipping. Use of uranyl nitrate solution for coating showed improvement

Fig.6 The flow-sheet of fabrication of ThO_2–4% UO_2 pellet by impregnation process

in microstructure and homogeneity of fuel pellets as compared to the CAP route in which coating was made with U_3O_8 powder. The use of CAP route for fabrication of $(Th,^{233}U)O_2$ mixed oxide fuel results in sticking of powder to processing equipments and glove boxes. This trouble is avoided in the IAP route which reduces man-rem further as compared to the CAP route. As received ThO_2 powder was milled in attritor at 200 rpm for 40 min using high chromium steel ball so as to break its platelet morphology. The milled ThO_2 powder was converted into free flowing spheroids by extrusion. The extrusion route involves mixing of milled ThO_2 powder with organic binder (polyethylene glycol), lubricant (oleic acid) and water in an appropriate proportion (1:1:8 wt.%) with the help of planetary mixer. The ThO_2 paste obtained was extruded through the perforated rollers. ThO_2 extrudes so obtained were dried by heating in an oven at $70–100^oC$ for 1 h to achieve sufficient handling strength for spherodization. The dried extrudes were converted into the spheroids with the help of spherodiser. The spheroids obtained from spherodiser were sieved to remove the fines. All the above operations were carried out in normal alpha tight glove box facility, since only ThO_2 was handled up to the sieving stage. The following operations were carried out in the shielded facility:

(a) Spray coating of ThO_2 spheroids with uranyl nitrate solution and drying of coated spheroids.

(b) Compaction of coated spheroids.

(c) Sintering in air and reducing atmosphere (N_2 + $7\%H_2$).

(d) Pellet loading and encapsulation into fuel rods.

1.7 Molten Salt Reactor Fuel

These reactors are still at the design stage but will be very well suited for using thorium as a fuel. The unique fluid fuel incorporates thorium and uranium (U-233 and/or U-235) fluorides [24] as part of a salt mixture that melts in the range $400-600^oC$, and this liquid serves as both heat transfer fluid and the matrix for the fissioning fuel. The fluid circulates through a core region and then through a chemical processing circuit that removes various fission products (poisons) and/or the valuable U-233. Certain MSR designs will be designed specifically for thorium fuels to produce useful amounts of U-233 eventually leading to the self-sustaining use of thorium as an energy source. The Oak Ridge National Laboratory (USA) designed and built a thorium-based demonstration MSR using U-233 as the main fissile driver. The reactor ran over 1965-69 and operated at powers up to 7.4 MWt. The lithium-beryllium-thorium salt worked at $600-700^oC$ and ambient
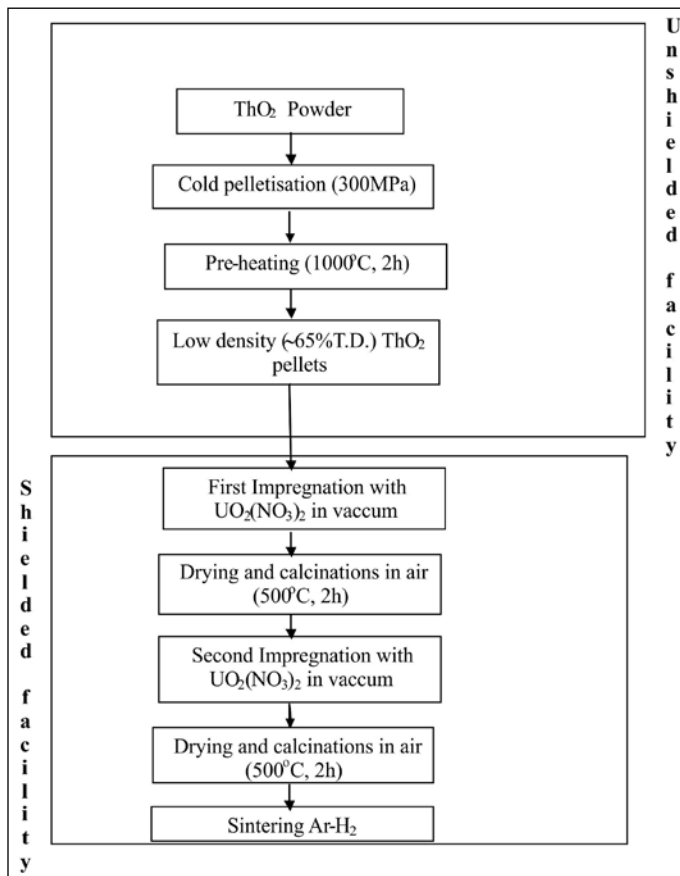
pressure. The R&D program demonstrated the feasibility of this system and highlighted some unique corrosion and operational issues that need to be addressed if constructing a larger pilot MSR. There is significant renewed interest in developing thorium-fuelled MSRs. Projects is underway in China, Japan, Russia, France and the USA. It is notable that the MSR is one of the six 'Generation IV' reactor designs selected as worthy of further development (see information page on Generation IV Nuclear Reactors). The thorium-fuelled MSR variant is sometimes referred to at the Liquid Fluoride Thorium Reactor (LFTR).

References

1. V. N. Vaidya and D. D. Sood, Presented at the Indo-Japanese Seminar on Thorium Fuels, BARC, Bombay, 86, (1990).

2. N. K. Rao, H. C. Katiyar, R. Rajendran, B. P. Pande, J. B. Patro and K.V.A.Chandramouli, IAEA/SM-233/33, (1979).

3. P. Balakrishna, B. P. Varma, T. S. Krishnan, T. R. R. Mohan and P. Ramakrishnan, *J. Nucl. Mater.*, 160 (1988) 88.

4. P. E. Hart, C. W. Griffin, K. A. Hsieh, R. B. Mathews and G. D. White PNL 3064, UC-78, Pacific Northwest Laboratory, Richland, Washington 99352 (1979).

5. P. V. Hegde, T. R. G. Kutty, S. Majumdar and H. S. Kamath Presented at the Int. Conf., 2002, Hyderabad, Allied Publishers, New Delhi, India (2003).

6. R. L. Beatty, R.E. Norman and K.L. Notz, ORNL-5469, 1979.

7. IAEA-TECDOC-412, IAEA, Vienna (1987) 27.

8. H. D. Ringel and E. Zimmer, *Nucl. Technol*. 45 (1979) 287.

9. J. B. W. Kanij, A. J. Noothout and O. Votocik, IAEA-161, IAEA, Vienna (1974).

10. N. Kumar, R. K. Sharma, V. R. Ganatra, S. K. Mukerjee, V. N. Vaidya and D.D. Sood, *Nucl. Technol*. 96 (1991) 169.

11. A. Kumar, T. V. Vittal Rao, S. K. Mukerjee and V. N. Vaidya, *J. Nucl. Mater.*, 350 (2006) 254.

12. G. Schileo (Proc. 2nd Intl. Symp., Gatlinburg, Tennessee, 1966), Edited by R.G.Wymer, US Atomic Energy Commission (1968) 299.

13. R. E. Brooksbank, J. P. Nichols and A.L. Lotis, ibid (1968) 321.

14. G. Orsenigo and S. Cambi, Presented at the 2nd Internatl. Thorium Fuel Cycle Symposium, Gatlinburg, Tennessee, USA, May 3-6, 1966, (Ed.) by WYMER, R.G., Published by US Atomic Energy Commission (1968) 547.

15. Thorium Utilisation in PWRs, Final Report (1979-1988), German- Brazilian Co-operation, Kernforschungsanlage, Juelich, Germany (1988).

16. IAEA-TECDOC-978, IAEA,Vienna (1997) 106.

17. C. Ganguly, H, Langen, E. Zimmer and E. Merz *Nucl. Technol*.73 (1986) 84.

18. R. V. Pai, S. K. Mukerjee, V. N. Vaidya, *J. Nucl. Mater.*, 325 (2004) 159.

19. T. R. G. Kutty, K. B. Khan, P. S. Somayajulu, A. K. Sengupta, J. P. Panakkal, Arun Kumar, H. S. Kamath, *J. Nucl. Mater.*, 373 (2008) 299.

20. T. R. G. Kutty, R. V. Kulkarni, P. Sengupta, K. B. Khan, K. Bhanumurthy, A. K. Sengupta, J. P. Panakkal, A. Kumar, H. S. Kamath, *J. Nucl. Mater.,* 373 (2008) 309.

21. T. R. G. Kutty, P. S. Somayajulu, K. B. Khan, A. Kumar, H. S. Kamath, *J. Nucl. Mater.*, 384 (2009) 303.

22. R. V. Pai, J. V. Dehadraya, Shovit Bhattacharya, S. K. Gupta, S. K. Mukerjee, *J. Nucl. Mater.,* 381 (2008) 249.

23. P. M. Khot, Y. G. Nehete, A. K. Fulzele, C. Baghra, A. K. Mishra, Mohd. Afzal, J.P. Panakkal, H.S. Kamath, *J. Nucl. Mater.*, 420 (2012) 1.

24. ORNL report- 4812, August, (1972) 65.

Dr. N.Kumar joined BARC in 1981 after graduating from Poona University in 1980. He obtained his Ph.D. from University of Mumbai in 2006. Since his joining, he has been actively involved with the development of sol-gel process for the fabrication of ceramic nuclear fuels of ThO2, UO2, mixed (U,Pu)O2 etc. He has set up a sol-gel demonstration facility for the preparation of (Th,U)O2 microspheres on a 1 kg/day scale and also engaged in development of sol gel microsphere pelletization (SGMP) process for the fabrication of AHWR fuel at a laboratory scale. Presently he is working on the preparation of 500 μm size, high density UO2 microspheres for studies related to coated particle fuel development program of the department.

Shri Rajesh V. Pai joined Fuel Chemistry Division, BARC after graduating from the 40th batch of Training School in the year 1997 after completing his M.Sc. (Applied Chemistry) from Cochin University of Science & Technology. He is mainly associated with the development of sol-gel process for nuclear materials and high technology ceramics. He has developed many flow sheets suitable for fabrication of thoria-urania and urania-plutonia based fuels by sol-gel process. He also gained experience in synthesis and characterization of nano-size powders of mixed oxides by various techniques. His current area of interest is development of coated fuel kernels suitable for Compact High Temperature Reactor.

Dr. S.K. Mukerjee joined Bhabha Atomic Research centre in year 1981 through BARC training school. Since then, he is working in the field of fabrication of ceramic nuclear fuels using sol-gel method in the form of microspheres. He has developed flow sheets for sol-gel preparation of various U, Pu oxides, carbides and for thoria based oxides. His current area of interest is fabrication of thorium carbide, (U,Pu)O2 microspheres having 50mole% Pu microspheres (700μm) for the fabrication of vipac test fuel pin for irradiation in FBTR. He is also working for the preparation of 500 micron UO2 microspheres having different surface morphology for the carbon/SiC coating studies, fabrication of porous thoria microspheres for uranyl nitrate impregnation studies & development of microwave gelation column and modification of the process for the fabrication of Lithium titanate pebbles to improve the utilisation of Li in ITER blanket.

Studies on the preparation and properties of thoria and urania-thoria

S. Anthonysamy and P. R. Vasudeva Rao

Chemistry Group
Indira Gandhi Centre for Atomic Energy, Kalpakkam 603102
E-mail: sas@igcar.gov.in

1. Introduction

India has vast reserves of thorium as monazite yet to be utilized. Utilization of thorium can reduce uranium consumption and diversify the nuclear energy resources for a long term nuclear energy programme. High-density thoria pellets are used in pressurized heavy water reactors for flux flattening and in the blankets of fast breeder reactors. The chemical inertness and high melting point (3573 K) of thoria make it suitable for applications in other industries as well. Most of these applications require the use of thorium oxide bodies with a sintered density better than 96% theoretical density (TD). Homogeneous solid solutions containing uranium and thorium oxides with U/(U+ Th) < 0.3 are being developed as fuels for thermal breeder reactors and advanced gas-cooled reactors.

High-density compacts of thoria and their solid solutions with urania are commercially produced by powder metallurgical methods which are energy intensive processes. In addition, radioactive dust is generated during the preparation of these ceramics through the powder metallurgical route, which are hazardous to the operating personnel. Hence, attempts have been made at IGCAR to develop advanced techniques of synthesis which are energy-efficient and can be cost-effective for the production of these nuclear ceramics. Key to the success of the development of such methods is to initially prepare, through chemical methods, nanocrystalline sinteractive press feed that could be cold compacted and sintered to high density at relatively low temperatures. Advanced methods such as microwave-assisted combustion synthesis, co-precipitation, de-agglomeration and de-agglomeration-cum-doping techniques have been extensively studied at our centre for the synthesis of nanocrystalline, surface active powders of thoria and urania-thoria. Optimization of process parameters through extensive characterization of the powders obtained at various stages during the preparation process, with the help of various analytical and metallurgical characterization techniques was found to be the major step in the development of these advanced methods for the preparation nano-crystalline powders with enhanced surface activity. The feasibility of these advanced techniques was successfully demonstrated to prepare highly homogeneous powder feed that could be cold compacted without binder or lubricant and sintered to a high-density (≥ 96 % TD) at relatively low temperatures.

The physicochemical properties such as enthalpy, heat capacity, oxygen potential oxidation behaviour and thermal expansion of thoria and urania-thoria solid solutions are needed for reactor physics and safety calculations as well as to assess their behaviour at high temperatures during reactor operation. However, there is paucity of these data on thoria–urania mixed oxides. Hence the enthalpy increments of $(U,Th)O_2$ solid solutions were measured in the temperature range 473–973 K by using a drop calorimeter developed in our laboratory, with a view to generate more data on the thermal properties of these solid solutions. The oxygen potentials of $(U_y Th_{1-y})O_{2+x}$ solid solutions with y ranging from 0.54 to 0.90 were measured at 1073 and 1173 K, with a view to elucidate the behaviour of uranium rich solid solutions which in turn will help to understand the U-Th-O system completely. The kinetics of oxidation of urania-thoria solid solutions were examined by means of thermogravimetry. The mechanism of the oxidation process was determined from the analysis of thermogravimetric data. The kinetic parameters of the oxidation process were generated for the first time. The thermal expansion of $(U_{0.13}Th_{0.87})O_2$, $(U_{0.55}Th_{0.45})O_2$ and $(U_{0.91}Th_{0.09})O_2$ was measured over the temperature range from 298 to 1973 K.

Information on the binding energies of U $4f_{7/2}$ and Th $4f_{7/2}$ electrons of $(U_y Th_{1-y})O_2$ solid solutions is important to understand the chemical bonding in the solid solutions, which has a bearing on various physicochemical properties of the solid solutions. Hence, the binding energies of U $4f_{7/2}$ and Th $4f_{7/2}$ electrons of $(U_{0.13}Th_{0.87})O_2$, $(U_{0.55}Th_{0.45})O_2$ and $(U_{0.91}Th_{0.09})O_2$ were experimentally determined by X-ray photoelectron spectroscopy.

2. Synthesis of thoria

2.1 Modified precipitation technique

Studies on thorium oxalate precipitation and subsequent pyrolysis for the preparation of thorium dioxide have been extensively reported in the literature. However, the effect of the washing medium on the powder characteristics has not been studied. The effect of using a different wash

medium other than distilled water on the characteristics of the powder and the density of the compacts obtained from the powders has been studied at our Centre [1]. For this purpose, ethyl alcohol was used instead of distilled water as the wash medium.

The specific surface area of the thorium dioxide is not affected when ethyl alcohol is used instead of water as the washing medium. However, changing the washing medium influences the particle size distribution. The powders obtained by washing the thorium oxalate precipitate with ethanol and subsequently calcined had a smaller aggregate size than that obtained from water washed precipitate. Compacts made using powders obtained by using different wash liquids did not show any significant effect on the density of the compacts. However, the microstructures were different for the pellets obtained from powders prepared using different wash liquids. The compacts which were made using powder prepared by the calcination of the ethanol washed thorium oxalate powder at 1273 K or less, showed uniform grains. The granular structure indicated that the powders prepared from ethanol washed thorium oxalate were soft aggregates that could be crushed, compacted and sintered to high densities. However, sintering could be effected only at 1773 K or more to get 95 % TD.

2.2 Combustion synthesis

The feasibility of the combustion synthesis of thorium dioxide powder from aqueous thorium nitrate solution, using polyvinyl alcohol (PVA), urea and citric acid as fuels has been studied. In addition, the effect of using microwave energy to carry out the synthesis on the powder characteristics was also studied.

2.2.1 Combustion synthesis of thorium dioxide using PVA as fuel

The synthesis was carried out by heating a mixture of aqueous solutions of thorium nitrate and PVA in microwave oven. In order to study the role of PVA in the synthesis, aqueous solutions containing 0, 5, 8 and 10 % (w/v) PVA were mixed with (~ 1 M) aqueous solutions and heated [2]. Powders obtained by PVA aided denitration as well as direct denitration were nanocrystalline. The synthesis using PVA resulted in a porous mass which, on subsequent calcination at 873 K, resulted in a free flowing thorium dioxide powder. The specific surface area of the PVA aided denitrated powder was ~12m^2g^{-1} while that of direct denitrated powder was ~ 45 m^2g^{-1}. The synthesis was also carried out on hot plate for the purpose of comparison. The specific surface area of the hot plate denitrated powder was only ~7 m^2g^{-1}.

The density of the sintered compacts, prepared from powder obtained by the PVA aided denitration employing a microwave oven and sintered at 1573 K, was ~94% TD. The density of the pellets from the powder prepared by denitration in the absence of PVA was only ~85 % TD, and that for pellets from powder prepared by PVA aided denitration but employing hot plate heating was ~90%.

2.2.2 Combustion synthesis using urea or citric acid as fuel

In these experiments, the synthesis of thorium dioxide was carried out using either urea or citric acid as fuel. The effect of microwave heating on the powder characteristics and the density of the sintered compacts prepared from them have been studied. The synthesis reaction went to completion in the case of urea as fuel, irrespective of the mode of heating (whether it was microwave or hot plate heating). The synthesis using citric acid as fuel was completed only on heating using a hot plate and the as-prepared product itself was free flowing thorium dioxide powder. However, the as-prepared product of the synthesis employing microwave heating was a white mass which had to be calcined in a furnace. The calcined product was found to be crusty. The calcined powders obtained by using either urea or citric acid were nanocrystalline, with the size of the crystallites larger when urea was used (almost double the size of crystallites obtained using citric acid). The surface area of the powder obtained using urea was only ~1 m^2g^{-1}as compared to ~12 m^2g^{-1} for the powder obtained using citric acid [3].

The density of the sintered compacts prepared using citric acid as fuel and sintered at 1573 K was ~96% TD, while the pellets prepared from powder made using urea as fuel was only 90% dense. The microstructure of the surface of the pellet obtained using SEM showed large uniform grains, with porosity on the grain boundaries. The results of the synthesis, calcination and sintering studies are compared in the following Table 1.

Combustion synthesis, developed for the first time for thorium dioxide is a better alternative for the preparation of thorium dioxide powder. Among the fuels for the combustion synthesis, the use of urea seems to be least effective, since it results in a powder that can be sintered to a maximum of 90% TD even at 1773 K. PVA aided denitrated powder yielded pellets with 94% TD on sintering at as low a temperature as 1573 K, without any sintering aid. The powder obtained by PVA aided denitration was found to contain carbon in the form of filamentary structures (Fig.1). However, sintering in air was effective in bringing down the carbon content to within acceptable limits of 100 ppm.

Table 1. A comparison of the methods explored

Property	Oxalate	PVA	Urea	Citric acid
Surface area	~10 m²g⁻¹	~12 m²g⁻¹	~1 m²g⁻¹	~12 m²g⁻¹
Particle size	~8 μm	~0.7 μm	120 μm	~350 μm
Crystallite size	~25nm	~10 nm	~30 nm	~10 nm
C in calcined powder	1000 ppm	~1500 ppm	~500 ppm	~1000 ppm
C content in the sintered pellet	~50 ppm	~80 ppm	~50 ppm	~50 ppm
Sintered density (mg.m⁻³)	~9.5 (1773 K)	~9.4 (1573 K)	~9.0 (1773 K)	~9.6 (1573 K)
Microstructure	Uniform	Highly porous	Highly porous	Uniform
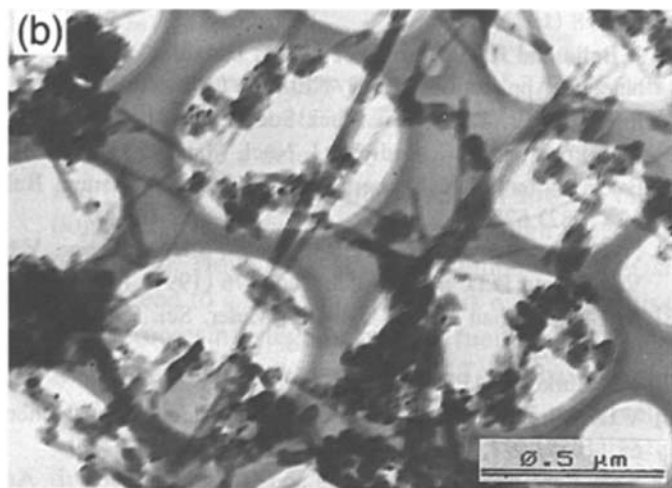
Fig. 1 CTEM image of PVA aided thoria

With citric acid as fuel, thorium dioxide powder press feed which can be sintered at 1573 K to 96 % TD can be prepared. Thorium citrate being transparent to microwaves could not be decomposed into thorium dioxide by microwave heating. However, initial evaporation of the aqueous solutions can be carried out using microwave heating. The decomposition can be carried out either on a hotplate or inside a conventional furnace. The powder obtained by combustion synthesis using citric acid as fuel on calcinations resulted in a free flowing powder that can be sintered to 96% of the theoretical density.

2.2.3 De-agglomeration of thorium oxalate – a method for the synthesis of sinteractive thoria

Thorium oxalate was obtained by precipitation in water and in non-aqueous solvents (methanol, ethanol, propan-2-ol and propan-2-one) and de-agglomerated by ultrasonication in both aqueous as well as non-aqueous (methanol, ethanol, propan-2-ol and propan-2-one) media. Sinteractive thoria (crystallite size 6–20 nm) was obtained from a thorium oxalate precursor that was de-

agglomerated by ultrasonication. It was demonstrated that ultrasonic de-agglomeration could be a useful method for obtaining sinteractive thoria. The dispersion medium did not influence the properties of thoria significantly. Thoria derived by this procedure could be sintered to a density of 97 % TD at a temperature as low as 1673 K. The de-agglomeration technique is simple and does not pose the problems associated with self-sustained, uncontrolled burning encountered in the methods based on the combustion synthesis. Thoria powder derived through the non- aqueous precipitation (methanol, ethanol, propan-2-ol and propan-2-one) was found to be nanocrystalline (2–5 nm) and did not exhibit desirable powder properties. The thoria powder derived through the precipitation in propan-2-ol, exhibited de-sintering when sintered beyond 1473 K [4-5].

2.2.4 Sintering of thoria employing sintering aids

Nanocrystalline powders of pure thoria as well as thoria doped with calcia and magnesia were synthesized by using the oxalate de-agglomertion method [6]. It was observed that the concentration of the dopant ion (Ca²⁺ and Mg²⁺) had a marginal influence on the bulk density and specific surface area while it did not affect the crystallite size of these powders. The residual carbon content was found to be of the same order in all the powders irrespective of the concentration of the dopant. The reduction in the triple line defects in the doped oxide powder suggests that the dopant species has a beneficial effect on the consolidation process even at temperatures far below the sintering temperature. The TEM investigations of these powders reaffirmed that the dopants were uniformly distributed into the host matrix. Thus, this method is a novel procedure for syntheisizing nanocrystalline thoria homogenously doped with cations of Group 2 elements at relatively low temperatures. The powders were irregular nanocrystallites agglomerated as cuboidal particles pseudomorphic with the oxalate precursor. These powders exhibited good compactibility

and yielded green compacts with a density as high as 50 % TD. A density as high as 98.8 % TD could be obtained by doping calcia into thoria and sintered at a temperature as low as 1673 K. This is so far the highest density reported in calcia doped thoria. Further, calcium doping was found to prevent de-sintering, a common behaviour observed with most nanocrystalline powders.

Studies were also carried out by doping the cations M^{5+} (M = V, Nb and Ta) in thoria through gel-combustion synthesis using citric acid as fuel. For the first time it was demonstrated that apart from niobia, even tantala and vanadia could bring about accelerated sintering in thoria if they are doped through a wet chemical route viz., the gel-combustion procedure. The maximum densities obtained by doping with vanadia (0.02 mol%), niobia (0.50 mol%) and tantala (0.50 mol%) were 9.8 Mgm^{-3} (1573 K), 9.68 Mgm^{-3} (1423 K) and 9.69 Mgm^{-3} (1623 K), respectively. It was also demonstrated, that the optimum concentration of the dopant required to cause accelerated sintering in thoria, when the doping is done through a wet chemical route, could be higher than the optimum concentration of the dopant required for conventional powder-metallurgical procedures. It was further demonstrated for the first time that doping of tantala and vanadia in thoria through a wet chemical route brings about significant acceleration of the sintering process. A more homogeneously doped oxide results when the doping is done through a wet chemical route. Thus, the gel-combustion synthesis is advantageous when the end use calls for a high degree of homogeneity of the distribution of the dopant in thoria [7].

2.3 Combustion synthesis of (U,Th)O$_2$ solid solutions

Studies on the combustion synthesis of the solid solutions of uranium and thorium dioxides containing the two oxides in various compositions were carried out using PVA as fuel. Microwave heating was employed for the synthesis. The as-prepared product of the combustion synthesis was solid solution of the two dioxides corresponding to the initial composition of the uranium and thorium in the aqueous solutions. Single-phase crystalline solid solutions were obtained irrespective of the uranium content in the initial aqueous solutions. The conventional calcination of the as-prepared product resulted in a second phase hexagonal α-U_3O_8 when the uranium oxide content in the solid solution was > 50 %. Uranium and its compounds couple effectively with microwave energy. This property was used for calcination and sintering of the products of the combustion synthesis of the (U,Th)O$_2$, with U/(U+Th) $\geq$0.5. The calcinations using microwave heating resulted in relatively phase pure solid solution. However, only when the sintering was carried out in a conventional furnace could compacts with ~93% TD be obtained [8].

The feasibility of the combustion synthesis using citric acid (CA) as the fuel was also studied in order to prepare a homogeneous mixture of uranium dioxide-thorium dioxide feed powder that could be cold compacted without binder or lubricant and sintered to a high density ($\geq$ 95% TD) at relatively low temperatures ($\leq$ 1573 K). High density ($\geq$ 95% TD) compacts of $(U_yTh_{1-y})O_2$ solid solutions with y $\leq$ 0.5 can be prepared by combustion/denitration of a mixture of aqueous uranyl nitrate, thorium nitrate and CA with a CA/NO_3^- ratio of 1.0 in a microwave oven, calcinations of the resultant powder in air at 973 K for 5 h followed by sintering the compacts at 1573 K in a flowing argon-2vol.% hydrogen gas mixture for 5 h. High-density ($\geq$ 95% TD) compacts of $(U_yTh_{1-y})O_2$ solid solutions with y > 0.5 can be prepared by the same procedure described above excepting the change in sintering temperature from 1573 K to 1773 K [9]. The microwave-processed powders yield compacts that can be sintered to relatively high densities compared to the hot plate-derived powders. CA is a better combustion fuel than PVA for the preparation of ThO_2 as well as $(U_yTh_{1-y})O_2$ solid solutions through the combustion route [10]. During the combustion/denitration process, a large amount of gaseous material is evolved and hence the combustion product is highly porous with fractured surfaces as shown in Fig. 2. The products obtained through the combustion route were found nanocrystalline, highly free flowing and porous powders that were found to be suitable as the feed material for making high density compacts.
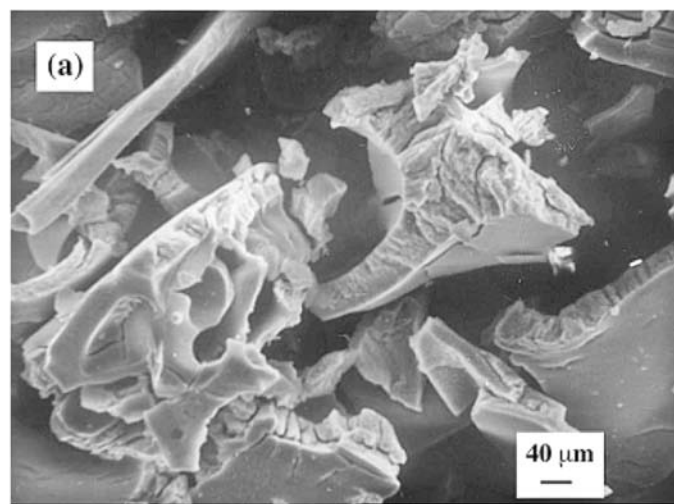

Fig. 2. SEM of micrograph of typical microwave-derived, calcined powder of $(U_{0.3}Th_{0.7})O_{2+x}$ showing fractured surfaces and pores

3. Physicochemical properties of urania-thoria solid solutions

3.1 Oxygen potentials of $(U_yTh_{1-y})O_{2+x}$ solid solutions

The oxygen potentials of $(U_yTh_{1-y})O_{2+x}$ solid solutions (y varying from 0.54 to 0.9) in the oxygen potential range -510 to -220 KJ mol^{-1} and $2.000 \leq O/M \leq 2.035$ at 1023 to 1173 K were measured for the first time to supplement the data already existing in the literature for $(U,Th)O_2$ solid solutions of other compositions [11]. The results are shown in Fig.3. The following systematic trends were observed:

a) The oxygen potentials of $(U_yTh_{1-y})O_{2+x}$ solid solutions increase with increasing temperature at a give O/M ratio and compostion of the solid solution.

b) The oxygen potentials decrease with increasing urania content of the solid solution at a given temperature and O/M ratio.

c) The results of the present measurements confirm that the oxygen potentials of $(U_yTh_{1-y})O_{2+x}$ solid solutions are a function of both the uranium valence and the U/(U+Th) ratio.

Partial molar enthalpies and entropies of solution of oxygen in the solid solutions with $y \geq 0.5$ and $x \leq 0.01$ were computed from the temperature dependence of the oxygen potentials. The partial molar enthalpies and entropies of oxygen for $(U_yTh_{1-y})O_{2+x}$ solid solutions with $y \geq 0.5$ and $x \leq 0.01$ were generated for the first time. The study indicated that the values of the partial molar enthalpies for $(U_yTh_{1-y})O_{2+x}$ solid solutions with $y \geq 0.5$ increasd with increasing oxygen content and urania content. However, the decrease in the partial molar entropy values with increasing oxygen content or thoria content was not significant.

The activity coefficients of urania in $(U_{0.54}Th_{0.46})O_{2+x}$, $(U_{0.77}Th_{0.23})O_{2+x}$ and $(U_{0.9}Th_{0.1})O_{2+x}$ solid solutions were also computed from the measured oxygen potential values. The results of the calculations indicated an increasing positive deviation from ideality with increasing oxygen content of the solid solutions. The equilibrium partial pressures of $UO_3(g)$, $UO(g)$, $ThO_2(g)$, $ThO(g)$ and O_2 over $(U_{0.54}Th_{0.46})O_{2+x}$, $(U_{0.77}Th_{0.23})O_{2+x}$ and $(U_{0.9}Th_{0.1})O_{2+x}$ solid solutions at 2000 and 2300 K were also computed [12].

3.2 Calorimetric studies on $(U_yTh_{1-y})O_2$ solid solutions

The enthalpy increments of $(U_yTh_{1-y})O_2$ solid solutions with y = 0.1, 0.5 and 0.9 were measured in the temperature range 473 to 973 K by using a drop calorimeter of isoperibol type [13]. A generalized expression for the enthalpy increments of $(U_yTh_{1-y})O_2$ solid solutions, as a function of both temperature and compositon, is given below:

$H^0_T - H^0_{298.15}$ (J mol^{-1}) = [$-13.2219 \times y^2 + 13.7481 \times y + 70.6804$] × T + [$0.01 \times y^2 - 0.0059 \times y + 0.004$] × T^2 + [$-0.647 \times 10^6 \times y^2 + 0.7467 \times 10^6 \times y + 1.0038 \times 10^6$] × (1/T) + [$0.5228 \times 10^4 \times y^2 - 0.6084 \times 10^4 \times y - 2.4791 \times 10^4$]

This expression is valid for y = 0 to 1 and T = 400 to 1000K.

The heat capacity of $(U_{0.1}Th_{0.9})O_2$, $(U_{0.5}Th_{0.5})O_2$ and $(U_{0.9}Th_{0.1})O_2$ solid solutions were derived from the measured enthalpy increments (Fig 4).

Cp (J mol^{-1} K^{-1}) = [$0.0199 \times y^2 - 0.0117 \times y + 0.0079$] × T + [$0.647 \times 10^6 \times y^2 - 0.7467 \times 10^6 \times y - 1.0038 \times 10^6$] × T^{-2} + [$-13.2219 \times y^2 + 13.7481 \times y + 70.6804$]

This expression is valid for y = 0 to 1 and T = 400 to 1000 K. A comparison of the measured enthalpy increments with the values computed by applying the molar additive rule of Neumann-kopp indicates that the
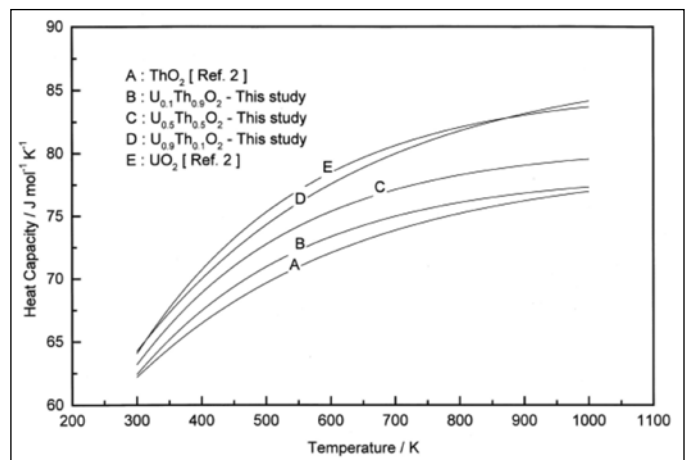

Fig. 3. Oxygen potentials of $(U,Th)O_2$ solid solutions

Fig. 4. Variation of heat capacities of $(U_{0.1}Th_{0.9})O_2$, $(U_{0.5}Th_{0.5})O_2$ and $(U_{0.9}Th_{0.1})O_2$ solid solutions with temperature.

measured enthalpy increments of $(U_{0.1}Th_{0.9})O_2$, $(U_{0.5}Th_{0.5})O_2$, and $(U_{0.9}Th_{0.1})O_2$ over the temperature range 473 to 973 K obey the Neumann-Kopp molar additive rule within the experimental uncertainty.

The enthalpy increment data of this study were used to compute other thermodynamic functions such as entropy and free energy function of the solid solutions at various temperatures.

3.3 Oxidation of urania-thoria solid solutions in air

The kinetics of oxidation of $(U_{0.15}Th_{0.85})O_2$, $(U_{0.30}Th_{0.70})O_2$ (low-urania solid solutions), $(U_{0.72}Th_{0.28})O_2$ and $(U_{0.77}Th_{0.23})O_2$ (high-urania solid solutions) powders was examined by means of thermogravimetry to determine the stability of these compounds in air [14]. The mechanism of the oxidation process was determined from the analysis of thermogravimetric data. The kinetic parameters of the oxidation process are reported for the first time. The oxidation was carried out under both isothermal as well as non-isothermal conditions. In general it is observed that the average O/M ratios of the oxidized $(U,Th)O_2$ solid solutions increase with increasing urania content in the mixed oxide. The oxidation of $(U_{0.15}Th_{0.85})O_2$ and $(U_{0.30}Th_{0.70})O_2$ occurred in a single step and the oxidized products were single-phase solid solutions with fluorite structure. The oxidation of $(U_{0.72}Th_{0.28})O_2$ and $(U_{0.77}Th_{0.23})O_2$ also occurred in a single step and the oxidized product in each case was a biphasic mixture containing cubic MO_{2+x} fluorite phase (M = U + Th) and orthorhombic U_3O_8 phase. The kinetics of oxidation of $(U,Th)O_2$ powder was found to be controlled by random nucleation mechanism (F1 mechanism). The activation energies derived from both isothermal kinetics and non-isothermal kinetics were found to be in reasonable agreement with each other and this confirms the correctness of the mechanism deduced form this study for the oxidation of $(U,Th)O_2$ solid solutions in air.

3.4 Studies on thermal expansion and XPS of urania-thoria solid solutions

Thermal expansion of polycrystalline $(U_{0.13}Th_{0.87})O_2$, $(U_{0.55}Th_{0.45})O_2$ and $(U_{0.91}Th_{0.09})O_2$ was measured over the temperature range 298 to 1973 K, by means of X-ray diffraction technique [15]. The percentage linear thermal expansions were evaluated from the temperature variation of lattice parameter in the range 298 to 1973 K (Fig.5).

A generalized equation for the percentage linear thermal expansions of $(U_yTh_{1-y})O_2$ solid solutions as a function of both temperature and composition of the solid solutions is given below:
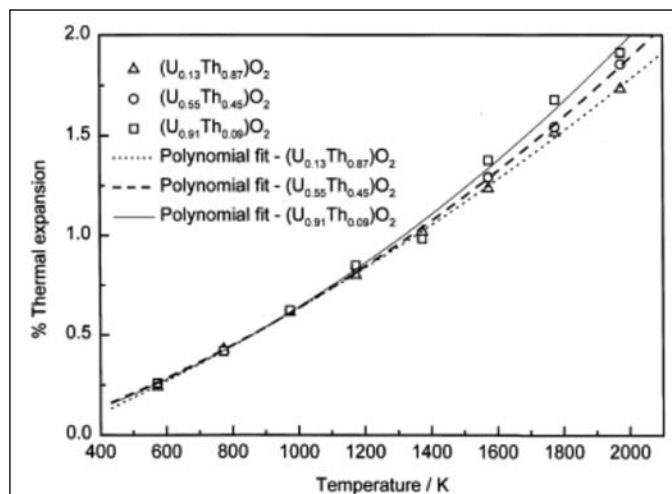
Fig. 5 The percentage linear thermal expansions of $(U,Th)O_2$ solid solutions

% Expansion = $[0.3671 \times 10^{-3} \times y^2 - 0.6948 \times 10^{-3} \times y + 0.7250 \times 10^{-3}] \times T + [-0.1106 \times 10^{-6} \times y^2 + 0.3070 \times 10^{-6} \times y + 0.1299 \times 10^{-6}] \times T^2 + [-0.2442 \times y^2 + 0.3835 \times y - 0.2204]$

It is observed that the linear thermal expansion of urania, thoria and urania-thoria solid solutions are almost identical up to 1200 K. Above 1200 K, the linear thermal expansion of urania-thoria solid solutions lie between values for pure urania and thoria.

A generalized equation for the instantaneous linear thermal expansion coefficients (α) of $(U_yTh_{1-y})O_2$ solid solutions as a function of both temperature and composition of the solid solutions is given below:

$\alpha = [-0.012 \times 10^{-8} \times y^2 + 0.3148 \times 10^{-8} \times y + 0.2484 \times 10^{-8}] \times T + [0.0795 \times 10^{-5} \times y^2 - 0.2823 \times 10^{-5} \times y + 0.7401 \times 10^{-5}]$

A generalized equation for the temperature dependence of the coefficient of average linear thermal expansion ($\dot{\alpha}$) of $(U_yTh_{1-y})O_2$ solid solutions as a function of both temperature and composition of the solid solutions is given below:

$\dot{\alpha} = [-0.006 \times 10^{-8} \times y^2 + 0.1574 \times 10^{-8} \times y + 0.1242 \times 10^{-8}] \times T + [0.0777 \times 10^{-5} \times y^2 - 0.2354 \times 10^{-5} \times y + 0.7771 \times 10^{-5}]$

The values of the average linear thermal expansion coefficients for $(U_{0.13}Th_{0.87})O_2$, $(U_{0.55}Th_{0.45})O_2$ and $(U_{0.91}Th_{0.09})O_2$ are 10.33×10^{-6}/K, 10.83×10^{-6}/K and 11.45×10^{-6}/K, respectively.

A comparison of percentage linear thermal expansion measured in this study with those calculated by applying the equations for linear thermal expansion of pure urania and thoria indicates that stoichiometric $(U,Th)O_2$ solid solutions are almost ideal atleast up to 2000 K.

3.5 Binding energies

The binding energies of U $4f_{7/2}$ and Th $4f_{7/2}$ electrons of $(U_{0.1} Th_{0.9})O_2$, $(U_{0.25} Th_{0.75})O_2$, $(U_{0.50} Th_{0.50})O_2$, $(U_{0.75} Th_{0.25})O_2$ and $(U_{0.90} Th_{0.10})O_2$ were experimentally determined by X-ray photoelectron spectroscopy. The study showed the presence of only U^{4+} and Th^{4+} chemical states in the stoichiometric urania-thoria solid solutions as identified from binding energy (379.9 eV for U $4f_{7/2}$ and 334.0 eV Th $4f_{7/2}$) and satellite peak positions [15].

4. Conclusion

Advanced methods such as microwave-assisted combustion synthesis, co-precipitation, de-agglomeration and de-agglomeration-cum-doping techniques have been developed for the synthesis of nanocrystalline, surface active powders of thoria and urania-thoria. These powders could be cold compacted and sintered to high densities at relatively low temperatures. The physicochemical properties of urania-thoria solid solutions relevant for the understanding of the system U-Th-O have been generated.

Acknowledgement

The authors sincerely acknowledge the contributions from Dr. V. Chandramouli and Dr. K. Ananthasivan in developing advanced methods for the synthesis of nanocrystalline thoria and urania-thoria solid solutions.

References

1. Study of the feasibility of the combustion synthesis for the preparation of thorium dioxide V. Chandramouli, Ph.D Thesis, University of Madras, May 1999

2. V. Chandramouli, S. Anthonysamy, P.R. Vasudeva Rao, R. Diwakar, D. Sundararaman *J. Nucl. Mater.,* 231(1996)213.

3. V. Chandramouli**,** S. Anthonysamy, P.R. Vasudeva Rao *J. Nucl. Mater.,* 265(1999)255.

4. K. Ananthasivan, S. Anthonysamy and P.R. Vasudeva Rao, *J. Nucl. Mater.,* 306(2002) 1.

5. K. Ananthasivan, S. Anthonysamy, V. Chandramouli, I. Kaliappan and P.R. Vasudeva Rao, *Trans. Powder Metallurgy Association of India* 26 (1999) 104.

6. K. Ananthasivan, S. Balakrishnan, S. Anthonysamy, R. Diwakar, E. Mohandas and V. Ganesan *J. Nucl. Mater.*, 434 (2013) 223.

7. K. Ananthasivan, S. Anthonysamy, C. Sudha, A.L.E. Terrance and P.R. Vasudeva Rao, *J. Nucl. Mater.,* 300 (2002) 217.

8. V. Chandramouli, S. Anthonysamy, P.R. Vasudeva Rao, R. Diwakar and D. Sundararaman *J. Nucl. Mater.,* 254 (1998) 55.

9. S. Anthonysamy, K. Ananthasivan, V. Chandramouli, I. Kaliappan and P.R. Vasudeva Rao *J. Nucl. Mater.,* 278 (1999) 346.

10. S. Anthonysamy, K. Ananthasivan, V.Chandramouli, I. Kaliappan and P.R. Vasudeva Rao *Tans. Powder Metallurgy Association of India* 26 (2000) 47.

11. S. Anthonysamy, K. Nagarajan, P.R. Vasudeva Rao *J. Nucl. Mater.,* 247 (1997) 273.

12. Studies on the preparation and some solid state properties of the solid solutions of urania and thoria S. Anthonysamy, Ph.D Thesis, University of Madras, April 2000.

13. S. Anthonysamy, Jose Joseph, P.R. Vasudeva Rao *J. Alloys and Compounds* 299 (2000) 112.

14. S. Anthonysamy, K. Joseph, T. Gnanasekaran, P.R. Vasudeva Rao *J. Nucl. Mater.,* 280 (2000) 25.

15. S. Anthonysamy, G. Panneerselvam, S. Bera, S.V. Narasimhan, P.R. Vasudeva Rao *J. Nucl. Mater.,* 281 (2000) 15.

Dr. S. Anthonysamy *is currently Head, Materials Processing Chemistry Section, Chemistry Group and Project Engineer, Demonstration Facility for Metallic Fuel Fabrication (DFMF). He obtained his M.Sc degree in Physical Chemistry from University of Madras, M.Sc (Engg.) from Indian Institute of Science and Ph.D from University of Madras. He is a professor at the Homi Bhabha National Institute (HBNI). He joined IGCAR in 1983 after completing one-year orientation course from BARC training school. His Research areas include studies on the preparation and thermochemical properties of nuclear fuel materials and control / shielding materials.*

Dr. P.R.Vasudeva Rao *is currently the Director of Indira Gandhi Centre for Atomic Research (IGCAR) and General Services Organization and also Director of Chemistry Group, IGCAR at Kalpakkam. He obtained his PhD Degree from Bombay University in 1979. He shifted to IGCAR in 1978 and was instrumental in setting up of the Radiochemistry Laboratory. He is a senior professor at the Homi Bhabha National Institute (HBNI). He has nearly 250 publications in peer reviewed international journals. His interests include actinide separations, development of advanced fuel cycles for fast reactors, chemical education and science history*

Thorium-based Metallic Alloys as Nuclear Fuels: Present Status, Potential Advantages and Challenges

D. Jain, V. Sudarsan and A. K. Tyagi*

Chemistry Division
Bhabha Atomic Research Centre, Mumbai – 400085
**E-mail: aktyagi@barc.gov.in*

1. Introduction

Use of thorium for extracting its nuclear energy has been envisaged since the very early developments in nuclear technology in India. The main reasons, for which thorium; which as such is a fertile element, has been given significant importance and is considered to play an important role in ensuring the long-term sustained supply of nuclear energy are the following. (i) It is naturally more abundant (nearly thrice) than uranium and widely distributed in easily extractable forms. (ii) Structural, physical, chemical, thermal and thermophysical properties of thorium-based fuels are superior than those based on uranium and/or plutonium (iii) ^{232}Th and ^{233}U have attractive fertile and fissile characteristics (nuclear properties), respectively (^{233}U is formed upon neutron capture by ^{232}Th followed by two successive beta decays inside a nuclear reactor). (iv) Irrespective of their chemical state, thorium-based nuclear fuels are inherently safe and non-proliferative., etc.

However, in order to realize the practically achievable and economically viable extraction of energy from thorium, it is required to initially sustain the fission chain reaction, until a self-sufficient inventory of ^{233}U is bred out of ^{232}Th inside a nuclear reactor. Once this is attained, it can be argued that such a reactor system, in principle, can become a self-sustaining and renewable source of energy, if the ratio of ^{233}U-breeding (from ^{232}Th) and ^{233}U-burning (to give the fission energy) remains near unity or more. To realize this, several methodologies have been proposed/being developed. These include (i) coupling the thorium with conventional fissile elements (^{235}U, ^{239}Pu or both) initially and keeping the system near-critical until sufficient ^{233}U is generated *in-situ* (or chemically separated after reprocessing the spent fuel) to sustain the chain reaction (ii) using molten salt fuel forms (ca. molten LiF-BeF$_2$-ThF$_4$-UF$_4$) with an online reprocessing capability, by continuously taking out part of the irradiated fuel to extract the as-bred ^{233}U as well as remove the undesired fission products (these fission products act as neutron poisons and thus adversely affect criticality) (iii) providing the required supply of extra neutrons by using appropriate particle accelerators (spallation neutron source) so as to operate the reactor in a slightly sub-critical mode (ADS

sub-critical reactors), etc. Given the present scenario of well proven and industrially practiced reactor technologies based on conventional fuels like ^{235}U, natural U and ^{239}Pu; the first approach may be the preferred choice for most of the reactor developers. Studies related to development of these thorium-based fuels (Th-^{235}U, Th-^{239}Pu, Th-^{235}U-^{239}Pu and more recently, those involving minor actinides also) are underway in few countries, which have continued their efforts towards developing thorium-based reactor technologies. On the other hand, the other two approaches of developing (i) thorium-based molten salt reactors or (ii) accelerator driven sub-critical (ADS) systems, which have immense promise towards bringing out a paradigm shift in nuclear technology sector from conventional uranium-based reactors to innovative and inherently safe thorium-based reactors, are still in their early stages of research and development.

Before bringing out the main subject of the present article on status, potential and challenges associated with thorium-based metallic alloy fuels, it is important to summarize the inherent aspects of thorium-based fuel cycles in general. This, although has comprehensively been covered by excellent articles [1-2] and technical documents [3], a brief mention of the same is presented here.

2. Salient features of thorium-based fuel cycles

a. Thorium is naturally more abundant than uranium. In a situation of steadily increasing demand and possible price escalation of uranium, it is argued to adopt the inclusion of thorium into large-scale nuclear technology at the earliest.

b. From nuclear characteristics, ^{233}U; which is bred from ^{232}Th, is the best fissile nuclei among ^{235}U, ^{239}Pu and ^{233}U for nearly all practically achievable neutron energies (thermal, epithermal and fast neutron spectrum). The value of eta ('η' is the average neutron yield per fission to neutron absorbed) is highest for ^{233}U. Further, given the value of 'η' being more than 2 for thermal as well as fast neutron spectrum, breeding is possible with ^{233}U in thermal reactors also (thermal breeders).

c. Breeding of ^{233}U from ^{232}Th, as compared to breeding of ^{239}Pu from ^{238}U, is more attractive and beneficial as

it generates lesser long-lived higher actinides (trans-uranics) during the breeding chain (for thorium being on the left side of actinide series in periodic table) and therefore considerably eases out the issue of nuclear waste management in the end.

d. Fission products generated in thorium cycle have smaller gross neutron capture cross section (poisoning effect) as compared to those produced during fission of ^{235}U or ^{239}Pu, which is important for neutron economy in thermal reactors, though not in fast reactors.

e. Two major safety parameters namely, negative sodium void coefficient (positive for uranium cycle) and negative Doppler coefficients (less negative for uranium cycle) associated with thorium cycle favor it in fast reactors.

f. Thorium and its compounds (oxides, carbides, etc.) have higher structural and chemical stability as well as superior thermal and theromophysical properties as compared to their uranium (or plutonium)-based counterparts. This results into their capability of high temperature operation and attaining higher burnups. However, the same aspect makes its front-end (fuel fabrication) and back-end (reprocessing), relatively challenging.

g. Iso-structural nature of ThO_2, UO_2 and PuO_2 (all crystallizing in isotropic fluorite structure) coupled with their complete range of solid-solubility with each other result into easier selection of mixed oxide fuels with desired fissile-fertile compositions so as to attain higher burnups and longer in-pile irradiation times.

h. Longer half-life of ^{233}Pa ($t_{1/2}$ = 27 days) formed in the thorium cycle may lead to reactivity related issues during the start-up as well as shut-down scenario of thorium-based reactor systems, which need to be addressed.

i. Presence of ^{232}U; formed by (n, 2n) reactions in ^{232}Th-^{233}U cycle, causes radiological challenges due to its hard gamma emitting daughter products. This however, has now been considered more like a weighted advantage in terms of the inherent non-proliferative nature of both spent as well as reprocessed fuels based on thorium cycle. The challenge remains therefore, is to develop suitable and safe remote handling technology for large scale handling of reprocessed ^{233}U and fuel fabrication thereafter.

j. Dissolution of sintered thoria in concentrated acidic media is still an unresolved challenge and needs extra addition of HF as well as buffer agents (ca. aluminum nitrate or zirconium salts) to reduce the extent of corrosion (in process vessel and associated circuitry) caused by the presence of aggressive fluoride ions in the dissolution cycle.

k. The THOREX process for thorium-based mixed oxides is not fully developed yet to an industrially matured level in comparison of PUREX process for U-Pu MOX fuels.

l. Higher toxicity of both, freshly prepared as well as aged thorium-based fuels due to hard beta and gamma emitting daughter nuclides is a cause of concern and necessitates appropriate shielding requirements/remote handling during large quantity material handling.

3. World energy scenario and thorium

With the growing population in developing countries as well as rapidly increasing development, the energy requirements for such regions, which are steadily increasing at present, are surely set to escalate drastically in the near future. This would press towards a huge increase in consumption of our fossil-fuel energy sources such as coal, gas, oil, etc. and also, would therefore lead to enhanced environmental concerns due to large quantity of CO_2 emission and green-house effects. In such a scenario, where availability of energy is going to dictate the pace of overall development, the role of nuclear energy; a clean and sustainable source of energy, towards attaining the energy security of our planet will become more and more significant. This would not only result into continuing operation of existing reactors with better efficiency and for a longer period of time, but would also require the construction of a number of additional reactors. Further, design; development and construction of new generation innovative reactors for specific requirements would also be needed. The specific requirements would depend upon the area specific needs of a nation/region and may require (i) need of small modular reactors that are easy to build & operate, safe, transportable and after completion of its life cycle at the user site, can be decommission safely (ii) need of very large high energy density reactors with enhanced safety and performance features (iii) reactors capable to extract energy from the depleted uranium resources (iv) efficient convertor or breeder reactors capable of producing energy as well as additional fissile inventories for future reactors or reactor cycles. In such a dynamic scenario of inevitable growth of nuclear technology, and given the potential of thorium-based fuel cycles, the role of thorium is certainly going to be an important and major factor.

3.1 Fuel options for thorium-based cycle and current status

Introduction of thorium into nuclear reactors is largely conceived in three different fuel forms: (i) ceramic (oxides, carbides, nitrides) (ii) metallic alloys and (iii) molten salts (especially fluorides). Out of these, the oxides fuel form (ThO_2, $Th_{1-x}U_xO_{2\pm\delta}$, $Th_{1-x}Pu_xO_{2-\delta}$, etc.) has been investigated to the maximum extent and still continues to be the preferred option. On the other hand, metallic and molten salt fuel forms have received relatively limited attention of exploration by the nuclear industry community. Carbide and nitride fuel forms have perhaps been the least studied. The principal factors for nearly unified attention to oxide fuel forms could be (i) well established uranium-based oxide fuel technology (both front- as well as back-end) for majority of nuclear reactors; worldwide (ii) possibility to go to very high temperatures and therefore achieve higher burnups and increased efficiency, etc.

In general, as compared to uranium (or U-Pu)-based fuels, the fuel options for thorium, either oxides or metallic alloys (Th-U, Th-Pu, Th-U-Pu, Th-U-Pu-Zr, etc.) show superior properties in respect to their thermal and structural stability, chemical compatibility with peripheral components (such as clad, coolant, etc.) and radiation stability. Table 1 and 2 lists the comparison between the metal and oxide form of thorium, uranium and plutonium.

It is these properties of thorium and its compounds, which, when coupled with the its favorable neutronic properties, have led researchers to explore their potential as promising fuels for variety of reactors. Good amount of experience exists on development and in-pile irradiation behavior of thorium-based fuel assemblies in several research/power reactors. Whereas USA has contributed towards the research and development of thorium-based fuel options since the very inception of nuclear technology, other countries including Germany, Great Britain, Japan, France, Canada, Russia have also explored the potential of thorium fuel options in their reactors/research facilities. Currently, in view of the large abundance of its indigenous thorium reserves and a well envisaged three-stage nuclear power program with closed fuel cycle [4] by late Dr. Homi Jahangir Bhabha, India is continuing its R&D activities on thorium-based fuels in a major way. Some of the ongoing studies/development include: (i) irradiation studies on thorium oxide fuel assemblies in their research as well as power reactors (ii) continuing the operation of only existing research reactor fueled with [233]U (KAMINI) [3] and (iii) developing the unique Advanced Heavy Water Reactor (AHWR), designed to give majority of electrical energy by thorium utilization [5].

In-spite of enormous work carried out during 1960s-1980s, focused towards development and performance evaluation of thorium-based fuels, these fuels have not yet

Table-1

Property	Thorium metal	Uranium metal	Plutonium metal
Structure	FCC (RT-1673 K) BCC (1673-T_m)	Orthorhombic (RT-935 K) Tetragonal (935-1045 K) FCC (1045 K – T_m)	Six allotropes (Monoclinic at RT)
Lattice parameter (Å) *(for RT phase)*	5.07	a = 2.85 b = 5.87 c = 4.95	a = 6.18 b = 4.82 c= 10.97 $\beta = 101.80^o$
Melting point	2025 K	1405 K	913 K
Boiling Point	5060 K	4405 K	3508 K
Theoretical density *(g/cc at 298 K)*	11.68	19.05	19.86
Specific Heat At RT (J/mol.K)	26.2	27.7	35.5
Thermal conductivity *(W/m.K) at 773K*	43.1	30	30
Coefficient of thermal expansion *(ppm/K)*	11.9 (30-600 K)	14.2 (30-600 K)	56 (mean value α-phase)

Table-2

Property	ThO$_2$	UO$_2$	PuO$_2$
Structure	FCC (CaF$_2$-type)	FCC (CaF$_2$-type)	FCC (CaF$_2$-type)
Lattice parameter (Å) *(at RT)*	5.597	5.466	5.397
Melting point	3643 K	3123 K	2623 K
Density *(g/cc at 298 K)*	10.0	10.96	11.46
Specific Heat *At 873 K (J/mol.K)*	64.9	71.4	94.9 (at 1523 K)$^\$$
Thermal conductivity *(W/m.K) at 773K*	6.20	4.80	4.48
(W/m.K) at 1773K	2.40	2.40	1.97
Coefficient of thermal expansion *(ppm/K)*	9.67 (RT-1223K)	10.0 (RT-1223K)	11.4 (RT-1223K)

$ *Specific heat data at 873 K are not traceable*

acquired their place as a proven and routinely used fuel in power reactors. The reasons are possibly a combination of both technical and economical orientation, in light of (i) redundant and proven performance of uranium-based fuels (ii) improvement in the uranium supply across the globe and (iii) ill-addressed issues of relatively challenging fuel-fabrication and reprocessing of thorium-based fuels. However, there is a renewed interest worldwide towards these fuels and their timely induction in power reactors. The present scenario is mainly focused on development of suitable advanced fuel options, which (i) are capable of providing nuclear energy for a long-term (practically inexhaustible) in an economically viable, sustainable and renewable manner (ii) minimize the issues related to nuclear waste management and (iii) are inherently non-proliferative in nature. Thorium-based fuels are perhaps the best suited for fulfilling all these requirements.

Among the possible options for future generation reactors, metallic fuels are also gaining attention [6]. This is possibly due to the inherent advantages that metallic fuels bring-in, especially, in terms of their capability of faster breeding (shorter doubling times), amenability to electrochemical reprocessing, inherent safety and non-proliferative nature, etc. In-spite of having an established fuel cycle expertise on oxide fuels for a large number of reactors; currently operational worldwide,

it is accepted that metallic fueled reactors will be major contributors towards rapid expansion of nuclear energy in future. Although the extensive work, presently being pursued on metallic fuels, is based on U-Zr and U-Pu-Zr alloys, it is a matter of time and focused development efforts, when thorium-based metallic fuels will also find their place in future nuclear reactors. Hence, it is desirable to take stock of the past and present status of development of these alloy fuels, their potential advantages and challenges that these fuels offer.

4. Attributes of metallic nuclear fuels

The development of nuclear technology, in its primitive and pioneering period, initiated with an all metal fuel concept. This was the most obvious choice, for simple reasons, like well-known chemical and physical behavior of metals and their alloys, ease of fabrication, simple and smaller core designs and production of artificial fissile inventory (^{239}Pu/^{233}Th). Although the global interest shifted towards oxide fuels (for thermal/fast reactors) during late 1960s, extensive research and irradiation experience continued on alloy fuels for over three decades. These studies demonstrated their high burnup capability (up to ~10 at.%) with inherent safety features. Their behavior during transient events was also found to be safe. Further, the unique approach of electrometallurgy

(pyrochemical reprocessing) to reprocess the spent alloy fuel had been demonstrated, thereby successfully closing the all metal fuel cycle. Excellent reviews on metallic fueled reactors have been written [6-7], which detail the progress made till now. However, for the sake of completeness, some of the important attributes of metallic fuels are mentioned as follows:

a. Metallic fuels are ideal for fast reactors as they produce very hard neutron spectrum.

b. Proper design of the fuels has demonstrated irradiation up to very high burnups.

c. Metallic fueled fast breeder reactors have shorter doubling time.

d. Metallic fuels, in general, have very high thermal conductivity

e. Inherent safety features of metallic fuels have been amply demonstrated in several intentional transients situations created during EBR-II experiments [7].

f. Amenability to electro-refining technology makes the metallic fuel reprocessing straightforward with lower waste generation.

g. Remote handling required for metallic fuel reprocessing (due to highly radioactive nature of both spent as well as reprocessed fuel) brings-in proliferation resistant attribute.

h. Electro-refining of the metallic spent fuel causes retention of long-lived higher actinides with the reprocessed fuel, which can be put back into reactor for burning. This in turn provides fission energy from these actinides as well as reduces the time duration required for long-term storage of nuclear waste from tens of thousands of years to hundreds of years.

4.1 Metallic fuels and thorium

Given the above general attributes of metallic fuels, it is apparent that they have significant potential as prospective fuels for future reactors. India also have; in principle, decided to build their next generation fast reactors fueled with metallic alloys after running the first few fast reactors with mixed oxide fuels [8]. U-Pu-Zr-based metallic alloy fuels are presently being considered for these future reactors. The selection is based on the fact that U-Pu-based fuel cycle has favorable nuclear characteristics in fast reactors and comprehensive information on their development and irradiation performance is available [6-7, 9].

Thorium-based metallic fuels, on the other hand, are apparently better than their uranium-based counterparts

on the basis of (i) inherent advantages of thorium fuel cycle and (ii) superior physico-chemical & thermophysical properties of thorium metal as compared to uranium [3, 10]. However, these fuels have still not been explored fully, from the standpoint of qualifying them for large-scale utilization in power reactors. There had been a comprehensive program, mainly in USA during 1950s-1970s, on developing thorium-based metallic alloy fuels. Quantum of activities pursued during that period can be seen from the amount of literature present in the form of technical reports. However, the same is not reflected in other parts of the world as well as in open journals literature. Reasons for this could be (i) enhanced uranium availability with diminishing need of further exploring thorium for large-scale utilization and (ii) nearly unanimous shift of world's nuclear community towards oxide fuels for LWR technology during late 1960s. Another factor could be a less intense approach towards production of [233]U for non-power applications, an important reason for which Th-U cycle had been researched in USA [2]. Of the technical difficulties in the perspective of LWR technology development during that period, limited compatibility of thorium metal and its alloys with the LWR-clad materials and coolant (water) as well as radiological challenges (associated with all fuel forms of thorium) perhaps would have contributed to the declining interest in these alloy fuels [11]. In India also, much of the efforts have focused on ThO_2-based fuels with very little towards metallic fuel development. It is however, difficult to identify the exact reasons for the little attention given to these alloys, while their merits over uranium-based alloy fuels have been emphasized time and again. Interestingly, there has been a recent surge of discussions and activities worldwide, advocating the use of thorium fuels in metallic alloy forms [12-13], so as to achieve the energy security in a sustainable, renewable, non-proliferative and environmentally benign way.

Based on the above, and given our three-stage program of optimum utilization of thorium resources for power production, it is worthwhile to summarize the salient features of thorium-based metallic alloy fuels (advantages and challenges), review the existing experience and current scenario of development and future prospects. The same is attempted in the following sections of the article.

4.2 Modern metallic fuel concept and thorium-based fuels

In light of ample experience gained in developing uranium-based metallic fuels (U-10Zr, U-Pu-Zr alloys, etc.) and availability of exhaustive database on them [6-7, 9], it is imminent that these fuels will serve the needs of immediate and near future reactors. They also have

ample scope of improvement in respect to safety, extended burnups, transuranic burning, etc. The current directions, in research activities related to metallic fuel development, is therefore focused on superior fuel performance coupled with safety and minimum long-term waste management issues. The attention is towards development of targeted alloys for achieving ultra-high burnups with controlled irradiation-induced swelling, burning the long-lived transuranics, better in-pile performance with improved resistance to fuel-clad interaction, advanced fuel fabrication methods, etc. [14]. Improved and/or innovative options for reprocessing the spent metallic fuel, like electro-refining, zone-refining, etc., are also being explored. Availability of modern computational tools, which are capable of simulating the fuel behavior, will also come handy in this respect as the development would require relatively modest experimental efforts in conjunction with the simulation results.

On the other hand, metallic fuels based on thorium, which in several aspects, appear to better-off their uranium-based counterparts, are still far from developed from the standpoint of large-scale utilization. Development of these fuels therefore, would require systematic and comprehensive research efforts in lieu of limited availability or scarcity of existing research and irradiation performance database.

4.3 Potential thorium-based metallic fuels

Being purely fertile in nature, thorium has to be combined with a fissile element (enriched uranium or plutonium or even minor actinides) before it can be used as a fuel. Many alloys have been proposed and studied in this regard. However, the potential candidates are thorium rich Th-U, Th-Pu, Th-U-Pu, Th-Pu-Zr, Th-U-Pu-Zr alloys with varying fissile to fertile compositions. More recently talked about, are the alloys with limited incorporation of minor actinides (MA), so as to burn them for energy production as well as minimize the nuclear waste for long-term management. Since addition of plutonium to thorium reduces the alloy solidus temperature more than that of uranium addition lowers it, co-doping of uranium and plutonium or U/Pu with some stabilizing element (such as Zr) is also recommended to optimize the alloy properties like, ease of fabrication, suitable structural and thermal properties, compatibility with clad & coolant, irradiation stability, amenability to reprocessing by electro-refining, etc. In one of the detailed report by Blumenthal *et al.*, two alloy compositions, namely 80Th-10U-10Pu and 70Th-20U-10Pu (in wt.%) have been proposed to be the prospective candidates for fast reactor fuels [15]. Similarly, irradiation experiments have been carried out on 90Th-10U, 80Th-20U and 80Th-20Pu alloys. Exact selection of the fuel, however, would depend upon the type of reactor, the envisaged irradiation conditions, target burnup and reprocessing aspects of the spent fuel. Some other alloys, which have been studied as potential fuels for advanced liquid metal cooled fast breeder reactors include Th-20Pu-4U, Th-20Pu-4U-8Zr, etc. (all compositions in wt.%) [3].

4.4 Advantages of thorium-based metallic fuels over uranium-based metallic fuels

There are several inherent features of thorium-based alloys, which make them better candidates as fuels and are derived out of the basic properties of thorium metal (Table-1). Some of these advantages are briefly mentioned as follows:

a. Higher melting point of thorium (~ 2025 K) as compared to uranium (~1405 K) renders better chemical stability to thorium-based alloys. Further, energy extraction with improved efficiency and higher burnups can be achieved by irradiating the fuel with higher centerline temperatures.

b. With higher melting point of thorium, the solidus temperature of Th-U-Pu ternary alloys is sufficiently high for their use in fast reactors with average outlet coolant temperature of 923 K [16]. This is an important advantage over U-Pu alloys, where the solidus temperature drops down to levels where melting within the fuel becomes inevitable under typical fast reactor conditions.

c. Thorium has much higher thermal conductivity (~54 W/m.K @ RT) and lower coefficient of thermal expansion (11.9×10^{-6}/K within RT-600 K) compared to uranium (~27 W/m.K @ RT & 14.2×10^{-6} /K within RT-600 K). Further, the conductivity increases with increasing temperature as in case of uranium.

d. The lower heat capacity of thorium metal and higher thermal conductivity, as compared to uranium metal as well as that of UO_2 or ThO_2 (Table 1 & 2) indicate the potential of better fuel performance during off-normal events such as under cooling (LOCA) or transients.

e. The cubic crystal structure of thorium metal (FCC up to 1723 K and BCC up to melting temperature 2025 K) is an important advantage. This practically means the fuel to remain in the same FCC phase during normal irradiation conditions and therefore suggests for lesser dimensional variation upon irradiation and/or thermal cycling. On the contrary, uranium has three allotropic transformations from anisotropic orthorhombic

structure (α-pase) to isotropic cubic structure before melting {(Orthorhombic (RT-935 K) → tetragonal (935-1045 K) → Cubic (1045 K-melting)}. This results, not only in anisotropic swelling of the α-phase during irradiation, but also causes co-existence of all the three phases along the radial direction within a fuel pin during normal irradiation conditions and lead to higher dimensional deformations.

f. Thorium has higher creep resistance and better ductility as compared to uranium metal, which are desired attributes for an alloy fuel element.

g. Due to isotropic and less dense (11.55 g/cc at RT) crystal structure of thorium, it is expected that fission products may be better retained within the thorium matrix (lattice) as compared to uranium (anisotropic and dense structure, 19.05 g/cc at RT) and thereby reduce the fission product-induced swelling/deformation. Higher solidus temperatures of thorium-based alloys also tend to retard the diffusion of both solid as well as volatile/gaseous fission products. This indicates a higher fission gas retention capacity and lesser extent of fission gas-induced swelling characteristics, even upon prolonged irradiation [17], which is one of the major reasons for fuel pin failure through fuel-clad contact followed by FCMI (Fuel-Clad Mechanical Interaction) or FCCI (Fuel-Clad Chemical Interaction) under irradiation conditions. Early in-pile studies on thorium-based alloys have revealed the same.

h. Thorium metal and its alloys are, easier to work with (hot/cold rolling, swaging, etc.) and form into various fuel shapes as compared to uranium metal and alloys. This gives an advantage in the fuel-fabrication front, when the fuel is required in specific shape/form. Between hot and cold rolling options, hot thorium is found to be easily rolled into desired forms without the need of intermediate annealing while as-cast thorium may have larger grain size, which may lead to crack formation upon cold rolling.

i. Thorium-based metallic fuels are expected to have higher breeding gains compared to other fuel forms of thorium (such as oxides, carbides, etc.) [17].

j. Th-Pu and Th-TRU alloys are promising fuel options in fast reactors for efficient burning of plutonium and transuranic (TRU) inventory, which is stockpiled in LWR spent fuels or separated during reprocessing of spent fuel. These alloys have the potential to incinerate these higher actinides without compromising the safety characteristics of the fuel and thereby reduce the long-term waste storage liability [18].

k. The inherent advantages of negative sodium void coefficient and more negative Doppler coefficient with thorium fuel cycle are still larger with the metallic fuel form and therefore give added safety attributes to fast reactors utilizing them [1].

l. Like other metallic fuels, thorium-based metallic fuels are also amenable to pyrochemical reprocessing as well as remote fabrication, for which substantial research experience exists.

4.5 Challenges with thorium-based metallic fuels

Several advantages are attributed to thorium-based metallic fuels, which indicate their superior potential over other metallic fuels such as uranium-based ones. However, these fuels have not been developed to the expected extent where they can be qualified for their large-scale use in power reactors. The possible reasons for this under-development could be policy as well as need-driven in light of (i) well performing ceramic fuels technology and (ii) more research exposure towards uranium metal fuels. However, there are some inherent scientific and technological challenges also, which have retarded/impeded the full-scale development of thorium-based metallic fuels in particular and overall thorium-based fuel cycle at large. Some of these issues, pertinent to metallic fuels are presented in the following text:

a. Higher melting point of thorium brings-in a technological issue during fabrication of high thorium containing alloy fuel pins using injection-casting (the method employed for large-scale manufacturing of metallic fuel pins). Due to higher solidus temperatures, conventional casting moulds, usually made of fused-quartz or Vycor, pose the limitation of softening or even breaking-down during the casting. Other prospective moulds such as graphite have not been developed fully till now and require a lot of efforts to (i) obtain suitably impervious and leak tight graphite tubes and (ii) avoid excess carbon uptake by the alloys during casting, etc. [16]. Other methods of fuel fabrication such as (i) arc-melting followed by swaging/rolling (ii) tilt-pour casting, etc., although used at various scales, are not yet preferred for large-scale applications.

b. While powder metallurgy is perhaps the best route for ceramic fuel fabrication and is practiced on industrial scale worldwide (with several advantages such as, control over the pin/pellet dimensions, scalability, control over density and microstructure, etc.), the same for metallic alloys comes with challenges of (i) preparation of high purity fine metal powders (ii) handling these highly reactive (pyrophoric) powders

and (iii) radiological issues in powder handling. Given these issues, the fuel fabrication has to be done in highly controlled atmosphere glove boxes and with additional remote handling for re-processed powders. Very little experience exists on thorium-based metallic fuels in this aspect. One potential route however, for these alloy fuels, involves the steps of (i) preparation of metal hydrides using bulk metals (ii) blending the hydrides in appropriate ratio (iii) de-hydriding cum sintering using vacuum hot pressing and (iv) final alloy shaping [19].

c. Unlike well established oxide-fuel technology and reasonably existing information on uranium-based metallic fuels, very limited data is available on thorium-based metallic fuels. Also, the data available is either limited to lower burnups or detailed post irradiation analysis (PIA) has not been carried out/reported [20].

d. Limited solubility of uranium in thorium metal (>1 wt.% U up to 1273 K) is also a concern. Beyond this content, uranium (present in Th-U alloy fuels) tends to segregate at grain boundaries (uranium dispersed in thorium matrix) and above 20 wt.% U, it usually makes a continuous network of metallic uranium phase, which is undesired from the point of view of irradiation swelling and dimensional stability [20]. The possible solution is either to keep the uranium content below a certain limit to avoid dimensional instability or to develop methods resulting into suitable alloy microstructure so as to minimize anisotropic swelling of the fuel [21].

e. In few studies conducted on thorium fueled fast reactors in respect to breeding ratios, it has been reported that only marginal advantage is gained with metallic fuels, in comparison of oxide fuels. Even this margin has been considered as doubtful [22], given the limited experimental swelling data available on thorium metal and its alloys. Similar argument of in-significant advantage has been placed for replacing ThO_2 blankets by the thorium metal. Clearly, large amount of experimental work is needed to address this ambiguity.

f. Issues of higher fission gas induced swelling are reported for these alloy fuels attaining very high burnups. Thermal expansion coefficients of as high as 25×10^{-6}/K have been reported for irradiated thorium-uranium (Th-11wt.%U) alloys [23], which is more than twice the value for un-irradiated alloys.

g. Due to large difference in melting points and densities of thorium in comparison with uranium/plutonium as well as their limited mutual solubility [15] (unlike ceramic fuels, which have wide range solid-solubility), obtaining homogenous thorium-based alloys is a challenging process, which needs to be developed.

h. The inherent issue of back-end of thorium fuel cycle, which remains the major challenge in realizing thorium-based nuclear energy regime, stays equally or little less with metallic fuels also. The radiological issues during handling and reprocessing of ^{232}Th-bearing spent fuels (especially oxides) containing noticeable amounts of ^{232}U in it, to extract the as-bred ^{233}U and its re-fabrication into fresh fuel assemblies are not completely resolved and will require complete automation and remote handling to comply with the modern-day's radiological protection standards. The concern however, is somewhat less serious for metallic fuels, given the applicability of relatively clean approach of molten salt electro-refining or more recently discussed zone-refining [12] methods for metallic fuel reprocessing.

i. Although the presence of ^{232}U in the thorium fuel cycle poses challenges in terms of complete automation and remote handling in fuel fabrication, fuel reprocessing and other related processes, the nuclear community at large, is presently looking at it more in terms of a beneficial tag associated with ^{233}U, which makes the fuel system extremely proliferation and diversion resistant, limiting its use for peaceful applications only.

4.6 Existing experience on thorium-based metallic fuels

Although limited information is available in open literature on development and performance evaluation of thorium-based metallic alloy fuels, still a sizable account of experience accumulated in the past can be retrieved, mainly contributed by results of the work carried out at national laboratories in USA as well as few other institutes. Alloys of thorium with fissile ^{235}U/^{239}Pu have been tested in several experimental facilities/power reactors for breeding ^{233}U and understanding their in-pile performance [3]. This information is very useful and can be fruitfully used for a deeper understanding of properties and behavior of these alloys and evaluating their potential as prospective fuels for future reactors. The summary of this existing information is provided in two subsections, namely (i) Early literature on thorium-based metallic fuels and (ii) Recent interest on thorium-based metallic fuels.

4.7 Early literature on thorium-based metallic fuels

The research and development activities related to studies on all metal fuel, based on alloys of thorium with

limited additions of uranium could be traced back to as early as 1952, when some work had been initiated in USA on Th-U (~1.2 wt.% U, enriched with ^{235}U up to 93.5%) plate type alloy fuels clad with aluminum. The intention for these experiments perhaps was sizable production of ^{233}U from ^{232}Th, which was considered equally better fissile material for defense applications. Irradiation of these alloys was carried out in a high power research reactor (MTR) up to an integrated neutron flux of 2.6 x 10^{21} n/cm^2, corresponding to an estimated burnup of ~1 at.% [24]. The PIA results on irradiated alloys have been reported in respect of variation of several properties like dimensional stability, density, fuel-clad bonding characteristics, fuel & clad hardness, chemical analysis, extent of ^{233}U buildup, etc. The results of these studies have indicated the dimensional stability of both, core as well as clad, and explained in terms of excellent radiation stability potential of these alloys. The irradiated fuel core was found to be hardened while no such effect was seen for the aluminum clad. Interestingly, an issue of increased air-borne radioactivity was also noted while handling the irradiated samples. Similar observations of substantially better radiation stability of Th-U alloys (up to 10 wt.% U), as compared to uranium-based alloys were made in another report [25]. Results of full-scale engineering level irradiation testing; carried out on Th-U , U-Zr and U-Mo alloys to a typical burnup of 850 MWd/MTU, also indicated the promising nature of Th-U and U-Mo alloys as suitable nuclear fuels [26].

Studies have also been carried out to understand the physical and chemical behavior of thorium-based alloys during the early years. These include corrosion testing on thorium metal and Th-M alloys (M = Cr, Nb, Zr, Ti doped individually or together and M content ≤ 6 wt.%) in distilled water at around 368 K for 30 days [27]. The results indicated significant variation in the extent of corrosion depending upon the extent of cold-rolling of starting metal/alloy. The reasons for such notable differences, though not reported/investigated then, could be due to the metallurgical history of the metal/alloys such as impurity contents, microstructure variations, texture, etc.

In order to improve upon the alloy properties as well as irradiation performance, several Th-U binary alloys with varying microstructures had been developed [28]. The alloys were developed using thorium metal of varying purity as well as employing variety of processing techniques like melting technique, hot/cold working, post-alloying heat treatment, etc. The results revealed that arc-melted alloys exhibited the ideally suited morphology, with small uranium particles uniformly dispersed in the base thorium matrix. Quantitative effect of uranium incorporation on work hardening as well as alloy re-crystallization has been explained. Doping with different metals (Zr, Nb and Mo; individually as well as in conjunction) had been attempted in order to stabilize the FCC gamma-uranium phase and thereby improve upon the irradiation resistance and high temperature strength of these alloy fuels. The beneficial effect of Mo and Nb towards gamma-phase stabilization and that of Zr for improving the water corrosion resistance has also been discussed.

Effect of alloying elements on physical, mechanical and structural properties of Th-U alloys (Th-5U & Th-10U, in wt.%) has been investigated [29]. Results with several alloying elements such as zirconium, niobium, molybdenum, carbon, aluminum, beryllium, etc. have been presented. In general, alloying has been shown to result into significant enhancement of high temperature tensile and stress-rupture strength, which is indicative of improvement in radiation-induced swelling resistance at elevated temperatures (up to 1073 K). The most pronounced effect has been reported with 2 to 5 wt.% zirconium incorporation. The improvement in alloy properties has been attributed to a combined effect of (i) solid-solution strengthening and (ii) dispersion strengthening of Th-U alloys. It is claimed that alloys with controlled morphology could be produced by appropriate process control during arc-melting and solution heat treatment. Results of irradiation testing on few of the most promising alloys at 1073 K and target burnups of 10,000, 20,000 and 30,000 MWd/t have also been briefed [29].

A number of experimental studies have also been reported on the neutron irradiation behavior of Th-U alloys, although the extent, to which the results are available, is limited in comparison to uranium-based alloys. Kittel *et al.,* [30] investigated the irradiation behavior of several Th-*x* wt.% U alloys ($0 \le x \le 31$, total ten compositions), prepared/processed by different methods like rolling, swaging, chill-casting, etc. Irradiation was carried out under different conditions of (i) total burnup achieved (from as low as 0.3 to as high as 10 atom %), (ii) irradiation temperatures (ranging from 318 K 1273 K), etc. As an important observation, the authors have reported that the irradiation-induced swelling for all the alloys was significantly less than that observed for the best uranium-based alloy under identical irradiation conditions. The exceptional resistance towards high temperature radiation induced swelling has been attributed to a combination of two main factors. The first being the low density; isotropic crystal structure of thorium metal and the second, the effect of Th-U alloy morphology involving uniform dispersion of tiny uranium precipitates

in the base thorium matrix. These two effects have been reported to result into enhanced possibility of fission recoils to escape from the uranium particles (which show anisotropic swelling) and immobilize into the relatively less-dense and cubic thorium metal structure. Based on these reports, similar behavior can be expected for Th-^{233}U, Th-Pu and other Th-based metallic alloys also. However, actual irradiation tests need to be carried out to understand their in-pile irradiation behavior. In an another report, burnup and specific power calculations on Th metal and Th-5.4wt.% U alloys have been attempted [31].

A notable evidence for the work that had been pursued in USA during 1960s – 1970s, to explore the potential of thorium-based alloys as prospective fuels for fast reactors, can be found in two detailed reports [15-16]. The first report [15] covers a comprehensive account of choice of Th-U-Pu alloys, their preparation & characterization and results obtained on binary (Th-U, Th-Pu, U-Pu) and ternary phase diagram (Th-U-Pu) evaluation using combination of experimental techniques (metallography, RT-XRD, HT-XRD, dilatometry, DTA, etc.). It has been identified that most ternary alloy compositions show coexistence of FCC-thorium with different (U-Pu) phases. Further, based on the studied influence of uranium addition on reducing the solid-solubility of plutonium in thorium, the useful composition ranges for fuel purpose have been identified. Two prospective alloys, namely 80Th-10U-10Pu and 70Th-20U-10Pu (in wt.%), have been identified as candidate fast reactor fuels. The study has also emphasized the need of further investigations that are required for a complete understanding of the ternary system and exploit the useful regions for fuel development.

The second part of this work [16] is focused mainly on mechanical, thermal & thermophysical properties of Th-U-Pu alloys and their irradiation performance. Main results have been reported for 80Th-10U-10Pu and 70Th-20U-10Pu alloys. The main findings of this work [16] indicated the qualification of these alloys as fast reactor fuels with nearly un-altered fuel microstructure up to a burnup of 5.6 at.% with average 7.3% irradiation-induced swelling per at.% burnup and safe release of nearly 70% of the total fission gases into the plenum volume of the test pins. Regarding the stability of the two-phase morphology of Th-U-Pu alloys at high temperatures (1173-1273 K), it is indicated that the two-phase alloys (Th-Pu solid-solution matrix with different (U-Pu) phases dispersed in it) are suitable as fuels for irradiation in a reactor operating at a maximum temperature of 923 K (typical metal cooled fast reactors), still with a safety margin of around 200 K. Results of thermal cycling experiments performed in molten NaK between 723 to 1073 K for more than 100 cycles revealed significantly smaller variations in density and dimensions of Th-U-Pu alloys as compared to uranium-based alloys (U-Pu-Zr, U-Pu-Ti, etc.).

During the same period, Copeland had reviewed the then existing literature on Th-U alloys (with special reference to Th-20 wt.% U alloy) in respect to their use as possible fuel elements for the sodium cooled Unclad Metal Breeder Reactor (UMBR) program [23]. In this report, the author has summarized and compared different methods of Th-U alloy preparation and casting methods, mechanical properties of un-irradiated as well as irradiated alloys, thermo-physical and thermodynamic properties, performance under different irradiation temperatures and burnup levels, etc. Based on the review, he has proposed that Th-20% U alloy fuels may give quite safe and optimum performance under operating conditions of <923 K and <4.3 at.% burnup with isotropic swelling characteristics. However, here again, it has been emphasized that more work is still needed to be done, especially on high temperature properties of the irradiated alloy fuels as well as compatibility issues with molten metal coolant.

Regarding the reprocessing of irradiated thorium-based alloy fuels, very early reports can be found that mentioned the use of vacuum induction drip melting method and demonstrated the development of remote handling system for reprocessing [32]. Limited work has also been reported on separation of uranium as well as fission products from thorium, present in U-Th-Mg alloys using pyro-metallurgy [33]. Solubility of uranium is Th-Mg alloys (Th-55Mg, Th-65Mg, Th-84Mg & pure Mg, all in wt.%) were determined and various processes were considered for removal of small quantities of fission products from Th-Mg alloys. Further purification of thorium from magnesium had been studied by (i) vacuum distillation of magnesium or (ii) precipitation of thorium as ThH_2 at ambient pressures and high temperatures, etc. Hensen [34] has reported the application of electro-refining to obtain pure Th/U metals or Th-U alloys in a fused salt medium using impure thorium or uranium metal as anode material. The electro-refined metals/alloys, obtained in molten cathode medium were separated from cathode using vacuum distillation.

However, in-spite of few reports as referred above, information on reprocessing of thorium-based metallic fuels on large-scale is relatively scarce. Results obtained by thermo-chemical modeling of reprocessing Th–U–Pu–Zr metallic fuels using pyrochemical electro-refining, indicated the possibility of thorium being retained in the

anode basket along with zirconium and noble metals while other elements like U, Pu and MA; along with rare-earth fission products would be co-deposited in molten cathode (cadmium) media from where they could be separated using vacuum distillation [3].

Potential of thorium-based metallic alloys had also been studied for light water reactors (LWRs) [35]. In comparison with ThO_2-fueled LWBR as well as UO_2-fueled PWR, the metallic thorium has been attributed with several benefits along with uranium resource conservation. It has been suggested that metallic thorium fuels would have better compatibility with water coolant, which is quite poor for uranium metal. In another report [36], based on calculation of average fuel-rod temperature as compared to moderator temperature, followed by estimation of energy stored within a fuel, it has been indicated that the stored energy would be several times less (1/4th as compared to UO_2 fuels and 1/20th, if the fuel-clad gap is avoided) for metallic thorium fuel, attributed to the lower heat capacity of thorium. As a result, the peak clad temperatures also would be lower during a situation like LOCA (Loss-of-Coolant Accident). Also, it is indicated that stored energy within the fuel would be removed faster from metallic thorium fuel by the departing coolant through conduction due to its higher thermal conductivity.

From a sight of above reports, detailing the early experience on thorium-based metallic fuels, it can be said that in several aspects, these alloys have notably superior properties as compared to uranium-based alloys and therefore certainly have the potential to be used as prospective reactor fuels with safe and optimum irradiation performance. Different experiments, carried out worldwide, have also proven that in-line with the basic characteristics of thorium and its alloys, such fuels can be used with an excellent behavior at higher coolant temperatures also. Finally, it has been proposed that the existing information has put forward these alloys as an alternative fuels with safe and self-sustained mode of operation of future reactors, where the burnt ^{233}U could be replaced by the neutron capture-induced breeding of the additional ^{233}U from the fertile ^{232}Th [37].

4.8 Recent interest on thorium-based metallic fuels

In recent years, as the concept of going back to metallic fuels for various future generation nuclear reactors is gaining stronger grip, there has been a renewed interest on exploring the potential of thorium-based metallic fuels with equal efforts, as being made for uranium-based metallic fuels. Few reports have come in open literature, emphasizing the importance of an early development of newer and better metallic fuels based on Th-U, Th-Pu

binaries, Th-U-Zr, Th-Pu-Zr, Th-Pu-MA-Zr ternaries and other related systems.

One of the most attractive propositions in favor of thorium-based metallic fuels came out of the computational results of studies conducted at Pacific Northwest National Laboratory, USA and presented by M/s Thorenco LLC, San Francisco [12], where it has been proposed that use of metallic thorium fueled reactors could bring in a paradigm shift in nuclear technology from present day uranium-based technology to a thorium-based, sustainable and renewable one. The study has claimed to find ways for future generation nuclear reactors. Based on computational results, use of thorium-based metallic fuels in fast spectrum reactors has been given the beneficial attributes of (i) minimum production of Pu and other TRUs as well as efficient burners of their existing stocks (ii) fuel stability over longer durations (iii) amenability to remote zone refining-based recycling of fuel rods and (iii) proliferation resistant nature of the fuel, etc. Out of these, the possibility of using zone-refining is quite attractive. By using this method, the low melting fission products can be removed from the high temperature Th-based alloys without any wet-chemical steps, essentially. The report has also proposed new Pb-^{7}Li or Pb-cooled fast reactor concepts (400 MWth) for burning existing plutonium or TRU stockpile, in form of Th-U, Th-Pu or Th-TRU-based metallic fuels, which not only burn these higher actinides but also seem capable to produce nearly similar amount of ^{233}U fissile inventory during a decade of operation. Although the reported claims appear quite ambitious, it is worthwhile to look into each aspect with greater interest while carrying out advanced R&D in this direction.

Few other studied have primarily focused on the following aspects: (i) better understanding of the phase equilibria in thorium-based binary and ternary alloy systems using existing database and modern tools of computational thermodynamics [38] and evaluating various thermodynamic properties using the results (ii) neutron irradiation studies on hydrided Th-U-Zr alloys [39], which are being promoted as a new type of potential future nuclear fuel [40].

In a full scale simulation study using combination of theoretical methods and codes such as MCNP5, ORIGIN2.2, MONTEBURNS2.0, etc. [13, 18], the actinide burning behavior of Th-TRU-Zr alloy fuel {with maximum of up to 30 at.% TRU i.e., (MA+Pu) contents} has been evaluated and compared with U-TRU-Zr and U-Pu-Zr alloy fuel matrices in an advanced sodium cooled fast reactor (PRISM) design, fueled by the spent fuel of LWRs. Results of fuel performance modeling have been reported at single

fuel pin level, single assembly level as well as full core levels and the results are virtually same at each level. The analysis has shown that thorium-based alloys outperform their uranium-based counterparts in terms of higher actinide burnups, discharging higher proliferation resistant spent fuel and depletion of the plutonium isotopes. The net isotopic destruction rates, achievable with thorium-based alloy fuels (-1.0384 g/MWd) is shown to be significantly higher than that achievable with uranium-based fuels (-0.3206 g/MWd). It has been argued that the potential of thorium-based alloy fuels has been overlooked since several decades. Once again, the authors have emphasized for the need of a detailed assessment of these alloy fuels from economic perspectives so as to ensure that they remain in the future nuclear technology scenario without significantly affecting the economic competitiveness of nuclear electricity.

In an another strategy, use of thorium-based alloys (Th-U-Zr alloys) for effective power flattening feasibility in liquid metal cooled large scale CANDLE (*Constant Axial shape of Neutron flux, nuclide densities and power shape During Life of Energy production*) burning reactors has been analyzed by core modeling (SRAC code with JENDL 3.2 nuclear data library) and computational methods [41]. The modeling results have indicated flattened power density profiles for these reactors by uniform addition of thorium in the inner core region and also indicated a significant drop in the radial peaking factor from 1.87 for only U-10Zr alloy fuel to 1.44 for mixed core (Th-U-10Zr in the inner and U-10Zr in the outer region). This has been attributed as an attractive potential as such core designs could realize increased average discharge burnup with lower fuel requirements.

Potential of thorium-based metal fuels has also been claimed for fast neutron accelerator driven sub-critical (ADS) systems. Design analysis of such systems has indicated that metallic or nitride fuels forms would be more suitable for efficient actinide incineration in such systems [3]. Other benefits of minimized TRU production, limited reactivity variation during repeated cycling and [233]U breeding have also been proposed for such systems with thorium alloy fuels.

4.9 India and thorium-based metallic fuels

Given that our three-stage nuclear power program incorporates the essential objective of large-scale thorium utilization for energy production in the long term, significant experience is being obtained in thorium-based fuels. However, existing literature suggests that nearly the entire work is devoted to oxide-based fuels with very little information on thorium-based metallic fuels. Although we have operational experience of facilities like PURNIMA-III (critical facility), fueled with [233]U/Al alloy and ongoing irradiation in KAMINI (world's only operating research reactor fueled with Al-20 % [233]U alloy), it has no direct relevance with thorium-based metallic fuels since the [233]U for these reactors has been extracted from irradiated oxide fuels and not metallic fuels.

Recently, Some work on preparation of pure (>99%) thorium metal powder with the aim of developing thorium-uranium alloys [17] and their thermal and thermo-physical characterization [42] has appeared in literature, being pursued in our organization. However, it must be mentioned here that timely and indigenous developmental efforts are very much required in this direction so as to understand the potential of these metallic fuels.

5. Conclusion and future scope

From the brief account of information discussed in the article, it is clear that ample potential exist in thorium-based metallic alloys to be used as potential fuels for future nuclear reactors, both in thermal and fast neutron spectrum. However, the conditions (physical, chemical and neutronic), in which these fuels are expected/required to operate safely for longer durations to achieve high burnups, needs extensive research database on fuel fabrication, in-pile/out-of-pile behavior, reprocessing aspects and waste-form characteristics, etc. Accumulation of such an extensive database is challenging as well as time consuming. In an inevitable scenario of (i) growing role of nuclear technology in obtaining energy security across the globe and (ii) need of high performance, safe and sustainable nuclear fuel options with minimum waste burden, it is highly desirous to carry out systematic R&D efforts towards timely development of thorium-based metallic fuels. Potential of modern computational and simulation methods, a very useful tool in modern day science, should be utilized fully in this direction to zero-in the most desirous fuel options and design experiments, which need to be performed to understand them.

Most of the ambitious and extensive projects, which started during 1950s-1960s, aimed at exploring the potential of thorium-based alloy fuels, stopped virtually around 1980s. Nearly all the results of these works have indicated the inherent advantages and prospects of using these fuels for electricity generation. The reasons for the decline in R&D efforts towards these fuels could be multifold such as (i) complexity of the projects (ii) increased availability of uranium and moderation (or even decline) in its price rise during 1970s-80s (iii) USA, by and large opting for a nuclear strategy based on open fuel cycle and thereby completely banning the option of

reprocessing, a step without which thorium-based fuel cycle can not be envisaged, etc.

Furthermore, due to the inherent radiological issues associated with the thorium fuel cycle, the fabrication, reprocessing and re-fabrication technology for thorium-based metallic fuels, as compared to their uranium-based counterparts, would be relatively challenging, as they are for the ThO$_2$-based fuel options. However, with the ever increasing technological breakthroughs (such as those being seen in advanced fuel fabrication and remote handling of U-Pu MOX fuels spin-off), it should not be treated as a limitation and more emphasis should be given towards optimizing the process flow sheets. Once the flow sheets for each of these steps in thorium-based metallic fuel cycle are established, it is likely to serve for our future energy security in a significant way. Los Alamos National Laboratory has already started to develop the required computational codes that feature novel thorium fuels [12]. With the inevitable requirement of a sustainable, environment friendly, non-proliferative, safe and waste intensive nuclear energy supply, it is certain that thorium-based fuels will sooner; once again find their place in the mainstream of research, development and appropriate usage in future reactors.

Acknowledgement:

References:

1. P. Rodrigues, C.V. Sundaram, *J. Nucl. Mater.*, 100 (1981) 227.

2. M. Lung and O. Grem, *Nucl. Engg. Design* 180 (1998) 133.

3. "*Thorium fuel cycle-Potential benefits and challenges*", IAEA-TECDOC-1450, International Atomic Energy Association (April 2005).

4. S. Banerjee, R.K. Sinha, S. Kailas, *J. Phy.: Conf. Series* 312 (2011) 062002.

5. R.K. Sinha and A. Kakodkar, *Nucl. Engg. & Design* 236(7-8) (2006) 683.

6. W.J. Carmak, D.L. Porter, Y.I. Chang, S.L. Hayes, M.K. Meyer, D.E. Burkes, C.B. Lee, T. Mizuno, F. Delage and J. Somers, *J. Nucl. Mater.*, 392 (2009) 139.

7. G.L. Hoffman, L.C. Walters and T.H. Bauer, *Prog. Nucl. Energy* 31(2) (1997) 83.

8. S.C. Chetal, P. Chellapandi, P. Puthiyavinayagam, S.Raghupathy, V.Balasubramaniyan, P. Selvaraj, P. Mohanakrishnan and B. Raj, *Energy Proc.,* 7 (2011) 64.

9. L.C. Walters, *J. Nucl. Mater.,* 270 (1999) 39.

10. "*Thermophysical properties of materials for nuclear engineering: A tutorial and collection of data*", IAEA-THPH, International Atomic Energy Agency, Vienna (2008).

11. S.M. Oggianu, H.C. No, M.S. Kazimi, *Nucl. Tech.,* 143(3) (2003) 256.

12. C.S. Holden, "*Rapid computational path for sustainable and renewable nuclear energy using metallic thorium fuels*", Presented at 2nd Thorium energy conference ThEC-2010, Mountain View CA (2010).

13. S.Z. Ghrayeb, K.N. Ivanov, S.H. Levine, E.P. Loewen, *Nucl. Tech.,* 176 (2011) 188.

14. R.D. Mariani, D.L. Porter, S.L. Hayes, J.R. Kennedy, *Proceedia Chemistry* 7 (2012) 513.

15. B. Blumenthal, J.E. Sanecki and D.E. Busch, "*Thorium-uranium-plutonium alloys as potential fast power reactor fuels; part-I: Thorium-uranium-plutonium phase diagram*", report no.: ANL-7258, Argonne National Laboratory, Illinois (September 1968).

16. B. Blumenthal, J.E. Sanecki, D.E. Busch and D.R. O'Boyle, "*Thorium-uranium-plutonium alloys as potential fast power reactor fuels; part-II: Properties and irradiation behavior of thorium-uranium-plutonium alloys*", report no.: ANL-7259, Argonne National laboraty, Illinois (October 1969).

17. S. Das, R. Kumar, S.B. Roy, A.K. Suri, "*Development study on metallic thorium and uranium-thorium alloy*", BARC Newsletter-Founder's Day Special issue (2011) 72.

18. S.Z. Ghrayeb, "*Investigations of thorium-based fuels to improve actinide buring rate in S-PRISM reactor*", M.Sc. thesis, The Pennsylvania State University (December 2008).

19. R.G. Wymer, D.A. Douglas Jr., "*Status and progress report for thorium fuel cycle development for period ending December 31, 1964*", report no.: ORNL-3831, Oak Ridge National laboratory, Tennessee (May 1966).

20. A.E. Waltar, D. Todd, P.V. Tsvetkov, "*Book: Fast Spectrum reactors*", Springer (2011).

21. S. Peterson, R.E. Adams, D.A. Douglas Jr., "*Properties of thorium, its alloys and its compounds*", report no.: ORNL-TM-1144, Oak Ridge National laboratory, Tennessee (June 1965).

22. D.R. Marr, D.A. Cantley, J.C. Chandler, D.C. McCurry, R.P. Omberg, "*Performance of thorium fueled fast breeders*", report no.: HEDL-SA-1327-FP, Hanford Engineering Development Laboratory, Richland, USA (October 1977).

23. G.L. Copeland, "*Evaluation of thorium-uranium alloys for the unclad metal breeder reactor*", report no.: ORNL-4557, Oak Ridge National Laboratory, Tennessee (June 1970).

24. R.M. Carroll, "*The effects of reactor irradiation on thorium-uranium alloy fuel plates*", report no.: ORNL-1938, Oak Ridge National Laboratory, Tennessee (August 1955).

25. B.R. Hayward, P. Corzine, "*Thorium uranium fuel elements for SRE*", Presented at 2nd U.N. international conference on the peaceful uses of atomic energy, Geneva (October 1958).

26. J.L. Ballif, B.R. Hayward, J.W. Walter, "*Engineering evaluation of a mixed alloy fuel element irradiated at elevated temperatures in SRE*", Technical report no.: NAA-SR-3888, Atomics International Division, North American Aviation Incorporation, California, USA (June 1960).

27. A.R. Olsen, "*Thorium and thorium alloys: Preliminary corrosion tests*", report no.: ORNL-1066, Oak Ridge National Laboratory, Tennessee (November 1951).

28. M.S. Farkas, A.A. Bauer and R.F. Dickerson, "*Development of thorium-uranium-base fuel alloys,*" report no.: BMI-1428, Battelle Memorial Institute, Columbus, Ohio (March 1960).

29. R.H. Cole, L.E. Wilkinson, "*Development of high strength ternary and quaternary thorium-uranium base alloys*", technical report no.: ATL-A-128, Advanced Technology Laboratory, California (1961).

30. J.H. Kittel, J.A. Horak, W.F. Murphy, S.H. Paine, "*Effect of irradiation on thorium and thorium-uranium alloys*", technical report no.: ANL-5674, Argonne National laboratory, Illinois, USA (April 1963).

31. A.L. Bement, "*Burnup and specific power calculations for the thermal neutron irradiation on thorium-uranium alloys*", technical report no: HW-56631, General Electric Co. Hanford Atomic Products Operation, Richland, Washington (1958).

32. F.W. Dodge, E.W. Murbach, L.A. Hanson, *Nuclear Science and Engineering* 6 (6) (1959) 533.

33. P. Chiotti, A.F. Voigt, "*Pyrometallurgical Processing*", Technical Report: A/CONF.15/P/517; ISC-1018, Ames Laboratory, Iowa (October 1958).

34. W.N. Hensen, "*Electrolysis of thorium and uranium*", US-Patent no.: US 2951793 (1960).

35. G.B. Zorzoli, *Nucl. Tech.,* 20 (1973) 109.

36. F. Correa, D.J. Driscoll, D.D. Lanning, "*An evaluation of tight pitch PWR cores*", technical report no.: MIT-EL-79-022, Massachusetts Institute of Technology, Cambridge, Massachusetts (1979).

37. M. Lung, "*A present review of the thorium nuclear fuel cycles*", European commission report no.: EUR-17771-EN, (1997).

38. Z.S. Li, X.J. Liu, C.P. Wang, *J. Alloys & Comp.,* 473 (2009) 193.

39. T. Yamamoto, H. Suwarno, F. Ono, H. Kayano, M. Yamawaki, *J. Alloys & Comp.,* 271-273 (1998) 702.

40. T. Yamamoto, H. Suwarno, H. Kayano, M. Yamawaki, *J. Nucl. Sci. Tech.,* 32 (1995) 260.

41. T. Okawa, H. Sekimoto and S. Nakayama, "*Design study on power flattening to sodium cooled large scale CANDLE burning reactor with using thorium fuel*", in Presented at 18th international conference on Nuclear Engineering, ICONE18, China, 2010.

42. D. Jain, C.G.S. Pillai, "*Thermophysical characterization of Thorium and Uranium-based metallic fuels and alloys*" ITAS Bulletin, Indian Thermal Analysis Society, 2012.

Shri Dheeraj Jain *joined BARC in 2004 after graduating from 47th batch of BARC Training School in Chemistry discipline.* Since then he has been pursuing his research activities in the field of thermophysical characterization of thorium-based nuclear fuels and related materials and investigation of sintering kinetics of nanomaterials, solid-state chemistry, etc. His current research activities include assessment of thermophysical properties of uranium and thorium-based metallic fuels and related materials, development of CVD diamond thin films for radiation detector applications under harsh environments, sintering kinetics of nuclear materials, and electrical characterization of oxides using ac impedance spectroscopy. He has been the recipient of TA-ITAS Young scientist award (2012) in recognition of his work in the area of thermal analysis.

Dr. V. Sudarsan *joined Chemistry Division of BARC in the year 1994 after graduating from 37th batch of BARC Training School. He received his Ph.D. degree in Chemistry from Mumbai University in the year 2002. Subsequently he worked for a period of two years at the University of Victoria, British Columbia, Canada in the area of luminescence of lanthanide ions which are doped in nanoparticles of inorganic hosts. Currently he is working on the optical and structural properties of lanthanide ions doped nanoparticles and glasses. In recognition of his work, he was conferred with DAE Scientific and Technical Excellence Award (2010). He is also associated with BARC Training School activities. Presently, he is heading Materials Chemistry Section of Chemistry Division.*

Dr. A. K. Tyagi *is presently Head, Solid State Chemistry Section, Chemistry Division, Bhabha Atomic Research Centre (BARC), Mumbai and also a Professor (Chemistry) at Homi Bhabha National Institute (HBNI). He joined BARC, Mumbai in 1986 through BARC-Training School. Since then he has been working in the field of Chemistry of nanomaterials, functional materials and nuclear materials. He was a Max-Planck Fellow at MPI, Stuttgart, Germany during 1995-96. In recognition of his work, Dr. Tyagi has been conferred with several prestigious awards such as Homi Bhabha Science & Technology Award, Gold Medal of Indian Nuclear Society, MRSI Medal, CRSI Medal, Dr. Laxmi Award by ISCAS, Rheometric Scientific-ITAS Award, and IANCAS-Dr. Tarun Datta Memorial Award, RD Desai Memorial Award of ICS, Rajib Goyal Prize in Chemical Sciences, DAE-SRC Outstanding Researcher Award, CRSI's Prof. C.N.R. Rao National Prize for Chemical Sciences and ISCB award for excellence in chemical sciences. He is a Fellow of Royal Society of Chemistry, UK (FRSC), National Academy of Sciences, India (FNASc), Maharashtra Academy of Sciences (FMASc) and Indian Academy of Sciences (FASc). He has been a visiting scientist to several countries like Germany, USA, Canada, France, Spain, Sweden, Portugal, Russia, Japan, Israel, China, Singapore, Malaysia and Australia.*

Thermochemistry of thoria based compounds and its relevance to the safety of Advanced Heavy Water Reactors (AHWR)

S. R. Dharwadkar

Department of Chemistry
University of Mumbai, Kalina, Mumbai 400098
E-mail: srdharwadkar@hotmail.com

Abstract

This paper deals with the thermochemistry of some thorium based compounds which could be formed during irradiation of thoria-based nuclear fuel in Advanced Heavy Water Reactor (AHWR) and its relevance on the safety of such reactors during operation. The issues related to the techniques employed for the acquisition of such data and the care to be exercised in such measurements to obtain reliable thermodynamic data are also discussed.

1. Introduction

The third stage of nuclear power program of India envisages the use of thoria based fuels [1]. The fuel will contain 2-4 % of fissile isotopes of uranium (^{233}U) having the fission yield profile almost identical to that of ^{235}U [2] or plutonium (^{239}Pu) in mixed oxide. The fuel with > 90 mol % thorium content will be utilized for power generation in nuclear reactors through in situ breeding of the ^{233}U isotope. Several elements (more than 40) in the periodic table are produced during the fission of heavy elements, in quantities which can be determined by normal analytical techniques. For smooth and safe operation of nuclear reactors, it is important to look into the chemical reactivities of the fission products of these elements (uranium and plutonium) with the fuel matrix, the clad and among each other. The chemical interactions of these elements with thoria matrix could result in the formation of low density compounds, which could adversely affect the performance of the fuel due to swelling, the changes in properties such as thermal expansion and thermal conductivity of the fuel and the transport of the volatile fission products from the fuel to the fuel clad gap.

The present paper is confined to the work done on the thermodynamic investigations on some ternary Thorium-based oxides. The influence of formation of such compounds in the thoria matrix on the fuel swelling due to retention of fission products within the fuel pellet and the release of the volatile and corrosive fission products to the fuel–clad gap can be predicted from such data. The literature though replete with such data for the urania based fuel [3, 4], is too scanty for thoria based fuels. The reactivity of thoria is expected to be different compared to urania by virtue of the stable 4$^+$ oxidation state of thorium. The thermochemical data for the compounds of fission

products with thoria is therefore invaluable and would greatly facilitate prediction of the performance of such fuel during irradiation. Further, it will also enable improvement in the fuel design to minimize the detrimental effects caused due to the formation of such compounds.

The existence of relatively lower density ternary oxide compounds of several fission products, including those of alkali and alkaline earth elements with thorium, is known but the possibility of formation of such compounds under the conditions prevailing in the fuel pin during irradiation (varying oxygen potential) can be predicted only if the thermodynamic data such as standard free energy of formation for such compounds are available with fairly high degree of accuracy. Several groups in different units of the Department of Atomic Energy in India are engaged in such activity and have contributed significantly to the acquisition of such an important basic data, necessary for prediction of fuel performance during irradiation. The contributions of these groups to this important activity are reviewed and the predictions made for the formation of these compounds in the fuel pin during irradiation are briefly discussed.

The standard Gibbs free energy of formation is the most important thermodynamic parameter for the substances which enables prediction of the feasibility of the reactions in which these substances participate as the reaction components, under a given set of experimental constraints such as temperature, pressure and composition. It can be determined either directly or by the combination of their enthalpy and entropy of formation employing the Gibbs –Helmholtz equation. All the thermodynamic quantities are tabulated under the standard condition of 298.15K and normal atmospheric pressure. Several reactions have been found to be thermodynamically feasible at

this temperature, but do not occur at an appreciable rate because of large kinetic barrier. Normally, the reactions are carried out at elevated temperatures at which these are kinetically favorable and the data obtained at these temperatures are converted to 298.15K using the heat capacity of the reactants and the products, employing the Kirchoff law. The measurement of thermodynamic properties essentially involves acquisition of the standard enthalpy of formation of the compounds, and their heat capacity as a function of temperature from which their standard free energy of formation can be derived .The other measurements involve direct determination of standard free energy of formation. The methods for acquisition of such data are briefly reviewed in the following section.

2. Techniques for the measurement of thermodynamic quantities

Calorimetry, vapor pressure and the galvanic cell electromotive force measurements are the most frequently used techniques for the acquisition of the thermodynamic data for the materials. An excellent book on these techniques has been published by Kubaschewski, Alcock and Spencer [5].

2.1 Calorimetry

Calorimetry is mainly employed for the determination of the heat capacity and the enthalpy changes accompanying the physical and chemical processes. Different types of calorimeters have been developed and used for the acquisition of the standard enthalpy of formation and heat capacity over a wide temperature range .The techniques and their continuous evolution have been adequately described in number of excellent books, monographs and special reviews [6,7]. The calorimeters have been classified in different categories. These are I. Isothermal calorimeter, II. Isoperibol calorimeter, and III. Adiabatic calorimeter. In isothermal calorimeter the temperature of the calorimeter remains constant as the physical or chemical process takes place in the calorimetric vessel. Bunsen ice calorimeter and the diphenyl ether calorimeter fall in this category. The amount of heat evolved or absorbed is determined from the amount of the phase transformed due to the heat evolved or absorbed from the two phase mixture. Since the latent heat of fusion are known for such substances, the volume change occurring in the mixture due to increase or decrease of temperature caused due to physical or chemical phenomena in the calorimeter can be transformed to the amount of heat released or absorbed in the process. This is one of the oldest types of calorimeters, but has been successfully used in several investigations [5].

In isoperibol calorimeter, the calorimeter vessel is placed in a thermostat maintained at the constant temperature. The calorimeter essentially consists of a double walled Devar flask placed in a copper vessel. The annular space between the wall of the Devar flask and copper vessel is filled with a thermally insulating material like thermocole. A solvent in which the reaction has to be carried out is placed in the Devar flask. A thermistor, miniature heater, a stirrer and the glass tube with a thin walled sample bulb are located in this solvent through the top lid of the calorimeter. The experiment consists of the establishment of thermal equilibrium of the calorimeter vessel with its contents, with the thermostat. This is concluded from the attainment of constant time-temperature base line recorded for the solvent contained in the Devar flask .The reaction of the solid or liquid with the solvent is then initiated by breaking the bulb located in the solvent and establishing the contact of the reactant with the solvent. The change in temperature due to the reaction is indicated by the temperature –time plot from the microvolt signal produced by a thermister located in the solvent. The magnitude of this signal is proportional to the amount of heat generated in the reaction. The calorimeter with the amount of solvent used in the experiment is calibrated electrically, prior to the dissolution step, by passing the known amount of current in it from the stabilized power supply. Alternately , it can also be calibrated using the heat of dissolution of some NIST recommended calibration materials like TRIS for which the enthalpy of dissolution is known with high degree of accuracy. The temperature changes of the order of thousandth's of degree can be measured in these experiments. A schematic of typical
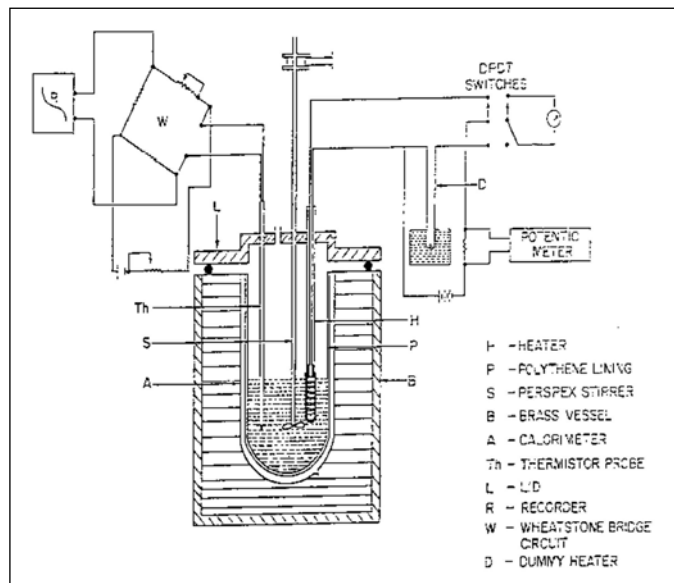

Fig.1: A schematic of typical isoperibol calorimeter

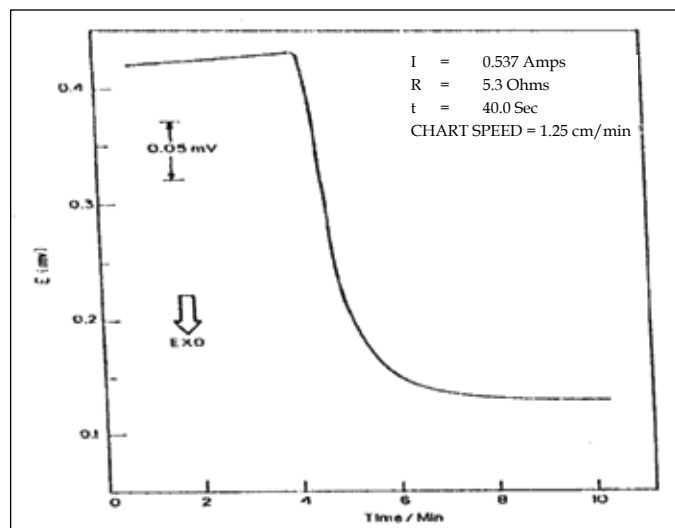|		
I	=	0.537 Amps
R	=	5.3 Ohms
t	=	40.0 Sec
CHART SPEED = 1.25 cm/min		

Fig.2: An electrical calibration plot for isoperibol solution calorimeter

isoperibol calorimeter is shown in Fig.1. An electrical calibration plot obtained for the calorimeter along with its contents is shown in Fig.2. Several investigations using this calorimeter were carried out in the author's laboratory.

In adiabatic calorimeter the sample located in the furnace is surrounded by a shield. The temperature change in the sample is maintained identical to that of the shield by adjusting the power to the furnace. Under these conditions, there is no heat transport from the sample to the shield and the sample is virtually heated under adiabatic condition. If the energy input to the shield needed for maintaining the zero temperature difference between the sample and the shield is known, then the heat capacity of the sample can be determined directly. Similarly the heat evolved or absorbed can also be determined by using such calorimeter. Such calorimeters can be employed to follow the heat changes accompanying slow reactions, but the accuracy of the measurements decreases at high temperatures due to the radiation losses which cannot be readily compensated to strictly maintain the adiabatic conditions. Similar heat capacity data can be obtained from the enthalpy increments employing the drop calorimeter [6, 7]. However, this procedure requires relatively more time for the measurements.

In addition to these, there are other calorimeters which fall under the category of 'heat flux' and 'power compensation calorimeters' [8]. These calorimeters operate in dynamic conditions when the samples under investigation are subjected to the constant programmed heating and cooling. Though the time involved in the data acquisition is relatively less, the accuracy of the data obtained with these calorimeters, frequently do not match with that obtained by conventional calorimetric techniques.

A special type of calorimeter called 'bomb calorimeter' is used for the determination of the reaction enthalpy directly. Such calorimeters have been employed for the determination of the heat of formation of oxides, nitrides; halides etc. and involve the measurement of heat released when the metals react to produce these compounds when heated in the respective gaseous environments. The measurements are carried out in closed vessels with the fixed volume of the reactant gas. These experiments generally measure the internal energy change during the reaction, which can be converted to the enthalpy change if the change in number of moles of the gaseous reactants during the reaction can be obtained.

Needless to say that for all accurate calorimetric measurements careful calibration of temperature and enthalpy measuring instruments is extremely important. The key role of calorimetry in thermodynamic property measurements has been highlighted in several books and monographs [7, 8].

2.1.1 Determination of the entropy change for the reaction

The acquisition of the standard free energy change for the reaction by calorimetry needs enthalpy as well as entropy of formation for the reactants as well as the products. The enthalpy change for the reaction, as seen from the foregoing description, can be obtained by the direct calorimetric measurements but it is not possible to measure the entropy directly. The determination of entropy change for the reaction requires the measurement of the entropy of formation of each of the chemical species appearing in the reaction. This involves the measurement of the heat capacity of the materials under equilibrium conditions upto absolute zero of temperature and plotting the curve of heat capacity versus temperature down to absolute zero. The curve is extrapolated to absolute zero fitting the low temperature part of the curve to the Debye equation. The area under the curve of C_p/T versus T at any temperature gives the entropy of any substance under investigation at that temperature. The entropy change in any reaction can thus be evaluated from the measured entropies of all the species appearing in the reaction and can be used for the determination standard free energy of formation of the substance under investigation by calorimetry employing the Gibbs-Helmholtz equation.

The probable errors in the enthalpy and heat capacity measurements by calorimetry:

The enthalpy and the heat capacity data obtained by calorimetry are subject to different types of errors which need to be recognized. Some of the factors which can contribute to the errors are 1.improper characterization of the material from the point of phase purity and composition, 2. Establishment of thermal equilibrium, 3. Improper knowledge of the reaction species in solution and 4. Energy losses due to the temperature gradients and the gaseous species evolved in the reactions. In several cases, as in the case of solution calorimetry, it is necessary to use lot of auxiliary data from the literature to transform the measured enthalpy values to the standard state. In such cases the data adopted from the literature has to be properly assessed for its accuracy.

The standard free energy of formation of materials obtained by calorimetry generally has larger uncertainties in view of the fact that it is derived from two independent measurements combined through the Gibbs-Helmholtz equation.

2.2 Vapor pressure measurement

Until the end of the first half of the last century, the standard Gibbs energy of formation of materials was determined mainly by the calorimetric technique. Dissociation pressure measurements employing, mercury or oil manometers and sickle gauges were also used wherever possible. The latter method was employed mainly for the heterogeneous reactions in which the permanent non condensable gases were formed as one or more of the reaction products. The rapid progress in the instrumentation in the second half of the twentieth century facilitated the measurement of vapor pressure of materials yielding the non-condensable vapors. Among the several methods, the transpiration and Knudsen effusion methods have contributed greatly to the acquisition of thermodynamic stability data for large number of materials which vaporized yielding the condensable vapors. Several variants of the transpiration and Knudsen effusion techniques have evolved over the years [9, 10]. The automatic recording transpiration apparatus are now built [11] which can be used in any inert or reactive gaseous environments. In addition to enthalpy of vaporization, transpiration technique can also provide information on identity of the vapor species and the stoichiometry of the vaporization reaction in some selected type of systems [12]. The discovery of metal clusters [13] , volatile transition metal oxides such as CrO_3 [14], oxides of uranium, molybdenum and tungsten [15] and the hydroxides of

transition metals [16] and uranium in vapor phase [17] are among the few such examples.

In the transpiration experiment, the amount of vapor transported by the known amount of the carrier gas swept over the vaporizing sample maintained at the constant temperature in uniform temperature zone of the furnace is measured under nearly equilibrium condition. The partial pressure of the vapor in the mixture of the carrier gas is derived by the application of the Dalton's law of partial pressure to the mixture of the carrier gas saturated with the vapor. The equilibrium between the condensed phases and the vapor is first confirmed by measuring the apparent vapor pressure as a function of the flow rate of the carrier gas at some selected flow rate in the temperature range of measurements. The flow independent region of the apparent pressure indicates the range over which the equilibrium is maintained between the vapor and the condensed phase. In this experiment it is assumed that the transport of the vapor is by the carrier gas alone and the contribution to the mass loss of the sample by any other process such as diffusion of the vapor caused due to temperature and concentration gradient in the reaction system is negligible. If the mass loss in the sample is monitored by gravimetry then it is necessary to confirm that the container material is thermally inert and does not contribute to the mass loss. The mean enthalpy of vaporization reaction over the
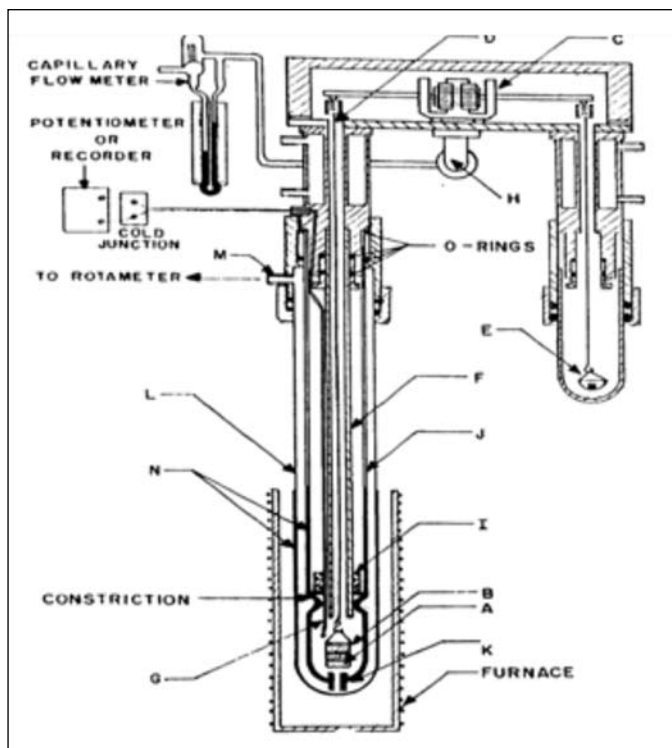

Fig.3. A schematic of the automatically recording transpiration assembly

temperature range of measurements is derived from the slope of the lnp versus 1/T plot. The standard enthalpy of formation of the condensed phases as well as the vapor species can be derived from such measurements. Any slope change in the lnp versus Temperature plot indicates either the change of state of the vaporizing material such as melting or polymorphic transformation or polymerization of the vapor species with the increasing temperature when the condensed vaporizing phase/s and the vapor are in equilibrium. A schematic of the automatically recording transpiration assembly is shown in Fig.3.

The Knudsen effusion technique was used initially for the measurement of the flux of the vapor emanating from the orifice of the Knudsen cell resulting from the sample enclosed in the cell and heated in vacuum .The vapor pressure was then evaluated from the measured flux using the Knudsen equation derived based on the kinetic theory of gases applied to gases at low pressures. As in the case of transpiration technique, it is necessary to establish that the vapor effusing from the Knudsen cell orifice does not disturb the equilibrium between the condensed phase and the vapor in the Knudsen cell. This is done by obtaining the apparent vapor pressure as the function of the orifice diameter. Under equilibrium condition the apparent vapor pressure should be independent of the size of the orifice diameter. The vapor pressure by Knudsen effusion technique is determined following various methods, which include

1. Forward collection technique:

    In this approach a fraction of the vapor effusing from the Knudsen cell orifice is collected on a planchet located at certain distance from the orifice. The fraction of the vapor collected on the planchet is dictated by the diameter of the collimeter and the distance of the planchet from the orifice of the Knudsen cell. Several planchets are stacked one above the other in a cylindrical copper cartridge, cooled by water, located vertically above the Knudsen, cell coaxial with the orifice. These planchets can be ejected in a sequence into the glass pouch by exposing to the molecular beam of vapor for known length of time. The vapor pressure is then deduced from the chemical assay of the amount of the vapor deposited on the planchet in a fixed time interval. A schematic of one such instrument is shown in Fig.4.

2. The Mass Loss Method:

    This method involves the measurement of the mass loss of the material due to vapor effusing from the Knudsen cell in vacuum which is monitored employing
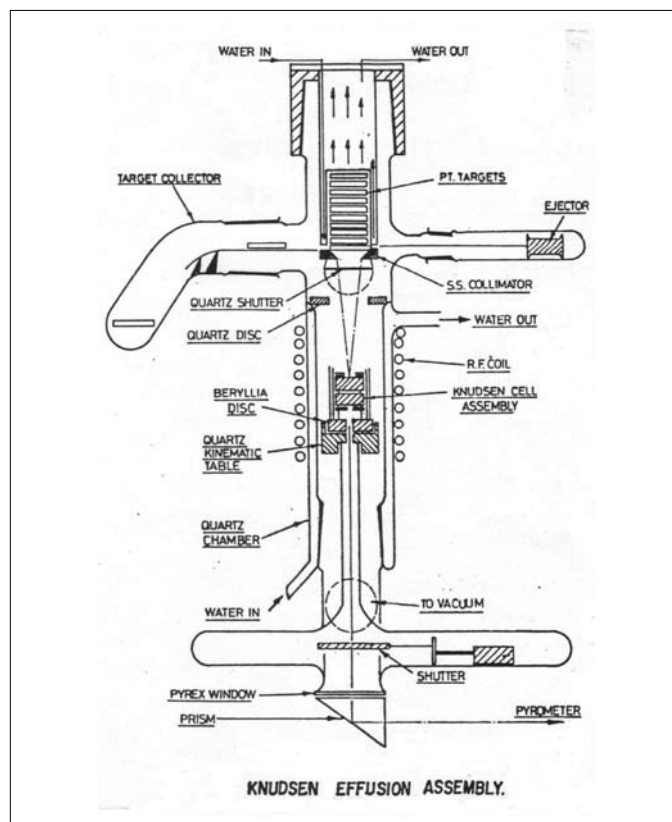

Fig.4: Schematic of Knudsen Effusion Assembly

the thermo microbalance. It is however important to ensure that the mass loss is originating only from the vapor effusing from the Knudsen cell and the sample container is thermally inert, not contributing to the mass loss by its vaporization. Further, it is important to confirm that the vaporizing material does not interact chemically with the container .In order to avoid this situation the inside part of the Knudsen cell is often coated with the inert material liner such as recrystallized alumina or zirconia which separates the vaporizing material from the container surface.

In Knudsen cell vapor pressure measurements the cell has to be located in the uniform temperature zone of the heater to avoid condensation of the vapor on the orifice which could interact chemically and be the factor responsible for the change of the effective diameter of the orifice either by condensation of the vapor around the orifice or chemical reaction. Such observation was made during the vapor pressure measurement of liquid uranium. The temperature gradient between the liquid uranium contained in the cell and the lid of the cell resulted in the chemical interaction of the liquid uranium condensed near the orifice surface with the tungsten lid, thereby increasing its effective diameter and disturbing the equilibrium between the vaporizing liquid uranium

and its vapor [18]. In transpiration as well as Knudsen effusion technique it is imperative to know the molecular weight of the vapor species in order to calculate the vapor pressure , which often is assumed to be the same as that of the condensed phase. This assumption is often incorrect since in several systems the vaporization proceeds incongruently. Also in several cases the vaporization can yield several polymeric species in the vapor phase with their relative importance changing with temperature. In order to derive the thermodynamic stability data of the condensed phase as well as the vapor species, it is therefore necessary to know the nature of the vapor species formed in the vaporization process. This problem however, has been successively resolved by coupling the Knudsen cell assembly with the mass spectrometers. Several commercial organizations currently supply the custom built units for such measurements.

2.2.1 Knudsen Effusion Mass Spectrometric [KEMS} technique for vapor pressure measurement

In Knudsen effusion Mass Spectrometric (KEMS) measurements the molecular beam emerging from the Knudsen cell is introduced in the ion source and the vapor species contained in the molecular beam are ionized and drifted in the mass analyzer under the applied potential which subsequently enters the channeltron, or Faraday cup in the analyzer, which converts it into ion current. The ion current is the measure of the vapor pressure of the species entering the analyzer. The observed ion current is then converted into the partial pressure of the species entering the mass analyzer, using the equation relating ion current with the vapor pressure of the species under consideration by the equation

$$p_i = k \times \frac{I_i T}{\gamma A_i \sigma_i}$$

Where p_i is the partial pressure of the vaporizing species I, k is the instrumental factor, I_i is the intensity of the species I, T is the absolute temperature, γ is the multiplier gain of the instrument, A_i is the isotopic abundance for the species 'i' and σ_i is the ionization cross section of i. An excellent critical review on Knudsen Effusion Mass Spectrometry is published by Hilpert [19] which could serve as a guide for the scientists working in this area. The total pressure in the cell is evaluated in terms of the ion current by evaporating the known amount of sample in the cell and measuring the total ion current produced.

The advantage of KEMS apart from identifying the individual vapor species and their relative abundance is that it is possible to evaluate the enthalpy of vaporization of each of the vapor species from the condensed phase

and also the energy of polymerization in the vapor phase in case the material yields the polymeric species in the vapor phase. The details of deriving such information from KEMS are available in the books edited by Margrave [9] and Hastie [10].

One of the most important factors in the measurement of vapor pressure by mass spectrometry is that the vapor species observed in the vapor may not originate from the vaporizing phase alone. There can be substantial contribution to the vapor from the fragments of higher mass number to the low mass number species as a result of the fragmentation of the former subjected to the potential needed for their ionization. It is however possible to segregate the contribution due to this factor from the variation of the partial pressure of the species under consideration with temperature. The partial pressures of the species originating from the condensed phase/s indicate exponential dependence on temperature but those formed by the fragmentation of higher molecular mass species are independent of temperature, which can be separated from total ion current. The plot of the log of the product of ion current for the particular species and temperature versus 1/T yields the enthalpy of vaporization of that species from the condensed phase. The procedure for the derivation of the thermodynamic parameters from these data is identical to that followed in other normal Knudsen effusion techniques.

2.3 Solid Electrolyte Galvanic Cell Technique

The galvanic cells provide direct method for the acquisition of standard Gibbs energy of formation of the compounds from the electromotive force generated due to the reaction involving the formation of the compound. The procedure involves setting of Galvanic cell and measuring the EMF between the two electrodes. One of the electrodes serves as a reference and at the other electrode we have the cell reaction involving the formation of the compound. The EMF of the cell is the sum of the potentials generated at the two electrodes. Hence by knowing the EMF of the half cell reference electrode, that for the formation of the compound at the other electrode can be evaluated. The relation between the cell EMF and the standard free energy change is given by the Nernst equation which can be represented as

$\Delta G = -nFE$

The use of solid electrolyte galvanic cells for thermodynamic property measurement of solid compounds was reported in the work of Kiokkula and Wagner [20] who first used such cells to determine the oxygen potentials. They measured the free energy of formation of oxides

from EMF measurements using ZrO_2 and ThO_2 based solid electrolytes which conduct only by oxide ions. The cell can be represented as the oxygen concentration cell. The EMF of the cell is generated by the difference in oxygen potential at the two electrodes separated by an oxide electrolyte. An excellent monograph on solid electrolytes and their applications in thermodynamic property measurements has been edited by Subba Rao [21].

The EMF measurements involve the recording of the open cell potential developed between the two electrodes separated by an electrolyte. The EMF measurement instrument should have high input impedance so that negligible current flows through it and the cell operates virtually under open circuit condition, where the cell output is maximum. When any system undergoes reversible process at a constant temperature T and pressure P, the decrease in free energy 'G' of the system equals the maximum work, ' Wmax' done by the system(which does not include the mechanical (PV type) work. The standard free energy change for this process is related to the maximum work which the system can perform by the relation

$-\Delta G° = \Delta Wmax = nFE$

In the process involving transport of electric charge across the electric potential difference, the work performed is obtained as the product of the charge transported 'q'(coulombs) and electric potential difference E. The unit of such work is 'Joule'(Volt×Coulomb).

A system which is capable of performing electric work as a result of occurrence of the chemical reaction is called a Galvanic Cell. The overall chemical reaction represented by a chemical equation is called the cell reaction. If n gram ions of valency Z are transported through the voltage difference E maintained between the electrodes of the cell then $\Delta W = n.F.E$. If the transportation is conducted 'reversibly' then the electric potential between the electrodes is termed as the standard electro motive force (EMF), 'E' of the cell which can be expressed as: $Wmax = n.F.E = -\Delta G°$

The standard Gibbs energy of formation of a number of solid substances has been determined using solid electrolyte galvanic cell measurements. Application of solid electrolyte galvanic cells for the determination of standard free energy of formation ($\Delta G_f°$) of solids should satisfy the following criteria.

1. It is necessary to establish that a single, unambiguous cell reaction takes place 'reversibly' on passage of infinitesimal charge, and that only this reaction is responsible for the measured EMF.

2. It is necessary that the charge transport through the cell obeys the Faradays laws of electrolysis. This necessitates, that there is one phase which is purely ionic separating the two electrode compartments. This requirement severely limits the number of solids that can be used as solid electrolytes in solid state galvanic cells. The oxides and fluorides are commonly used in such measurements. These are predominantly O^{2-} and F^- ion conducting electrolytes.

Majority of the solid electrolyte galvanic cell measurements employ solid oxide electrolytes, viz. calcia stabilized zirconia (CSZ) and yttrium doped thoria (YDT). The oxygen pressure ranges corresponding to their ionic domains are p_{O2} = 1 to 10^{-20} atm. and p_{O2} =1 to 10^{-30} atm. for CSZ and YDT respectively. The electrolytes , CSZ and YDT can be categorized under the extrinsic defects electrolytes, where oxygen transport from cathode to anode take place through the oxygen vacancies created by doping zirconia and thoria by lower oxidation state ions, namely Ca^{2+} and Y^{3+} respectively. The calcium fluoride electrolyte however, has intrinsic vacancies which facilitates migration of the fluoride ions through the electrolyte. The concentration of these vacancies increase exponentially with increase in the temperature.

Typical Galvanic Cell Systems studied employing CSZ and YDT

1. **Free energy of formation of binary oxides**

   The cell reaction can be represented by: A(s), AO(s) / electrolyte/ B(s), BO(g). The representative net reaction is A(s) + BO(s) = B(s) + AO(s), where A(s), B(s) are Cu, Ni, Co, Fe, Mn, Sn, Cr, V, Nb. Etc.

2. **Free energy of formation of ternary oxides**

   The cell can be represented as: A(s), AB_2O_4(s), B_2O_3(s) /electrolyte/ A(s), AO(s). The net reaction can be represented as B_2O_3(s) + AO(s) = AB_2O_4(s). This is applicable for ferrites, cobaltites, silicates, molybdates etc.

3. **Activities of the alloys**

   The cell can be represented as: A(s), AO /electrolyte/ [A]B(s), AO. The reaction involves dissolution of B in a resulting in the formation of an alloy.

4. **Study of single phase non-stoichiometric oxides**

   Cell representation: MO_{1-x}(s) /electrolyte/A(s), AO(s), where M and A are metals. The typical reaction is $1/y$ MO_{1-x}(s) + ½ O_2(s) = $1/y$ MO_{1-x-y}(s). Examples UO_{2+x}, FeO_{1-y}, NiO etc.

5. Thermodynamics of oxygen dissolved in molten metal

Cell: [O]M(s) / electrolyte/ A(s), AO(s) (or Oxygen). Similar cells can be set up employing CaF_2 as a solid electrolyte.

2.3.1 A Solid Electrolyte Galvanic Cell set up

A typical solid state galvanic cell set up consists of a stack of three pellets. The pellets comprising of anode and cathode made from the phase composition of the electrode materials are separated by dense high purity CSZ or YDT electrolyte pellet. The electrolyte pellet has to be of high purity to ensure that the conduction through it is purely ionic. The surfaces of the pellets are smoothened and polished to obtain flat uniform surfaces. This ensures proper surface contact between the surfaces of the anode, electrolyte and cathode materials. The contact between the pellets during the experiment is maintained employing the spring loaded mechanism which adjusts any mechanical change in the stack of the pellets due to thermal expansion during the measurements. The cell assembly comprising of the anode, cathode and the electrolyte is operated in highly purified inert carrier gas such as argon, which is totally free from any traces of oxygen or water vapor. The gas from the cylinder is therefore passed over the molecular sieves such as copper impregnated BASF catalyst and titanium metal sponge maintained at an appropriately high temperature to get rid of any traces of moisture and oxygen. The cell configuration can either be open or the anode and the cathode may be isolated from each other by a dense impervious electrolyte tube to prevent short circuiting of the cell through the vapor phase, particularly when the absolute magnitude of the oxygen pressures at the two electrodes are high(in the case of oxide systems). An open stack assembly can be used even when the difference in the partial pressures between the two electrodes differ by orders of magnitude when the absolute magnitudes of these pressures are very low. The extremely slow kinetics at the electrode surfaces does not readily facilitate short circuiting of the cell through the gas phase and such cells can be used in highly purified gases like argon for sufficient length of time. In the case of oxide cells, it is extremely important to ensure that there is no carbonatious matter present in the cell assembly which could introduce drift in the cell EMF due to the side reactions involving oxidation of this matter. The establishment of the equilibrium within the cell has to be ensured by thermally cycling the cell or by passing infinitely small amount of current in the cell and observing the voltage response when that much amount of current is withdrawn. The EMF of the cell has to remain constant once the thermodynamic equilibrium is attained

within the cell. The cell assembly has to be tested prior to the main measurements with the standard electrodes comprising of the couples Fe, FeO_{1-x}, Cu, Cu_2O, Ni, NiO etc. Asymmetry in the cell EMF, if any, between the two electrodes has to be tested by using the same standard electrodes on both sides of the electrolyte pellets. It is also important to confirm that there is no chemical interaction of the electrode materials with the electrolyte and the
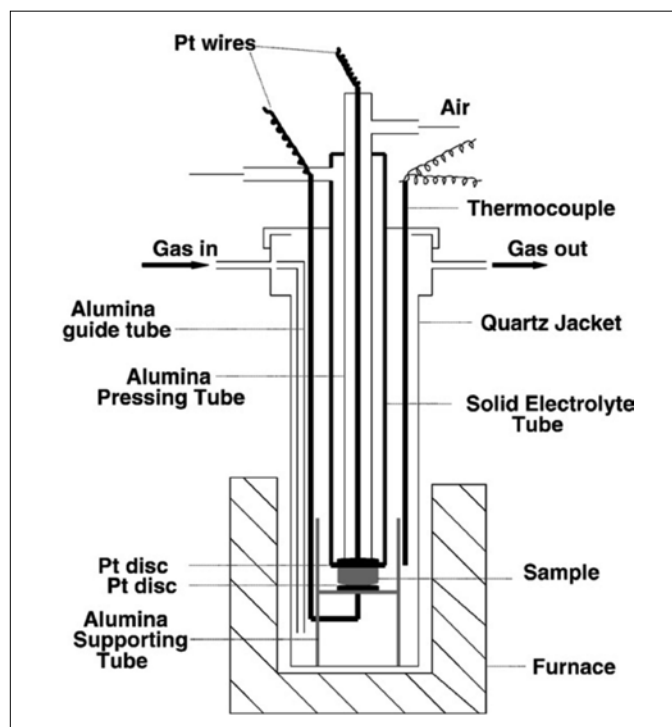

Fig.5. Schematic diagram of the solid state electrochemical cell

contact material plates connected to the measuring Leeds, which normally are made of the platinum group metals. A schematic of typical EMF cell assembly used in such experiments is shown in Fig.5. The Standard Gibbs energy change from the measured EMF is calculated using the Nernst equation mentioned above.

3. Some Selected Examples of Thermochemical Data obtained employing the techniques described above

Thermochemical data such as standard enthalpy and Gibbs energy of formation for some compounds of thoria with selected fission products were obtained with the techniques outlined, after calibrating the instruments following the standard protocol. The temperature measuring thermocouples were calibrated against the melting points of the metals recommended by NIST which included Zn, Sb, Ag, Gold and Cu[22]. The disappearing filament optical pyrometer used for high temperature measurements was calibrated at the gold point using the

sector technique to extend the temperature range to higher values [23].The black body cavity in the Knudsen cell heated using electron bombardment or radio frequency was simulated in its base by drilling the hole of appropriate length and diameter. The cells were made from either graphite or refractory metals such as tungsten, tantalum or molybdenum. The vapor pressure measuring instruments were calibrated by measuring the vapor pressure of standard materials like silver. Likewise the performance of the galvanic cell system was tested by making use of the standard electrode potentials in which the difference in the standard electrode potentials were measured for different combinations.

Thermochemical data for the following thorium compounds was obtained by synergistic use of different techniques and procedures to establish the accuracy of the measurements. The compounds investigated were (1) Molybdenum thorate, (2) Barium thorate, (3) Strontium thorate, (4) Cesium thorate and (5) Rubidium thorate. Prior to the measurements on thermodynamic properties of thorium compounds, several investigations had been carried out in the laboratories mentioned earlier to test the synergy of the different types of measurements on one and the same compound by different techniques. Examples were chosen from U-Te-O, Zr-Mo-O and Hf-Mo-O systems. The standard enthalpy and free energy of formation of $UTeO_5(s)$ and $UTe_3O_9(s)$ were determined employing the vapor pressure measurements [24, 25], calorimetry [26] and Solid Electrolyte Galvanic Cells [27].The vapor pressure in these studies was measured using two different techniques. In the case of $ZrMo_2O_8(s)$ and $HfMo_2O_8(s)$ same three techniques were employed. However, in this case two groups made the measurements employing the solid electrolyte galvanic cells [28-30]. The standard enthalpy and Gibbs energy of formation of the phases $UTeO_5(s)$ and $UTe_3O_9(s)$ obtained by two independent methods of vapor pressure measurements by two different groups in different laboratories and by employing solid electrolyte galvanic cell measurements and calorimetry showed excellent agreement within the stipulated experimental errors. This indicates that if enough care is exercised in these measurements considering all the precautions outlined in the above discussion, it is possible to obtain reliable and reproducible thermodynamic data. Mishra and co-investigators [24] determined the vapor pressure of $UTeO_5$ in one atmosphere of flowing oxygen employing the transpiration technique. The vaporization reaction could be represented as $3UTeO_5(s) = U_3O_8(s) + 3TeO_2(g) + 1/2O_2(g)$. The standard free energy of formation of $UTeO_5$ evaluated from the vapor pressure data in the temperature range of measurement could be expressed as: $\Delta_fG° = -1614.2 +$

0.45T/K (kJ/mol), whereas, the measurements of Krishnan et.al [25] for the same reaction by Knudsen effusion mass loss method yielded the expression: $\Delta_fG° = -1616 + 0.4T/K$ (kJ/mol). Similarly for UTe_3O_9, the Standard Gibbs energy of formation obtained from the vaporization reaction studied by transpiration method for the reaction $UTe_3O_9 = UTeO_5 + 2TeO_2(g)$ could be expressed as: $\Delta_fG° = -2313.1 + 0.89T/K$ (kJ/mol). Krishnan et.al [26] as in the previous case studied the same reaction using the Knudsen effusion technique involving the total mass loss. Their results could be represented as: $\Delta_fG° = -2318.0 + 0.08T/K$ (kJ/mol). The transpiration as well as Knudsen effusion measurements were carried out in almost identical temperature regions.

The standard enthalpies of formation deduced for $UTeO_5(s)$ and $UTe_3O_9(s)$ from the vapor pressure measurements by transpiration using the second law method were -1595.4 ± 12 kJ/mol and –2282.2 ±18.0 kJ/mol respectively, which compared very well with the values -1606.3 ± 3.5 and -2287.2 ± 9.5 kJ/mol obtained from isoperibol calorimetric measurements[26]. The Gibbs energy of formation of $UTeO_5(s)$ was determined by Singh and co-investigators [27] by electro-chemical method using the calcia stabilized zirconia (CSZ) as the solid electrolyte and could be expressed as a function of temperature by the equation: $\Delta_fG° = -1642.5 + 0.4784T/K$ (kJ/mol). The standard enthalpy of formation derived from their data by the second and third law treatment was given as -1638.8 ± 9 kJ/mol and -1601.6 ± 10 kJ/mol respectively. It can be seen that the standard enthalpy of formation for $UTeO_5(s)$ derived from electrochemical measurement by third law treatment is in close agreement with that determined by vapor pressure measurements by second law method (- 1595.4 kJ/Mol) and that reported from calorimetric measurements (- 1606.3 kJ/mol) but differed significantly from that obtained by the third law treatment of the electrochemical data (-1638.8 kJ/mol).

In the case of the measurements done on the molybdates of Zirconium and Hafnium, two different laboratories derived the Gibbs energy of formation of these compounds employing the solid electrolyte galvanic cell technique under almost identical conditions. The Gibbs energy of formation of molybdates of zirconium and hafnium determined by the two groups could be expressed as: $\Delta_fG°(ZrMo_2O_8) = -2535.4 + 0.6247T/K$ (kJ/mol), Z. Singh et.al [28] and $\Delta_fG°(ZrMo_2O_8) = -2552.7 + 0.6335T/K$ (kJ/mol), Pankajvalli and Sreedharan [29]. The standard free energy of formation of these two compounds derived from the vapor pressure measurements by transpiration technique [31] could be expressed as $\Delta_fG°(ZrMo_2O_8) = -2525.5 + 0.6115T$ (kJ/mol). It can be seen from these

observations that the agreement of the results obtained by galvanic cell and vapor pressure measurements are mutually consistent. The Gibbs energy of formation of $HfMo_2O_8$ obtained from galvanic cell measurements of Singh et.al [28] and Pankajvalli and Sreedharan [30] could be expressed as: $\Delta_f G°(HfMo_2O_8)$ = -2551.4 + 0.6128T/K (kJ/mol) and $\Delta_f G°(HfMo_2O_8)$ = -2603.8 + 0.6179T/K (kJ/mol) respectively. The expression for the Gibbs energy of formation for this compound derived from the vapor pressure measurement could be expressed as: $\Delta_f G°(HfMo_2O_8)$ = - 2548.8 + 0.6060T/K (kJ/mol). The large difference between the galvanic cell measurements of Singh et.al [28] and Pankajvalli and Sreedharan [30] is attributed to the different values for the standard free energy of formation of HfO_2 used by these two investigators. The standard free energy of formation value for HfO_2 used by Singh et.al [28] in their galvanic cell measurement was the best assessed value taken from the IAEA compilation [32]. Same value was used by Bharadwaj et.al [33] in their reassessed vapor pressure data from which the above equation was derived. The standard enthalpy of formation at 298.15 K obtained by isoperibol calorimetry [34, 35] and second law treatment of the vapor pressure data of Samant et.al [33] agreed very well. These are compared below:

	Vapor Pressure	Calorimetry
$ZrMo_2O_8$	-2577.8 ± 18.2 kJ/mol	-2575.0 kJ/mol
$HfMo_2O_8$	-2592.0 ± 22.0 kJ/mol	-2582.4 kJ/mol

The foregoing examples indicate the importance of the use of multiple techniques for obtaining reliable self consistent thermodynamic stability data on materials and augment our understanding about these techniques. Thermodynamic stability for the following selected compounds was obtained using these proven techniques.

3.1 Thermodynamic Property Measurements on Thoria based Compounds

The standard Gibbs free energy of formation for five compounds of thorium in the pseudo binary oxide systems was determined employing the vapor pressure measurements and the standard enthalpy of formation derived from the second law treatment of the data was compared with that obtained by direct calorimetric measurements wherever these measurements were made. The compounds included two alkali metal thorates, two alkaline earth metal thorates and thorium molybdate. The vapor pressures of Cs, Rb, Ba and Sr thorates were measured by forward collection Knudsen effusion technique.

3.1.1 Vapor pressure measurement method

The most important issue pertaining to the vaporization reaction is the establishment of the vaporization reaction in which the phases co-existing with the vapor have to be identified which should be consistent with the known phase diagram of the system. It is also necessary to have the knowledge of the species in the vapor phase co-existing with the condensed phase /s. In the case of vaporization of the alkali metal thorates Cs_2ThO_3 and Rb_2ThO_3 the solid phases co-existing with their vapor were identified as the parent compounds co-existing with ThO_2. In the case of vaporization of Cs_2ThO_3 the vaporization reaction could be represented by the equation [36]

$Cs_2ThO_3(s)$ = $ThO_2(s)$ + Cs_2O (g), but for Rubidium thorate [37], the reaction was represented as

$Rb_2ThO_3(s) = ThO_2(s) + 2Rb(g) + ½ O_2(g)$. The equations for the standard Gibbs energy of formation for the above two thorates could be expressed as: $\Delta_f G°(Cs_2ThO_3, s)$ (± 20 kJ/mol) = -1780.1 + 0.437T/K and $\Delta_f G°$ (Rb_2ThO_3, s) (± 5 kJ/mol) = -1794.7 + 0.42T/K respectively. It is obvious from the above equations that the thermodynamic stability of these two thorates is not much different. Thermodynamic calculations indicated that under the maximum oxygen partial pressure of oxygen in the fuel pin amounting to the oxygen potential of -375 kJ/mol, there is hardly any possibility of stress corrosion cracking of the clad by iodine vapor formed due to the consumption of oxygen in the formation of these compounds. The concentration of iodine produced will be far below the threshold limit for the stress corrosion cracking of zircalloy.

In the case of alkaline earth thorates different types of reactions were used to derive the standard Gibbs energy of formation. For barium thorate, $BaThO_3$, these were $BaThO_3(s) = ThO_2(s) + BaO$ (g) [38] and $BaThO_3(s) + H_2O$ (g) = Ba $(OH)_2$ (g) + ThO_2 (s) [39]. The former vaporization reaction was followed using the forward collection Knudsen effusion and the latter by employing the reactive carrier gas transpiration technique using water vapor saturated argon as a carrier gas. The dependence of Gibbs energy of formation obtained in the two cases could be expressed as $\Delta_f G°(BaThO_3, s)$ (± 8.0 kJ/Mol) = -1807.7 + 0.276T/K (Knudsen Effusion) and $\Delta_f G°$ ($BaThO_3$, s) (± 38 kJ/mol) = -1775.8 + 0.266T/K (Transpiration).

The large uncertainty in the Gibbs energy derived from transpiration measurements is attributed to the larger uncertainty in the Gibbs energy of formation of Ba $(OH)_2$ gaseous species[40]. The standard enthalpy change for the reaction $BaThO_3(s) = ThO_2(s) + BaO$ (g) derived from the Knudsen effusion measurements by second as well as third law treatment of the data showed excellent agreement. (i.e.

-445.8 ± 6.1 kJ/mol and -445.1 ±25 kJ/mol by third and the second law, respectively). The feasibility of formation of $BaThO_3$ in the fuel pin from the component oxides $BaO(s)$ and $ThO_2(s)$ during the irradiation of the fuel pin evaluated from the thermodynamic data obtained in this investigation indicated the finite possibility of formation of $BaThO_3$.

The high temperature reactions used for the acquisition of thermodynamic data for $SrThO_3$ involved the estimation of the strontium vapor produced as a result of the reactions [41] $5SrThO_3(s) + W(s) = Sr_2WO_5(s) + 5ThO_2(s) + 3Sr(g)$ and $4SrThO_3(s) + W(s) = SrWO_4(l) + 3Sr(g)$. The possibility of these reactions was prompted by the observation of the pink glow emerging from the orifice of the Knudsen cell containing the $SrThO_3$ sample. The X-ray diffraction patterns of the residues left over after partial vaporization of the $SrThO_3$ sample at different temperatures helped in identification of the condensed phases co-existing with the strontium vapor.

The standard Gibbs energy of formation of $SrThO_3$ derived from the vapor pressure measurement in the two high temperature ranges could be expressed as: $\Delta_f G°(SrThO_3, s)$ (± 5kJ/mol) = -1953.6 + 0.367T (1670<T/K<2040) and $\Delta_f G°(SrThO_3, s)$ (± 7.0kJ/mol) = -1960.2 + 0.369T/K (2135<T/K<2420). Prasad et.al [42] determined the standard Gibbs energy of formation of this compound at much lower temperatures by the galvanic cell method using calcium fluoride as a fluoride ion conducting electrolyte. They used two different types of cells represented by (-)O_2 (g), Pt/SrO (s) + SrF_2(s) // CaF_2 // $SrThO_3$ (s) + ThO_2(s) + SrF_2(s) / Pt, O_2 (g) (+) and (-)O_2 (g), Pt/$SrThO_2$(s) + SrF_2 (s) + ThO_2 (s) // CaF_2 // CaO(s) + CaF_2(s) /pt, O_2 (g) (+). The Standard Gibbs energy values obtained from these two electrochemical cells as a function of temperature could be represented by the equations $\Delta_f G°(SrThO_3, s, T)$ (± 10 kJ/mol) = -1829.2 + 0.2735T/K (978<T/K<1154) and $\Delta_f G°(SrThO_3, s)$ (± 20kJ/mol) = -1853.5 + 0.2867T/K (1008<T/K<1168).

It can be seen that these equations differ significantly from the equations derived from the vapor pressure measurements. This can however be understood in terms of the difference in the standard states of the co-existing phases in the different temperature ranges in which these measurements are done. These investigators however, calculated the Gibbs energy values for $SrThO_3(s)$ from both the data at selected temperatures of 1100 and 1800 K and concluded that the Gibbs energy value obtained by galvanic cell was about 20 kJ/mol less negative compared to that derived from vapor pressure measurement at 1100 K and this difference was 34 kJ/mol more negative at 1800 K.

The experimentally derived thermodynamic properties of $SrThO_3(s)$ both by vapor pressure as well as Galvanic cell measurements suggests that the formation of strontium thorate from its constituent oxides $SrO(s)$ and $ThO_2(s)$ is thermodynamically feasible at the normal operating temperatures of the reactors based on thoria fuel. However, because of the marginal stability of this compound, there is high possibility that the strontium oxide will be fixed within the fuel pin by the formation of more stable perovskite such as $SrZrO_3(s)$.

3.1.2 Thermodynamic stability study of Thorium Molybdate by vapor pressure measurement

The standard Gibbs energy of formation of thorium molybdate was determined from its vapor pressure measured by transpiration technique employing oxygen as a carrier gas [43] in the temperature range 1195<T/K<1292. The Gibbs energy could be expressed as a function of temperature by the equation: $\Delta_f G°(ThMo_2O_8, s)(±12.8\ kJ/Mol) = -2682.6 + 0.595T$. The standard enthalpy of formation $\Delta_f H°_{298.15K}$ derived from the mean enthalpy of formation obtained in the temperature range of measurement and the estimated heat capacity for the compound was -2737 ± 15 kJ/mol. The standard molar enthalpy of $ThMo_2O_8$ determined by isoperibol calorimetry experiments [44] was -2742.2 ± 4.5 kJ/mol, which is in excellent agreement with that obtained by vapor pressure measurements.

4. Conclusion

Attempt is made in this article to present the overview of the thermodynamic property measurement activities of different groups in DAE family related to AHWR thoria based fuel. This review is by no means exhaustive but presents the glimpses of such research activities, the meticulousness with which such activities have to be carried out to obtain highly reliable data and the role such data would play in assessing the feasibility of any reaction of our interest under given set of constraints. Factors are identified and outlined which need recognition to claim the precision and accuracy of the data obtained. Needless to say that the quantities such as Gibbs free should be determined with the utmost accuracy since these are used to calculate various properties of the material depending exponentially on temperature in which this quantity appears in the exponential term. A small error in the measurement of such quantities could therefore reflect in significant error in the derived quantity such as equilibrium vapor pressure which is exponentially dependent on temperature. Examples are selected in this article to show how reproducibility of data for one and the same material could be obtained

by adopting different techniques following completely different routes, which establishes the accuracy of such measurements. The data included in this article pertains to only few compounds of uranium and thorium but the methodology adopted in the acquisition of this data applies equally to several other systems.

An additional interesting issue highlighted in the review pertains to the methods designed to study the vaporization reactions. Quite often when the vapor pressure of the material is too small to measure by normal means, other procedures can be adopted to enhance the vapor pressure. Berylia (BeO) is known to be the best refractory material having negligible vapor pressure in vacuum at high temperatures. However, its vapor pressure is enhanced by several orders of magnitude in presence of water vapor due to the formation of volatile beryllium hydroxide, $Be(OH)_2$. Such observations can be used to obtain the thermodynamic properties of refractory materials with negligible vapor pressure. The investigation on Barium thorate described above is the example in this category.

The other interesting observation is the use of reaction of such materials to yield the more volatile vapor species by interaction with the known materials. In the case of Strontium thorate use is made of its reaction with tungsten metal at high temperatures which produces strontium metal vapor which can be estimated by normal analytical means employing the techniques such as flame photometry. The accidental observation of observing the pink glow originating from the Knudsen effusion cell orifice from the strontium thorate sample contained in the Knudsen cell made of the tungsten metal provided a clue that the vapor phase contained the strontium metal bearing species which could easily be analyzed by flame photometry. Such approach for obtaining the thermodynamic properties of vapor species resulting from the interaction of the sample with the container material was adopted by Gingerich [45].

Standard Gibbs energy of formation of the ternary thorium compounds determined by employing various techniques indicate the possibility of formation of these compounds but because of the competing other possible reactions such as formation of more stable zirconates of some elements produced in fission, may not contribute to the failure of the clad due to stress corrosion. This aspect has been discussed by Basu et.al in their recent exhaustive review [46]

Acknowledgement

References

1. R. K. Sinha and A. Kakodkar, *Nucl. Eng. Des.*, 236 (2006) 683.
2. D. D. Sood, A. V. R. Reddy and N. Ramamoorthy, Fundamentals of Radiochemistry, Indian Association of Nuclear Chemists and Allied Scientists, 4th Edition(2010), Mumbai.
3. H. Kleykamp, *J. Nucl. Mater.*, 131(1985) 221.
4. E. H. P. Kordfunke and R. J. M Konigs, Thermochemical Data for Reactor Materials and Fission Products, Elsevier, (1990), Amsterdam.
5. O. Kubaschewski, C. B. Alcock and P. J. Spencer, Materials Thermochemistry, 6th Ed. (1993), Pergamon , New York.
6. K. Nagrajan, presented at 16th Natl. Symp. and Workshop on Thermal analysis (Feb. 2008), Kalpakkam, India, ed. K. V. Govindan Kutty et.al.
7. S.C.Parida, presented at the Workshop on Thermal Analysis (2012), Mumbai, India, ed. Renu Agarwal et.al.
8. H. Hohne, W. Hemminger and H. Hammerschein, Differential Scanning Calorimetry-An Introduction for Practioners, Springer Verlag, (1996) Berlin.
9. The Characterization of High Temperature Vapors, J. L. Margrave (Ed.) John Wiley Sons, (1967) New York.
10. Techniques in Metal Research, Vol.4, Part1, Wiley, New York, E. D. Carter(Ed.) in Characterization of High Temperature Vapors and Gases, Vol.1& 2 J. W. Hastie Ed., NBS Special Publication(1971).
11. S. R. Dharwadkar, A. S. Kerkar and M. S. Samant, *Thermochim Acta.,* 217(1993)175.
12. S. R. Bharadwaj, R. Mishra, M. Ali (Basu), A. S. Kerkar, S. R. Dharwadkar, *J. Nucl. Mater.,* 275 (1999)201.

13. D. D. Sood, S. K. Mukerjee, V.N. Vaidya and V. Venugopal, *J. Metals, Materials and Process,* 5(1993)13.

14. V. Peres, L. Favergeon, M. Andrieu, J-C Palussiere, J. Balland, C. Delafoy, M. Pojolat, *J. Nucl. Mater.,* 423(2012)93.

15. R. J. Ackermann, R. J. M. Tetenbaum and C. Alexander., *J. Phys. Chem.,* 64(1960)350.

16. O. Glemser and H. G. Wendlandt, Advances in Inorganic and Nucl. Chem., H. J. Emelius and A. G. Sharp (Eds.) Academic Press (1961) 215-258.

17. S. R. Dharwadkar, S. N. Tripathi, M. D. Karkhanavala, M. S. Chandrasekharaiah in Thermodynamics of Nucl. Mater. IAEA-SM-190/92(1975) p.445.

18. D. Das, S. R. Dharwadkar and M. S. Chandrasekharaiah, *J.Nucl.Mater.,*130 (1985)217.

19. High-temperature Mass Spectrometry in Materials Research, K.Hilpert, *Rapid Comm. mass spec.,* 5 (1991) 175.

20. Kiokkula and Wagner, *J. Electrochem Soc.,* 104(1957)379.

21. Basics of Electromotive Force Measurements; E. C. Subba Rao, Plenum Press, New York.

22. O. M. Sreedharan, A. S. Kerkar, and M. S. Chandrasekharaiah BARC-261(1973).

23. D. Das, M. S. Chandrasekharaiah, *High Temp. Science.,* 21(1987)161

24. R. Mishra, P. N. Namboodiri, S. N. Tripathi, S. R. Bharadwaj and S. R. Dharwadkar, *J. Nucl. Mater.,* 256(1998)139.

25. K. Krishnan, G. A. Rama Rao, K. D. Singh Mudher and V. Venugopal, *J. Nucl. Mater.,* 254(1998)49.

26. M.Basu, R. Mishra, S. R. Bharadwaj, P. N. Namboodiri, S. N. Tripathi, A. S. Kerkar and S. R. Dharwadkar, *J. Chem. Thermodyn.,* 31(1999)1259.

27. Z. Singh, S. Dash, K. Krishnan, R. Prasad and V. Venugopal, *J. Chem. Thermodyn.,* 31 (1999)197.

28. Z. Singh, S. Dash, R. Prasad, V. Venugopal, *J. Alloys & Comp.,* 244(1996)85.

29. R. Pankajvalli and O. M. Sreedharan, *J. Nucl. Mater.,* 172 (1990)151.

30. R. Pankajvalli and O. M. Shreedharan, *J. Nucl. Mater.,* 175(1990)194.

31. M.S. Samant, S.R. Bharadwaj, A.S. Kerkar, S.R. Dharwadkar, *J. Nucl. Mater.,* 200 (1993)157.

32. P. J. Spencer, Physico-chemical properties of its compounds and alloys, K. L. Komarek (Ed.), Atomic Energy Review , Special issue No.8(IAEA, Vienna,(1981).

33. S. R. Bharadwaj, S. R. Dharwadkar and M. S. Samant, *J. Nucl. Mater.,* 211 (1994) 244-247

34. S. R. Bharadwaj, M. S. Samant, S. R. Dharwadkar, S. S. Savant and R. Kalyanraman, *J. Chem. Thermodyn.,* 27 (1995)863.

35. S.R. Bharadwaj, M.S. Samant, R. Mishra, S. R. Dharwadkar, S. S. Savant, R. Kalyanaraman, *J. Alloys & Comp.,* 218 (1995) 135.

36. M. Ali (Basu), R. Mishra, K. N. G. Kaimal, S. R. Bharadwaj, A. S. Kerkar, D .Das and S. R. Dharwadkar, *J. Nucl.Mater.,* 282 (2000)261.

37. M. Ali (Basu), A.N. Shirsat, C. Kumar, S. R. Bharadwaj and D. Das, *J. Nucl. Mater.,* 323 (2003) 68.

38. R. Mishra, M. Basu(Ali),S. R. Bharadwaj, A. R. Kerkar, D. Das and S. R. Dharwadkar

39. S. R. Bharadwaj, R. Mishra, M. Ali (Basu), A. S. Kerkar and S. R. Dharwadkar, *J. Nucl. Mater.,* 275 (1999)201.

40 I. Barin, 3rd Edn. Thermochemical Data of Pure Substances, Vol.1VCH, (1995) Weinheim.

41. M. Ali (Basu), R. Mishra, S. R. Bharadwaj, A. S. Kerkar, S. R. Dharwadkar and D. Das, *J. Nucl. Mater.,* 299(2001)165.

42. R.Preasd, S.Dash,S.C.Parida,Z.Singh, V.Venugopal, *J. Nucl. Mater.,* 312(2003)1.

43. M.Basu, R.Mishra,S.R.Bharadwaj, A.S.Kerkar and S.R.Dharwadkar, *J. Nucl. Mater.,* 257(1995)185.

44. M.Ali, S.R.Bharadwaj,R.Mishra, A.S.Kerkar and D.Das, *Thermochim. Acta.,* 346(2000)129.

45. I.Shim,M.Sai Baba,K.A.Gingerich, *Chem. Phys.,* 277(2002)9.

46. M.Basu,R.Mishra and D.Das, *J. Nucl. Mater.,* 403(2010)204.

Dr. S. R. Dharwadkar joined the 5th batch of BARC training school in 1961 after graduating with first class in Chemistry from Mumbai University. After successfully completing the training, he joined the Chemistry Division of BARC (1962) and specialized in High Temperature and Solid State Chemistry. Over the period spanning more than 36 years of service in BARC he contributed significantly to the research leading to the acquisition of important data on thermodynamics of nuclear materials useful in the prediction of the nuclear reactor safety during irradiation and safe disposal of nuclear radioactive waste. As a part of this research work he, in collaboration with his colleagues developed several thermoanalytical techniques indigenously. Dr. Dharwadkar has published more than 170 papers in peer reviewed National and International journals. Dr. Dharwadkar takes keen interest in teaching and has taught thermodynamics and solid state chemistry to several batches of BARC training school. Currently he is Adjunct Professor of Physical Chemistry in Mumbai University and Guest Facalty of the Centre for Excellence in Basic Sciences at Mumbai University, Kalina. Dr. Dharwadkar is the Life Member and Fellow of several scientific organizations.

Thermo-chemical Investigations of thorium based oxide and carbide ceramic nuclear fuels

V. Venugopal

Raja Ramanna Fellow, Radiochemistry & Isotope Group
Bhabha Atomic Research centre, Mumbai 400085, India
E-mail: vvgopal@barc.gov.in

1. Introduction

India has a very ambitious three stage nuclear power programme to explore the potential of different types of fuel such as thorium and mixed oxides of Th, U and Pu, their irradiation and in-pile behaviour [1]. In recent years there has been renewed interest by experts for thorium as a nuclear fuel in place of uranium to create nuclear power. The thorium fuel cycle offers enormous energy security benefits in the long-term – due to its potential for being a self-sustaining fuel without the need for fast neutron reactors. It is therefore an important and potentially viable technology that seems to be able to contribute to building credible, long-term nuclear energy. India has about 31% of the world's estimated deposits of thorium. The reserves could have been several times more if systematic surveys are carried out for thorium in the geologically promising terrains of India. Presently India is working on Advanced Heavy Water Reactor (AHWR), Compact High temperature Reactor (CHTR) and accelerator driven subcritical system (ADS) using thorium-based fuel for nuclear energy production. The nuclear reactors use ceramic fuels of the fluorite structure (UO_2, $(U,Pu)O_2$, $(Th,U)O_2$, $(Th,Pu)O_2$) or of rock-salt structure ($(U,Pu)C$). The oxides are largely ionic; the carbides have covalent or metallic bonding. All these materials have high melting points. The oxides are the most common fuel materials in commercial power reactors. Mixed carbide $(U,Pu)C_{1+x}$ is being used as a driver fuel in the Fast Breeder Test Reactor (FBTR). $(U,Th)C$ along with $(U,Th)O_2$ has been proposed as a fuel in CHTR. The performance of the oxide and the carbide fuels is characterized by their chemical potential which is a driving force for numerous reactions taking place in the reactor. The chemical potential of the fuels is, in turn, closely linked with the oxygen and carbon potentials of the oxide and carbide fuels respectively. In this paper, the role of oxygen and carbon potentials as parameters for judging the fuel performance as well as the different techniques used for their measurements will be discussed.

1.1 Ceramic Oxide fuels

The commercial Pressurized Heavy Water Reactors (PHWRs) use UO_2 as common fuel material. To meet the sustained energy need of India, $(U_{1-y}Pu_y)O_{2-x}$ is being considered as fuel for Proto-type Fast Breeder Reactor (PFBR) [1]. $(U,Th)O_2$ and $(Th,Pu)O_2$ will be used as fuel for Advanced Heavy Water Reactor (AHWR) for the utilization of thorium [2]. The behavior of the oxides of uranium and plutonium is more complex than that of other metal oxides, as these metals can exist as ions in a number of valence states. Both uranium and plutonium oxides show broad ranges of non stoichiometry where oxygen to metal ratio (O/M) differs substantially from 2. The oxygen pressure over a single phase is usually strongly dependent upon O/M. The most significant chemical property in an oxide fuel pin is the equilibrium pressure of oxygen in the gas phase within the fuel element. The mixed oxide fuel at a particular temperature is characterized by a definite partial pressure of oxygen which is in thermodynamic equilibrium with it. The oxygen potential over solid oxide can be calculated from thermodynamics:

$$\mu(O_2) = G^o(O_2) + RT \ln p(O_2). \tag{1}$$

where $G^o(O_2)$ is the Gibbs energy of pure oxygen gas at temperature T and pressure at one atmosphere. The quantity $RT \ln p(O_2)$ is the oxygen potential of the fuel. It is the difference between the chemical potential of oxygen in the solid and that of pure gaseous state at the same temperature and one atmosphere pressure. The oxygen potential of the fuel determines the physical states of fission products, their migration, oxidation of the metallic cladding, O/M ratio and actinide redistribution of the oxide fuel.

Additionally, the control of fuel compositions during fabrication requires knowledge of the compositional variation of oxygen potential.

2. Influence of chemical states of fission products on oxygen-availability

Fission products are formed during irradiation of fuel pins. The chemical state of the fission product elements/ oxides/complex compounds influences the availability of oxygen within the fuel rod which in turn controls the oxygen potential of the fuel. The chemical state of fission

products can be calculated from its affinity for oxygen from the following reaction

$$\frac{2}{v} \, (FP) + O_2 \, (g) = \frac{2}{v} \, (FPO_n). \tag{2}$$
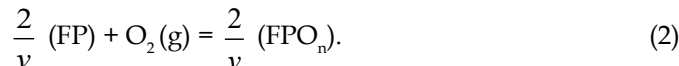
where FP and $(FP)O_n$ represents a fission product element and its oxide respectively and the v is the valence of the fission product cation. The oxygen pressure at which both the element and its oxide coexist is given by applying the law of mass action to Eq.(2), which yields

$$p(O_2) = \exp\left(\frac{\Delta_f G^0(FPO_n)}{RT}\right) \tag{3}$$

where $\Delta_f G^o(FPO_n)$ is the Gibbs energy of formation of the fission product oxide per mole of oxygen at temperature T. Whether or not a particular fission product oxide is stable as an element or an oxide in the presence of the fuel depends on the difference between the Gibbs energy of formation of fission product oxides and oxygen potential of the fuel. The oxygen potential of mixed oxide fuel is roughly bounded by -170 and -670 kJ/mol. If the Gibbs energy of formation of fission product oxide is smaller than -670 kJ/mol, the element will be capable of removing oxygen from the fuel matrix and forming a stable oxide. On the other hand, fission products for which $\Delta_f G^o(FPO_n)$ is larger then -170 kJ/mol will exist as elements in the fuel under all reactor conditions. The Gibbs energy of formation of MoO_2 is very close to that of stoichiometric mixed oxide fuel and this fission product may be present either as an element or an oxide (or both simultaneously). In hypo-stoichiometric fuel the oxygen potential are low enough to reduce MoO_2 to molybdenum metal and the high oxygen pressure over hyper-stoichiometric fuel favors formation of MoO_2. For nearly stoichiometric fuel, Mo is distributed between the fuel matrix as MoO_2 and as the metallic inclusion. It prevents drastic changes in the oxygen potential of the fuel by converting between element and oxide.

The oxygen potential diagrams for the formation of the ternary oxides that can coexist with liquid sodium in PFBR were calculated [3]. Recently chemical states of fission products in irradiated $(Th_{0.94}U_{0.04})O_2$ fuel with burn ups have been computed in our laboratory [4]. Additionally, the control of fuel compositions during fabrication requires knowledge of the compositional variation of oxygen potential.

2.1 Gibbs energy of formation of fission product oxides

The $\Delta_f G^o_m(T)$ of fission product oxides are required to determine chemical sate of fission products and their reaction with clad, coolant and fuel materials. The solid electrolyte Galvanic cell technique using oxygen ion conducting electrolyte has been used to measure Gibbs energy of formation of fission product oxides. A typical Galvanic cell for investigation of $\Delta_f G^o_m(SrThO_3,s,T)$ using CaF_2 is given as:

(-)Pt,O$_2$/SrO(s)+SrF$_2$//CaF$_2$//(SrThO$_3$+
ThO$_2$(s)+SrF$_2$}/O$_2$,Pt(+) \hfill (4)
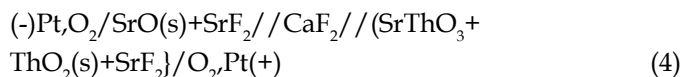
Using similar type of cell, $\Delta_f G^o_m(T)$ for fission product compounds in Sr-Th-O, Ba-Th-O, Rb-Th-O, Na-Mo-O, Na-Cr-O,Ba-Mo-O, Ba-U-O, Sr-Mo-O, R-Fe-O(R =rare earth) and Cs-U-O systems were determined [5].

2.2 Oxidation of stainless steel clad.

The oxygen potential of an oxide fuel material significantly influences the extent of fuel clad chemical interaction. The oxidation of chromium in stainless steel is possible when oxygen partial pressure satisfies the equilibrium of the reaction:

$$4/3 \text{ Cr (solid solution in steel)} + O_2(g) = 2/3 \text{ Cr}_2O_3(s). \tag{5}$$

When the law of mass action is applied to this reaction, the equilibrium oxygen pressure over stainless steel clad that contains some chromium oxide is given by:

$$RT \ln p(O_2) = (2/3)\Delta_f G^o(Cr_2O_3) - \frac{4RT}{3} \ln a_{Cr} \tag{6}$$

where a_{Cr} is the activity of chromium in the stainless steel. For equilibrium between the fuel and the cladding, the oxygen pressure in Eq. (6) must also be in equilibrium with the fuel. Thus, Eq. (6) should be equated to the oxygen potential of the fuel. Incorporating $\Delta_f G^o(Cr_2O_3)$ from the literature and activity of chromium in steel as 0.18, the oxygen potential of the fuel is calculated as -544 kJ/mol. Hence, when oxygen potential of the fuel surface reaches -554 kJ/mol, oxidation of the cladding is thermodynamically possible. From plot of O/M versus oxidation potential of mixed oxide fuel, it is found that if the O/M of fuel surface could be maintained just below exact stoichiometry, oxidation of cladding could not take place. The fresh fuel for fast reactors is purposely fabricated with an O/M of 1.96 for just this reason.

2.3 Measurement of oxygen potential

The oxygen potential over the material can be measured by isopiestic, transpiration, Knudsen effusion mass spectrometry, thermogravimetry and Galvanic cell methods. Latter two methods have been used in our laboratory to measure oxygen potential of different type of oxide fuels.

2.3.1 Thermogravimetric method

This method is based upon weight changes of a sample in a controlled gas atmosphere. The stoichiometry of the sample held in the furnace is first adjusted to a known value

by equilibrating the solid with a gas phase containing a known partial pressure of $O_2(g)$. Then its partial pressure is changed to a known new value, which causes the O/M ratio of the solid to assume a new equilibrium value. The loss or gain of oxygen by the solid is measured by the change in weight of the sample. In hyperstoichiometric fuel the gas phase used is a mixture of $CO(g)$ and $CO_2(g)$. For hypostoichiometric $(U_{1-y}Pu_y)O_{2-x}$ fuel the equilibrium oxygen pressure is fixed by reaction mixture of $H_2(g)$ and $H_2O(g)$. The required low H_2O/H_2 ratios are obtained by controlling the inlet gas temperature.

2.3.2 E.m.f. method

In this method, the oxygen potential of mixed oxide is determined by solid oxide Galvanic cell. The zirconia solid electrolyte (zirconium oxide containing either 5-10 mole % of yttrium oxide or 15 mole % of CaO) provides a means by which oxygen ion can communicate between the sample (mixed oxide) and the reference electrode {Ni(s)+NiO(s)}. The cell e.m.f. is measured using a high impedance electrometer. The oxygen potential of mixed oxide can be determined from the generated e.m.f.s as a function O/M and temperature

2.4 Oxygen potential measurements of $(U_{1-y}Pu_y)O_{2-x}$, $(Th_y U_{1-y})O_{2-x}$ and UO_{2+x}

The oxygen potentials for mixed oxide fuel $(U_{1-y}Pu_y)O_{2-x}$ with y= 0.21 and 0.28 for PFBR were measured by employing a gas equilibration and e.m.f. measurement techniques. Measurements were initiated by equilibrating the fuel sample to an O/M of 2 by heating it to 1073 K while exposing it to an atmosphere with an oxygen potential of -400 kJ/mol. The behavior of fuels with high plutonium content $(U_{1-y}Pu_y)O_{2-x}$ with y=0.4 has also been studied. The oxygen potentials of $(U_{1-y}Pu_y)O_{2-x}$(x= 0.21,0.28, 0.4) are shown in Fig. 1.

The large scale utilization of thorium in India requires $(Th_y U_{1-y})O_{2+x}$ fuel based AHWR reactor system. The oxygen potential of UO_{2+x} (x=0.0598) and $(Th_{1-y}U_y)O_{2+x}$ (y = 0.1,0.15 and 0.9, x = 0.008 to 0.098) have been measured in our laboratory using a solid oxide galvanic cell [6]. Thoria-urania pellets were initially reduced under flowing Ar+8% H_2 mixture in a micro-balance at 973 K. The O/M ratio thus obtained was assumed to be 2.000. The pellets were then treated with argon containing 250 ppm oxygen impurity to obtain $(Th_{1-y}U_y)O_{2+x}$, by varying the temperature and duration of oxidation, pellets having different O/M ratio were prepared. The solid state Galvanic cell employed was:

$$Pt/Ni(s)+NiO(s)/CSZ/(Th_{1-y}U_y)O_{2+x}/Pt \qquad (7)$$
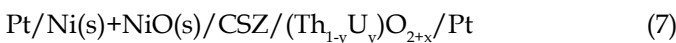
The overall cell reaction can be represented by:

$$(Th_{1-y}U_y)O_{2+x}+ 2\ Ni(s) = (Th_{1-y}U_y)O_{2+x'}(s) + 2\ NiO(s). \qquad (8)$$
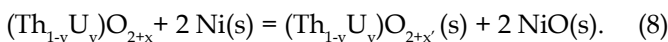
The Gibbs energy change for the above reaction can be given by:

$$\Delta_r G^o = -\ 4\ FE = RT \ln p(O_2) - 2\ \Delta_f G^o(NiO,s). \qquad (9)$$

The oxygen potential over $(Th_{1-y}U_y)O_{2+x}$ is

$$\Delta\mu(O_2) = -4FE + 2\ \Delta_f G^o(NiO) \qquad (10)$$

The oxygen potential thus evaluated for different $(Th_{1-y}U_y)O_{2+x}$ as a function of O/M is shown in Fig.2.

2.5 Carbide fuel

The mixed carbide of uranium and plutonium is an attractive alternative to the mixed oxide as fuel in FBTR [7].
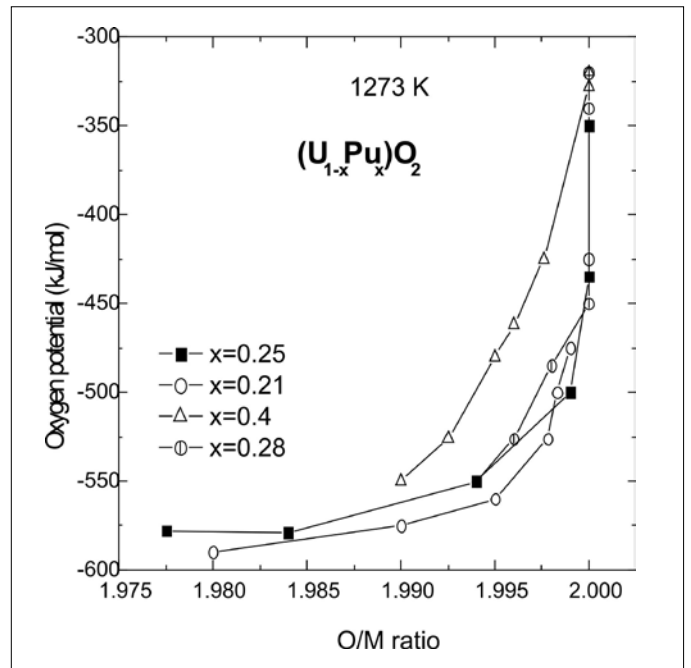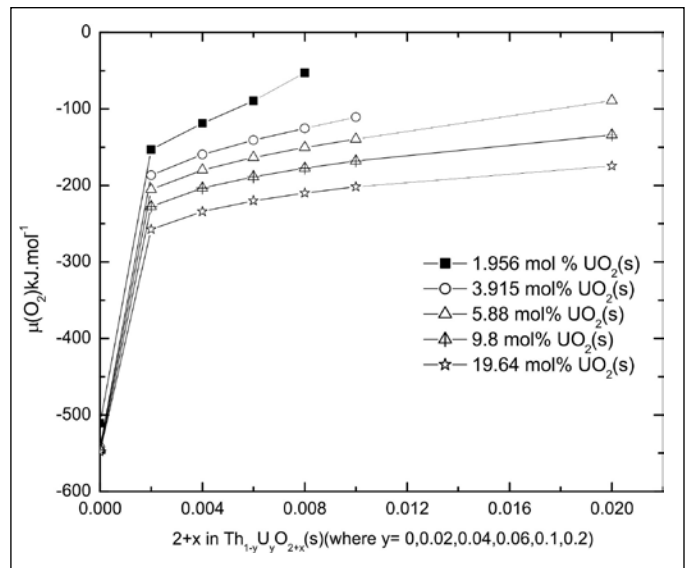

Fig 1 μ (O₂) for various Pu Content.

Fig. 2 μ (O₂) of $(Th_{1-y}U_y)O_{2+x}$ as function of O/M

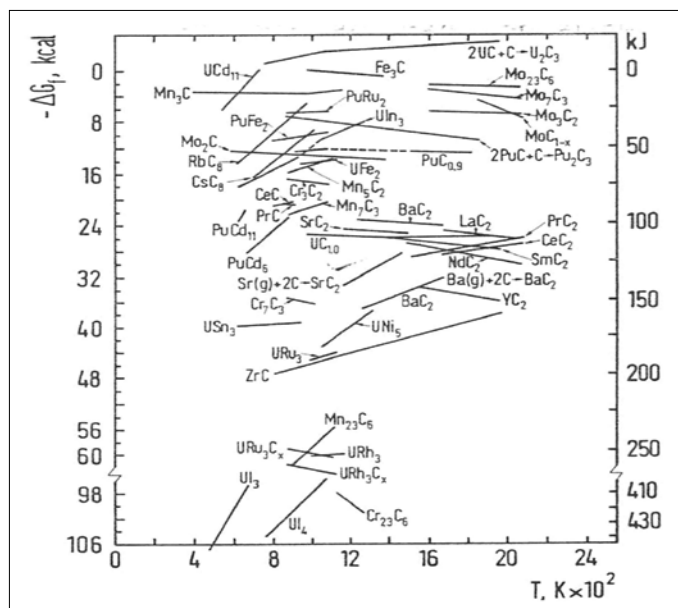*Fig. 3. Carbon potential of fission products*

The fuel of fast Breeder Test Reactor (FBTR) of Kalpakam in India is a mixed carbide fuel with Pu/(U+Pu) = 0.7. It is a biphasic fuel containing monocarbide phase (U,Pu)C, in equilibrium with sesquicarbide phase $(U,Pu)_2C_3$. The ternary phase diagram of the U-Pu-C system shows that the monocarbides of uranium and plutonium have very narrow non-stoichiometry. Hyper-stiochiometric carbide should consist of $(U,Pu)C+(U,Pu)_2C_3$ phase and the hypo-stoichiometric carbide should consist of (U,Pu)C+(U,Pu) phases. The C/M decreases to less than one at high burn ups, because fission products tie up more carbon than the fissioning atom. Thus, sesquicarbide phase will disappear and a low melting metallic phase will appear. To predict the burn-up at which metallic phase may appear in the carbide fuel, it is important to know the change in C/M with burn up. The C/M ratio is related to carbon potential of the fuel.

2.5.1 Carbon potential

The most significant chemical property of carbide fuel is the carbon potential of the fuel pin. The carbon potential of fuel is defined as RT lna_C. The carbon activity in carbide fuel depends on C/M ratio. The usual procedure to measure the carbon potential of metals and alloys is by gas equilibration method where the sample is equilibrated with CH_4/H_2. From the composition of the gas mixture at equilibrium, the carbon potential is calculated by appropriate thermodynamic considerations. Carbon potential can be measured by various methods.

2.5.1.1 Isopiestic method

In this case a metal or alloy of accurately known carbon activity concentration relationship is equilibrated with the sample under investigation. By analyzing the former after equilibration, the carbon activity in the sample is calculated.

2.5.1.2 E.m.f method

This method uses an electrochemical carbon meter which is established in IGCAR [8] for measurement of activity of carbon in fuel. In this method, the sample is immersed into sodium at high temperature until carbon potential becomes equal. The carbon potential of sodium is then measured using an electrochemical carbon meter. The carbon meter has been validated by a study of the carbon potential of nickel.

2.5.2 Measurement of carbon potential of carbide fuel

The carbon potentials in fuel (μ_C^{fuel}) and sodium (μ_C^{Na}) are given by

$$\mu_C^{fuel} = \mu_C^o + RT \ln a_C^{fuel} \tag{11}$$

$$\mu_C^{Na} = \mu_C^o + RT \ln a_C^{Na} \tag{12}$$

where μ_C^o is the carbon potential in the standard state, which is chosen as unity for graphite. At equilibrium $\mu_C^{fuel} = \mu_C^{Na}$ and hence $a_C^{fuel} = a_C^{Na}$. Thus, by measuring carbon activity of sodium, carbon activity of fuel is measured. The electrochemical carbon meter is based on the principle of concentration cell and is represented as:

Reference electrode/Na_2CO_3/Li_2CO_3/$[C]_{Na}$ (13)

where $[C]_{Na}$ represents the carbon dissolved in sodium in equilibrium with carbide fuel. The reference electrode is a thin-walled nickel capsule filled with graphite powder. The e.m.f., *E* generated is given as:

E= (RT/nF) ln a_C^{Ref}/a_c^{Na} (14)

Thus, by measuring the e.m.f., the carbon activity in sodium can be calculated, which is the measure of carbon activity of carbide fuel.

2.5.3 Fuel-Clad compatibility in the carbide fuel

The cladding material is stainless steel in FBTR. Carburization of clad is one of the principal concerns while using mixed carbide fuel. There are two methods by which stainless steel clad can be carburized. In the first mode, transport of carbon to and from the clad could occur at the interface between the fuel and the clad, depending upon the difference in the carbon potential between them. In the second mode, carburization is brought about by the pressure gradient of CO(g) within fuel pin. Hence any change in carbon content resulting from carbon transport could have a detrimental effect on the mechanical integrity of the steel. Hence, the carbon potential of fuel and stainless steel are important.

The carbon potential of carbide fuel is measured using electrochemical carbon meter and is calculated as -69.3 kJ/mol at 913 K. The carbon potential of stainless steel cladding material is -40 kJ/mol at 950 K. Thus mixed carbide fuel material is not likely to carburize the AISI 316 cladding material.

2.5.4 Clad-Coolant Interactions

Liquid sodium, which is used as the coolant in the fast breeder reactor, is compatible, in the pure state with austenitic and ferritic steel structural materials. Even parts of million (wppm) levels of oxygen causes corrosion in the high temperature section of the sodium loop and the corrosion products get transported through liquid sodium medium to cooler parts. Under the normal operating conditions of a sodium-steel circuit, the ternary compound that is observed is $NaCrO_2$. Threshold oxygen level above which this compound would form is an important parameter. This can be obtained by measuring the oxygen potential in Na-$[Cr]_{ss}$-$NaCrO_2$ phase field. This value was measured in our laboratory using solid oxide Galvanic cell technique [9].

2.6 Chemical state of Fission products

The C/M of the carbide fuel is related to the chemical states of the fission products. The equilibrium state of the fission products is a result of many competing chemical reactions. The chemical state of fission products in carbide fuel have been computed in our laboratory [10]. Fission products generated in the matrix of carbide fuel during irradiation are dissolved in the lattice or precipitates within the fuel structure. Zirconium was found to be completely soluble; Mo and rare earth were partially dissolved where as alkali and alkaline earth metals formed separate phase and the composition of metallic (Tc, Pt) phase depends on the carbon potential of the fuel. The carbon potential of different fission products has been calculated from the standard Gibbs energy formation values and is given in Fig. 3.

3. Conclusion

It is evident from above discussion that oxygen and carbon potential of oxide and carbide fuels containing actinides are of paramount importance in nuclear technology. These data are extensively used in the entire nuclear fuel cycle, starting from fuel fabrication to nuclear west management. Several intricate problems associated with nuclear fuel could be solved by thorough assessment of the chemical potentials of the nuclear fuel.

References

1. A. Kakodkar, *BARC News Letter*, 2007, p 3.
2. K. Anantharaman, V. Shivakumar, and D. Saha *J. Nucl. Mater.*, 383(2007)119.
3. Smruti Dash, D.D. Sood, and R. Prasad, *J. Nucl. Mater.,* 228 (1996) 83.
4. Renu Agarwal, B.K. Sen, and V. Venugopal,presented at the Sixteenth National Symposium on Thermal Analysis (Feb 4,2008), Kalpakam, India.
5. V. Venugopal, presented at the International Symposium on Material Chemistry (ICMC, Dec 4,2006), Mumbai, India.
6. V.S. Iyer, Ph.D thesis submitted to Mumbai University, 1991.
7. C. Ganguly, G.C. Jain, J.K. Ghosh, and P.R. Ray, *J. Nucl. Mater.,* 153(1988)178.
8. S.R. Pillai, S. Anthonysamy, P.K. Prakashan, R. Ranganathan, P.R. Vasudev Rao , and C.K. Mathrws, *J. Nucl. Mater.* 167(1989)105.
9. V. Venugopal, V.S. Iyer, V. Sundaresh, Ziley Singh, R. Prasad, and D.D. Sood, *J. Chem. Thermodyn.*, 19(1987)19.
10. Renu Agrawal, and V. Venugopal, *J. Nucl. Mater.,* 359(2006)122.

Dr. V. Venugopal, *M.Sc.,Ph.D, is presently a Raja Ramanna Fellow at BARC and retired as the of Director of Radio Chemistry and Isotope Group at BARC, Mumbai in June 2011. He is a specialist in the field of thermal/ thermodynamics of plutonium based fuels at high temperature, chemical quality control of fuel, X-ray and solid state chemistry and Nuclear Materials Safeguards. He had overseen the Radioisotope and Radiation Technology Programs at BARC. During 2007-2011, He served as a member Standing Advisory Group for Safeguards (SAGSI) of IAEA to advice Director General IAEA on safeguard issues. He was officer in-charge on "Nuclear Materials and Control" in all the units of DAE since 1997. He has to his credit more than 370 publications out of which 190 are published in reputed international journals. He is widely acclaimed as an expert in the area of thermodynamics and attended international conferences on thermodynamics of nuclear materials. He is the vice president of Indian Nuclear Society (INS). He has been the President of Indian Association of Nuclear Chemists and allied scientists (IANCAS) and Indian Thermal Analysis Society (ITAS). He has given lectures on "Radiochemistry and Applications of Radioisotopes", in more than 70 universities in India. He is also a member of several professional bodies. He has received many awards including the Netzsch-ITAS award in 2001, ISCAS silver medal in 2002, MRSI medal for 2003-04, INS award for 2005, DAE award in 2007 and Dr. Athavale memorial award for his contribution to analytical chemistry.*

He was on Deputation on Indo-German collaboration and worked in Nuclear Research Centre, Julich, Germany for one and half years and attended several conference abroad to give lectures in the field on thermodynamics of Nuclear Materials. He had led a delegation to South Korea and Argentina for bilateral meetings for cooperation in Nuclear Science and Technology.

As a guide for PhD in Mumbai University, so far 26 students have obtained PhD/MSc. under his guidance.

Thorium fuel utilization in thermal reactor systems

Umasankari K. and P. D. Krishnani

Reactor Physics Design Division, Reactor Design and Development Group
Bhabha Atomic Research centre, Mumbai 400085, India
E-mail: uma_k@barc.gov.in

Abstract

Thorium is a potential fuel for nuclear reactors. Thorium utilization is expected to be the mainstay of the third stage of the nuclear power programme of India. The major disadvantage with thorium is that it is not associated with any fissile species. One has to convert ^{232}Th to ^{233}U in a reactor, and energy is obtained by the fission of ^{233}U. Thorium fuel will have to be used in a closed fuel cycle in order to exploit the complete potential of thorium. However, separating the ^{233}U from irradiated thorium and fabricating newer fuel with the bred ^{233}U are technologically challenging. This aspect coupled with the fact that thorium fuel reprocessing requires remote handling and not as simple as uranium fuel processing has contributed to the lagging behind of thorium as energy source. Several reactor concepts have been developed over the past decades in almost all kinds of neutron spectra from thermal to fast and from light water cooled to molten salt cooled reactors. There have been continued research efforts in all aspects of the thorium fuel cycle. In this paper, the physics aspects of current research projects being pursued in Bhabha Atomic research Centre, namely, Advanced Heavy Water Reactor (AHWR) and the new high temperature reactors are briefly summarized. Also some studies on thorium utilization in thermal reactors are also presented. This paper will also give a description of the critical facility which has been designed and built at BARC for performing experiments with AHWR fuel.

1. Introduction

India would have to launch thorium cycle at the earliest for its energy security and sustainability [1]. We have been developing the thorium technology over the years, with a number of R&D programs and commercial application in our PHWRs. Currently, India is engaged in the design and development of an Advanced Heavy Water Reactor (AHWR) which will serve as a technology demonstrator for the complete thorium cycle from fabrication to irradiation and reprocessing. The newer high temperature reactors like Compact High Temperature Reactor (CHTR) and Innovative High Temperature Reactor (IHTR) also use thorium fuel.

The fuel cycle for thermal reactor systems utilizing thorium would have to use ^{235}U or plutonium as the initial fissile content. Plutonium recycle i.e. using plutonium back into reactors and thereby reducing its radio-toxicity has been a main attractive feature and there have been many designs with thorium as a carrier for plutonium. The problem of associated radio-toxicity of the daughter products of ^{232}U generated in the thorium cycle is an issue and requires remote handling technologies.

In this paper we discuss the various physics aspects of thorium fuel cycle and the thorium based reactors being designed in India.

2. Neutronic characteristics of thorium fuel

The thermal neutron absorption cross-section of ^{232}Th (7.4 b) is about three times higher than that of ^{238}U (2.7 b). Thorium (^{232}Th) having a higher absorption cross section than ^{238}U offers the possibility of absorbing the extra neutron thereby aiding a better conversion [2]. An important aspect of the Thorium fuel is that because of the higher absorption in Thorium itself, the fissile inputs would have to be higher than that of a comparable uranium cycle. The neutronic characteristics for some of the isotopes of importance in the Th and U cycles are given in Table 1. In the thermal spectrum, ^{233}U has best neutronic properties among the fissile isotopes (Table 1). The neutronic parameters in the table have been generated from the PREPRO code system [3]. The major difficulty is that, Thorium cannot be introduced directly as fuel for the buildup of initial quantities of ^{233}U and some other fissile material topping in the form of ^{235}U or ^{239}Pu is required for this purpose.

An important nuclear characteristic favoring thorium cycle is the η value of bred fissile material ^{233}U. ^{233}U has an η value greater than 2.0 per thermal neutron absorbed, which remains constant over a wide energy range, in thermal as well as epithermal regions, unlike ^{235}U and ^{239}Pu, which makes the thorium fuel cycle less sensitive to the type of reactor.

The value of η which is a measure of the excess neutron available for fertile-to-fissile conversion is plotted in Fig. 1 for ^{233}U, ^{235}U and ^{239}Pu. The value of η remains constant below 2 eV. However, it has a sharp dip around 2-3 eV (Fig 1, Table 1).

The thorium fuel cycle also has associated radiological problem in ^{232}U, whose daughter products are hard gamma emitters. The two long-lived Minor Actinides (MAs) associated with thorium cycle are ^{231}Pa and ^{237}Np. Another important product is ^{234}U, which has a significant absorption cross section and acts as a load in thorium-fuelled systems. The actinide build-up chain in the thorium cycle is presented in Fig. 2.

From a design standpoint the higher thermal absorption cross section in ^{232}Th as compared to ^{238}U would lead to a harder neutron spectrum in thorium based reactors [4]. This means that the effective thermal flux would be lower in such systems. Because of the in-situ generation of ^{233}U or better conversion, the reactivity loss in thorium-based systems is lower.
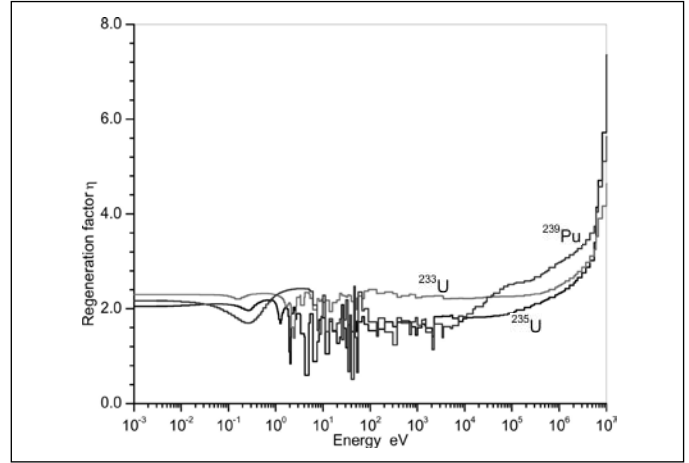
Fig. 1 η of the fissile nuclides ^{235}U, ^{233}U and ^{239}Pu

Table 1 Neutronic properties of some fissile and fertile isotopes

	^{232}Th	^{233}U	^{234}U	^{235}U	^{236}U	^{238}U
Thermal data : Cross sections at (0.0253 eV)[*] (Maxwellian average are given in brackets) (Temperature = 0.0253 eV ; Range 1.0E-05 to 10 eV)						
σ_a barns	7.34	576.45	100.96	683.77	5.18	2.68
σ_c barns	7.34 (3.446)	45.24 (35.18)	100.89 (115.88)	98.69 (50.60)	5.13 (39.14)	2.68 (18.02)
σ_f barns	0.00 (0.00)	531.21 (308.674)	0.067 (.07304)	585.09 (269.1357)	.047 (0.456)	1.679E-05 (1.575E-05)
α^1	-	0.085	-	.169	-	-
v^2 (at 0.0253 eV)	-	2.497	2.365	2.437	2.371	2.493
η^3	-	2.301	-	2.085	-	-
Maxwellian average (Range 1.0E-05 to 0.1 eV)						
σ_a barns	6.88	541.05	94.45	631.90	4.89	2.53
σ_c barns	6.88	43.22	94.39	92.27	4.84	2.53
σ_f barns	0.00	497.84	0.063	539.63	0.044	1.582E-05
Resonance Integral (0.5 eV – 100 keV)						
Absorption barns	83.73	907.47	631.53	408.75	345.07	274.81
Capture barns	83.73	140.81	630.83	139.79	340.61	274.81
Fission barns	5.701E-06	766.67	0.7026	268.96	4.45	0.0023
α	-	.184	-	.520	-	-
Fast energy data (Fission spectrum averaged one group cross section) (Range 1.0 keV to 20 MeV)						
Fission barns	0.731	2.026	1.15	1.339	0.56	.295
Capture barns	0.135	0.102	0.149	0.157	0.151	.106
ν	2.4	2.89	2.79	2.82	2.74	2.81
η	1.91	2.86	2.64	2.74	2.65	2.69

[1]*α is the capture-to-fission ratio*

[2] *ν is the average number of neutrons produced per fission*

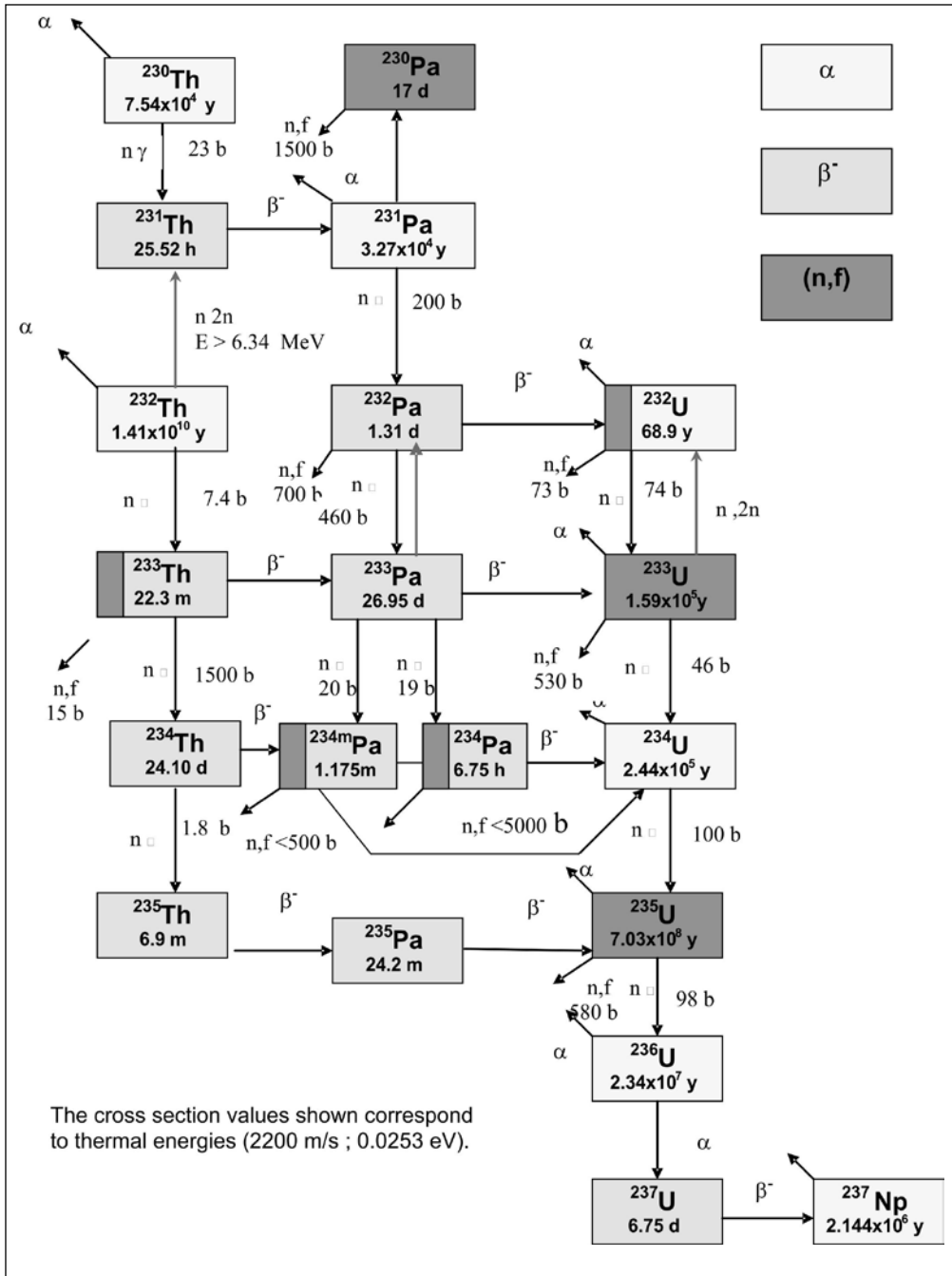[3]*η is defined as the average number of neutrons produced per thermal neutron absorbed*

Fig. 2 Actinide build-up chain of the thorium cycle

1.0% at burnups of 33 GWD/T. In contrast the bred fissile material in thorium systems reaches a maximum of 1.5% in a thermal spectrum. But for such fissile performance one would have to go for high burn-up i.e. about 45 GWD/T or above [6]. It can be seen from Figure 3 that initially [235]U enrichment in thorium gives lower burn-up as compared to that in thorium. This is due to the parasitic absorption in [232]Th. But for enrichments of the order of 3.0% or above, thorium gives a distinct advantage in terms of burn-up. In thorium, for a given enrichment of [235]U, the initial reactivity is relatively low due to the higher absorption of thermal neutrons in thorium.

There is a steady in-situ conversion of thorium to [233]U. As η for [233]U is much higher than that for a [235]U (Table 1), the subsequent fall in reactivity on account of [235]U burn-up is low. In contrast in the case of [238]U as the fertile host, i.e. Low Enriched Uranium (LEU) fuel, the fuel utilization though much better initially decreases steadily thereafter. Subsequently, due to neutron capture in fissile plutonium, reactivity and fraction of fissile plutonium falls.

2.1 Performance potential of thorium

A study based on the performance of [232]Th and [238]U as a fertile host in a thermal spectrum like the one in PHWR shows that [235]U in thorium gives a better fuel utilization. In the case of [238]U as the fertile host, i.e. Low Enriched Uranium (LEU) fuel, the fuel utilisation though much better initially decreases steadily after attaining a maximum value at a moderate burn-up of about 25 GWD/T and the bred fissile material, Pu saturates at a low 0.6 % [5]. In a typical PWR spectrum, the plutonium contents are about

2.2 Conversion and breeding in thorium fuelled systems

Thorium has high thermal absorption cross section and does not have any intrinsic fissile element. By feeding the neutron to thorium, not only is the excess reactivity suppressed but also ensures production of [233]U, which is used as fuel within the same reactor. The production of fissile [233]U in an ambient thermal spectrum from a pure thoria fuel is illustrated in Fig. 4. It can be seen that at higher thermal fluxes, faster is the rate of [233]U generation and also the [233]U saturates or reaches an asymptotic level. The ambient thermal flux in the vicinity of thoria rods can

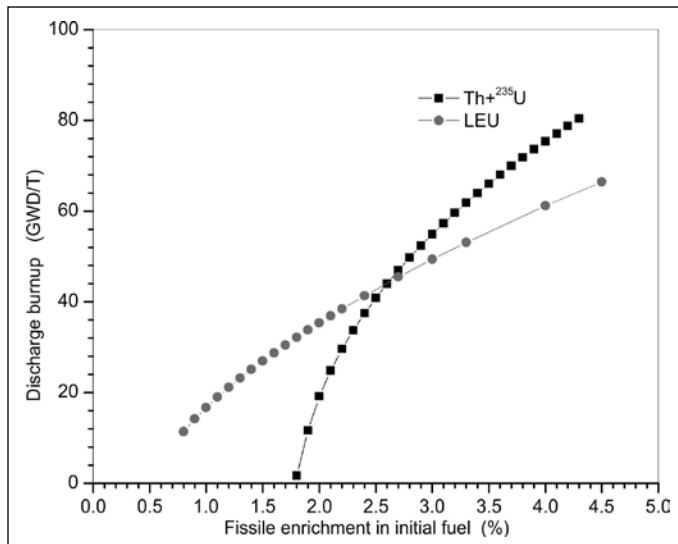*Fig. 3 Performance potential fissile topping in thermal spectrum to ^{238}U*

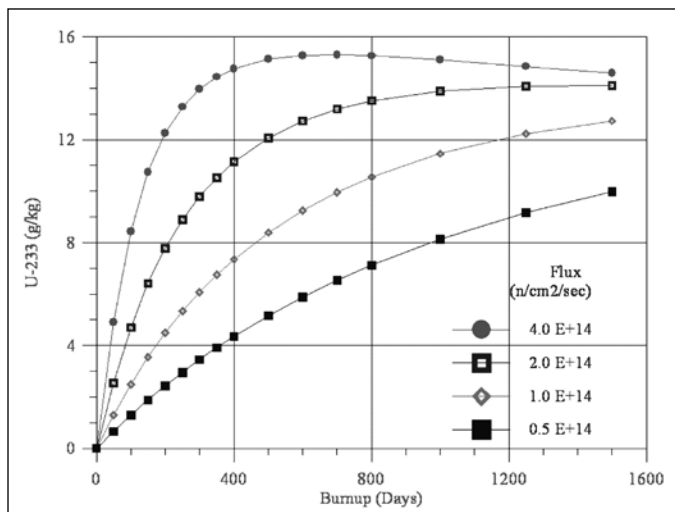*Fig. 4 ^{233}U production as a function of thermal neutron flux*

be increased by design. This feature is exploited in the conceptual ATBR design [7].

3. Thorium utilisation in India

3.1 Thorium irradiation in Research reactors [8]

- Thoria rods (J-rods) have been continuously irradiated in CIRUS in the reflector region (between the inner and outer graphite reflectors) and ^{233}U has been accumulated. These rods have then been reprocessed. These J-rods have about ~2-3 ppm of ^{232}U in uranium (being irradiated in the reflector region where the fast neutron fluxes are low).

- **PURNIMA-II** (1984 -1986) **:** India initiated thorium studies as early as seventies and the first research reactor built with ^{233}U fuel generated in J-rods in

the CIRUS was PURNIMA-II. Experiments were performed in PURNIMA-II facility with uranyl nitrate solution containing **^{233}U** reflected by BeO blocks. Variation of critical mass with different H/**^{233}U** ratio was measured. Measurements of various reactivity parameters and neutron lifetime were also performed. These experiments also gave confidence in handling U-233.

- **PURNIMA-III** (1990-93) **Experiments with ^{233}U- Al Dispersion Fuel:** Experiments were performed with ^{233}U-Al dispersion fuel in the form of plates in PURNIMA-III. BeO canned with zircaloy was used as reflector. Void coefficient and temperature coefficient of reactivity were also measured. These measurements helped in finalising the core of KAMINI reactor. They also helped in validating the cross sections of ^{233}U and Be.

- **KAMINI Reactor:** A reactor based on **^{233}U** fuel in the form of U-Al alloy was commissioned at Kalpakkam in 1996 (IGCAR). It is the only operating reactor in the world with ^{233}U as fuel. The reactor power is 30 KW and has very high flux to power ratio. It has 3 beam holes used for activation analysis and facility for neutron radiography of Fast Breeder Test Reactor fuel.

- **Irradiations in Pressurized Water Loop of Cirus Reactor:** Advanced fuels using thorium was irradiated in dedicated engineering loops in CIRUS in a power reactor environment. A mixed cluster B-C-8 which also included (Th,Pu)MOX fuel pins and a plain Thoria cluster was irradiated upto 18,000 RMWD (Reactor Mega Watt Days).

- Thoria bundles irradiated in the blanket zone of FBTR (^{232}U content in U will be low ~10 ppm)

- ^{233}U based PFBR fuel irradiation testing in FBTR.

3.2 Critical facility for AHWR

A critical facility for AHWR has been built in order to perform various kinds of experiments to validate the design parameters and the calculation models. It would also help to validate the multi-group nuclear cross section data used for design applications. The Critical Facility went critical on 7th April, 2008. The observed critical height for the reference core configuration was 226.7 cm which agreed well with the estimated value of 226.5 cm [9].

CF has been designed with three types of core

1. Reference core – 55 locations with natrural UO_2 (19 rods clusters with pin dimensions of Dhruva pins) ; 6 shut-off rods locations

2. AHWR core – a variant of the reference core, central 9 clusters will be replaced with 54 pin AHWR D5 clusters.

3. PHWR core 63 locations having 37 rods natural UO_2 clusters of 500 MW(e) PHWR design, 6 locations for shut-off rods

The core layout of the Reference core of AHWR-CF is shown in Fig. 5a. Several experiments were performed which included, measurement of critical height for various cores, calibration of reactivity devices, Neutron Spectrum measurement on central cluster, Cadmium ratio measurement at infinite dilution, fine structure flux measurement inside the central lattice of Nat. Uranium and thorium clusters. The various experiments proposed to be performed in the CF are measurements of level coefficient of reactivity, reaction rates, neutron spectrum, flux disadvantage factor, epithermal flux ratios at various points in and around experimental cluster, and shut-off rods. It is also proposed to do void reactivity measurements in the 9 AHWR clusters. Kinetic parameters like prompt neutron decay constant will be measured using noise analysis technique. Recently integral experiments with ThO_2-U mixed pin cluster and ThO_2-PuO_2 cluster (Fig. 5b) were performed by loading them in the central E-5 and several other locations.
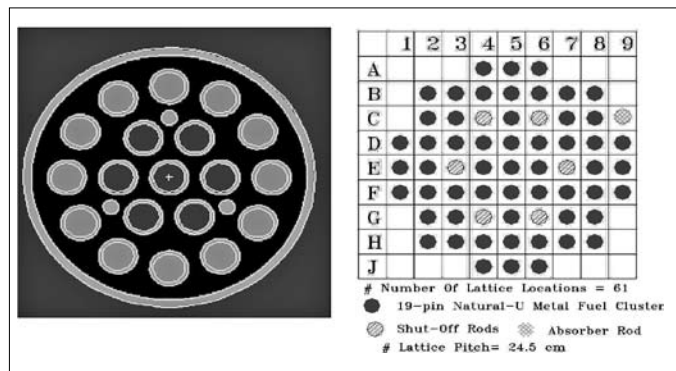
Fig. 5a Core layout of AHWR-CF Fig. 5b Mixed Pin (Nat. U-ThO$_2$) experimental cluster

3.3 Flux flattening in PHWRs by using Thorium

As an alternative to using depleted uranium, thorium has been used in the fresh core of 220 MW(e) PHWRs. 35 lattice locations in the 220 MW(e) PHWR core were optimised for loading one thoria (ThO_2) bundle in each channel such that it provides the required flux flattening without any loss of burnup in UO_2 fuel and without compromising the worth of Shut Down Systems [6]. The maximum operating power can be improved by flattening of the flux. In earlier reactors like RAPS, MAPS and NAPS, depleted uranium was used for this. For the first

time such a loading was experimented in 1991 at KAPS-1. The same loading pattern was followed in the subsequent reactors like KAPS-2, KGS 1 and 2 and RAPP-3 and 4. This represents a unique way of utilizing thorium and about 210 thoria bundles have been irradiated. The Post irradiation examination (PIE) of this irradiated thoria fuel was also done to estimate the uranium composition [10]. The uranium isotopic content in this bundle has been analysed experimentally by chemical and spectrometric studies and found to match well with theoretical estimations [11].

4. Advanced Heavy Water Reactor

The Advanced Heavy Water Reactor **(**AHWR) is a unique reactor designed for large scale commercial utilisation of thorium and integrated technological demonstration of the thorium cycle [12]. The AHWR is designed to maximise power production from thorium. The AHWR is a 920 MWth, vertical pressure tube type thorium-based reactor cooled by boiling light water and moderated by heavy water. Thus we are able to incorporate our experience in design, operation and safety analyses/ aspects of PHWR and BWR and extend it further. In keeping with current day norms of enhanced safety features, AHWR is designed with several passive safety features such as negative coefficient of coolant void reactivity, heat removal through natural circulation of coolant and passive containment cooling system. Two different AHWR designs are being developed with thorium-plutonium and thorium-uranium cycles, in both closed and open cycle options. The plutonium topped version which is the reference AHWR design, AHWR-Ref and the LEU topped variant is called as the AHWR-LEU.

The main features of AHWR physics design are

i) Achieving negative coolant void coefficient of reactivity

ii) Strong coupling between neutronics and thermal hydraulics

iii) Use of axially graded enrichments to achieve better thermal hydraulic margins

iv) Maximise the power from thorium

v) Achieve near self-sustenance in [233]U

In the reference design, the basic fuel cycle is based on the fact that the AHWR core should be self-sustaining in [233]U. The plutonium inventory will be kept a minimum and will come from fuel irradiated in PHWRs. The [233]U required is to be bred in situ, which implies that the initial core will be based solely on thorium-plutonium fuel. There will be gradual transition from the initial core which will not contain any [233]U to an equilibrium core, which will have

(233U, Th) MOX fuel pins also in a cluster called composite cluster. And, during this transition phase a relatively large quantity of plutonium may be required. The fuel cluster design converged on a composite cluster (D5) - 54 pin circular cluster (12 (Th,233U) MOX / 18 (Th,233U) MOX / 24 (Th,Pu) MOX) pins with a central displacer to achieve all the features mentioned above [13]. The cross section of the fuel cluster optimized for the design objectives of the AHWR Reference design is shown in Fig. 6a.
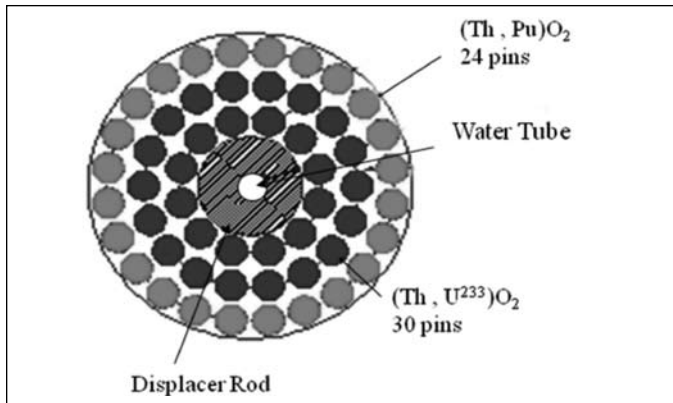

Fig. 6a Cross section of the AHWR fuel cluster
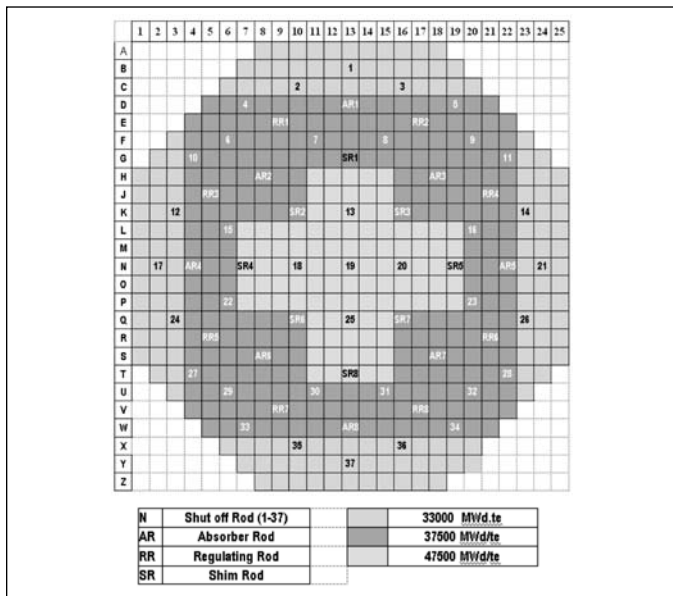
Fig. 6b Layout of AHWR equilibrium core

The core configuration of the AHWR core is shown in Fig.6b. The strong coupling between the neutronics and thermal hydraulics puts an extra requirement of flat radial power characteristics [14].

The reactor core of AHWR consists of 513 lattice locations in a square lattice pitch of 225 mm. Of these, fuel assemblies occupy 452 locations and 61 locations are reserved for the reactivity control devices and shut down

system-1 [15]. Among the 61 locations for the reactivity devices, 37 locations are used for locating Shutoff Rods (SORs). The remaining 24 are used for locating control rods (CRs) for short-term reactivity compensation and power maneuvering during normal operation. The control element is boron carbide (B_4C) packed in SS tubes placed between SS shells both for control rods and shut off rods. The main core design features are tabulated in Table 3.

Table 3 Important Design Parameters of AHWR

Reactor Power	300 MWe (920MWth)
Fuel	54 pin cluster (Th,233U)MOX+(Th,Pu) MOX or (Th,LEU fuel)
Coolant	Boiling Light Water
Moderator	Heavy Water
Total No. of Channels	513
No. of Fuel Channels	452
Lattice Pitch	225 mm
Primary Shut down System	37 shut off rods (B_4C absorber)
Secondary Shut down System	Liquid poison injection in moderator (Gadolinium Nitrate injected into moderator)
No. of Control Rods	24
Passive Poison Injection	Poison injection through a passive valve due to increase in steam pressure

4.1 Pu as fissile topping

The equilibrium fuel cycle is based on the conversion of naturally available thorium into fissile 233U driven by plutonium as external fissile feed. The uranium in the spent fuel will be reprocessed and recycled back into the reactor. The basic fuel cycle is based on the fact that the AHWR core should be self-sustaining in 233U. The 233U required is to be bred *in situ*, which implies that the initial core will be based solely on thorium-plutonium fuel. There will be gradual transition from the initial core, which will not contain any 233U to an equilibrium core, which will have composite clusters. During this transition phase a relatively larger quantity of plutonium is required. 233U is then recycled into the same core operating in a closed fuel cycle. The fuel cycle is thus involved with a three way reprocessing for the outer (Th,Pu)MOX pins. The initial content of the fuel in the composite cluster is about 34.5 g/kg of 233U fuel. With burnup, the loss of fissile 233U in the (Th, 233U)MOX pins has to be compensated by the conversion of fertile 232Th in the (Th, Pu)MOX to fissile 233U. This can be seen in Fig.
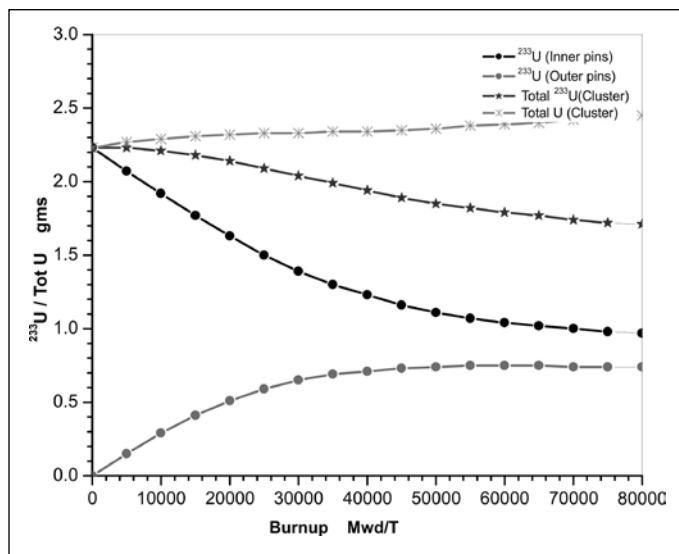
Fig. 7 ^{233}U and uranium build-up in the AHWR equilibrium core cluster with Pu topping

7. It was shown that 75% of power comes from Th-^{233}U in the equilibrium cycle [16].

4.2 LEU-Th fuel cycle in AHWR

The physics design of AHWR has been focused on the Th-LEU fuel in an open cycle configuration. With ^{235}U content of about 4.2% a discharge burnup of about 60GWD/T has been achieved [17]. The equilibrium fuel cluster is loaded with 30% LEU in ThO$_2$ in the inner 12 pins, 24% LEU in the middle ring of 18 pins and an average of 16% LEU in the outermost 24 pins. Gd is used as burnable poison to suppress power ripples in two pins on the inner ring. The cross section of the fuel cluster is shown in Fig. 8. The AHWR-LEU core, by design has enhanced safety and proliferation resistance characteristics. The spent uranium fuel is denatured by the presence of ^{238}U Also, the presence of ^{232}U in discharged U and ^{238}Pu in discharged Pu enhances its proliferation resistance characteristics. The power from Th/^{233}U would be about 39%.
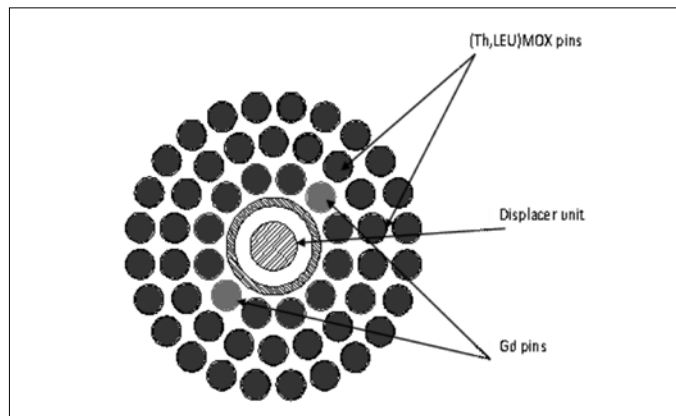
Fig.8 AHWR equilibrium Core Cluster with Th-LEU fuel

The AHWR-LEU fuel management has posed several challenges from managing a flat power/flux profile across the core as the Gd burns to managing the in-core peaking at the empty reactivity device locations. Several fuel management schemes through mini batch-fuelling are being studied as the core advances from initial to equilibrium phases. Presently the core is being re-optimised in order to get better shut down margins.

5. Thorium fuelled High Temperature Reactors

BARC is designing high temperature reactor systems for different objectives. The designs being pursued for the high temperature reactor project is the Compact High Temperature Reactor (CHTR) and the 600 MWth Innovative High Temperature Reactor (IHTR). The CHTR is being designed as a nuclear power pack for supplying energy in remote areas for a long period of time. The IHTR utilizes the process heat to dissociate water into its constituent gases H$_2$ and O$_2$. The main components of CHTR are BeO moderator, Th-^{233}U or HEU fuel, Lead Bismuth Eutectic (LBE) coolant with vertical prismatic type design rated for 100 kWth power. It has 19 Fuel assemblies. Each fuel assembly of CHTR consists of 12 fuel bores filled with fuel compacts made of TRISO coated particles. Other salient design features are passive core heat removal by natural circulation of liquid heavy metal coolant, compact design to minimize weight, longer core-life (~15 years) [18].
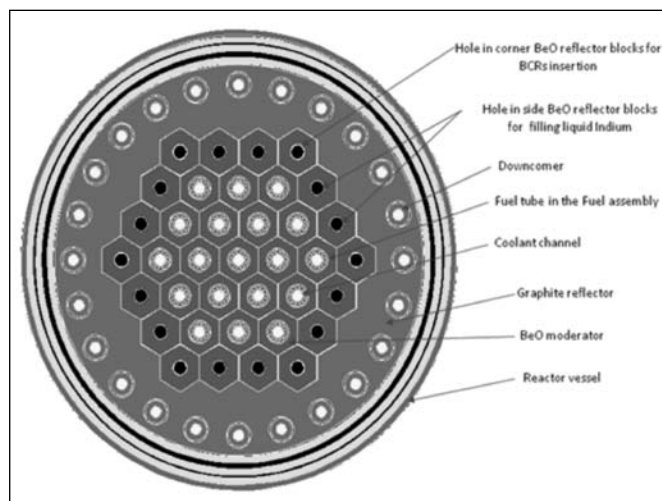

Fig.9 Cross section of the CHTR core

In the current conceptual design of CHTR, the core has primary shutdown system based on six absorber rods to be inserted in inner coolant channels and liquid poison injection of Indium in 12 BeO reflector holes acting as secondary shut down system. The cross section of the CHTR core is shown in Fig. 9.
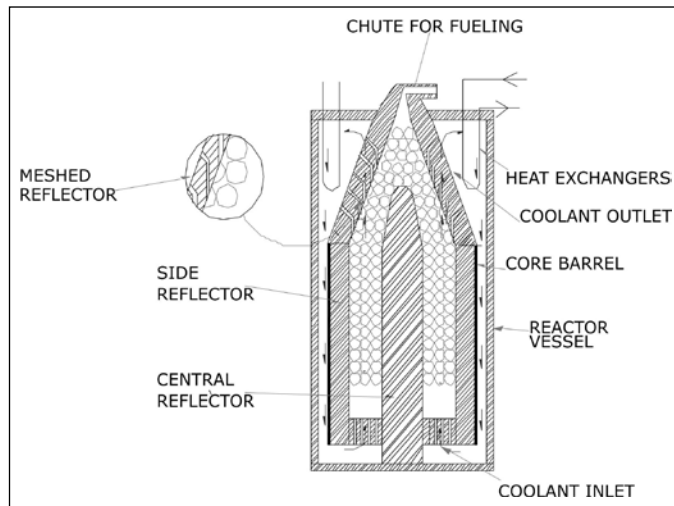
Fig.10 The pebble bed IHTR

The **IHTR-Core** is being designed with 150000 pebbles floating in the coolant in annular core of 150cm thickness and graphite as moderator [19]. The schematic of the pebble bed in IHTR core is shown in Fig. 10. The fuel particles, called TRISO coated particles has a kernel of 250 µm radius that contains the heavy metal ($^{233}UO_2+^{232}ThO_2$), where 7.6 wt % UO_2 of total heavy metal) and is surrounded by four carbon-based coating layers, forming a total outer radius of 450µm. The proposed coolant consists of mixture of fluoride salts (FLiBe) which has a freezing point of 400°C and a boiling point of ~1400°C at atmospheric pressure. Operating temperature of IHTR is about 1000°C. Presently the packing fraction of the pebbles in the core is being re-optimised to get desired negative coolant void reactivity characteristics.

6. Summary

Thorium utilisation has been the significant objective of many reactor systems due to the superior properties of the bred fissile material. It is also well established that the implementation of the thorium fuel cycle is involved and there have been significant progress in all aspects of the thorium fuel cycle. In this paper we have tried to focus our attention on the use of thorium in thermal reactor systems which are currently being designed in the Reactor Physics Design Division. The technological feasibility of the thorium fuel cycle would be realized with the help of AHWR. Th experience gained in irradiating thorium in research and power reactors has also helped in the design of newer reactors with thorium fuel. It has also been emphasized that thorium would have to be used in a closed fuel cycle option in order to exploit its complete potential. To this end post irradiation examination of the irradiated thorium fuel would be a very useful tool for fuel cycle studies.

References

1. R.K. Sinha, presented at the *Annual Conference of the Indian Nuclear Societ y(INSAC-2006)*, Mumbai, India.

2. M. Lung, Report No. EUR 17771, European Commission, 1997.

3. D. E. Cullen, PREPRO2000, ENDF/B Preprocessing codes, IAEA-NDS-39, Rev. 10, April 2000.

4. K. Umasankari, S. Jayashree, A. Kumar, P. D. Krishnani, K. Anantharaman, and R. Srivenkatesan, Thorium fuel and its use in AHWR, IAEA consultants meeting on *Role of Heavy Water Reactors for efficient Fuel utilization*, 2006.Mumbai, India.

5. K. Balakrishnan, *BARC Newsletter*, 183(April, 1999).

6. K. Balakrishnan, and A. Kakodkar, *Annals of Nucl. Energy*, 21(1993)1.

7. V. Jagannathan, U. Pal, R. Karthikeyan, , S. Ganesan, , R. P. Jain, and S. U. Kamat, *J. Nucl. Technol.*, 133(2001)1.

8. IAEA,. Thorium Fuel Utilisation: Options and Trends. TECDOC-1319, 2002**.**

9. N. Prasad et al., "Reactor Physics and Shielding (Chapter 4) of Final Safety Assessment Report (FSAR) of Critical Facility for AHWR & 500 PHWR, May 2008.

10. S. Ganesan, 2004., "Progress in the preparation of Indian experimental benchmarks on thorium irradiations in PHWR and KAMINI reactor," P. 42-43, Summary Report of the Second Research Coordination Meeting of the *IAEA Co-ordinated Research Project* on "Evaluated Data for the Thorium-Uranium fuel cycle," IAEA, Headquarters Vienna, Austria, 6 – 9 December 2004, INDC(NDS)-468, IAEA NDS, Vienna, Available online at: www-nds.iaea.org/publications/indc/indc-nds-0468.pdf

11. K. Umasankari, S. Ganesan, and R. Srivenkatesan, Estimation of ^{232}U concentration of spent thoria fuel of PHWR using the updated WIMSD library. RPDD / AHWR / FC /20(2002).

12. R. K. Sinha, and A. Kakodkar, *Nucl. Eng. Des.*, 236(2006)683.

13. A. Kumar, *Proc. of annual conf. on Power from Thorium – Status, Strategies and directions*, 1(June 1-2, 2000)52, Mumbai, India.

14. R. Srivenkatesan, A. Kumar, K. Umasankari, V.K. Raina, M. K. Arora, S. Ganesan, and S. B. Degwekar, presented at the Indian Nuclear Society Annual Conference, INSAC, June 2000, Mumbai, India.

15. A. Kumar , K. Umasankari, N. Prasad, P. Baltej Singh,

A.Thakur, A. Kumar, S. Mukerji, B. Krishna Mohan, A. Gupta, A. K. Mallick, and P. D. Krishnani, Safety analysis report - Preliminary; Physics Chapter. RPDD / AHWR / 130 / Nov. 2009.

16. K. Umasankari, N. P. Pushpam, A. Kumar, S. Ganesan, P. D. Krishnani, R. Srivenkatesan, and R. K. Sinha, Physics design aspects of Thorium Fueled Advanced Heavy Water Reactor (AHWR)". *Paper presented Advances in Nuclear Fuel Management IV (ANFM 2009) April 12-15, 2009,* Hilton Head Island, South Carolina, USA.

17. A. Thakur, B. Singh, N. Prasad, V. Bharti, K. Umasankari, P. D. Krishnani, and R. K. Sinha,presented at the Int. Conf. on Future of Heavy Water Reactors (FHWR -2011, Oct 02-05), Ontario, Canada.

18. D. K. Dwivedi, A. Gupta, A. Kumar, P. D. Krishnani,presented at the International Conference on Peaceful Use of Atomic Energy 2009, New Delhi, India.

19. I. V. Dulera, and R. K. Sinha, *J. Nucl. Mater.,* 383(2008)183.

Dr. Krishnani joined Bhabha Atomic Research Centre in the year 1974 after taking Post-graduate degree in Physics from Lucknow University and has received his Ph.D. from Mumbai University while working in BARC. He is from the 17th batch of BARC Training School. Presently, Dr. Krishnani heads Reactor Physics Design Division of BARC and is also a Senior Professor of Homi Bhabha National Institute and has nearly 38 years' research experience. He has developed a number of lattice analysis codes for PWRs, BWRs, HTRs and PHWRs which are most sophisticated and state-of-the-art software for reactor design. He has contributed towards the study of utilization of thorium and MOX fuel in TAPS-1/2 as well as 220 MWe PHWR. He is also associated with the design of PHWRs and PWRs. Presently, he is in-charge of physics design of Advanced Heavy Water Reactor, Compact High Temperature Reactor and Innovative High Temperature Reactor for Hydrogen production. He is also Chairman of Programme Implementation Committee of Nuclear Data Physics Centre of India. He is member of number of safety committees in AERB and BARC. He has more than 380 publications to his credit in the international journals, National and International symposia and in the form of reports.

Dr. Umasankari Kannan is from the 29th batch of the BARC training school. She has over 26 years of experience in the field of Reactor Physics. She joined the Reactor Engineering Division in 1986.   She has been mainly involved in the Physics design of Advanced Heavy Water Reactor. Her other areas of specialisation include, thorium utilisation, Nuclear Data Physics for the thorium fuel cycle, fuel cycle physics and experimental irradiation in Research Reactors and. She acquired her PhD from University of Mumbai and her PhD topic was "Development of new nuclear databases for advanced reactor systems utilising thorium".

She is currently heading the Fuel Cycle Studies Section of the Reactor Physics Design Division and is a professor of Homi Bhabha National Institute. She has over 165 publications including 30 papers in peer reviewed Journals and International conferences.

Perspectives of Thorium based Nuclear Fuel: Mixed Oxide Estimation Techniques

**A. A. Melvin[a]* and B. Gupta[b]**

[a]*Department of Chemistry, University of Pune, Ganeshkhind, Pune 411007, India*
[b]*Surface and Nanoscience Division, Materials Science Group, Indra Gandhi Centre of Atomic Research, Kalpakkam, Tamilnadu 603102, India*
*Email: ashwinmelvin08@gmail.com

1.1 Introduction:

The growth of nuclear power around the world is under progressive improvement, especially in terms of its operating performance with the existing reactors and also in its economic competitiveness that comes out in electricity markets. In 2002, 16% of global electricity was generated from some 441 nuclear power plants, with total installed capacity of 358 GW(e). In reference to this current situation, the annual average rate growth of world nuclear capacity would be expected to be in the range of 0.9% up to the year 2025 that corresponds to the nuclear power of some 438 GW(e). For the fulfilment of this objective there is a requirement in the substitution of existing nuclear fuel which is largely available in the surroundings. Thorium (Th) supplies are several times greater than that of uranium (U) and is widely distributed in nature and explored as an easy resource in many countries [1]. Thorium does not contain any 'fissile' component and is composed of the 'fertile' ^{232}Th isotope in contrary to U which contain ~0.7% 'fissile' ^{235}U isotope. Hence, Th and Th-based fuel in different chemical forms, could be explored for the possibility of their utilization along with more feasible 'fissile' ^{235}U or ^{239}Pu in nuclear research and power reactors; thereby opening a source for 'fissile' material as shown in the following equation. The final 'fissile' element is ^{233}U and not higher minor actinides.
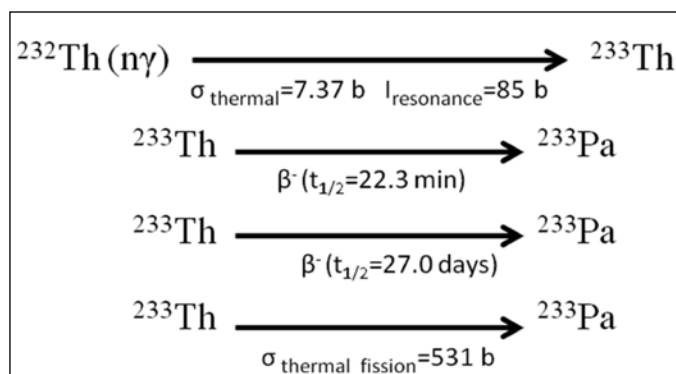
Thorium fuels and fuel cycles are particularly of interest in those countries where there is limited uranium reserve but very large thorium deposit. Applicability of Th based fuel is in wide range of nuclear reaction like high temperature gas cooled reactors (HTGR), light water reactors (LWR), pressurized heavy water reactors (PHWRs), liquid metal cooled fast breeder reactors (LMFBR) and molten salt breeder reactors (MSBR). In addition, theoretical database is also available in many documents *viz.* reviews and conference proceedings published by US Atomic Energy Commission [2], US Department of Energy [3], [4], KfA, Germany [5] and IAEA [6]. In addition, proceedings of IAEA meetings on Thorium Fuel Utilization: Options and Trends cover the activities and research projects related to the thorium fuel cycle in its Member States [7]. The two main international activities, namely Innovative Nuclear Reactors and Fuel Cycles Programme (INPRO) initiated by the IAEA and the US-led Generation IV International Forum (GIF), are intricately involved with research with thorium fuels and fuel cycles. Initially Th-based fuels and fuel cycles were unable to get more attention among the developing countries, due to discovery of new U deposits and their improved availability. India has been a forerunner and has actively persuaded the development of Th as a potential nuclear fuel. The initiative for India's nuclear energy programme was taken and laid by nuclear pioneer Homi Bhabha in 1954. The advanced heavy water reactor (AHWR) projected by nuclear power corporation of India (NPCIL), can have ground breaking results and could fulfil India's 60-year vision for thorium based nuclear energy production. Recently, various factors like proliferation-resistance, higher burn-up, longer fuel cycles, improved waste form characteristics; reduction of plutonium (Pu) inventories and *in-situ* use of bred-in fissile material turned our interest towards Th-based fuel. Following are the benefits and challenges of Th-based fuels and fuel cycles:

1.2 Benefits of Th based fuel:

Amongst various nuclear fuels, Th based fuels have their own unique advantages in terms of availability, relatively small absorption cross section and less radio toxicity *etc.* Following sub-section describes some of the points briefly.

1. Thorium is widely distributed in nature and hence makes it an easily exploitable nuclear fuel resource in many countries; however, it has not been exploited for commercial purpose. Thorium can be considered as a complement of uranium fuels and ensure nuclear power as an important source for a long time.

2. Th is considered as a better 'fertile' material than ^{238}U in thermal reactor; however, thorium is not able to compete with depleted uranium as a 'fertile' material in fast reactor. Fertility is estimated in terms of absorption cross-section for thermal neutrons of ^{232}Th (7.4 barns) which about three times that of ^{238}U (2.7 barns). Hence, ^{232}Th can produce a larger amount of ^{233}U in comparison to the reaction ^{238}U to ^{239}Pu.

3. Th fuel cycle produce very less radiotoxic waste with long term prospect. In addition, incineration process of weapons grade plutonium (WPu) or civilian plutonium makes transition into Th a safe nuclear fuel.

4. For the 'fissile' ^{233}U nuclei, the breeding of neutron is more than 2 times over absorbed one which varies with the thermal energy of neutron spectrum opposite to that of ^{235}U and ^{239}Pu. Thus, ^{238}U–^{239}Pu cycle is based on fast neutron spectra; however, the ^{232}Th–^{233}U fuel cycle can operate under three condition *viz.* with fast, epithermal or thermal spectra.

5. Chemical stability and radiation resistance of thorium dioxide is higher than uranium dioxide. The rate of fission for ThO$_2$–based fuels is less than that of UO$_2$ by about one order of magnitude. Apart from that, ThO$_2$–based fuels are also supposed to have better in–pile performance and favorable thermo-physical properties than that of UO$_2$ Better thermo-physical properties correspond to higher thermal conductivity and lower co-efficient of thermal expansion.

6. Chemical inactivity makes the possibility of long term interim storage and permanent disposal of spent ThO$_2$–based fuel without the problem of oxidation.

7. Proliferation-resistance of Th based fuel is very high due to the formation of ^{232}U with half life of 73.6 year along with ^{232}Th, ^{233}Pa and ^{233}U which emit strong gamma (γ) radiation through daughter nuclei. Above feature makes the utility of ^{232}U as an attractive carrier of highly enriched uranium (HEU) and weapon grade plutonium (WPu) to avoid non-peaceful outcomes [8].

8. Usually ^{232}Th–^{233}U fuel cycle, forms very less amount of Pu and Minor Actinides (MA: N_p, Am and C_m) having long life of decay, thereby reducing the chance of radiotoxicity.

1.3 Mixed oxide nuclear fuel:

Mixed oxides of ^{232}Th either with ^{233}U or ^{239}Pu are considered as efficient fuels for the third stage of power production utilizing Advanced Heavy Water Reactors (AHWR) [9, 10]. Before utilizing ^{233}U as an actual fuel, there is a requirement of research related to the preparation of mixed oxides of natural U and Th using powder metallurgical routes, wherein the optimization of composition and homogeneity of U and Th are kept into consideration. The following techniques have been developed so far for the preparation of ThO$_2$ based mixed oxide fuels:

1.3.1 Powder-pellet route: Powder pellet route is used for the preparation of high density fuel pellets of ThO$_2$, UO$_2$ and PuO$_2$. Here, the respective oxides are taken in the form of powders. The formed pellet is used as stack and encapsulated in cladding tubes for further use [11].

1.3.2 Vibro-sol route: This method involves the preparation of fuel microspheres in a gel form by an internal or external gelation process, where the gelating agent is "ammonia". After ammonia treatment, the microspheres are found to separate out in the form of hydrated gel. Later on microspheres are sintered and vibro packed in cladding tubes followed by encapsulation [12]. Precursors for the above process are nitrate solutions of U, Pu and Th for adopting the gelation process.

1.3.3 Sol-gel microsphere pelletisation: This method is not only dust-free but also free-flowing and involves sol-gel derived oxide fuel microspheres, that are used for direct pelletisation and sintering [13].

1.3.4 Impregnation technique: This technique can be carried out in two ways 1) with Relatively low density ThO$_2$ pellets after partially sintering or 2) 'porous' ThO$_2$ microspheres are vacuum impregnated in nitrate solution of U or Pu–nitrate. This is followed by calcination and sintering, resulting into high density ThO$_2$-based mixed oxide fuel pellets and can be stored in cladding tubes after encapsulation [14].

1.4 Composition analysis of metal oxide mixture:

The composition of U, Th based fuel should be specific for nuclear energy plan and requires strict quality control. It is also necessary to make use of minimum amount of sample for estimation purpose. As we are dealing with nuclear materials of both U and Th, hence, reduced risk of nuclear radiation caused by ^{238}U, ^{235}U and ^{232}Th and their daughter products is required to be studied in respect to the sample amount. As per the requirement of chemical quality control, composition characterization of U and Th oxide fuel should be accurate as well as precise. Compositional

characterization of mixed oxide samples were done by conventional chemical methods like mass spectrometry and biamperometry [15-17]. These methods give precise results only after chemical dissolution, which limits their applicability. Total reflection X-ray fluorescence (XRF) method was used to determine U and Th in presence of each other only in the dissolved state [18]. The track etching technique was used for the same purpose without chemical separation. But, this method is also having some drawbacks *i.e.* lengthy sample preparation procedure, development of tracks and also nonspecific [19, 20]. Recently various methods have been reported which make oxide estimation in a long range with high precision and without dissolution as described below:

1.4.1 Instrumental neutron activation analysis (INAA):

INAA is a feasible method for determination of mixed form in one stream without chemical dissolution and separation. Two types of reactor neutrons namely thermal NAA (TNAA) and epithermal NAA (ENAA) were optimized and employed for the determination of U and Th in their mixed oxides. Process happened in two steps, first the sample is subjected to a neutron flux and formation of radioactive nuclides followed by estimation of emitting γ rays with energies that are characteristics of their respective nuclei. Acharya *et al.* applied a very facile methodology of oxide estimation by the above mentioned technique. Cellulose matrix was used as the base material for the preparation of slandered and synthetic samples of U–Th mixed oxide. Irradiation had been carried out in pneumatic carrier facility (under pressure) of Dhruva reactor as well as at self serve facility of CIRUS reactor under cadmium cover (0.5 mm) [21]. After irradiation, γ-emitting daughter products ^{238}U (^{239}U and ^{239}Np) and ^{232}Th (^{233}Th and ^{233}Pa) were formed and used as a prototype of ^{238}U and ^{232}Th for estimation purpose. High-purity germanium detector (HPGe-40% relative efficiency) was used for radioactive assay of the nuclei. The estimation results revealed the value of U and Th of 4–8% U–Th matches well with the expected values (within ±3%). Results are quite reproducible (1.6% for U and 0.1% for Th) for four batches of samples having 4% U–Th mixed oxide. Detection limits was found to be the best in case of ENAA method of 0.1 and 0.3l g for U and Th respectively.

1.4.2 Energy dispersive X-ray fluorescence (EDXRF):

EDXRF methods is known because of its multiple advantages *viz.* simple and quick analysis steps, environmental friendly, applicability for a wide concentration range (100 ppm level to 100%) and analysis of many elements in one step process. EDXRF technique is very less reported in literature especially for its application

in the nuclear field; however, some reports [22, 23] are available for the determination of solution processed actinide elements. V. Natarajan *et al.* explored EDXRF method for the determination of U content in (Th–U) mixed oxides and found it to achieve large dynamic range (2–80%) [24]. Similar comparative estimation has been done by some other standard estimation technique to ensure the accuracy of the method. The experimental parameters for the sample preparation were optimized with 1 cm diameter pellets in which base material is cellulose, however, the wt. % of Th–U oxide is 1:1. Calibration plots were made on the basis of both L_a as well as L_b peaks intensity in case of U and, L_a peak intensity for Th respectively. Typical feature of calibration plot is shown in Fig. 1. The experiment outputs of concentration measurement of synthetic samples were found to be in good agreement with standard values. Moreover, the method was found to be useful in various temperature ranges, where the sample could be either cooled or heated.
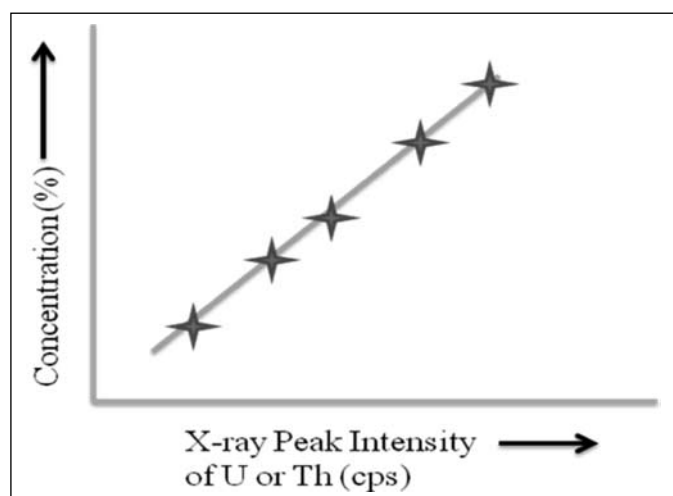

Fig. 1: Typical form of calibration plot of EDXRF measurement.

1.4.3 Non-destructive assay technique:

The high resolution gamma-ray (γ-ray) spectrometry is one of the older and non-destructive methods available for the estimation of U to Th ratio in mixed oxide kind of samples. Naturally occurring isotopes of U emits very low energy γ-rays and some of the nuclei like ^{232}Th do not emit any such rays of its own. However, fission product (daughter nuclei) of ^{238}U and ^{232}Th emit intense γ-ray which can be used for the analysis purpose. Determination of U can conveniently be done by this method as it decays quickly (~5 month) to attain equilibrium with daughter nuclei. But in case of ^{232}Th the decay is found to be very long (~35 year). In this case, γ-spectrometric can be used for the determination of Th of known time history, since, it is found that γ-spectrometric method has the limitation

of radon loss which leads to uncertainty in the estimation of Th. Estimation protocol follows the assay of γ-rays with varying energy according to the nuclei *i.e.* 1001 keV for ^{238}U and 2614.6 keV for ^{232}Th. It is also a requisite for the best detection that all the samples have a same geometry. T. N. Nathaniel *et al*. describes this technique [25] for oxide estimation using closely spaced high energy γ-rays in the region of 4000 keV to 4150 keV which is applicable for samples of any geometry and thickness and also not facing the problem of any correction for γ-ray attenuations and detection efficiencies. For thicker samples, higher energy prompt γ-rays were chosen. Since the chosen γ-rays were closely spaced this method can be appled for any shape and size of the sample. The results comes out in the form of peak area ratios and the ratio of ^{238}U to ^{232}Th makes its applicable for the estimation of the different components in fuel materials as well as the finished products at any stage of fuel cycle.

1.4.4 Laser-induced breakdown spectroscopy (LIBS):

LIBS is a type of emission spectrometric technique with several advantages and potentially applicable in nuclear field. A. Sarkar *et al*. have developed LIBS methodology to determine U and Th in aqueous solutions individually as well as in the mixture [26]. LIBS is also applicable for the determination of trace constituents in a thoria matrix [27]. Recently, this method has been applied for Th–U mixed oxide fuel samples in solid form [28]. The mixed oxide pellets were prepared from 1:1 (w/w) mixture of Th-U mixed oxide standards where boric acid was used as a binder. In the instrument part, high power Q-switched Nd:YAG laser is used which set to generates 200 mJ of pulse energy. Finally, the emission from plasma is collected in front side at an angle of 45° to that of the laser source. Estimation process involves two steps: the collection of plasma emission on 15-mm diameter imaging lens focused onto silica optical cable fibers followed by signaling on CCDs through spectrographs (Czerny–Turner configuration). Calibration curves were established for different emission lines of U *i.e.* U(II) 263.553 nm, U(II) 367.007 nm, U(II) 447.233 nm and U(II) 454.363nm. Reproducibility of the experiment was carried out with two different synthetic mixed oxide samples and it was found that the calibration curve matches well with that of the expected values. In this method U(II) 263.553 nm emission line did not depict a saturation effect caused by self absorption. The method is highly reproducible upto to ±2% (1σ). The result supports strong potential of the LIBS method in nuclear industry even though the addition of boron in nuclear material is undesirable because it explores the possibility of the usage of carbon-based binder such as starch and nitrocellulose as an alternative for boron based materials.

The technique for utilization of Th and Th based fuel is still under development process. It has many unique properties but also has some challenges which need to be overcome as mentioned in the following section.

1.5 Challenges with Th fuel:

1. Sintering temperature of Th based fuel is more than >2000 °C due to its high melting point (2800 °C) (much higher compared to that of UO_2). Admixing of CaO, MgO, and Nb_2O_5 *etc* considered as 'sintering aid' is required to achieve dense pellet at lower temperature.

2. ^{232}U is a byproduct of irradiation on Th or Th–based fuels which produce strong γ-irradiation from its very short half-lived daughter products *i.e.* ^{212}Bi and ^{208}Tl. The consequence of Th fuel cycle causes significant build-up of radiation dose. Hence, such process needed automated reprocessing and re-fabrication in highly protected hot cells at remote area which finally causes the problem of high cost.

3. Long time boiling of THOREX [13 M HNO_3+0.05 M HF+0.1 M $Al(NO_3)_3$] at ~393 K is required for dissolution of ThO_2 due to its inertness. The presence of required amount of HF in concentrated HNO_3 causes corrosion problem for stainless steel equipment in reprocessing plants; however, it can be overcome up to a certain extent by the addition of aluminum nitrate.

4. ^{233}Pa is an intermediate radioactive nuclei in Th fuel cycle which is having long decay time (~27 days) as compared to ^{239}Np (2.35 days-product of uranium fuel cycle) and so it requires minimum one year cooling time for completing the conversion of ^{233}Pa to ^{233}U. Thus it is essential to separate Pa from the spent fuel prior to the separation of ^{233}U and thorium by any conventional extraction process.

5. The process of three component separation like U, Pu and Th from spent mixed oxide fuel is still not optimized.

6. Literature data dealing with Th-based fuels and Th fuel cycles is very scarce in comparison to UO_2 and (U, Pu)O_2 fuels, and hence it needs to be well discussed before commercial utilization of thorium fuels and fuel cycles with large scale financial program.

1.6 Conclusion:

Chemical stability and better solubility of thoria, attracts greater attention towards thoria based fuels in

nuclear plant. It also helps in better disposal of the nuclear wastes. To utilize these beneficial and attractive qualities of thoria based fuels two things are required—first (a) an appropriate fuel fabrication technique and second (b) an estimation process which gives rise to an acceptable degree of microscopic homogeneity and quality control. Mainly by keeping the objective of enhancing the intrinsic proliferation barriers, the utility of Th–based fuel cycles will come out as an evolutionary alternative into existing and near-future nuclear power plants. Apart from that, the superior neutronic properties of [233]U and improved stability for long term storage open up a wide possibility for the utilization of Th–based fuel.

References:

1. IAEA, ISBN 92–0–103405–9 (2005).

2. R. G. Wymer, presented at the 2nd Int. Symp. on Thorium Fuel Cycle, Ten. USA, 1966, US Atomic Energy Commission (1968).

3. P. E. Hart, C. W. Griffin, K. A. Hsieh, R. B. Mattews and G. D. White, *PNL 3064, UC-78, 99352* (1979).

4. J. Belle and R. N.Berman, *DOE/NE-0060, DE85 006670* (1984).

5. Nuclebra's, Final Report (1979-1988), Nuclebra's, Siemens KWU, Nukem and KFA-Juelich, Germany (1988).

6. IAEA, Utilization of Thorium in Power Reactors, Technical Reports Series No. 52, IAEA, Vienna (1966).

7. IAEA-TECDOC-1319, Vienna (2002).

8. J. Tommasi, European Commission (2000) 58.

9. R. K. Inha and A. Kakodkar, *Nucl Eng Des.*, 236(2006)683.

10. T. R. G. Kutty, M. R. Nair, P. Sengupta, U. Basak, A. Kumar and H. S. Kamath, *J. Nucl. Mater.*, 374(2008)9.

11. P. V. Hegde, T. R. G. Kutty, S. Majumdar, and H. S. Kamath, presented at the Int. Conf., (2003), Hyderabad, India.

12. IAEA-TECDOC-412, IAEA, Vienna (1987) 27.

13. C. Ganguly, H. Langen, E. Zimmer, and E. Merz, *Nucl. Tech.*,73(1986)84.

14. T. R. G. Kutty, presented at the Int. Conf.,(2003), Hyderabad, India.

15. P. R. Nair, M. Xavier, K. A. Mathew, P. M. Shah, S. K. Agarwal and H. C. Jain, *ESARDA Bull.*, 26(1996)23.

16. M. Xavier, P. R. Nair, K. V. Lohithakshan, S. G. Marathe and H. C. Jain, *J. Radioanal. Nucl. Chem.*, 148(1991)251.

17. N. V. Sreekumar, B. Narayana, R. A. Nazareth, N. G. Bhat, P. Hegde and B. R. Manjunatha, *Chem. Anal.*, 47(2002)759.

18. V. Natrajan, M. J. Kulkarni, N. K. Porwal, B. A. Dhawale, N. S. Hon, S. V. Godbole and V. K. Manchanda, *Nucl Instr Meth A.*, 266(2008)3290.

19. A. F. Hafez and M. A. Naim, *Nucl. Instr. Meth.*, B69(1992)373.

20. B. B. Srivastava, S. Mazumdar and J. K. Ghosh, *Nucl. Instr. Meth.*, B69(1992)370.

21. R. Acharya, Ruma Gupta and P. K. Pujari, *Radioanal Nucl Chem.*, 294(2012)121.

22. R. S. Day and A. R. Vigil, *J. Radioanal. Nucl. Chem.*, 194(1995)107.

23. N. C. Jayadevan, K. L. Chawla, K. D. Singh Mudher and D.M. Chackraburrthy, *Report- BARC-891* (1976).

24. V. Natarajan, M. J. Kulkarni, N. K. Porwal, B. A. Dhawale, N. S. Hon, S. V. Godbole and V. K. Manchanda, *Nuclear Instruments and Methods in Physics Research B* 266(2008)3290.

25. T. Newton Nathaniel, K. Sudarshan, A. Goswami and A. V. R. Reddy, *J. Radioanaly. and Nucl.Chem.*, 279(2009)481.

26. A. Sarkar, D. Alamelu, and S. K. Aggarwal, *Appl. Opt.*, 47(2008)G58.

27. D. Alamelu,A. Sarkar, and S.K. Aggarwal, presented at the *National LaserSymposia-6*, (2006), 90.

28. A. Sarkar, D. Alamelu and S. K. Aggarwal, *Talanta* 78(2009)800.

Ambrose A. Melvin is presently working as a postdoctoral fellow at National Chemical Laboratory (NCL), Pune. His research interest is in synthesis and fabrication of nanomaterials for different technological application. He's also involved in synthesis of nanometal composites through γ-radiolytic method for fuel cell application.

Dr. Bhavana Gupta is presently working as a visiting scientist (DST-ISPIRE-Fellow) at Indra Gandhi Centre for Atomic Research (IGCAR), Kalpakkam. Her major research interest is synthesis of nanomaterials for catalysis, biosensing and energy storage devices

Dissolution of thorium dioxide and its mixed oxides in nitric acid

G. K. Mallik

Post Irradiation Examination Division, Nuclear Fuels Group,
Bhabha Atomic Research Centre, Mumbai – 400094
E-mail : gatiwant@barc.gov.in

1. Introduction

Indian nuclear energy programme has been oriented to gain self-reliance by ultimately utilizing its rich indigenous thorium resources. Consequently, multi dimensional R & D studies are being carried out for the development of thorium based closed nuclear fuel cycle and innovative reactors [1]. A critical facility with thorium based fuel is running and an Advanced Heavy Water Reactor (AHWR) is in the offing. At both front and back ends of the thorium fuel cycle, the dissolution of thorium dioxide (ThO_2 or thoria) in nitric acid (HNO_3) is one of the most important processing steps. But, unfortunately, the dissolution of ThO_2 in only pure HNO_3 is chemically and thermodynamically unfavourable [2] and therefore, is a challenging manoeuvre.

A review of the Gibbs free energy values of Table-1 [2] suggests that spontaneous dissolution of only uranium dioxide (UO_2 or urania) is favourable in HNO_3 whereas that for plutonium dioxide (PuO_2 or plutonia) and thorium dioxide (ThO_2 or thoria) is not. The endothermic dissolution of PuO_2 and ThO_2 in pure HNO_3 is extremely difficult specifically when they are crystallized and sintered ones. High negative value of ΔH for $UO_2(NO_3)_2.6H_2O$ as compared to $Pu(NO_3)_4$ and $Th(NO_3)_4$ is the main reason for favorable dissolution of UO_2 in HNO_3.

In aqueous HNO_3 medium, Uranium (U) and Plutonium (Pu) exhibit more than one oxidation states whereas Thorium (Th) exhibits single oxidation state as Th (IV). The irreversible oxidation of U(IV) to U(VI) in HNO_3 in the form of more stable UO_2^{2+} ion is an energetically favored phenomenon on the basis of its smaller ionic radius [3] than U^{4+}. Pu has also the tendency to exhibit III, IV, V and VI oxidation states. Hence, UO_2 easily dissolves

in HNO_3 in presence of air and PuO_2 can be dissolved by employing oxidative-reductive [4, 5] and electrolytic [6] techniques. However, these techniques are non-amenable to ThO_2 due to single oxidation state exhibited by Th.
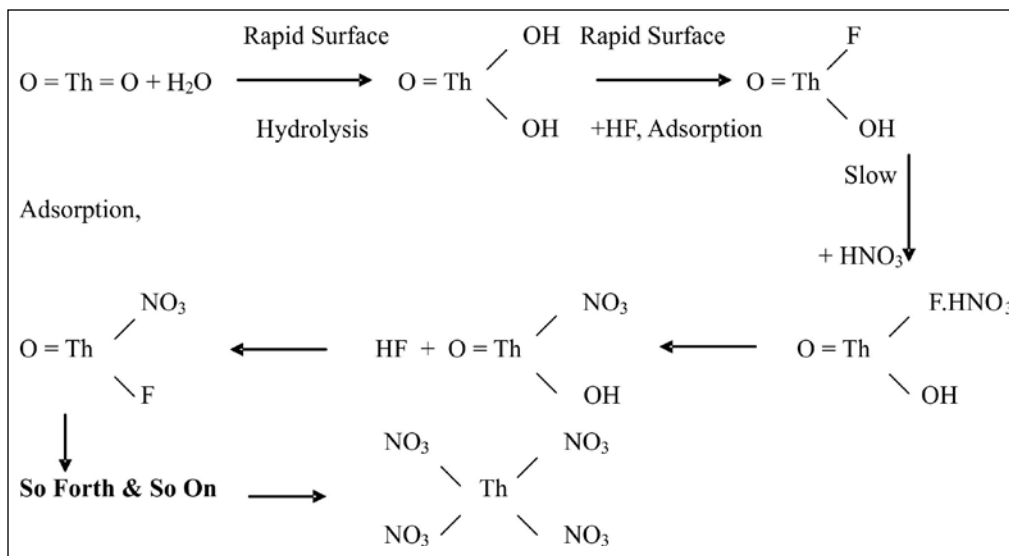
ThO_2 or $(Th,U)O_2$ may also be dissolved by solid state reaction method [7], using low melting $(NH_4)_2SO_4$, alkali metal bisulphates and pyrosulphates. But associated disadvantages of applying higher temperature (250-365°C) for fusion of salts and incorporation of non-volatile anions like SO_4^{2-} in the aqueous processing streams thereafter would require additional separation and purification steps.

Therefore, currently, using F^- ion along with HNO_3 appears to be the fittest technique for the endothermic dissolution of ThO_2. In heating modes, reflux (boiling the solute with solvent and condensing the escaping vapors of solvent) looks to be the most appropriate one. The F^- ion is chemically very reactive species and acts as a catalyst in the dissolution of ThO_2 in HNO_3 via following probable mechanism (Scheme 1) [8]:

Depending on the process flow-sheet, F^- ions may be boiled off almost completely from the solutions, after its role in dissolution is complete. Due to its high corrosive capability, F^- ion can shorten the life of metallic dissolution vessels. Due to volatility and penetrating capabilities, F^- ion can even prematurely damage the safety barriers of radiological containments, if not restricted properly. Hence, it would need a lot of precautions and efforts to avoid harmful corrosive attack of F^- ion. But, incidentally, F^- ion is required only in catalytic quantities for the dissolution of ThO_2 and, thus, some typical improvement on equipment concepts may resolve this issue.

Table-1: Thermodynamic parameters for the dissolution of UO_2, PuO_2 and ThO_2 in nitric acid

Sl. No.	Reaction	ΔG_{298} (kcal/mole)	Compound	ΔH_{298} (kcal/mole)
1.	$UO_2+3HNO_3+5H_2O = UO_2(NO_3)_2.6H_2O+HNO_2$	-16.9	UO_2 $UO_2(NO_3)_2.6H_2O$	-270 -764.3
2.	$PuO_2+4HNO_3 = Pu(NO_3)_4+2H_2O$	9.8	PuO_2 $Pu(NO_3)_4$ (aq)	-251 -340
3.	$ThO_2+4HNO_3 = Th(NO_3)_4+2H_2O$	10.3	ThO_2 $Th(NO_3)_4$ (aq)	-292 -380.5

Scheme 1

increase the reaction sites. The crushing of the high density thoria pellets would require severe mechanical means. This proposition of crushing for irradiated materials and spent fuels would not be viable on the grounds of spread of contamination on the walls of equipment and containments (glove-boxes or hot cells) specifically when the pellet(s) consists of neutron and γ-emitting nuclides like Pu and ^{232}U.

The concentration of F$^-$ ions within the acid mixture is also an important factor. Beyond a specified concentration limit of F$^-$ ions within the acid mixture, thorium precipitates out forming insoluble anionic fluoride complexes [13], which is very difficult to dissolve. It means that the concentration of F$^-$ ion is to be properly prefixed and controlled during dissolution.

Restricting the escape of F$^-$ ions, from the dissolution vessel, would be beneficial on two accounts. First, it would optimally maintain the adequate catalytic quantity of F$^-$ ion within the solvent medium and secondly it would effectively reduce the corrosive attack by the escaping F$^-$ ions on the peripherals outside the dissolution vessel.

2. History

Thoria, Thoria-Urania and Thoria-Plutonia [ThO$_2$, (Th,U)O$_2$ and (Th,Pu)O$_2$], with a requisite percentages of fissile U & Pu-isotopes, are generally used in high density (92-98% T.D.) cylindrical solid pellet forms as fuels. These fuels are normally fabricated from respective powder(s) by applying cold compaction and high temperature sintering route for heavy water reactors (HWRs). Therefore, apart from the powder forms, the dissolution techniques have to be more amenable to high temperature sintered - high densities thoria or its mixed oxides fuel pellets.

In laboratories, ThO$_2$, (Th,U)O$_2$ and (Th,Pu)O$_2$ are dissolved in hot HNO$_3$ + HF acid mixture by using infrared lamps, hot plates and reflux heating techniques [9]. Gradually microwave heating techniques using reflux or pressure vessels modes are also being introduced [10, 11, 12]. Acid mixtures can be heated below, at and above the normal boiling point of HNO$_3$ (i.e 120°C at atmospheric pressure) by using open vessels, reflux vessels and pressure vessels, respectively.

Lower is the surface area for the solid oxide-nitric acid reaction; lower would be the dissolution rate. The higher density pellets have the lower surface area and less open pores available for the reactions. For the ceramics like thoria powder, the dissolution rate is itself very low. The compaction of powder to pellet and sintering the pellet(s) to high density turns its dissolution rate extremely low. The sintering process highly densifies the particles within the pellet and reduces the pores / surface area for reaction within the pellet. Thus, for faster dissolution, either pellet is required to be crushed or there has to be some soluble species within the pellet matrix which selectively dissolve at faster rate and resultantly open pores to

3. Dissolution Studies

The results presented in Table-2 to 4 indicate the time of dissolutions of ThO$_2$ and its mixed oxides in pure HNO$_3$ and HNO$_3$ + F$^-$ mixture, impact of crushing of pellets, efficacies of heating modes, role of concentration of F$^-$ and benefits of use of NaF for a proper comparative understanding of rate and extent of dissolution. The experiments have been carried out over a long span of time but still would establish the beneficial trend and required conditions for implementing them at larger or industrial scale. In general, the used thorium dioxide and its mixed oxide pellets are sintered at 1500-1700°C and the density of the pellets is in the range of 93-96% T.D. The pellet has 14.2 – 14.6 mm diameter, 15.75 - 16.10 mm height and ~25 gms weight. The pellet is either dissolved intact or after crushing in mortar-pestle. 15.5 M LR grade HNO$_3$ has been used for all the experiments. Heating modes and dissolution vessels have been: (a) Infra red lamp - Platinum crucible (b) Hot plate - Platinum crucible (c) Heating mantle - Conventional glass reflux set-up (d) Microwave oven - MW reflux set up

Table-2 : Dissolution of ThO_2 and $(Th,U)O_2$ in 15.5M HNO_3

Material	Nature	Status	Weight (gms)	Dissolution Time (hrs)	Mode of Dissolution	ThO_2 Dissolution
ThO_2	Microwave Denitrated Oxide Powder	Powder	75	1	Microwave (Pressure)	>99%
ThO_2	Oxide powder via Th-Oxalate route	Powder	2	10	Conventional (Reflux)	<10%
ThO_2	Sintered Solid Pellet	Powdered	2	10	Conventional (Reflux)	<0.02%
ThO_2	Sintered Solid Pellet	Powdered	2	10	Microwave (Pressure)	<0.01%
ThO_2	Sintered Solid Pellet	Intact Pellet	6	17	Microwave (Reflux))	<0.03%
$(Th_{0.9675},U_{0.0325})O_2$	Sintered Solid Pellet	Intact Pellet	6	23	Conventional (Reflux)	<0.02%
$(Th_{0.9675},U_{0.0325})O_2$	Sintered Solid Pellet	Intact Pellet	6	23	Microwave (Reflux)	<0.03%
$(Th_{0.8},U_{0.2})O_2$	Sintered Solid Pellet	Intact Pellet	6	32	Microwave (Reflux)	<25%
$(Th_{0.8},U_{0.2})O_2$	Sintered Solid Pellet	Intact Pellet	6	84	Microwave (Reflux)	<39%

and (e) Microwave digestion system - PFA made controlled pressure vessels upto 120 psi.

In conventional heating, by infra red lamp, hot plate and reflux, only liquid (the acid / acid mixture) is heated directly whereas in microwave heating solid particles (UO_2 and PuO_2) may also be heated to higher temperatures simultaneously. Solid ThO_2 particles do not get heated with microwaves. In pressure vessels, the system is closed and does not allow the vapour to escape, so minimum F^- ions amount would be required. Due to unchanged concentration of F^- ion in pressure vessels, the dissolution time with 0.1M and 0.01M HF is almost same. In pressure vessels, the raising of pressure also increases the boiling temperature of HNO_3 and, hence, increases the dissolution rate. The microwave reflux set-up has been specially designed and used to compare its efficiency with conventional refluxing and microwave pressure vessel modes. The use of pressure vessel inside the glove-box and hot-cell is generally avoidable and, hence, the trials with microwave refluxing have been essential.

Table-3: Complete Dissolution of sintered ThO_2, $(Th,U)O_2$ and $(Th,Pu)O_2$ pellet in 15.5M HNO_3 + HF Mixture

Material	Nature	Status	Weight (gms)	Concentration of HF (M)	Dissolution Time (hrs)	Mode of Dissolution
ThO_2	Sintered Solid Pellet	Powdered	2	0.1	28	Infra Red Lamp
ThO_2	Sintered Solid Pellet	Powdered	2	0.1	22	Hot Plate
ThO_2	Sintered Solid Pellet	Powdered	2	0.1	0.75	Microwave (Pressure)
ThO_2	Sintered Solid Pellet	Powdered	2	0.01	0.9	Microwave (Pressure)
$(Th_{0.97},U_{0.03})O_2$	Sintered Solid Pellet	Powdered	2	0.1	26	Infra Red Lamp
$(Th_{0.97},U0_{.03})O_2$	Sintered Solid Pellet	Powdered	2	0.1	18	Hot Plate
$(Th_{0.97},U_{0.03})O_2$	Sintered Solid Pellet	Intact Pellet	2	0.1	14	Conventional (Reflux)
$(Th_{0.97},U_{0.03})O_2$	Sintered Solid Pellet	Intact Pellet	2	0.1	2	Microwave (Pressure)
$(Th_{0.97},U_{0.03})O_2$	Sintered Solid Pellet	Powdered	2	0.1	0.75	Microwave (Pressure)
$(Th_{0.96},Pu_{0.04})O_2$	Sintered Solid Pellet	Powdered	2	0.05	40	Infra Red Lamp
$(Th_{0.96},Pu_{0.04})O_2$	Sintered Solid Pellet	Powdered	2	0.05	1.5	Microwave (Pressure)

Table-4 : Complete dissolution of intact sintered pellets in 15.5M HNO$_3$ + HF / NaF in larger scale

Material	Nature	Status	Weight (gms)	Acid / Acid mixture (15.5M HNO$_3$)	Dissolution Time (hrs)	Mode of Dissolution
ThO$_2$	Sintered Solid Pellet	Intact Pellet	75	HNO$_3$+0.05M HF	168	Conventional (Reflux)
ThO$_2$	Sintered Solid Pellet	Intact Pellet	75	HNO$_3$+0.05M NaF	160	Conventional (Reflux)
ThO$_2$	Sintered Solid Pellet	Intact Pellet	75	HNO$_3$+0.05M HF	24	Microwave (Pressure)
ThO$_2$	Sintered Solid Pellet	Intact Pellet	75	HNO$_3$+0.05 M NaF	14	Microwave (Pressure)
(Th$_{0.9675}$,U$_{0.0325}$)O$_2$	Sintered Solid Pellet	Intact Pellet	450	HNO$_3$+0.05M HF	250	Conventional (Reflux)
(Th$_{0.9675}$,U$_{0.0325}$)O$_2$	Sintered Solid Pellet	Intact Pellet	450	HNO$_3$+0.05M HF	23	Microwave (Reflux)
(Th$_{0.9675}$,U$_{0.0325}$)O$_2$	Sintered Solid Pellet	Intact Pellet	450	1st stage : HNO$_3$	10	Microwave (Reflux)
				2nd Stage : HNO$_3$+0.05M HF	15	

In Table-3, it is observed that the dissolution rate of thoria pellet by the use of microwave pressure vessel is one order higher than the conventional refluxing (also see Fig.1). The dissolution of thoria pellet occurs by symmetric dissolution of pellet, as pellet(s) goes thinner and thinner, with cylindrical shape remaining intact, till last i.e. ~1mm diameter and then crumbles. It is also observed that the use of NaF in place of HF increases the dissolution rate which may be attributed to the higher availability of F$^-$ ions in medium with NaF as compared to HF. The last three experiments in Table-4 [12] have been specially carried out with (Th,U)O$_2$ pellets to assess whether initial leaching of UO$_2$, in absence of HF, can have any impact on dissolution scheme of ThO$_2$. It can be concluded that only leaching of UO$_2$ without HF at 1st stage and then dissolving ThO$_2$ with HF at 2nd stage, will reduce the contact time of HF with dissolution vessel for a significant duration of time (here, 8 hrs, i.e. one third of applied time).

The quantitative analysis of Thorium in solutions has been carried out by EDTA complexometric titrations using Xylenol Orange indicator [14]. The estimations of Uranium and Plutonium have been carried out using redox titrimetric method using potentiometric end point determination [15, 16].

The studies have been carried out to observe the role of F$^-$ ion concentration and pressure application on ThO$_2$ dissolution [10,11] along with impact of HNO$_3$+HF/NaF mixture with or without Al(NO$_3$)$_3$ on the leach rate of clad and corrosion rate of dissolution vessel materials [11]; shown in Fig.2 to 5.
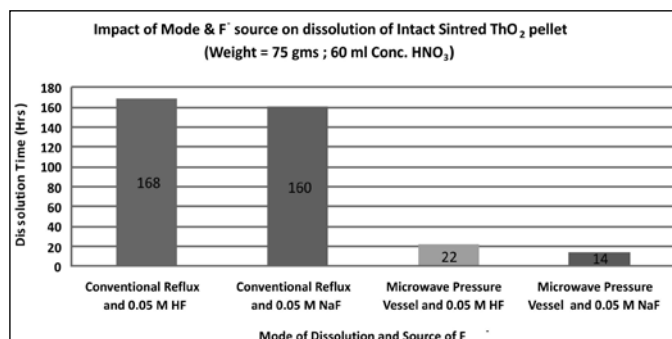

Fig.1 : Impact of microwave pressure vessel technique over conventional reflux along with effect of the use of NaF over HF on ThO$_2$ dissolution
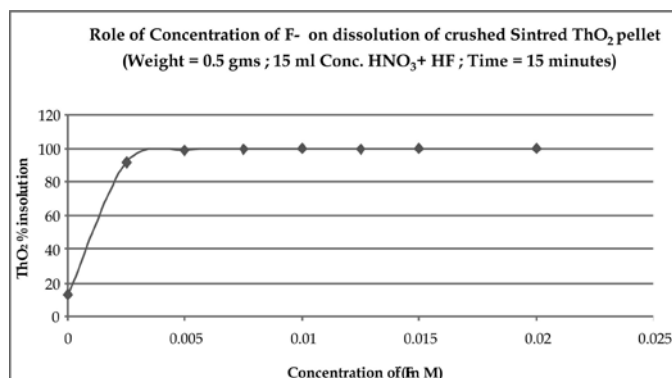

Fig.2 : Effect of concentration of F- ion

4. Salient Features And Summary

Based on the above mentioned facts and results, the important observations on dissolution of thoria and its mixed oxides can be summarised as follows:
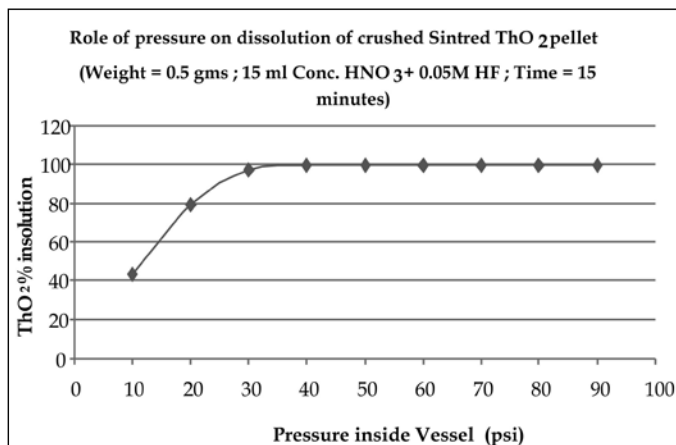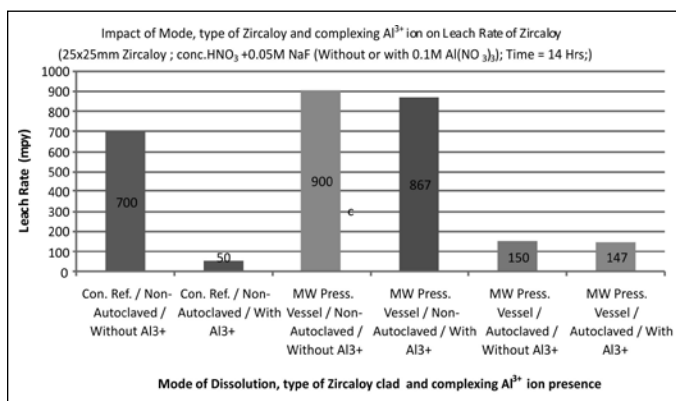
Fig.3 : Effect of elevation of pressure
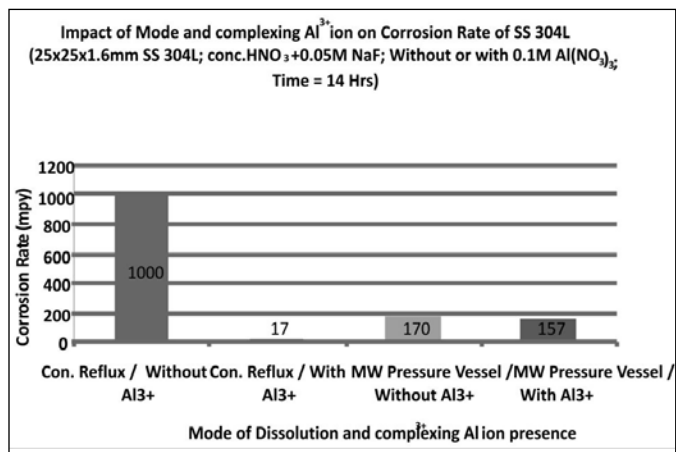

Fig.4 : Leach rate of Zircaloy

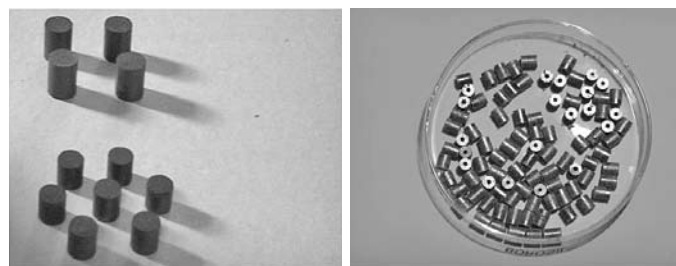*Fig.5 : Corrosion rate of SS 304L*

Fig.6   (a) Used Solid Pellets   (b) Annular Pellets

1. **Thorium dioxide and its various forms as fuels:** The nanocrystalline thoria powder, prepared by PVA-aided microwave denitration technique, may dissolve in only hot and pure conc. nitric acid, but other crystalline powder and sintered forms do not dissolve quantitatively [10,11]. ThO_2 is to be used as the fuel in sintered solid pellet forms with 92-98% TD with certain percentage of UO_2 or PuO_2. Higher is the density of the pellet; lower would be the dissolution rate. Higher the concentration of nitric acid, higher is the dissolution rate. The dissolution rate increases with increasing percentage of PuO_2 and UO_2 in ThO_2. The annular pellets dissolve at faster rates. Please see Fig.6(a) and (b) for various forms.

2. **Requirement of F- ions with concentrated HNO_3:** F- acts as a reactive catalytic species to accelerate and complete the dissolution of ThO_2 in nitric acid. Since F- ion is volatile in nature, its concentration in open vessels decreases during dissolution course and hence, there appears to be a variation in the use of reported concentrations of HF from 0.005 M to 0.1 M with HNO_3 by various groups. So, either F- ion should be replenished in open solvent medium or the solvent medium should be closed to avoid depletion of concentration of F-. Use of NaF, if Na does not interfere in any chemical processing step, would be better proposition than HF [10, 11], if added in same molar concentration.

3. **Crushing of ThO_2 pellet or doping in it with some fast soluble species:** Crushing of pellet to powder increases the surface area for reaction tremendously and, hence, the dissolution rate. Doping with either UO_2 or PuO_2 or any other soluble oxides within ThO_2 pellet would render their prevalent dissolution which consequently create pores and increase the surface area for reaction and dissolution rate. ThO_2 fuel would have UO_2 or PuO_2 as constituent (in driver fuels) or would have UO_2 or some other oxides, formed by neutron irradiation or fission (in spent fuels), to play the role of pore formers. If nitric acid soluble species are present within the solid ThO_2 fuel, a pretreatment step with nitric acid without F- ion would be of significant help for the dissolver vessel life. Spent fuels would dissolve more easily than fresh fuels due to defects, pores and solubility of fission products. Higher is the soluble species in pellet matrix, higher would be resulting surface area for reaction and the dissolution rate.

4. **Mode of heating and dissolution:** Endothermic dissolution of ThO_2 needs the application of heat. Heating may be carried out either by conventional

heating (infra red lamp or hot plate or reflux) or by microwave heating (reflux or pressure vessel). The former is surface heating, where heat is transferred from a hot source to the pellets. On the other hand, microwave heating is a volumetric heating where heat is produced at the molecular levels in the pellet, by interaction with electromagnetic radiations. So, along with heating of liquid, the solid particles (if microwave absorbers) are also heated to higher temperatures simultaneously resulting in the enhanced dissolution.

5. **Role of Pressure:** Heating of liquids may be carried out in reflux mode at atmospheric pressure (i.e. at the b.p.) and high pressure mode (i.e. above the b.p.). It may be noted that b.p. of nitric acid is 120^oC at atmospheric pressure which elevates to 160^oC at 7.5 kg/cm^2 or 120 psi pressure. Higher is the dissolution temperature, higher is the dissolution rate. But the experiments have shown that ~3kg/cm^2 or 40 psi pressure would suffice [10, 11].

6. **Role of addition of complexing agent for F^- ion:** F^- ions, though aid the dissolution of ThO_2, corrodes the metallic dissolution vessel. A complexing agent is required to complex the free F^- ions to minimise such corrosion, though depletion of F^- ions, by complexing, may also decrease the dissolution rate of ThO_2. Al^{3+} ions, added as $Al(NO_3)_3$, is expected to act as complexing agent. In microwave pressure vessel experiments earlier [10]**,** Al^{3+} addition does not decrease the dissolution rate of ThO_2, whereas in conventional reflux mode it decreases. It may be probably due to sufficiently longer dissolution time in conventional mode, whereby the F^- ions concentration drops significantly due to complexation with either added Al^{3+} ions or by in situ generated Th^{4+} ions. It is concluded that Al^{3+} addition is impractical, since Th^{4+} ion is a better complexing agent than Al^{3+} ion. And, for spent fuels scheme, in situ generated Zr^{4+} ion, from dissolution of Zircaloy clad pieces, is even better than Th^{4+} ion.

7. **Leaching of clad material:** For the chopped spent fuel pieces along with Zircaloy clad, the leaching of clad would play important role in the dissolution of spent thoria or its mixed oxide fuels, since the leaching of clad would loosen its grip over fuel piece. Non-autoclaved Zircaloy-4 (PHWR's clad) and autoclaved (treatment to form 3-4µm oxidised layer on clad surface) Zircaloy-2 (BWR's clad) coupons of (25x25 mm) have been subjected to leach studies. Using microwave pressure vessels, the leach rate of non-autoclaved Zircaloy is ~900 mpy on the weight loss basis whereas that of autoclaved Zircaloy is significantly less i.e. ~150 mpy

in HNO_3 + 0.05M NaF mixture [11] in 14 hrs, the time equivalent to quantitative dissolution of ThO_2 with same solvent. The values decrease insignificantly to 867 mpy and 147 mpy, if 0.1M $Al(NO_3)_3$ is used to complex free F^- ions. Experiments show that oxidation of zircaloy surface, by autoclaving, makes the Zircaloy resistant to F^- attack. With conventional reflux, the leach rate decreases from 700 mpy to 50 mpy, for non-autocaved Zircaloy, if 0.1M $Al(NO_3)_3$ is used.

8. **Corrosion of dissolution vessel material:** The life of dissolver vessel is of the utmost concern in radiochemical processing. The candidate materials for the use as dissolver vessel are SS304L or NAG SS304L. The corrosion rate of SS304L coupons (25x25x1.6mm) in HNO_3 + 0.05M NaF mixture is 170 mpy and 157 mpy without and with 0.1M $Al(NO_3)_3$, respectively [11] in 14 hrs, the period required for the quantitative dissolution of ThO_2. In conventional refluxing, the corrosion rate of SS 304L decreases drastically from 1000 mpy to 17 mpy with the use of 0.1M $Al(NO_3)_3$. The corrosion rate of SS 304L and leach rates of Zircaloy would decrease with Th^{4+} or / and Zr^{4+} ions, if used, in place of Al^{3+}.

Requirements

Mainly three categories of ThO_2 based fuel materials are expected for dissolution and accordingly their handling in (i) ventilated hoods : consisting of Natural Thorium, Natural Uranium and Low Enriched Uranium , (ii) normal glove-boxes : consisting of Plutonium and Uranium-233 with <50 ppm Uranium-232 and (iii) shielded glove-boxes or hot-cell : consisting of Uranium-233 with >50 ppm Uranium-232 or any irradiated fuel

5. Conclusions and Recommendations

(i) Use of catalytic amount of F^- ions with HNO_3 is essential. Use of NaF appears to be the better option than HF for the dissolution of crystalline and sintered ThO_2, $(Th, U)O_2$ and $(Th, Pu)O_2$.

(ii) Crushing of ThO_2 pellet(s) is to be avoided, specifically for Pu and ^{232}U bearing fuels.

(iii)The symmetric dissolution of thoria pellet(s) from all sides with cylindrical shape remaining intact, till ~1mm diameter, hints towards employing annular pellet(s), to allow dissolution from inside too. The time required for dissolution of one pellet would represent the approximate dissolution time for a batch.

(iv)A pre-treatment step, with pure conc. HNO_3 (without HF / NaF), is helpfully incorporable for doped pellets like $(Th,U)O_2$ and $(Th,Pu)O_2$, to reduce the F^- attack on metallic dissolution vessel for a reasonable duration.

If required, suitable oxidising-reducing agent may be added to accelerate the dissolution during 1st Stage. This stage would also generate requisite quantity of Th^{4+} (or/and Zr^{4+}) ions in the solution and avoid external addition of Th^{4+} (or/and Zr^{4+}) ions for complexing the F$^-$ ions.

(v) The reflux mode appears to be appropriate in view of safety concerns. Otherwise, 2-3 kg/cm^2 pressurised mode dissolution would be a better choice. The later, being a closed system, would restrict the escape of F$^-$ ions almost completely. It would (a) enhance dissolution rate and (b) avoid corrosive attack of F$^-$ ions on peripherals. Alternatively, escaping vapour in reflux should be closed cycled.

(vi) Periodic transfer of intermittent solutions during the course of dissolution and replenishing the solvent accordingly (semi-continuous mode) would increase the efficiency of dissolution. The transferred solution may be boiled off and condensed vapour may be returned to the dissolution vessel.

(vii) Microwave heating (MH) is material selective in nature whereas conventional heating is not. HNO$_3$, UO$_2$ and PuO$_2$ strongly absorb the microwaves but ThO$_2$ does not. Being volumetric in nature, MH is fast and vigorous. Therefore, MH increases the dissolution rates of ThO$_2$ by one order when pressure vessels are used as compared to conventional refluxing.

(viii) MH technique is fit for remote controlling, cavities (dissolution vessels) adaptation inside glove-box/hot-cell with almost zero-maintenance and customising the dissolution vessels. Dissolution vessels may also be provided with protective non-corrosive lining in MH technique, without affecting the dissolution rates. In MH, reflux and pressure, both modes can be used with same equipment.

(ix) An indigenous glove-box adaptable 3 kW microwave heating system (MHS), being continuously used for (U,Pu)O$_2$ mixed oxides dissolution and denitration in kilograms scale for more than fifteen years without a shut down, gives a reasonable technological base.

A hot-cell adaptable MHS has also been erected and tested. Systematic effort on vessel design may provide adequate scaled up outputs.

(x) Single microwave heating control unit with different cavities may be used for many liquid heating processes. It can act as dissolver, concentrator and denitration unit. So, it is useful where space-constraint troubles. MH techniques are also supportive of eco-friendly and non-proliferation aspects.

References

1. R. K. Sinha and A. Kakodkar, India HWR Activities Status Report, 5th meeting of IAEA Technical Working Group on Advanced Technology for Heavy Water Reactor, Vienna, June 25-28, 2001.
2. H.D. Greiling and K.H. Lieser, *Radiochimica Acta.,* 35(1984)79.
3. I. I. Chernayev, Complex compounds of Uranium (published at Moscow), 1-2, 1964.
4. J. C. Sullivan and E. H. Appleman, *Radiochimica Acta.,* 48(1989)151.
5. A. M. Shakila et.al, *Nucl. Technol.,* 79(1987)116.
6. P. B. Gurba, Studies on the electrolytic dissolution of Plutonium dioxide, Ph.D. Thesis, Bombay University, 1988.
7. Satyajeet Choudhary, M. Keskar, A. V. Patil, K. D. Singh Mudher and V. Venugopal, *Radiochimica Acta.,* 94(2006) **357.**
8. M. F. Shying, T. M. Florence and D. J. Carswell, *J. Inorg. Nucl. Chem.,* 34(1972)213.
9. A. K. Fulzele, D. J. Shah, P. K. Gedam, R. K. Malav, G. K. Mallik, J. P. Panakkal and H. S. Kamath, presented at NUCAR(Feb 2003, p-163) Trombay, India.
10. G. K. Mallik, A. P. Karande, R. Govindan, V. K. Bhargava, H. S. Kamath & D. S. C. Purushottam, presented at NUCAR (Dec 1992, p-155), Andhra University, India.
11. G. K. Mallik, R. K. Malav, K.Raju and H. S. Kamath, presented at NUCAR (Feb 2001, p-260), University of Pune, India.
12. G. K. Mallik, R. K. Malav and H. S. Kamath, presented at NUCAR (Jan 2009, p-145), SVKM's Mithibai College, Mumbai, India.
13. W. D. Bond, ORNL-2519, 1958.
14. A. I. Vogel, Text Book of Quantitative Inorganic Analysis, 3rd Edition, Longmans, Geen & Co. Ltd., London, 442.
15. W. Davies and W. Gray, *Talanta,* 11(1964)1203.
16. J. L. Drummond and R. A. Grant, *Talanta,* 13(1966)477.

Dr. Gatiwant Kumar Mallik, after obtaining his M.Sc. (Chemistry) degree from Bihar University, Muzaffarpur, graduated from 29th Batch of BARC Training School and joined Advanced Fuel Fabrication Facility, BARC, Tarapur. He appreciably contributed towards chemical quality control of nuclear fuels, specially U, Pu and Th based Mixed Oxide (MOX) fuels, erection of indigenous microwave heating systems, microwave processing of U, Pu and Th based nuclear materials and erection of a-active waste drum monitor. Presently, at Post Irradiation Examination Division, BARC, Mumbai, he is associated with PIE and chemical characterisation of fuel, control rod and structural components of nuclear reactors. He has authored / co-authored 56 publications in international / national journals and proceedings. Presently he is Heading, Chemical Characterisation Section, PIED, BARC.

Structural aspects of ThO$_2$ containing borosilicate glasses: Probed by solid state nuclear magnetic resonance technique

R. K. Mishra[1], V. Sudarsan[2], A. K. Tyagi[2] and C. P. Kaushik[1]*

[1]Waste Management Division, [2]Chemistry Division,
Bhabha Atomic Research Centre, Mumbai – 400094
E-mail: cpk@barc.gov.in

Abstract

Structural configurations of boron and silicon present in borosilicate glasses have been identified and quantified by ^{29}Si and ^{11}B solid state nuclear magnetic resonance (NMR) technique. Based on NMR studies on barium borosilicate glasses containing ThO$_2$, it has been established that there is no interaction between borosilicate network and Th^{4+} ions in these glasses. Whereas Si exists as Q^3 and Q^2 structural units in the ratio of ~0.7, boron exists in both trigonal (BO$_3$) and tetrahedral (BO$_4$) configurations and their relative concentrations are not affected by ThO$_2$ incorporation in the glass. Higher extent of ThO$_2$ incorporation in barium borosilicate glasses compared to sodium borosilicate glasses has been attributed to the increased number of non-bridging oxygen atoms present in the barium borosilicate glasses.

1. Introduction

Borosilicate glasses have wide application as materials for the immobilization of high level nuclear wastes [1-2]. Since India has vast thorium resources, Department of Atomic Energy is having an ambitious program to use thorium in the blanket zone of fast breeder reactors (in the second stage of nuclear energy program) followed by its induction as Th-U^{233}mox fuel in the same type of reactors in the third stage. Thorium will be one of the major components, along with fission products like Cs^{137}, Sr^{90}, Ru^{160} etc., present in the waste after the reprocessing of thoria containing spent fuel [3] generated form above mentioned type of reactors. This needs to be immobilized in glassy matrices before their long term disposal in repositories. Very few studies have been reported regarding structural aspects of ThO$_2$ incorporated silica based glasses mainly because of very poor solubility of ThO$_2$ in such glasses (~6 wt. %) [4, 5]. It is observed that most of the time phase separation occurs during glass formation. Structural aspects of Th^{4+} in silicate glasses have been investigated by Farge [5] using EXAFS technique and found that for 1-3 wt% of ThO$_2$ contents in the glass, Th^{4+} is octahedrally coordinated with a mean Th-O distance of 2.32±0.02 Å and above this concentration, Th^{4+} is also present in eight fold coordination with mean Th-O distance of 2.40±0.03 Å. Effect of ThO$_2$ incorporation on the structural aspects of phosphate glasses has been reported by Simon et al. [6, 7] and Pillai et al. [8] up to 10 mole% of ThO$_2$. Based on nuclear magnetic resonance and vibrational spectroscopic studies, these authors concluded that ThO$_2$ incorporation in the glass matrix is associated with the distortion and breaking of P-O-P structural units. Further they suggested that Th^{4+} ions occupy the network modifying positions in

these glasses. Destruction and distortion of P-O-P linkages is detrimental to the stability of the glass and such glasses are not suitable for the immobilization of radioactive waste. Similarly the network modifying action of ThO$_2$ has also been reported for TeO$_2$ based glasses [9].

Recently it has been reported that ThO$_2$ incorporation in borosilicate glasses can be significantly improved by addition of BaO in the feed mixture [10]. Detailed study of the structural aspects of these glasses is desirable to understand the bonding characteristics of Th^{4+} in the borosilicate network and their thermal stability. This information will also be useful for the development of glassy materials with improved waste immobilization characteristics. Solid-state NMR is an ideal technique to monitor the changes in the borosilicate network brought about by ThO$_2$ incorporation using ^{29}Si and ^{11}B as probe nuclei. In the following section brief description is given regarding the basic aspect of solid state nuclear magnetic resonance (NMR) technique and how it helps to understand the structural aspects of borosilicate glasses. This will be followed by discussion on structural information obtained through NMR technique on representative sodium and barium borosilicate glasses having compositions $(Na_2O)_{0.36}(SiO_2)_{0.39}(B_2O_3)_{25}$ and $(SiO_2 +B_2O_3)_{0.64}(Na_2O+BaO)_{0.36}$. As the barium borosilicate base glass having the general composition $[(SiO_2 +B_2O_3)_{0.64}(Na_2O+BaO)_{0.36}]$, is known [10] to exhibit enhanced solubility for ThO$_2$ a number of above base glass composition with varying concentrations of ThO$_2$ have been prepared and investigated by ^{29}Si and ^{11}B magic angle spinning nuclear magnetic resonance (MAS NMR) technique to understand the structural features and location of Th^{4+} ions in these glasses. To under stand role

of BaO in the glass, detailed NMR studies were also carried out for sodium borosilicate glasses without any BaO.

2. Details of glass preparation and characterization

Required amounts of analytical grade $NaNO_3$, $Ba(NO_3)_2$, SiO_2, H_3BO_3 were taken so as to get the base glass of above mentioned compositions. The compounds were mixed, well grounded and heated at 1000 °C for 4 hours in platinum crucible. The free flowing melt was quenched between two stainless steel plates. ^{29}Si and ^{11}B MAS NMR patterns of these glasses were recorded using a Bruker Avance DPX 300/500 machine. Powdered samples were packed inside 4 mm zirconia rotors and subjected to a spinning speed of 5 kHz. Typical 90° pulse durations for the ^{29}Si and ^{11}B nuclei are 4.5 and 2.09 μs, respectively with the corresponding delay times of 6 and 2 seconds. ^{11}B static NMR patterns were also recorded with same pulse duration and delay times as that used for MAS NMR experiments. ^{11}B NMR experiments were carried out with lower pulse durations also (upto 0.3μs) and the line shapes were found to be identical. The chemical shift values for ^{29}Si and ^{11}B NMR spectra are reported with respect to tetramethylsilane and 1M aqueous solution of H_3BO_3, respectively. All the ^{11}B NMR patterns were corrected for the boron nitride (BN) background arising from the Bruker MAS NMR probe.

3. Basic principle of NMR

Nuclear magnetic resonance spectroscopy is a technique that exploits the nuclear magnetic properties of atomic nuclei and can give valuable information about the structure, dynamics and chemical environment around a particular nucleus in a molecule/lattice/amorphous material. The important parameters obtained in NMR experiments are briefly described below.

Chemical shift: The chemical shift of any nucleus is defined as the difference between its resonance frequency and the resonance frequency of the same nuclei in a referance sample and can be expressed by the equation 1

$$\delta = \frac{\omega - \omega_0}{\omega_0} * 10^6 \qquad \text{.......................... (1)}$$

where ω, ω_0 represent resonance frequencies of nuclei in the sample and in the reference, respectively.

Chemical shielding interaction: Chemical shift arises because of the effective magnetic field felt by nuclei brought about by the polarization effect of electron cloud around the nuclei created by the applied magnetic field. Since this is particularly sensitive to the configuration of valance electrons, which is governed by the nature of chemical bonding, this aspect has been labeled as chemical shielding interaction. The Hamiltonian for this interaction can be written as [11]

$$H_{cs} = \gamma\, I_z \sigma\, B_0 \qquad \text{..................................... (2)}$$

where σ is a second rank (3x3) tensor known as the chemical shielding tensor. This tensor can be diagonalised for a specific principal axis system and σ_{11}, σ_{22}, σ_{33} are the corresponding diagonal components. The isotropic component of the chemical shift tensor can be expressed by the relation

$$\sigma_{iso} = \frac{1}{3}\left(\sigma_{11} + \sigma_{22} + \sigma_{33}\right) \qquad \text{.......................... (3)}$$

The symmetry parameter is defined as

$$\eta = \frac{\sigma_{22} - \sigma_{11}}{\sigma_{33} - \sigma_{iso}} \qquad \text{.................. (4)}$$

Due to the presence of chemical shielding anisotropy, the nuclear precessional frequency depends on the orientation of principal axis system with respect to the external applied magnetic field and can be expressed by the relation [11]

$$\omega_p\left(\theta, \phi\right) = \gamma\, B_0 \left\{\left(1 - \sigma_{11}\right)^2 cos^2\phi\, sin^2\theta + \left(1 - \sigma_{22}\right)^2 sin^2\phi\, sin^2\theta + \left(1 - \sigma_{33}\right)^2 cos^2\theta\right\}^{1/2} \qquad \text{...(5)}$$

where θ and Φ represent the orientation of principal axis system with applied magnetic field direction. For axial symmetry η = 0 and the precession frequency can be expressed by the relation

$$\omega_p\left(\theta\right) = \gamma\, B_0\left[1 - \sigma_{iso} - \Delta\sigma\cdot\left(3\cos^2\theta - 1\right)/3\right] \qquad \text{.... (6)}$$

For values of θ = 54.7° the term $3\cos^2\theta - 1$ becomes zero and the dependence of chemical shielding anisotropy term on Larmor frequency gets averaged out to a very small value.

In solution NMR spectroscopy, dipolar interactions and anisotropic effects are averaged out by the molecular motion, but this is not so in the solid state and the NMR spectra of solids tend to be broadened because of (a) magnetic interactions of nuclei with the surrounding electron cloud (chemical shielding interaction), (b) magnetic dipole – dipole interactions among nuclei and (c) interactions between electric quadrupole moment and surrounding electric field gradient. Hence it is difficult

to get any meaningful information from such patterns. However, by using suitable experimental strategies, such interactions can be averaged out, thereby improving the information obtained from solid state NMR patterns. One such technique used to get high resolution solid state NMR pattern in solids is the magic angle spinning nuclear magnetic resonance (MAS NMR) technique. In the following section brief account of the MAS NMR technique has been given.

3.1 Magic Angle Spinning Nuclear Magnetic Resonance (MAS NMR)

MAS NMR technique involves rotating the powder samples at high speeds, at an angle of 54.7° (magic angle) with respect to the applied magnetic field direction. When $\theta=54.7°$, the term $3\cos^2\theta$ becomes unity. Since Hamiltonian for different anisotropic interactions have $3\cos^2\theta - 1$ term, these anisotropic interactions get averaged out in time during fast spinning. This is schematically shown in Fig.1 and explained below.
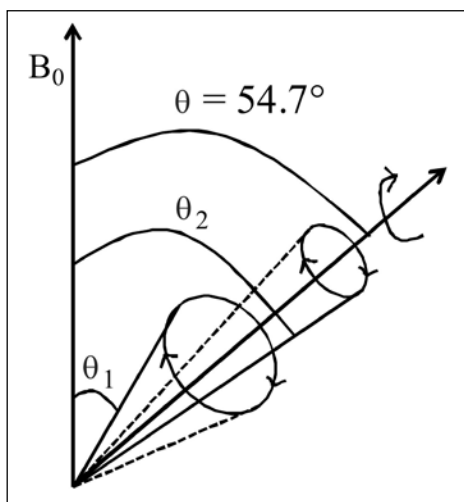

Fig.1. Principle of MAS NMR experiment

At sufficiently fast spinning speeds, the NMR interaction tensor orientations with initial angles of θ_1 and θ_2 relative to B_0 have orientaional averages of 54.7°, resulting in the conversion of $3\cos^2\theta - 1$ term in expressions corresponding to various interactions to a very small value, thereby giving rise to sharp NMR peaks. Thus the MAS NMR technique simplifies the solid state NMR patterns and individual chemical environments can be correlated with corresponding chemical shift values obtained from these samples [11].

Although, MAS is an efficient technique employed for getting high resolution NMR patterns from solid samples, in many cases, due to spinning, side bands, which are mirror images of the isotropic peak and spread from

the isotropic peak by integer multiples of the spinning frequency, appear along with the central isotropic peak for nuclei having wide range of chemical shift values. For nuclei which is having a nuclear spin value ½, sideband pattern is a measure of the chemical shift anisotropy and valuable information regarding the symmetry of the electronic environment around a probe nuclei can be obtained from the intensity distribution of sidebands. However, in presence of large number of isotropic peaks, the number of sidebands also increases, and there can be overlap between the sidebands and isotropic peaks, which makes the MAS NMR pattern complicated.

4. ^{29}Si and ^{11}B MAS NMR studies on borosilicate glasses

The main constituents in borosilicate glasses are boron and silicon, the local environment around both of them can be investigated by recording ^{29}Si and ^{11}B MAS NMR patterns. Fig. 2 shows ^{29}Si MAS NMR pattern of $(Na_2O)_{0.36}(SiO_2)_{0.39}(B_2O_3)_{25}$ glass. The pattern is characterized by a broad asymmetric peak with maximum around -100 ppm. The broad asymmetric peak can be de-convoluted into two peaks based on Gaussian fit with individual peaks around -102 and -89 ppm which are characteristic of Q^4 and Q^3 structural units of silicon respectively (where Q^n represents silicon structural units having "n" number of bridging oxygen atoms attached with it) [12,13]. The structural units schematically represented in Fig. 2 (a and b). With increase in network modifier concentration, it is observed that the silicon structural units undergo de-polymerisation to form Q^2 and Q^1 structural units. The physicochemical properties like, thermal expansion coefficient, glass transition temperature, leach resistance etc have got strong influence on the nature and relative concentration of different structural units present in the glass. Our studies have revealed that as the Q^4 structural units of silicon get converted to Q^3, Q^2 and then to Q^1 structural units sequentially, the thermal expansion coefficient of glass increases and the glass transition

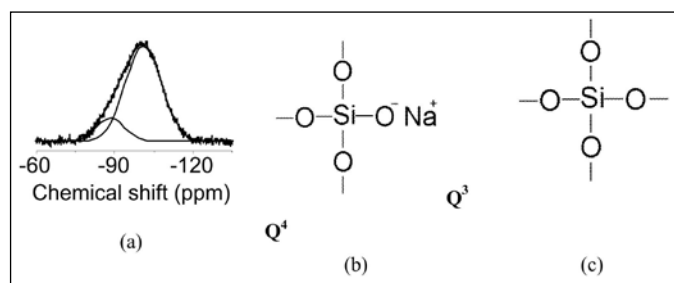*Fig 2. ^{29}Si MAS NMR pattern of (a) $(Na_2O)_{0.36}(SiO_2)_{0.39}(B_2O_3)_{25}$ glass. Schematic representation of Q^3 and Q^4 structural units are shown in Fig. 2 (b) and (c) respectively. (All chemical shift values are expressed with respect to tetra methyl silane (TMS)). Spinning speed was 5 kHz.*

temperature decreases. This is explained based on the conversion of more rigid structural units to less rigid ones brought about by the bridging to non-bridging oxygen atoms conversion. As mentioned earlier, ^{11}B MAS NMR also can give valuable information regarding the coordination environment around boron atoms in the glass and this is discussed in the following section.

^{11}B MAS NMR patterns of sodium borosilicate glass having composition $(Na_2O)_{0.36}(SiO_2)_{0.39}(B_2O_3)_{25}$ is shown in Fig. 3. The pattern consists of a sharp peak around -1 ppm and a broad peak around 11 ppm. Based on the previous ^{11}B MAS NMR studies [12] the sharp peak has been attributed to boron in tetrahedral coordination and broad peak to boron in trigonal coordination. As [11]B is a quadrupolar nucleus with spin I = 3/2, quadrupolar interaction around the nuclei will be quite significant when it occupies a site with non-cubic symmetry, like that in trigonal configuration (BO_3 structural units). Unlike this, in tetrahedral configuration (BO_4 structural units) boron is having cubic symmetry and hence negligible quadrupolar interaction. Thus BO_3 structural units give rise to broad NMR line shape and BO_4 structural units give rise to sharp NMR line shape. Taking into consideration of intensity of spinning sidebands and the detector efficiencies of BO_3 and BO_4 structural units (using the standard compound like borax), relative concentration of the two types of boron structural units in the glass can be calculated. Schematic representation of BO_3 and BO_4 structural units attached with silicon structural units in sodium borosilicate glass is also shown in Fig. 3. The relative concentration of BO_3 and BO_4 structural units are also found to have strong influence on the thermo-physical properties of glasses.
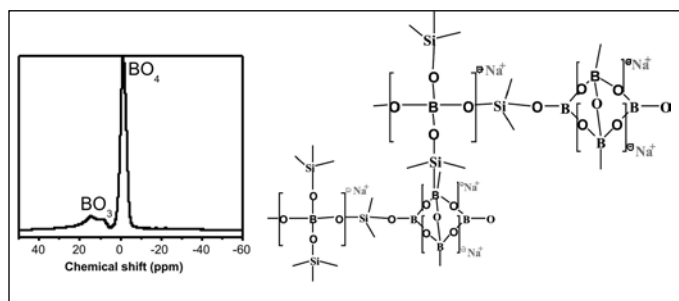

Fig 3. ^{11}B MAS NMR pattern (left) of $(Na_2O)_{0.36}(SiO_2)_{0.39}(B_2O_3)_{25}$ glass recorded in a 500 MHz NMR machine. Schematic representation of BO_4 and BO_3 structural units attached to silicon is shown in the right. (All chemical shift values are expressed with respect to 0.1M aqueous solution of H_3BO_3). Spinning speed was 10 kHz.

^{29}Si MAS NMR patterns for $[(SiO_2+B_2O_3)_{0.64}(Na_2O+BaO)_{0.36}]$ glasses containing different amounts of thorium is shown in Fig. 4 (left). For all the samples an asymmetric peak placed at –89.5 ppm is observed. Deconvolution of this

peak assuming a Guassian line shape resulted in two peaks around –95 and –86 ppm. Based on the ^{29}Si MAS NMR studies of borosilicate glasses [12-19], the peak around –95 ppm, characteristic of Q^3 structural units of silicon and that around –86 ppm is attributed to Q^2 structural units (where Q^n represents silicon structural units having 'n' bridging oxygen atoms). The variation of the relative concentration of Q^3 and Q^2 structural units along with The relative concentration of Q^3 and Q^2 structural units and their chemical shift values as a function of ThO_2 concentration is shown in Figure 4 (right). The relative concentration of Q^3 and Q^2 structural units and their chemical shift values are not affected by increasing ThO_2 concentration establishing the fact that the borosilicate network is unaffected by ThO_2 incorporation in the glass. Probable reason for this could be that the Th^{4+} along with Na^+ ions can get incorporated at the network modifying sites, which are formed by the significant amount of nonbridging oxygen atoms present in these glasses. Thus there is no detectable interaction between the Th^{4+} ions and the glass network.

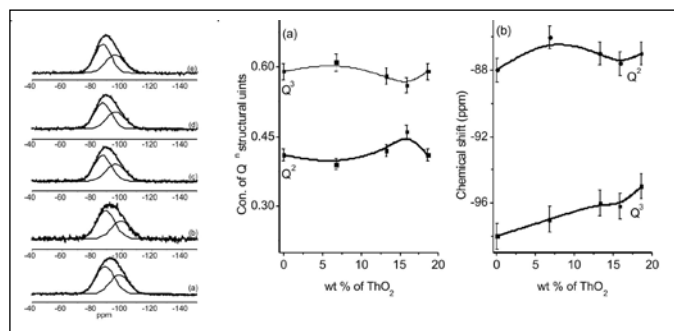*Fig 4. (Left): ^{29}Si MAS NMR patterns for barium borosilicate glasses containing (a) 0 wt%, (b) 6.8 wt%, (c) 13.2 wt%, (d) 15.8 wt% and (e) 18.6 wt% of ThO_2. (Right)Variation of (a) the relative concentration of Q^n structural units of silicon and (b) their chemical shift values as a function of ThO_2 contents in barium borosilicate glasses.*

In order to find out the role of BaO in the glass for ThO_2 incorporation, borosilicate glasses without any BaO and containing 0, 11 and 18 wt % ThO_2 were prepared and characterised (keeping all the remaining mole ratios same). XRD patterns for 11 and 18 wt % ThO_2 containing samples revealed that part of the ThO_2 got phase separated during quenching. ^{29}Si MAS NMR patterns of these glasses are shown in Figure 5. Borosilicate glasses without any BaO and ThO_2 (Fig. 5(a)) is characterised by an asymmetric peak centered around –100 ppm and deconvolution of which resulted in two peaks around –101 and –90 ppm characteristic of Q^4 and Q^3 structural units of silicon respectively. With addition of ThO_2 in the glass Q^4 structural units got partially converted to Q^3 structural units, indicating that the ThO_2 acts as a network modifier
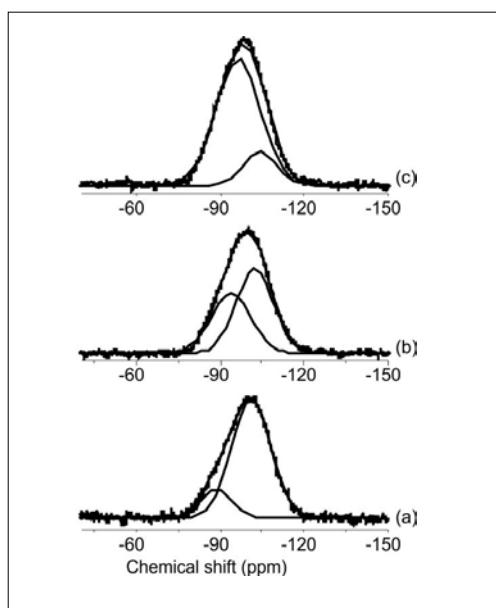
Fig 5. ^{29}Si MAS NMR patterns for borosilicate glasses without any barium and containing (a) 0 wt % (b) 11 wt% and (c) 18 wt% of ThO$_2$.
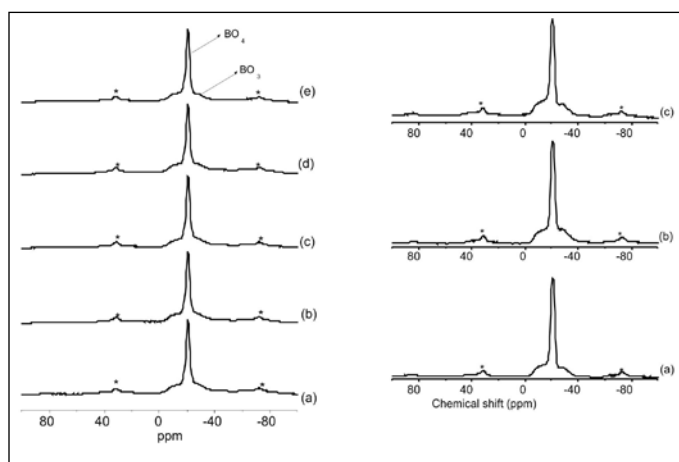

*Fig 6 (left). ^{11}B MAS NMR patterns for barium borosilicate glasses containing (a) 0 wt %, (b) 6.8 wt%, (c) 13.2 wt %, (d) 15.8 wt% and (e) 18.6 wt% of ThO$_2$. The corresponding patterns from borosilicate glasses without any barium and having (a) 0 wt % (b) 11 wt% and (c) 18 wt% of ThO$_2$ are shown in Fig. 6(right). Peaks marked " * " are spinning side bands. Experiments were carried out in 300 MHz NMR machine.*

in these glasses. Further the chemical shift values of Q^4 and Q^3 structural units shifted to more negative values with increase in ThO$_2$ incorporation in the glass. The possible reason for this could be due to the conversion of Si-O-Si to Si-O-B linkages [12]. Based on the ^{29}Si MAS NMR patterns for ThO$_2$ incorporated barium borosilicate and borosilicate glasses, it is inferred that the significant number of non bridging oxygen atoms present in barium borosilicate glasses, facilitates the Th^{4+} incorporation in the glass without breaking Si-O-Si linkages. These results further substantiate our previous conclusion that Th^{4+} along with

Na$^+$ ions get incorporated in the network modifying sites created by the significant number of non-bridging oxygen atoms present in barium borosilicate glasses.

Fig. 6 (left and right) shows the background corrected ^{11}B MAS NMR patterns of borosilicate glasses with and without BaO and containing different amounts of ThO$_2$. Barium borosilicate glasses without any ThO$_2$ (Fig. 6(a) left), showed a sharp peak (~ -20 ppm) superimposed over a broad peak . Based on the previous studies [12, 14-17, 19] of borosilicate glasses, the sharp peak is characteristic of tetrahedrally coordinated boron structural units and the broad peak is arising due to the trigonally coordinated boron structural units. The intensity and the line shape of both the components of these spectra remained almost unchanged with increase in ThO$_2$ contents, indicating that there is no interaction between ThO$_2$ and the boron structural units. For a half integer quadrupolar nucleus like ^{11}B ($I = 3/2$), quadrupolar interaction is significant when it has got trigonal (non cubic symmetry) environment compared to the tetrahedral environment (cubic symmetry). This results in the appearance of broad peak for trigonally coordinated boron atoms and a sharp peak for the tetrahedrally coordinated boron atoms. ^{11}B MAS NMR spectra corresponding to borosilicate glasses without any BaO and containing different amounts of ThO$_2$ are shown in Fig. 6(right). The patterns are essentially similar to those corresponding to barium borosilicate glasses. The relative concentrations of BO$_3$ and BO$_4$ structural units can be obtained from the ^{11}B MAS NMR patterns assuming a Gaussian line shape with negligible quadrupolar interaction for the BO$_4$ structural units and a quadrupolar broadened line shape for the BO$_3$ structural units. No distinction was made between the symmetric and asymmetric BO$_3$ structural units. It is observed that the relative concentration of BO$_3$ and BO$_4$ structural units in borosilicate glasses remained unchanged with increase in ThO$_2$ content in the glass.

5. Conclusions

Structural configurations of boron and silicon present in borosilicate glasses have been identified and quantified by ^{29}Si and ^{11}B solid state nuclear magnetic resonance (NMR) technique. Barium borosilicate glasses containing up to 18 wt. % of ThO$_2$ have been prepared by conventional melt quench method. Based on ^{29}Si & ^{11}B MAS NMR studies it has been concluded that the borosilicate network is not affected by such large ThO$_2$ incorporation. From ^{29}Si MAS NMR studies on ThO$_2$ incorporated, barium borosilicate and sodium borosilicate glasses, it has been concluded that significant number of non bridging oxygen atoms present in barium borosilicate glasses facilitates the Th^{4+} incorporation in the glass.

Acknowledgements:

References

1. P. G. Eller, G. O. Tarvinen, J. D. Purson, R. A. Penneman, R. R. Ryan, F. W. Lytle and R. B. Greegor, *Radiochim. Acta.*, 39 (1985)17.

2. A. J. Freeman, G. H. Lander (Eds.), Handbook on the Physics and Chemistry of the Actinides, Elsevier, 1987, pp. 271-312.

3. A. Kakodkar, presented at the international seminar on the role of Nuclear Energy for sustainable development (New Delhi, India, 1997), p. 62-76.

4. M. S. Sonavane, R. G. Yeotikar, S. S. Ali, presented at the Indian Nuclear Society Annual Conference 2003, Mumbai, India, p168-169.

5. F. Farges, Geochim. *Cosmochim. Acta.,* 55(1991)3303.

6. S. Simon, I. Ardelean, I. Bratu, D. U. Reckert, V. Simon, *Mater. Lett.*, 37(1998) 227.

7. V. Simon, *Eur. Phys. J. Appl. Phys.*, 25(2004)93.

8. C. G. S. Pillai, V. Sudarsan, M. Roy, A. K. Dua, *J. Nucl. Mater.*, 321(2003)313.

9. T. Sekiya, N. Mochida, A. Soejima, *J. Non-Cryst. Solids.*, 191(1995)115.

10. R. K. Mishra, A. K. Tyagi, P. Sengupta, G. B. Kale, C. P. Kaushik and K. Raj, presented at the DAE solid state Physics symposium 2005, Mumbai, India.

11. P. Boolchand, Insulating and semiconducting glasses, Series on directions in condensed matter physics, Vol.17, World scientific, Singapur, 2000.

12. V. Sudarsan, V. K. Shrikhande, G. P. Kothiyal, S. K. Kulshreshtha, *J. Phys.: Condens. Matter.*, 14(2002)6553.

13. G. Bhasin, A. Bhatnagar, S. Bhowmik, C. Stehle, M. Affatigato, S. Feller, J. McKenzie and S. Martin, *Phys. Chem, Glasses,* 39(1998)269.

14. R. Martens, W. Muller-Warmuth, *J. Non-Cryst. Solids,* 265(2000)167.

15. T. Nanba, Y. Miura, *Phys. Chem. Glasses*, 44(2003)244.

16. D. Chen, H. Miyoshi, H. Masui, T. Akai, T. Yazawa, *J. Non-Cryst. Solids* 345(2004)104.

17. H. Miyoshi, D. Chen, H. Masui, T. Yazawa, T. Akai, *J. Non-Cryst. Solids* 345(2004)99.

18. T. Nanba, M. Nishimura, Y. Miura, Geochim, *Cosmochim. Acta.*, 68(2004)5103.

19. J. G. Wood, S. Prabhakar, K. T. Mueller, C. G. Pantano, *J. Non-Cryst. Solids* 349(2004)276.

Dr. V. Sudarsan *joined Chemistry Division of BARC in the year 1994 after graduating from 37th batch of BARC Training School. He received his Ph.D. degree in Chemistry from Mumbai University in the year 2002. Subsequently he worked for a period of two years at the University of Victoria, British Columbia, Canada in the area of luminescence of lanthanide ions which are doped in nanoparticles of inorganic hosts. Currently he is working on the optical and structural properties of lanthanide ions doped nanoparticles and glasses. In recognition of his work, he was conferred with DAE Scientific and Technical Excellence Award (2010). He is also associated with BARC Training School activities. Presently, he is heading Materials Chemistry Section of Chemistry Division, BARC.*	
Dr. A. K. Tyagi *is presently Head, Solid State Chemistry Section, Chemistry Division, Bhabha Atomic Research Centre (BARC), Mumbai and also a Professor (Chemistry) at Homi Bhabha National Institute (HBNI). He joined BARC, Mumbai in 1986 through BARC-Training School. Since then he has been working in the field of Chemistry of nanomaterials, functional materials and nuclear materials. He was a Max-Planck Fellow at MPI, Stuttgart, Germany during 1995-96. In recognition of his work, Dr. Tyagi has been conferred with several prestigious awards such as Homi Bhabha Science & Technology Award, Gold Medal of Indian Nuclear Society, MRSI Medal, CRSI Medal, Dr. Laxmi Award by ISCAS, Rheometric Scientific-ITAS Award, and IANCAS-Dr. Tarun Datta Memorial Award, RD Desai Memorial Award of ICS, Rajib Goyal Prize in Chemical Sciences, DAE-SRC Outstanding Researcher Award, CRSI's Prof. C.N.R. Rao National Prize for Chemical Sciences and ISCB award for excellence in chemical sciences. He is a Fellow of Royal Society of Chemistry, UK (FRSC), National Academy of Sciences, India (FNASc), Maharashtra Academy of Sciences (FMASc) and Indian Academy of Sciences (FASC). He has been a visiting scientist to several countries like Germany, USA, Canada, France, Spain, Sweden, Portugal, Russia, Japan, Israel, China, Singapore, Malaysia and Australia.*	
Dr. C. P. Kaushik *shouldering the responsibility of Dy. Plant Superintendent (H),Waste Management Facility, Trombay. He is engaged in development and characterisation of glass formulations for vitrification of HLW from PHWR, FBR & AHWR. He is also responsible for Plant scale vitrification HLW after finalization of a suitable glass formulation. Other areas of his research cover- compatibility of materials at various stages of vitrification, characterizations of buffer and backfill materials for use in Near Surface Disposal Facilities and Geological Repositories, separation and recovery of valuables from radioactive waste. He has more than 120 publications in journals/international conferences and symposia to his credit. He is a recipient of INS gold medal award in the year 2005. He has also received Group Achievement awards in the year 2006 and 2012 for his contribution in commissioning of WIP, Trombay and 2010 for characterisation of refractory materials used in Joule Heated Ceramic Melter deployed for vitrification of HLW & Process development and bench scale synthesis of DCH18C6 and development and demonstration of recovery of Sr from thorium lean waste respectively.*	
Dr. R K Mishra *is associated with Process Control Laboratories of Waste Management Facilities, Trombay for providing analytical support to the waste immobilization plant. He is engaged in preparation and characterization of glass/glass ceramics matrices for immobilization of high level radioactive liquid waste generated during reprocessing of spent fuel from PHWR, FBR and AHWR. Other areas of his research experience cover separation and recovery of valuables from radioactive waste for industrial application, corrosion study of different alloys with nitric acid as well as molten glass matrix, synthesis and characterization of nano materials for decontamination of low level radioactive liquid waste. He has more than 75 publications to his credit. He is a recipient of DAE Special Contribution Award – 2008 and Group Achievement awards in the year 2010 for his valuable contribution in the field of Nuclear Science and Technology and to the programmes of Dept of Atomic Energy. During his Ph D, he has extensively worked on different types of borosilicate glasses for the purpose of immobilization of nuclear waste and based on this outstanding work, he has been bestowed with Prof. H J Arnikar best Ph. D thesis Award in the year 2011.*	

Separation Science related to the thorium fuel cycle

Jayshree R.

Analytical Chemistry Division
Bhabha Atomic Research Centre, Mumbai 400085, India
E-mail: jrk@barc.gov.in

1. Introduction:

The closed fuel cycle approach, with importance being given to reprocessing and recycling of spent fuel, has been adopted to meet the requirements of three stage Indian nuclear programme as visualized by Dr.Homi J.Bhabha in 1960's. The three stages are:

❖ Natural uranium fuelled Pressurised Heavy Water Reactors (PHWRs),

❖ Fast Breeder Reactors (FBRs) utilising plutonium based fuel,

❖ Advanced nuclear power systems for utilisation of thorium.

The first stage comprises of Pressurized Heavy Water Reactors fuelled by natural uranium which contains only 0.7% of fissile ^{235}U. The rest 99.3% is comprises ^{238}U which itself is not fissile, but can be converted in the nuclear reactor, to fissile element ^{239}Pu. The second stage, comprising of Fast Breeder Reactors (FBRs) are fuelled by mixed oxide of ^{238}U and ^{239}Pu, recovered by reprocessing of the first stage spent fuel. In FBRs, production of ^{239}Pu occurs thus leading to the name "breeder". Thus the FBRs produce energy and fuel, thus leading to the build up of ^{239}Pu inventory over a period of time. ^{232}Th is not a fissile material but can be converted to the fissile ^{233}U. Therefore ^{232}Th is known as fertile material. India has the world's third largest reserves of thorium. Therefore thorium is used as a blanket in fast breeder reactor. Moreover, development of innovative design of reactors for direct use of thorium is also in progress in parallel to three stage program. In this context, the frontier technologies being developed include the Accelerator Driven Systems (ADS) and Advanced Heavy Water Reactor (AHWR). The ADS essentially is a sub-critical system using high-energy particles for fission. The main advantage is the reduction of waste production as the actinides produced in ADS are `burnt' out. The AHWR is an innovative concept, which will act as a bridge between the first and third stage essentially to advance thorium utilization without undergoing second stage of the three stage program. It uses light water as coolant and heavy water as moderator. It is fuelled by a mixture of ^{239}Pu and ^{232}Th, with a sizeable amount of power coming from ^{232}Th. The three stages are closely interlinked with one another and the successful implementation of one stage leads to the onset of the other. Development of reprocessing technologies, waste treatment, immobilization technology, advanced decontamination and decomissioning procedures etc are important part of the back end of the fuel cycle. Reprocessing of irradiated thorium for the recovery of ^{233}U is the major focus of the back end of the fuel cycle. Hence it is obvious that such recent developments necessiate the need for separation procedures to be developed for thorium from mainly uranium.

In this chapter, the various studies relating to separation of thorium from different systems have been discussed. Various procedures adopted based on the need of the separation. The separation process may be applied to recovery of thorium from the ores or the reprocessing of the spent fuel and waste mangament or for the chemical analysis in complicated matrices. In the present article, the intial description will be based on the nature of separation procedure. At the end, a small description of the procedure applied for chemical analysis will also be discussed.

2. Liquid-Liquid Extraction:

Solvent extraction is an important separation process with various advantages of being simple and highly efficient. Liquid–liquid extraction, also known as solvent extraction and partitioning, is a method to separate compounds based on their relative solubilities in two different immiscible liquids, usually water and an organic solvent. It is an extraction of a substance from one liquid phase into another liquid phase. The term partitioning is commonly used to refer to the underlying chemical and physical processes involved in liquid–liquid extraction but may be fully synonymous. The term solvent extraction can also refer to the separation of a substance from a mixture by preferentially dissolving that substance in a suitable solvent. In that case, a soluble compound is separated from an insoluble compound or a complex matrix.

Solvent extraction has been used for the separation of thorium both in the recovery from the monazite sand as well as in the reporcessing stages. Recovery of thorium is carried out from the monazite sands which contain ilemenite ($FeTiO_3$) as a major constituent (65-80%) while

Table I. Degree of Extraction and Metal Selectivity Depends on Amine Type and Alkyl Structure (1M SO$_4$, pH 1 , ~1 gram metal ion/liter; phase ratio 1/1, 0.1M amine in kerosine)

Amine Type	Example	Metal Ion extraction E=M$_o$/M$_{aq}$		
		U(VI)	Th(IV)	Ce(III)
Branched primary	Primene JM[a], 1-(3-ethylpentyl)-4-ethyloctylamine	5-30	>20,000	10-20
Secondary with alkyl branching distant from the nitrogen	Di(trideeyl)amine[b]	80	>500	<0. 1
Secondary with alkyl branching on the first C	Amberlite LA-1[c], bis(1-isobutyl-3,sdimethylhexy1) amine	80-120	5-15	<0.05
Tertiary with no branching or branching no closer than the third C	Alamine 336[d], tri isooctylamine[e,f]	140	<0.03	<0.01

[a]Trialkylmethylamine, homologous mixture, 18-24 carbons. [b] Mixed C$_{18}$ alkyls from tetrapropylene by oxo process. [c]Dodecenyl-trialkylmethylamine, homologous mixture 24-27 carbons, [d]Trialkylamine with mixed n-octyl and n-decyl radicals. [e] Kerosine diluent modified with 3 vol. % tridecanol.[f] Mixed Cs alkyls from oxo process.

Table 2. Composition of Typical Monazite Sulfate Liquor

Ion	Concentration (g/L)
Th	5.3
U	0.2
Total rare earth oxides (including Ce$_2$O$_3$)	35
Ce$_2$O$_3$	16
La$_2$O$_3$	8.5
Pr$_2$O$_3$	1.7
Nd$_2$O$_3$	7
Sm$_2$O$_3$	1.3
SO$_4^{2-}$	128
PO$_4^{3-}$	26

monazite is only 0.5-1% along with useful minerals like zircon, rutile, garnet and silimanite. The processing of beach sands is carried out using gravitation and magnetic separations. Thorium is recovered from the monazite fraction. Monazite contains phosphates of thorium and rare earths. It contains 9% ThO$_2$, 60% rare earth oxides, 0.4% UO$_2$ and 27% phosphorus pentoxide. On treatment with concentrated sodium hydroxide, sodium phosphate and hydroxides of thorium, uranium and rare earths are formed. Sodium phosphate being water soluble can be recovered from solution and used in textile industry for water softening. The residual cake known as thorium concentrate is dissolved in excess of hydrochloric acid and thorium is precipitated as its sulphate using 50% sulphuric acid. The solution is then treated with sodium fluoride and hydrochloric acid to recover the remaining thorium,

uranium and rare earths. The thorium sulphate obtained is converted to thorium hydroxide by the addition of sodium hydroxide. The thorium hydroxide is then dissolved in hydrochloric acid and re-precipitated as sulphate to increase the purity. The sulphate is treated with ammonium carbonate and the resulting thorium hydrogen carbonate is dissolved in nitric acid and the solution is evaporated to obtain crystalline thorium nitrate. The thorium nitrate obtained thus is known as mantle grade and this is purified further for nuclear application by solvent extraction using tributyl phosphate. The thorium concentrate dissolved in nitric acid contains nitrates of thorium along with uranium and rare earth. The thorium is separated by the selective extraction of uranium using an organic solvent having 5-10% tributyl phosphate in kerosene. In the second stage, thorium is extracted into 40% tributyl phosphate in kerosene. Both thorium and uranium are separately back extracted into aqueous solution as nitrates and purified further by solvent extraction and finally concentrated to nitrates of thorium and uranium [1].

The Amex Process developed by Crouse Jr and Brown [2] for the extraction of thorium from the deposits in the Canadian Blind River district using alkyl amines. Alkyl amines are versatile extractants for economical recovery of relatively high grade thorium products from ore process sulfate liquors. Relative extraction power for thorium and other metal ions is strongly dependent on the amine type and alkyl structure (Table 1). Thus, appropriate choice of amine permits efficient recovery and separation in multicycle extraction operations. Thorium is present in the extract as a thorium-amine-sulfate complex, with excess amine sulfate and/or bisulfate. This complex contains three to four amine sulfates per thorium, depending on amine

type. When the extract is treated with neutral or acidic nitrate or chloride solutions, thorium is displaced with the nitrate or chloride anion. Nitrate is the more effective stripping anion. Following nitrate stripping the amine is regenerated to the free amine form for recycle by contact with a base such as ammonium hydroxide. This recovers the relatively expensive nitrate for recycle and maintains extraction efficiency by preventing contamination with nitrate.

Due to the high acidity and relatively high concentrations of sulfate and phosphate, the extraction coefficients of thorium from monazite liquors are appreciably lower than those shown in Table 1 but the relative extraction power of amines are similar (Table 1). The strong affinity of the primary amines for thorium is again apparent. In comparison, the extraction coefficient for di-(tridecy1) amine is low but adequate for process use. The Amex process was also used for the removing of thorium from the existing Blind River ion exchange plant raffinates. The liquor contained 1– 2 g/L of chloride or nitrate introduced to elute uranium from the anion exchange resins. Both ions have affinity for the amine extractants. The chloride and nitrate ions at the particular concentration do not affect the extraction efficiency of di (tridecy1) - amine or primary amines [2].

Various other studies have been reported in literature on the extraction of thorium from monazite leach solutions. Hughes and Singh [3] extracted thorium from sulfate leach solution using 0.1 M Adogen-383 (secondary amine) diluted in kerosene. Their counter-current extraction system consists of four stages extraction (0.1 M H_2SO_4), four scrub stages (0.1 M H_2SO_4) and three strip stages (1.0 M ammonium carbonate). The use of dimethylheptyl-methylphosphonate (DEHMP) and tributylphosphate (TBP) as extractants diluted in kerosene was carried out by Dong and Jinwen [4] for treatment of monazite–U–Th–alkaline cake leached with HCl. Hammad et al. [5] separated uranium from Egyptian monazite alkaline hydrous oxide cake concentrate dissolved in concentrated HCl solution by anion exchanger column containing Amberlite IRA-400. Thorium present in the effluent solution was purified by extraction from nitric acid medium by TBP diluted in kerosene. Ali et al [6] developed a flow sheet for the recovery of thorium from Egyptian monazite sands. The dissolution and leaching is carried out using alkaline carbonate solutions. This cake was dissolved in 4M HNO_3 and thorium was extracted selectively by a counter-current extraction system using a mixer–settler contactor and Aliquat-336 in kerosene as extractant. It was observed that 2 h of continuous operation was needed to reach the steady state condition for the

process. The extraction efficiency is found to be 80% and the stripping efficiency is 82%.

In the thorium fuel cycle, the irradiated fuel is reprocessed for the recovery of fissile U^{233} and remaining ^{232}Th. The procedure for the separation of uranium and thorium becomes very important. Whenever thorium fuel reprocessing procedures are considered, THOREX is first and foremost process which is to be discussed. The thorium fuel needs sufficiently long cooling time since the decay of ^{233}Pa to ^{233}U takes 1-2 years. Even then the fuel is highly radioactive due to the presence of fission products and the reprocessing is carried out remotely in hot cells having thick concrete walls of several feet. Since thorium oxide is insoluble in acid media, dissolution of thorium based fuels in nitric acid is very slow and therefore hydrofluoric acid is needed as a catalyst to enhance the dissolution rate. The presence of hydrofluoric acid results in severe corrosion of the stainless steel dissolver vessels which is partly overcome by the addition of aluminium nitrate during dissolution. Once in solution, ^{233}U and thorium are extracted into tributylphosphate. However, the extraction of thorium is very poor and the solubility of thorium nitrate in the organic medium is small. Moreover, the organic layer splits into two phases namely, thorium rich and thorium poor phases. Thus the amount of thorium that can be extracted into the organic layer becomes limited. Due to the poor extraction of thorium co extraction of fission products occurs resulting in contamination. Once thorium and uranium are extracted into the organic layer, the partitioning based on valency change is not possible as thorium has got only one valency. Thus the partitioning is based upon the lower extraction of thorium as compared to uranium. In the THOREX flow sheet, the dissolver solution containing thorium, uranium and fission products nitrates in 1 M nitric acid is contacted with 30% tributyl phosphate in the first column resulting in the extraction of both uranium and thorim. Any fission products extracted into the organic phase is scrubbed back using 1M nitric acid. The organic solvent is then contacted with dilute nitric acid (0.2 M) to ensure the extraction of thorium into the aqueous phase and has to be stored as it contains ^{228}Th and cannot be used for ten years. Uranium is stripped using 0.01 M nitric acid and this aqueous solution contains fission products and thorium also. Further purification is carried out using ion exchange method. Uranium is separated as ^{233}U from thorium rods. In this process, the rods are treated with caustic soda to remove the aluminium cladding. The bare thorium or thorium oxide is dissolved in 8 M nitic acid containg 0.05 M sodium fluoride and aluminium nitrate. The solution containing 200 g/L of thorium and 0.2 g/L of uranium is treated with 5% tributylphosphate to enable

selective extraction of uranium. Back -extraction and pre-concentration result in an aqueous solution containing 5-10 g/L of uranium [1].

The use of reagents like tetra (2-ethylhexyl) diglycolamide (TEHDGA) as an extractant by Sharma et al [7, 8] showed that the conditional acid uptake constant (K_H) of TEHDGA/n-dodecane was found out to be 1.72 and the ratio of TEHDGA to nitric acid was 1 : 0.96. The extracted species of uranium and thorium in the organic phase were found to be $UO_2(NO_3)_2$.2TEHDGA and $Th(NO_3)_4$.2TEHDGA. The separation factor (D_{Th}/D_U) was of the order of 300 in the nitric acid concentration range of 0.5- 1.5 M. Similar separation factor was also achieved at higher acidity when thorium was present in large concentration compared to uranium. These results indicate that TEHDGA solvent system could be a potential candidate for separation of thorium from uranium. The extraction efficiency of tris (2-ethylhexyl) phosphate (TEHP) in n-dodecane at 25°C evaluated by Pathak et al [9] showed that TEHP was a better choice than tri-n-butyl phosphate (TBP) for the separation of ^{233}U from the irradiated thorium matrix. Various kinds of organophosphorus extractants, both acidic and neutral ligands have been investigated for thorium extraction [10-13] and it has been found that the acidic extractants have shown very large distribution coefficients from nitrate media in the pH region. Karve et al showed that the distribution coefficient of thorium in 0.001M HNO_3 was around 110 [10]. For the neutral extractants, compared to tri-octyl phosphine oxide [TOPO] [11] and TBP [12], Cyanex 923 [13] resulted in high extraction efficiency of thorium.

Liquid-liquid extraction has been applied for separation and preconcentration prior to determination of trace levels of thorium in various samples like monazite sand, rare earths, sand, sea water, gas mantles etc. Various extractants like N-phenylbenzo-18-crown-6-hydroxamic acid (PBCHA) in dichloromethane [14], N-n-octylaniline in xylene [15] were used.

3. Solid-Liquid Extraction

3.1 Sorption

Sorption using simple and cheap adsorbents is gaining lot of importance due to its economic benefits as well as easy availability of different kinds of adsorbents. A great deal of research is carried out continuously to develop new sorbents which are cheap and easily available so that they need not be regenerated using expensive processes after their use for sorption. Hence the research in developing new adsorbents can be focused on the development of simple and economic procedures for the synthesis of the sorbents or on the development of methods for the reusability of these sorbents.

The use of adsorption for the nuclear waste treatment requires that apart from the other benefits it should have good radiation and thermal stability. Boro-alumino-silicate glasses are technologically important due to their high mechanical strength and chemical durability and are widely used in various applications like nuclear waste immobilization. In France, vitrification using R7T7 [16] and SON 68 [17] nuclear glasses, is the major procedure adopted for waste immobilization of fission products and minor actinides. 'R7T7' glass, named after the COGEMA La Hague vitrification units, is the reference alumino-boro-silicate glass selected to immobilize the radioelements arising from reprocessing light-water reactor fuel, whereas SON 68 is the inactive analog which is used. The use of boro-alumino-silicate glasses as room temperature sorbents for the separation of thorium and uranium has been carried out by Chandramouleeswaran et al [18]. It was seen that selective uptake of Th from a mixture containing uranium was achieved by adjusting the pH of the solution only and without the use of any complexing agent.

Solid phase extraction (SPE) is also an important technique which is gaining a lot of importance due to the various advantages of insolubility in aqueous phase, low rate of degradation and no hazardous waste being produced coupled with the ease of recycling. In SPE, the organic extractants are anchored to an inert polymeric support and several methods have been developed for actinide extractions. Modification of the Merrifield chloromethylated resin with octyl(phenyl)-*N*,*N*-diisobutylcarbamoyl-methylphosphine oxide (CMPO) [19] showed very high sorption capacity values of 0.960 mmol g−1 for U(VI), 0.984 mmol g−1 for Th(IV), 0.488 mmol g−1 for La(III) and 0.502 mmol g−1 for Nd(III) under optimum HNO_3 medium, respectively coupled with fast exchange kinetics (<5 min for 50% extraction) and greater preconcentration ability, with reusability exceeding 20 cycles. The developed grafted resin has been successfully applied in extracting Th(IV) from high matrix monazite sand, U(VI) and Th(IV) from simulated nuclear spent fuel mixtures. Solid phase extraction has been used for the determination of uranium and thorium in marine and soil reference samples. A catechol functionalized silica gel (CASG) [20] synthesized by chemically immobilizing catechol with diazotized aminopropyl silica gel was used for uptake of U and Th in the pH range of 3.5–6.0. The elution was carried out using 10 mL of 1.0 M HCl and determined by using an Arsenazo III spectrophotometric procedure.

Table 3: **Comparision of various biosorbents for thorium uptake**

Biosorbent		Qo (mg/g)	Operating conditions			
Name	Type		pH	T(°C)	Intial metal ion concentration (mg/L)	Amt. of biosorbent (g/L)
Pseudomonas fluorescens	bacterium	15	4-5	23	30-1000	n.a
Streptomyces niveus	bacterium	34	4-5	23	30-1000	n.a
Aspergillus niger	fungus	22	2-5	23	30-1000	n.a
		162	0-1	25	100-700	0.3-9
Rhizopus arrhizus	Fungus	185	2-5	23	30-1000	n.a
		116	0-1	25	100-700	1-13
Pennicillium chrysogenum	Fungus	150	4-5	23		n.a
Saccharornyces cerevisiae	Yeast	116	0-1	25		0.8-24

Biosorption is considered a potential instrument for the removal of metals from waste solutions and for precious metals recovery, an alternative to the conventional processes, such as those based on ion exchange, or adsorption on activated carbon. Table 3 gives a comparision of some of the biosorbents used for thorium uptake.

It was postulated that radionuclides present in an aquatic (sea) environment are sorbed by marine microorganisms [21]. Tsezos and Volesky [22] verified that thorium and uranium biosorption by fungal biomass of Rhizopus arrhizus is based on both physisorption and chemisorption. In physisorption, adsorption occurs in the cell wall chitin structure. In the chemisorption, a complex is formed between the nitrogen of the chitin network in the cell wall. This uptake was found to be selective and not influenced by the presence of other ions, like Fe^{2+} and Zn^{2+}.

Ion exchangers have been used for the separation of uranium and thorium. The adsorption of uranium from sodium carbonate solutions by means of strong basic ion exchange resins is applied to the recovery of uranium from monazite sand residues and to the exhaustive separation of uranium from thorium stocks [23]. The batch distribution coefficients of thorium, rare earths, and many other elements were determined on the strongly acidic cation exchanger Dowex 50 in mixed aqueous-organic solvent systems containing organic phosphorus compounds and nitric acid. These investigations showed that from some of these media, thorium is not retained on the resin while rare earths and numerous other metal ions are strongly adsorbed making possible their quantitative separation from thorium. The most suitable medium for the complete separation of tracer and milligram amounts of thorium is 0.1 M trioctylphosphine oxide (TOPO) in methanol containing 5 vol % of 12M nitric acid [23]. With this eluent, thorium is eluted before rare earths and other

cations with separation factors in the order of ~102-104. It was found that methanol was much better than other reagents like acetone, tetrahydrofuran, acetic acid, and methyl glycol. Similarly poor results were obtained on replacing nitric acid with HCl. The use of other extractants like bis(2-ethyl- hexyl)-orthophosphoric acid (HDEHP) or tri-n-butyl- phosphate (TBP) instead of TOPO resulted in lower elution of Th, thus showing that the organic extractants followed the order of TBP < HDEHP< TOPO with respect to their efficiency for thorium elution [23]. The utility of macroporous cation-exchange resins for the separation of uranium from thorium (relevant to the final purification of the product uranium after reprocessing of the thorium breeder fuel) was examined [24]. It was seen that separation was efficient when macroporous resins were used instead of the gel-type resin [24]. Amberlite IRA-400 (sulphate form) is used for sorption of thorium at pH 2.0 [25] whereas tervalent cerium and other rare earths are sorbed to only a slight extent. An ion-exchange method has been developed for the separation of thorium from these elements. The method has also been applied to the determination of thorium and rare earths in monazite concentrate [25].

3.2 Membrane Separation:

Membrane separation method is of interest as it has several advantages over other separation methods like cost effectiveness, energy efficient and offers a high pre-concentration factor with a high degree of selectivity. The carrier-facilitated transport of metal ions across a liquid membrane has been primarily studied due to the simplicity of operation. They have shown great potential, especially in the cases where solute concentrations are relatively low and other techniques cannot be applied efficiently, since they combine the processes of extraction and stripping in a single step operation [26]. The extraction chemistry is the same as that of liquid–liquid extraction except that it

is governed by a non-equilibrium mass transfer. Metal ion extraction in the liquid membrane system can be facilitated by carrier mediated transport. In the simple system having a single cation the best carrier for transport is a ligand that forms a moderately stable complex than very stable one for effective transport [27]. The use of hollow fibre supported liquid membrane for the removal of uranium and thorium was evaluated by Ura et al [28], using tributylphosphate (TBP) diluted in kerosene as an extractant and sodium hydroxide as a stripping solution. Uranium ions were extracted using 5 % TBP (v/v) by rejecting thorium ions into raffinate. It was further concluded that the rate-controlling step was the diffusion of the uranium complex ions through the liquid membrane.

3.3 Extraction Chromatography

Extraction chromatography combines the selectivity of liquid-liquid extraction with the rapidity of chromatographic methods. The separation of the radionuclides is based on the distribution of the cations of interest between an organic and an aqueous phase (neutral or acidic). The extractant is adsorbed on the surface of an inert support and corresponds to the organic, stationary phase. An extraction chromatographic separation of thorium and uranium from simulated waste was achieved by Fujiwara et al [29] using the commercially available UTEVA resin (for uranium and tetravalent actinide). Thorium and uranium in control solutions with $1\text{-}5\,mol/dm^3$ HNO_3 were extracted with UTEVA resin and recovered with a solution containing $0.1\,mol/\,dm^3$ HNO_3 and $0.05\,mol/dm^3$ oxalic acid to be separated from the other metallic elements. Extraction behavior of U in the sample solutions was similar to that in the control solutions, but extraction of Th was dependent on the concentration of HNO_3. Thorium was extracted from $5\,mol/dm^3$ HNO_3 sample solutions but not from $1\,mol/dm^3$ HNO_3 sample solutions. It was concluded that the thorium fluoride formation interfered with extraction of Th. Addition of $Al(NO_3)_3$ and $Fe(NO_3)_3$, which have higher stability constant with fluoride ion than Th, does improve extractability of Th from $1\,mol/dm^3$ HNO_3 sample solution [29]. Extraction chromatography has also been used for preconcentration of uranium and thorium prior to their determination in geological samples like uraninite ore, coral and granite reference materials [30, 31].

Ion-imprinted polymers (IIPs) are recently identified nano-porous polymeric materials which on leaching the imprint ion can rebind, sense or transport (when cast as membranes) selectively the target analyte in presence of closely related inorganic ions. The IIPs find interesting applications in solid phase extraction, sensors and membrane separations of inorganics. An IIP material with methacryloylamidoglutamic acid (MAGA) and EGDMA ethylene glycoldimethacrylate (EGDMA) was used for the selective preconcentration of thorium in presence of uranyl and other lanthanide ions [32].

4. Conclusions:

It is seen from the above discussions, various separation procedures are avaialable for the separation of thorium from different matrices. The separation has been applied to recovery, fuel reprocessing and waste management in plant scale. Separation procedures are used on laboratory scale for preconcentration and separation prior to analysis in various types of samples.

References:

1. D. D. Sood, in "Nuclear Materials" (1996) IANCAS Publications

2. D. J. Crouse, Jr., and K. B. Brown, *Ind. Eng.Chem.*, 51(1959)1461.

3. Hughes, K. C., Singh, R., *Hydrometallurgy* 6(1980)25.

4. Z. Dong, D. Jinwen, In: Guangxian, X., Jenei,X. (Eds.), New Frontiers in Rare Earth Science and Applications. (1985) Academic Press Inc., Orlando, FL, USA.

5. A. K. Hammad, E. E. Ibrahim and M .R. Hammad, Arab *J.Nucl.Sci.Appl.*, 19 (1986) 19.

6. A. M. I. Ali, Y. A. El-Nadi, J. A. Daoud, H. F. Aly, *Int.J.Miner. Process.,* 81(2007) 217.

7. J. N. Sharma, R. Ruhela, K.L.Harindran, S.L.Mishra, S.K.Tangri and A.K.Suri, *J.Radioanal.Nucl.Chem.,* 278 (2008) 173.

8. J. N. Sharma, R. Ruhela, K. K. Singh, Manoj Kumar, C. Janardhanan, P. V. Achutan, S. Manohar, P. K. Wattal, and A. K. Suri, *Radiochim Acta.,* 98 (2010) 485.

9. P. N. Pathak, R. Veeraraghavan, and V. K. Manchanda, *J.Radioanal.Nucl.Chem.,* 240 (1999) 15.

10. M. Karve and C.Gaur, *J. Radioanal Nucl. Chem.,* 270 (2006) 461.

11. R.B. Pathak and A. P. Argekar, *J. RadioanalNucl. Chem.,* 166 (1992) 503.

12. V.G. Maioro, A. I. Nikolaev, and O. P. Adkina, *Radiochem.,* 48 (2006) 576 .

13. B. Gupta, P. Malik, and A. Deep, *J. Radioanal. Nucl. Chem.,* 251 (2002) 451.

14. Y. K. Agrawal, and S. B. Vora, *Microchim. Acta.,* 142 (2003) 255.

15. R. J. Patti, N. B. Kadm Patti, and M. B. Chavan, *J. Radioanal. Nucl. Chem.,* 2 (1997) 179.

16. P. A. Bingham, R. J. Hand, *J. Haz. Mater.,* 119 (2005)125.

17. C. Guittonneau, S. Gin, N. Godon, J. P. Mestre, O. Dugne, P. Allegri, *J. Nucl. Mater.,* 408 (2011) 73.

18. S. Chandramouleeswaran, Jayshree Ramkumar, V. Sudarsan and A.V.R. Reddy, *J. Hazard. Mater.,*198 (2011) 159.

19. Ch. S.K.Raju and M.S.Subramanian, *J. Hazard. Mater.,* 145(2007)315.

20. P. Metilda, J. M. Gladis and T. P. Rao, *Radiochim. Acta.,* 93(2005)219.

21. F.Veglio' and F.Beolchini, *Hydromet* 44(1997)301.

22. M.Tsezos and B.Volesky, *Biotechnol.Bioeng.,* 24(1982)955.

23. J. Korkisch' and K. A. Orlandini, *Anal.Chem.,* 40(1968)1952.

24. R. K. Rastogi, M. A. Mahajan, and N. K.Chaudhuri, *Sep. Sci. Technol.,* 32(1997)1711.

25. R. A. Nagle, and T. K .S. Murthy, *Analyst* 84(1959)37.

26. Jayshree Ramkumar, S. K Nayak, B Maiti, *J. Memb. Sci.,* 196(2002)**2**03.

27. T. Revathi Reddy, Jayshree Ramkumar, S. Chandramouleeswaran, A.V. R. Reddy, *J. Memb. Sci.,* 351 (2010)11.

28. P. Ura, R. Prakorn, P. Weerawat, and H. Milan, *Ind. Eng. Chem.,* 12(2006)673.

29. A. Fujiwara, Y. Kameo, A. Hoshi, T. Haraga, and M. Nakashima, *J Chromatogr A,* 1140(2007)163.

30. H. E. Carter, P. Warwick, J. Cobb, and G. Longworth, *Analyst,* 124(1999)271.

31. S.Y.Tolmachyov, J. Kuwabara, and H. Noguchi, *J. Radioanal. Nucl. Chem.,* 261(2004)125.

Dr. Jayashree Ramkumar *joined BARC from the 37th batch of training school after the completion of MSc from University of Madras, Chennai. Subsequently she joined the Analytical Chemistry Division. Since then, she is involved in the development of new separation procedures for different metal ions and toxic substances using membranes and adsorbents. She was awarded Ph.D on her work on ion exchange and related studies using Nafion membrane. She has more than 36 international journal publications to her credit in the field of membrane separation. She pursued her postdoctoral research in 2009 as the MANA Research Fellow on the use of mesoporous materials for remediation studies in the National Institute of Materials Science (NIMS), Ibaraki, Japan. She is also an Assistant Professor Homi Bhabha National Institute, India and currently guiding students as a co guide for their PhD.*

Achievments, Honours and Awards received by the SMC members

Name of the member and Affiliation	Name of the award/honour	Conferred by
Dr. Ayyappanpillai Ajayaghosh CSIR-National Institute for Interdisciplinary Science and Technology	Infosys Prize	Infosys Science Foundation
	CRSI Silver Medal	Chemical Research Society of India
	INSA Fellow (FNA)	Indian National Science Academy
Dr. Rajendra N. Basu CSIR-Central Glass & Ceramic Research Institute, Kolkata	ISEAC Eminent Scientist Award	Indian Society for Electroanalytical Chemistry (ISEAC), BARC
Dr. H. N. Ghosh BARC, Mumbai	Fellow, Indian Academy of Sciences (FASc)	Indian Academy of Sciences
Dr. Vinita Grover Gupta BARC, Mumbai	INS Young Scientist Award	Indian Nuclear Society
Dr. V.K. Jain BARC, Mumbai	Prof. W.U. Malik Memorial Award	Indian Council of Chemists
Dr. Mainak Roy BARC, Mumbai	Young Achiever Award	DAE Solid State Physics Symposium
Dr. Saurabh S Soni Sardar Patel University , Vallabh Vidyanagar, Gujarat	DST Fast Track Young Scientist Award	DST, New Delhi
Dr. A. K. Tyagi BARC, Mumbai	Fellow, Indian Academy of Sciences (FASc)	Indian Academy of Sciences
Prof. Sandeep Verma Indian Institute of Technology, Kanpur	R C Mehrotra Commemoration Lecture (Gold Medal)	Indian Science Congress (2013, Centenary Session, Kolkata)
	Member, Editorial Advisory Board, Chemical Communications	Royal Society of Chemistry

In this issue

Feature articles